

Revised Groundwater Flow Model and Predictive Simulation Results

**Coso Operating Company
Hay Ranch Water Extraction and Delivery System
Conditional Use Permit (CUP 2007-003)**

**Prepared for County of Inyo
Independence, California**

January 28, 2011




Daniel B. Stephens & Associates, Inc.

6020 Academy NE, Suite 100 • Albuquerque, New Mexico 87109



Daniel B Stephens & Associates, Inc

The following people were responsible for producing this report:



T Neil Blandford, P G. No. 1034 (Texas)



Muthu Kuchanur, PhD, E.I.T.



Farag Botros, PhD, P.E. No. C 076531 (California)



Stephen J. Cullen, PhD, P.G. No. 7399 (California)
Principal-in-Charge



Table of Contents

Section	Page
1. Introduction	1
2. Groundwater Model Updates	2
2.1 Recharge from Precipitation	3
2.2 Geologic Unit Thickness	4
2.3 Haiwee Reservoir Seepage and Northern Rose Valley Water Levels	5
2.4 Historical Hay Ranch and LADWP Pumping	7
2.5 Model Grid	8
3. Model Calibration	9
3.1 Approach to Model Calibration	10
3.2 Boundary Conditions	10
3.3 Initial Conditions	13
3.4 Hydraulic Properties	14
3.4.1 Hydraulic Conductivity	14
3.4.2 Storage Coefficient	16
3.4.3 Comparison to Hay Ranch Aquifer Test Results	16
3.5 Simulation Results	17
3.6 Sensitivity Analysis	20
4. Predictive Simulation Results	21
5. Conclusions and Recommendations	24
References	26

List of Figures

Figure

- 1 Base Map
- 2 Well Locations
- 3 Base of Model Layer 1
- 4 Haiwee Reservoir Toe-Drain Discharge and Correspondence of Toe-Drain Discharge and Reservoir Stage
- 5 Geology and Wells South of Haiwee Reservoir



List of Figures (Continued)

Figure

- 6 Correspondence of Well VS360 Water Levels and Haiwee Reservoir Stage, No Lag
- 7 Correspondence of LADWP Well 816 Water Levels and Haiwee Reservoir Stage, 3-Month Lag
- 8 LANDSAT Image of Hay Ranch Area, June 17, 1985
- 9 Model Grid
- 10 Recharge from Precipitation
- 11 Boundary Conditions for Model Layer 1
- 12 Boundary Conditions for Model Layer 2
- 13 Boundary Conditions for Model Layers 4 and 5
- 14 Horizontal and Vertical Hydraulic Conductivity, Model Layer 1
- 15 Horizontal and Vertical Hydraulic Conductivity, Model Layer 2
- 16 Horizontal and Vertical Hydraulic Conductivity, Model Layer 3
- 17 Horizontal and Vertical Hydraulic Conductivity, Model Layer 4
- 18 Horizontal and Vertical Hydraulic Conductivity, Model Layer 5
- 19 Simulated and Observed Water Levels at HR1 and HR2 Shallow Cluster Wells
- 20 Recent Period Simulated and Observed Water Levels at HR1 and HR2 Shallow Cluster Wells
- 21 Simulated and Observed Water Levels at Wells RV090 and RV100 South of Hay Ranch
- 22 Recent Period Simulated and Observed Water Levels at Wells RV090 and RV100 South of Hay Ranch
- 23 Simulated and Observed Water Levels at Wells RV140 and RV150 South of Coso Junction
- 24 Recent Period Simulated and Observed Water Levels at Wells RV140 and RV150 South of Coso Junction



List of Figures (Continued)

Figure

- 25 Simulated versus Observed Water Levels for December 2009 and September 2010
- 26 Simulated December 2009 Water Table
- 27 Sensitivity Analysis Results for Layer 1, Hydraulic Conductivity and Specific Yield
- 28 Simulated Drawdown from 2009 Conditions at Time of Minimum Flow to Little Lake (Scenario A)
- 29 Simulated Drawdown from 2009 Conditions at Time of Minimum Flow to Little Lake (Scenario B)
- 30 Simulated Drawdown from 2009 Conditions at Time of Minimum Flow to Little Lake (Scenario C)

List of Tables

Table

- 1 Simulation Mass Balance for Steady-State and Transient (1985 and 2009) Simulations
- 2 Predictive Simulation Results

List of Appendices

Appendix

- A Recharge Modeling Analysis for Rose Valley
- B LANDSAT Images of Historical Irrigated Acreage
- C Simulated and Observed Water Levels
- D Report and Model Files



Revised Groundwater Flow Model and Predictive Simulation Results Coso Operating Company Hay Ranch Water Extraction and Delivery System Conditional Use Permit (CUP 2007-003)

1. Introduction

The purpose of this report is to document the updated and revised groundwater flow model and the updated predictive simulation results conducted by Daniel B. Stephens & Associates, Inc. (DBS&A) in accordance with Mitigation Measure Hydrology-4 of the Mitigation Monitoring and Reporting Program (MMRP) of Conditional Use Permit (CUP) 2007-003. For ease of reference, the updated model documented in this report is referred to as the “current model”, whereas the model on which CUP 2007-003 was based is referred to as the “previous model”. The final version of the previous model, completed by Geologica, is documented in Appendix C2 of the final environmental impact report (EIR) (MHA, 2008b). The previous model is an updated version of the groundwater model presented in the draft EIR (MHA, 2008a), which itself is an updated and modified version of the first groundwater model constructed for Rose Valley by Brown and Caldwell (2006).

CUP 2007-003 permits the extraction of groundwater from two existing wells on the Coso Hay Ranch LLC property (Hay Ranch) in Rose Valley (Figure 1). The water is extracted by Coso Operating Company (Coso) for injection at the Coso geothermal field in the northwest area of the China Lake Naval Air Weapons Station. The MMRP prescribed, among other things, monitoring a number of wells in Rose Valley. The locations of these wells, and others referenced in this report, are shown in Figure 2.

The current model implemented the following major changes to the previous model:

- Estimates of recharge to Rose Valley were conducted using the distributed parameter watershed model (DPWM), independent of the calibrated groundwater flow model.
- The model grid was refined in the horizontal and vertical dimensions.



- The thickness of the recent alluvium and underlying Coso lakebed geologic units were adjusted within the model domain based on the available well logs.
- Model hydraulic properties and layering were adjusted to better match the observed water levels in Los Angeles Department of Water and Power (LADWP) wells between Hay Ranch and Haiwee Reservoir, and available information was examined to better understand the correlation of water levels and Haiwee Reservoir levels in this region.
- Model boundary conditions in the Little Lake area were adjusted to improve the simulation of physical processes in this region.
- The model was recalibrated to historical transient conditions accounting for seepage from Haiwee Reservoir, previous Hay Ranch and LADWP pumping for irrigation, and project pumping that occurred through September 2010.

The updated (current) Rose Valley model was used to reevaluate future Coso pumping amounts that may be implemented as part of the Hay Ranch Water Extraction and Delivery System project without exceeding a 10 percent reduction in groundwater outflow to Little Lake. The bases for the updated model, the model calibration results, sensitivity analyses, updated predictive simulation results, and conclusions and recommendations are provided in the remainder of this report. Applicable data and reports already in the record for CUP 2007-003 are not replicated in this report. This report focuses only on the updated analysis, interpretations, and model simulation results. Newly collected field data prior to and during the first year of project pumping are documented in a series of monthly and quarterly reports produced by TEAM Engineering and Management, Inc., collectively referred to as the TEAM reports.

2. Groundwater Model Updates

This section provides a summary of the most significant groundwater model updates and the data or reports on which the updates are based.



2.1 Recharge from Precipitation

Recharge from precipitation was estimated using the DPWM. The DPWM is a “bucket” type soil-water-balance model, which evaluates precipitation, evapotranspiration, and resultant percolation through the soil column on a basin-wide scale. The modeling approach includes some of the same methods applied in similar basin and range locations by the USGS (e.g., Flint and Flint, 2007). Although there are insufficient data to determine highly accurate or precise estimates of recharge to the Rose Valley aquifer, application of the DPWM allows for quantitative estimates based on site-specific climatological, geologic, soils, and vegetation factors.

Application of this recharge model and the results obtained for Rose Valley are discussed in detail in Appendix A. Within the model domain, a total mean annual recharge from precipitation of 4,455 acre-feet per year (ac-ft/yr) was estimated using DPWM. Of this total amount, about 68 percent occurs as mountain front recharge from the Sierra Nevada, about 21 percent occurs as mountain front recharge from the Coso Range, and about 11 percent occurs as recharge beneath drainages within the interior portions of Rose Valley.

The estimated recharge from precipitation determined during development of the current model is similar to that used in the previous model, which was 4,191 ac-ft/yr, although the geographic distribution is different. In the previous model, the entire amount of recharge from precipitation is assumed to be derived from the Sierra Nevada range, whereas the estimated recharge from the Sierra Nevada range in the current model is about 3,030 ac-ft/yr.

The calculated mean annual recharge is applied for each simulation period (steady-state, historical, and predictive) in the model. Although it is possible that cyclical drought and wet periods may lead to corresponding changes in water levels, such changes are not discernable based on the observed water level dataset for Rose Valley. Furthermore, the effects on water levels of variable amounts of recharge that may occur from year to year will tend to be muted as the recharge moves through the fractured rocks and shallow alluvium of the mountain fronts toward the basin-fill sediments of Rose Valley that constitute the primary aquifer system. Water levels in wells close to drainages that are sources of significant recharge may respond to specific periods of higher and lower recharge, although this recharge mechanism is calculated



to represent only 11 percent of the total mean annual value. The approach of applying mean annual recharge may warrant reconsideration in future work as additional data become available.

2.2 Geologic Unit Thickness

The geology of Rose Valley or portions of Rose Valley is discussed extensively by MHA Environmental Consulting (MHA, 2008a and 2008b) and other reports referenced therein, such as Bauer (2002), Schaer (1981), Duffield and Smith (1978), Rockwell International (1980), Stinson (1977), Power (1958), Duffield and Bacon (1981), GeoTrans, Inc. (2004), and Whitmarsh (1997a and 1997b). One of the comments made by the U.S. Geological Survey (USGS) on behalf of the Bureau of Land Management concerning the previous model was that “The model developed for the EIR simulated a much greater thickness of the permeable fanglomerate-gravel unit than reported in available well logs” (USGS, 2009). Based on our review of the available data and well logs, DBS&A concurs with this comment; the thickness of the fanglomerate-gravel unit was reevaluated for implementation in the current groundwater model. Note that the fanglomerate-gravel unit referred to by the USGS is called recent fanglomerate by Schaer (1981) and recent alluvium by Bauer (2002), who uses the term to collectively include recent fanglomerates and recent alluvial fan deposits. The term recent alluvium is applied herein, consistent with Bauer (2002).

Available well logs indicate that the recent alluvium is 300 to 400 feet thick in the Hay Ranch–Coso Junction area (base elevation of about 3,100 feet above mean sea level [feet msl]) and overlies lacustrine Coso lakebed sediments of the Coso Formation. Although the lakebed sediments contain a noticeably higher proportion of fine-grained sediments (i.e., silt and clay) than does the recent alluvium, the lakebed sediments also contain significant layers of fine to coarse sand. The geophysical logs for the HR1 and HR2 cluster wells are similar to one another and clearly intersect the same geologic section (SGSI, 2009). Although the lithologic log for these wells indicates an increase in clay, silt, and very fine sand content at about 200 and 270 feet below ground surface (bgs) in HR1 and HR2, respectively, the geophysical logs do not support the interpretation in SGSI (2009) that these depths represent the top of the Coso lakebed sediments. Rather, the geophysical logs indicate an abrupt contact at 335 and 364 feet bgs in HR1 and HR2, respectively, that probably reflects the top of the Coso lakebeds.



The geologic logs for the Hay Ranch supply wells indicate the presence of blue clay (often associated with lacustrine sediments) at about 330 to 340 feet bgs, which is consistent with the above interpretation for the HR1 and HR2 wells. A blue silt is reported at 247 to 280 feet bgs in the Hay Ranch North well (RV050), but information from nearby wells suggests that this depth likely does not represent the top of the Coso lakebeds.

The geophysical log for LADWP well T889, north of Hay Ranch (Figure 2), indicates that fine-grained sediments predominate below about 398 feet bgs and the log character is as would be expected for lakebed sediments. The well logs for well T889 and the HR1 and HR2 cluster wells do not exhibit obvious lateral correlations. Available well logs for the Coso Junction area indicate the presence of blue clay (interpreted to be the top of Coso lakebed sediments) between about 300 and 400 feet bgs. Farther to the south towards Red Hill and Little Lake, the recent alluvium contains layers of scoria and basalt, but the wells (which are generally shallower than those in the north) do not appear to intersect the Coso lakebeds.

Figure 3 is a contour map of the current model layer 1 base elevation, with pertinent well data posted. In the central Rose Valley area, model layer 1 represents the thickness of recent alluvium. In the southern Rose Valley area, model layer 1 represents the recent alluvium and associated shallow layers and intrusions of igneous rocks. In northern Rose Valley, model layer 1 represents the narrow alluvial channel from Haiwee Dam south to the general vicinity of LADWP well 816 (RV020, Figure 2) called “the narrows” (Bauer, 2002). This region is discussed in detail in the following section. In the northern portion of Rose Valley west of the alluvial channel just described and west of South Haiwee Reservoir, model layer 1 represents the Dunmovin Hill debris flows discussed by Bauer (2002).

2.3 Haiwee Reservoir Seepage and Northern Rose Valley Water Levels

To support DBS&A’s investigation of the available data for Haiwee Reservoir and the potential causes of the observed water levels at wells in northern Rose Valley, LADWP, through the Inyo County Water Department, provided data on Haiwee Reservoir stage and toe-drain flows. The annual reported toe-drain flows are plotted in Figure 4a. From reservoir construction through the early 1990s, toe-drain discharge has generally been declining. Since the early 1990s, toe-



drain discharge has been steady or rising, although discharge values are not nearly as high as those observed in the early decades of Haiwee Reservoir operation (Figure 4a).

Figure 4b is a plot of monthly toe-drain discharge values versus South Haiwee Reservoir stage. The figure illustrates that there is a general positive correspondence between toe-drain discharge and stage (i.e., when the reservoir stage increases, the toe-drain discharge increases). Linear regression of the raw monthly data for the period 1992 through 2009 leads to a correlation coefficient of about 0.5, which is not particularly high, but is statistically significant at the 95 percent level. Review of the data sheets obtained from LADWP indicates that a significant change in the volume of flow from drain number 5 occurred between 2005 and 2006 (the volume of flow increases significantly for this drain beginning in 2006). Linear regression of the data broken out for two periods of time (1992 through 2005 and 2006 through 2009) produces higher correlation coefficients of 0.72 and 0.74 for the periods 1992 through 2005 and 2006 through 2009, respectively.

Review of aerial photographs and the Haiwee Reservoirs and Coso Junction 7.5-minute topographic maps indicated that the toe-drain discharge flows along an (apparently) unlined ditch that follows the east side of the approximately 1,000-foot-wide gap south of the Haiwee Dam known as the narrows (Bauer, 2002). Mr. Robert Harrington of the Inyo County Water Department visited the accessible part of the area on July 30, 2010 and noted water flow in the ditch terminating only several hundred yards north of LADWP well 816. There are several LADWP wells within the narrows (Figure 5). Furthermore, based on the well depths of about 200 feet and the cross section C–C' in Stinson (1977) (reproduced in part in Figure 5), it appears that the alluvial material south of Haiwee Reservoir is limited both horizontally and vertically by igneous rocks that likely have lower hydraulic conductivity than the adjacent alluvium. Bauer (2002) reports through personal communication with LADWP geologist L.A. Jackson in March 1999 that thickness of alluvial fill in the narrows portion of Haiwee Gorge is believed to be in the range of 150 to 200 feet.

Figure 6a is a plot of monthly Haiwee stage values versus the observed water level in well VS360, which is close to the toe of Haiwee Dam (Figure 5). The figure illustrates a direct correspondence between reservoir stage and water level in the well, confirmed by the linear regression presented in Figure 6b, which has a correlation coefficient of 0.84.



A similar analysis was conducted for LADWP well 816, approximately 1 mile south of Haiwee Dam (Figure 5). Initial analysis indicated a poor correspondence of water levels with reservoir stage; however, when the observed water levels are lagged by 3 months relative to the reservoir stage, a significant correlation emerges (Figure 7).

Previous reports (e.g., MHA, 2008a, Appendix C1) have noted an apparent lack of correspondence between water levels in Rose Valley and Haiwee Reservoir stage. The analysis provided above, however, indicates that there is a discernible correspondence at least as far south as LADWP well 816, and possibly as far as the Cal Pumice well RV030 (analysis not shown). All of the regression analyses presented above are statistically significant at the 95 percent level. LADWP well 816 is too far away from Haiwee Reservoir for changes in reservoir stage to influence water levels within a 3-month period through direct seepage from the reservoir. Rather, it appears that the link between reservoir stage and observed water levels is through the toe-drain flows that flow south along the alluvial channel and recharge the local groundwater system. Because well VS360 is shallow and very close to the toe drains, the effects of changing stage and drain flows are observed very quickly. LADWP well 816, however, is farther from the ditch and is likely deeper than well VS360 (no well log is available). It appears to take about 3 months for the effects of changes in drain flow infiltration to be observed at LADWP well 816.

2.4 Historical Hay Ranch and LADWP Pumping

Historical pumping for irrigation was implemented in the model for Hay Ranch and LADWP for the periods 1972 through 1985 and 1983 through 1985, respectively. The periods of pumping were determined through a series of LANDSAT images provided in Appendix B. Figure 8 is an example LANDSAT image for June 17, 1985 illustrating the irrigated region at Hay Ranch and the LADWP circular field to the north. Although the earliest LANDSAT images available are from 1972, the completion dates of the Hay Ranch north production well of March 18, 1971 is consistent with a 1971 or 1972 irrigation start date. The Hay Ranch south production well was completed on February 14, 1974; so evidently the first two to three years of irrigation was conducted using the Hay Ranch north well only. Because the historical distribution of pumping between the north and south wells is unknown, the assumption was made that each well pumped an equal volume of water.



The historical pumping amounts were estimated based on the estimated pumping for Rose Valley Ranch (Hay Ranch) of about 3,130 ac-ft/yr reported by Rockwell International (1980). Of this amount, Rockwell International (1980) estimated that about 30 percent of the extracted water returns to the aquifer as return flow, or water that is pumped and applied to the fields, but is not consumptively used. The amount of groundwater extraction estimated by Rockwell International (1980) equates to an application rate of about 10 ac-ft/yr per acre, of which 7 ac-ft/yr per acre would be consumptively used based on 30 percent return flow. In the current model, historical groundwater extraction from Hay Ranch is about 2,430 ac-ft/yr for the period 1972 through 1973, and about 3,220 ac-ft/yr for the period 1974 through 1985, reflecting an increase in the observed irrigated acreage after the first two years—from 243 acres to 322 acres as measured from the images provided in Appendix B. Return flows of 30 percent of the pumping values are assigned to model layer 1 beneath the irrigated field.

Pumping for irrigation of the LADWP circular field north of Hay Ranch was initially estimated based on the same consumptive use estimated for Hay Ranch irrigated acreage, but using a smaller return flow percentage (10 percent) more representative of center pivot irrigation systems, which are typically more efficient than other types of irrigation methods. The initial pumping estimates had to be scaled back, however, to avoid dewatering the aquifer in the historical simulations at LADWP well 816, the assumed source of pumping. The final pumping applied in the model for the three-year irrigation period is 450 ac-ft/yr, with an assumed return flow of 50 ac-ft/yr, or about 11 percent.

2.5 Model Grid

The model grid was refined in the horizontal dimension so that model cells in the current model are 660 feet on a side ($\frac{1}{8}$ mile), as opposed to 2,640 feet ($\frac{1}{2}$ mile) used in the previous model. This refinement was primarily to allow better resolution in the vicinity of Hay Ranch, where two series of new multi-level observation wells were constructed. The finer model grid also allowed better resolution for the implementation of hydrogeologic features (fault and alluvial channel) between Hay Ranch and Haiwee Reservoir. The current model grid is presented in Figure 9.

In the vertical dimension, the current model has 5 model layers, as opposed to 4 model layers used in the previous model. In the current model, the first model layer (layer 1) represents the



recent alluvium and laterally contiguous shallow sediments and rocks (i.e., igneous rocks to the south in the vicinity of Red Hill and Little Lake, and debris flow deposits of Dunmavin Hill and the shallow alluvium of the narrows in the north). Model layers 2, 3, and 4 represent the Coso lakebed deposits, and model layer 5 represents the Coso sand. Model layers 2 and 3 are each 150 feet thick. These layers were incorporated into the model so that in the Hay Ranch area, each multi-level observation well would be represented by a separate model layer. The top of model layer 2 is the same as the base of model layer 1 (Figure 3). Model layer 4 begins at the base of model layer 3, and represents the remainder of the thickness of the Coso lakebed unit. The base of the Coso lakebed unit (base of model layer 4) is the same as that used in the previous model. The thickness of the Coso sand unit (model layer 5) is also the same as that used in the previous model; however, the top and bottom elevations of this layer were shifted upward by 5 to 1,700 feet to avoid the construct in the previous model where the top of the model layer in the central portion of Rose Valley was set at an elevation below the base of adjacent cells. This adjustment has no effect on model calibration, but is more physically realistic.

3. Model Calibration

This section provides an overview of the general approach to model calibration, model calibration results, and the results of model sensitivity analysis. The current model consists of three simulation periods. The first simulation period is intended to be representative of quasi-steady-state conditions in Rose Valley prior to the construction and filling of Haiwee Reservoir in 1915. There are no observed data to which the model can be calibrated for this period; therefore, the purpose of the steady-state simulation is to provide initial hydraulic head values that are consistent with estimated recharge from precipitation and aquifer properties assigned in the model.

The second simulation period is the historical transient period from 1915 through 2010. This simulation period incorporates estimated hydrologic effects of Haiwee Reservoir and historical groundwater pumping at Hay Ranch and north of Hay Ranch by LADWP (Section 3.4), as well as recent project pumping by Coso. The ultimate goal of the historical model calibration period was to implement these historical occurrences within the groundwater modeling framework so



as to reasonably match observed historical water levels that are available only fairly recently. Observed data from the MMRP through September 14, 2010 were used in the model calibration. The third period is the predictive simulation period from December 25, 2009 through December 2044. The predictive simulation results are discussed in Section 5.

3.1 Approach to Model Calibration

The general approach to model calibration was that initial calibration runs were conducted using a manual trial and error approach. Once reasonable simulation results were achieved using this approach, the model input parameters were refined using inverse modeling (PEST) (Doherty, 2004). The first and second simulation periods were run sequentially during the model calibration process. The output hydraulic heads obtained from the first simulation period were used as the initial heads for the second simulation period. A number of model constructs were calibrated prior to achieving the current model; the process started with simple alterations of the previous model, such as inclusion of the updated recharge estimate.

The hydraulic conductivities of different zones, the conductances of the general head boundaries and the drains, specific storage, and specific yield were calibrated initially using the manual trial and error approach and then later refined using PEST. Mean recharge obtained from the DPWM was not adjusted during model calibration. There are no calibration targets available for the first (steady-state) simulation period. Available water level data from 25 wells were used to calibrate the second (historical transient) simulation period. The locations of the calibration targets are shown in Figure 2. The simulated groundwater discharge to Little Lake was used as a semiquantitative calibration target.

3.2 Boundary Conditions

The simulated recharge from precipitation applied in the current model is illustrated in Figure 10. As shown in Figure 10, the majority of the recharge occurs as mountain-front recharge along the basin margins, and a lesser amount of recharge (11 percent of the total) occurs along drainages within Rose Valley. The inter-drainage recharge as simulated using DPWM is negligible. The recharge is applied in the model to the topmost active (non-dry cell) layer. Throughout most of the model domain, the uppermost active model layer is layer 1; however, on the basin margins,



the uppermost active model layer is either model layer 2 or 3. The recharge indicated in Figure 10 is applied throughout the historical and predictive simulation periods.

Figure 11 illustrates boundary conditions other than recharge from precipitation applied to model layer 1 for the historical calibration. In the northern portion of the model domain, these conditions include prescribed hydraulic head at South Haiwee Reservoir, prescribed recharge along the narrows, and prescribed recharge from irrigation return flow at Hay Ranch and the LADWP irrigated field. Prescribed hydraulic head at Haiwee Reservoir is 3,730 feet, which is the average value for the period 1992 through 2009 (the period of data provided by LADWP).

The prescribed recharge from Haiwee Reservoir drain flows was set to 25 percent of the observed flow from 1915 through 1970, and 50 percent of the observed flows after 1970. The 50 percent value, or even a higher value, may be more realistic, but prescribing 50 percent of observed flows as recharge in the designated area led to simulated water levels above land surface at some locations during the earlier simulation periods, thereby requiring the reduction in assumed recharge percentage. Additional investigation and analysis in the Haiwee Reservoir area would lead to better estimates of the fate of the drain flow water.

Return flow from irrigated agriculture is assumed to be 30 percent of the pumping value for the Hay Ranch and 11 percent of the pumping value for the LADWP field.

In the southern portion of the model domain in the Little Lake area, drain cells are used to represent groundwater outflow to Little Lake, general head boundary cells are used to simulate subsurface groundwater outflow south of Little Lake, and evapotranspiration (ET) cells are used to simulate ET from vegetation adjacent to Little Lake. For the ET cells, an extinction depth of 15 feet was applied, and the maximum vegetation ET rate is 28 inches per year (in/yr) (MHA, 2008a; Danskin, 1998).

For the drain cells, the prescribed drain elevation was 3,144 feet msl, the approximate bottom elevation of the lake. The drain cell conductance of 8,710 square feet per day (ft²/d) was determined through model calibration. Conceptually, the simulated volume of groundwater that discharges to Little Lake at the drain cells is either evaporated from the lake surface or flows out of Rose Valley as surface water outflow from the lake. The estimated evaporation from Little



Lake is about 500 ac-ft/yr assuming a 75-acre lake surface and an annual evaporation rate of 80 in/yr (Bauer, 2002). Bauer (2002) also estimates a surface water outflow volume of 771 ac-ft/yr, and a groundwater inflow component to Little Lake of 1,233 ac-ft/yr. More recent data available in the TEAM monitoring reports indicate that the annual 2010 surface water outflow from Little Lake is about 200 ac-ft/yr (Rainville, 2010).

For model layer 2, the uppermost 150 feet of Coso lakebed sediments, the only boundary condition applied is a general head boundary south of Little Lake (Figure 12). This boundary condition allows for groundwater outflow. The prescribed hydraulic head associated with the general head boundary is 3,130 feet, and the conductance for each boundary cell is 26,400 ft²/d; both values were taken from the previous model. In addition, on the edges of Rose Valley, where model layer 1 cells are dry, simulated recharge is applied to model layer 2.

Figure 13 illustrates the boundary conditions for model layers 4 and 5, which represent the majority of the Coso lakebed thickness (layer 4) and the underlying Coso Sand (layer 5). Other than the adjustments to the top of the Coso lakebed elevation and top of Coso sand discussed previously, these layers were for the most part unchanged from the previous model. The only boundary condition prescribed for these deep layers is a general head boundary along the southeastern portion of the model domain. This boundary allows a fairly small outflow of water from the deeper sediments of Rose Valley to Indian Wells Valley. The conductance of these boundary cells is 18.2 ft²/d and the assigned head is 2,820 feet; both values were taken from the previous model.

Note that, as in the previous model, the extent of active grid cells for model layers 4 and 5 (and layer 3, not shown) do not extend south to Little Lake (Figure 13). Consequently, all groundwater outflow from these deeper layers either occurs through the southeastern general head boundaries or through upward leakage to model layer 2. Also, there is no prescribed recharge or hydraulic head condition for the deeper model layers, with the exception of a small amount of recharge to layer 3 where the overlying model cells in layers 1 and 2 are dry. Therefore, the water that occurs in these model layers must flow downward from surface recharge or mountain front recharge assigned to model layers 1 or 2. In the previous model, a prescribed head boundary was used along the northern model boundary for all model layers. This approach was not followed due to the uncertainty of prescribing this type of condition



through time and with depth. Similarly, prescribed flux and general head type boundary conditions were also rejected due to the uncertainty in hydrogeologic conditions and aquifer properties along and north of the northern model boundary. With regard to groundwater that flows from the Owens Valley groundwater system to the vicinity of Owens Lake (dry), Danskin (1998, p. 59) states:

The bulk of the ground water probably flows vertically upward and is discharged through evaporation from the dry lake. Minor quantities of water may flow at depth through the fractured bedrock beneath the Haiwee Reservoir to Rose Valley. . . .

In the current model, the approach is taken that aquifer water levels in the vicinity of the northern boundary are primarily a function of the presence of Haiwee Reservoir, and the inclusion of Haiwee Reservoir in the model as a prescribed head boundary (Figure 11) is sufficient for the purposes of assessing the future effects of Coso pumping. Some comments provided regarding the previous model discuss potential groundwater inflow to the Rose Valley at depth; however, available data to estimate such a recharge component, if one exists, are virtually non-existent. Consequently, incorporation of a significant amount of deep recharge to Rose Valley from the north (e.g., through the Coso sand) would be too speculative for inclusion in the current model.

3.3 Initial Conditions

The initial conditions for the transient simulation are taken from the results of the steady-state simulation. In the steady-state simulation, recharge from Haiwee Reservoir and Haiwee Dam toe-drain flows is zero, and the simulated water level in the narrows and the immediately adjacent region is below the base of model layer 1. Consequently this region of model cells is inactive in the steady-state simulation. The alluvium in the narrows is saturated, however, as indicated by water levels in LADWP wells (Section 2.3). In order to “activate” the model layer 1 cells in this region for the transient model calibration, the estimated water level in the narrows was read into the model as initial conditions. This approach leads to some simulation inaccuracy early in the transient simulation.



3.4 Hydraulic Properties

The aquifer properties used in the current model are presented in the following three subsections. The aquifer properties were determined through model calibration and through consideration of available aquifer test data and aquifer material characteristics based on well logs.

3.4.1 Hydraulic Conductivity

Figure 14 illustrates the assigned horizontal and vertical hydraulic conductivity values in the model for model layer 1. The central portion of Rose Valley in the Hay Ranch and adjoining areas has a model layer 1 (recent alluvium) horizontal and vertical hydraulic conductivity of 105 and 7 feet per day (ft/d), respectively. The correspondence of these values with Hay Ranch aquifer test data is discussed in Section 3.4.3. The southern portion of Rose Valley has a model layer 1 (recent alluvium and interbedded igneous rocks) horizontal and vertical hydraulic conductivity of 75 and 10 ft/d, respectively.

One goal of the model calibration was to eliminate, if possible, the zone of high horizontal hydraulic conductivity of 200 ft/d used in the southwestern portion of Rose Valley in the previous model. This magnitude of hydraulic conductivity seemed too high based on existing aquifer test data and well logs. As indicated in Figure 14, this goal was achieved in the current model. The previous model also had a zone of low hydraulic conductivity (1 ft/d) to represent the Red Hill area and associated volcanic rocks. This zone was considered in the current model, but was not required to achieve an accurate model calibration; it was therefore removed.

In the northern Rose Valley area, the largest zone of horizontal and vertical hydraulic conductivity of 3 and 0.03 ft/d, respectively, represents the surficial portion of the Dunmovin Hill debris flow. This region, as in the previous model, has relatively low hydraulic conductivity relative to the recent alluvium in Rose Valley, possibly representative of the poorly sorted sediments. The adjacent light green zone of horizontal and vertical hydraulic conductivity of 1 and 0.01 ft/d, respectively, represents the fractured volcanic rocks adjacent to Haiwee Reservoir and the narrows. The red zone in Figure 14 with horizontal and vertical hydraulic conductivity of 0.1 and 0.001 ft/d, respectively, represents the igneous rocks below Haiwee



Reservoir; most of the cells in this zone are prescribed hydraulic head (Figure 11); therefore, this zone has limited influence on simulation results.

The zone of yellow cells in Figure 14 with horizontal and vertical hydraulic conductivity of 10 and 0.1 ft/d, respectively, represents the model layer 1 alluvium in the narrows. The horizontal hydraulic conductivity of 10 ft/d is consistent with the aquifer test conducted at LADWP well 817 (LADWP, 2009) at the south end of this zone (Figure 2). The aquifer test consisted of pumping LADWP well 817 at about 824 gpm for 6.5 days. Water levels were measured in a number of wells during the test, but only the observed drawdown in LADWP well 816, 197 feet west of LADWP well 817, was used to determine aquifer properties (LADWP, 2009). Based on a screened interval of 200 feet for LADWP well 817, the average hydraulic conductivity obtained from several analytical solutions applied to evaluate the aquifer properties from the drawdown data was about 7 ft/d.

Adjacent to and south of the narrows, there is a linear zone of low hydraulic conductivity oriented slightly northwest to southeast. This model layer 1 zone represents a fault identified by Stinson (1977) immediately adjacent to LADWP well 816 (Figure 5). This zone was required during the model calibration to better replicate the high observed water levels (relative to other wells to the south) observed at LADWP well 816. The LADWP well 817 aquifer test report (LADWP, 2009) does not note the presence of a fault or low-permeability boundary based on the test data. It is possible that a longer test might delineate the boundary response, that the fault could be at a slightly offset location from that identified by Stinson (1977), or that the change in water levels may be attributable to other, unknown hydrogeologic features. The low-permeability fault feature is continued in the model into layers 2 and 3 only.

The hydraulic conductivity for model layer 2 is presented in Figure 15. Throughout central and southern Rose Valley, model layer 2 represents the first 150-foot section of the Coso lakebed sediments. Most of this layer has a horizontal and vertical hydraulic conductivity of 4.65 and 0.057 ft/d, respectively. The conceptualization that this layer has lower hydraulic conductivity than layer 1 is consistent with the Hay Ranch production well logs. In the far southern portion of Rose Valley, where igneous rocks are prevalent and interspersed with the alluvium and lakebed sediments, this layer has hydraulic conductivity the same as layer 1. In the northern portion of Rose Valley, the horizontal and vertical hydraulic conductivity values of 0.1 and 0.001 ft/d are



small, consistent with the previous model. This zone of low hydraulic conductivity in the north is continued downward through model layers 3, 4, and 5.

The hydraulic conductivity for model layers 3, 4, and 5 are illustrated in Figures 16, 17, and 18, respectively. The horizontal and vertical hydraulic conductivity across most of Rose Valley for model layers 3 (second 150-foot section of lakebed sediments) and 5 (Coso sand) are significant but small (i.e., 1 to 3 ft/d). Model layer 4, which represents the greatest thickness of Coso lakebed sediments, has low horizontal and vertical hydraulic conductivity values of 0.25 and 0.002 ft/d, respectively (Figure 17).

3.4.2 Storage Coefficient

A specific yield of 0.1 (10 percent) was used throughout the model domain except for the thin channel of alluvium in the narrows (the yellow cells in Figure 14), where a value of 0.25 was applied. The value of 0.1 best matched observed water levels in model layer 1 throughout the majority of Rose Valley, while the value of 0.25 led to a better match with observed historical water levels in the narrows.

For the confined portions of the Rose Valley aquifer system, a specific storage of 1×10^{-7} feet⁻¹ was applied based on model calibration. This value is approximately 10 times lower than that determined from the Hay Ranch aquifer test analysis (MHA, 2008a, Appendix C1), but is believed to be appropriate as the observed storage coefficient determined from that test reflects a combination of confined and unconfined conditions.

3.4.3 Comparison to Hay Ranch Aquifer Test Results

One of the conditions of the model calibration was to maintain consistency with the observed hydraulic properties obtained from the most recent Hay Ranch South well 14-day aquifer test conducted in November and December 2007 (MHA, 2008a, Appendix C1). Analysis of the results from this test determined the estimated aquifer transmissivity to be 14,750 ft²/d and the estimated vertical hydraulic conductivity to be 0.01 ft/d.

In the model, the Hay Ranch production well screened intervals occur primarily in model layers 1 through 3. The model aquifer transmissivity is therefore determined through the



summed transmissivity for each of these layers. The combined transmissivity for the Hay Ranch area is approximately 16,600 ft²/d, determined as follows:

- Layer 1 transmissivity: 150 feet saturated thickness x 105 ft/d = 15,750 ft²/d
- Layer 2 transmissivity: 150 feet saturated thickness x 4.65 ft/d ~ 700 ft²/d
- Layer 3 transmissivity: 150 feet saturated thickness x 1 ft/d = 150 ft²/d

Approximately the bottom 100 feet of the Hay Ranch production wells occurs in the top of model layer 4, which has low transmissivity due to the low horizontal hydraulic conductivity of 0.1 ft/d. The model transmissivity for the Hay Ranch area is therefore about 12 percent higher than that estimated from the aquifer test data, which is reasonably close agreement.

The vertical hydraulic conductivity applied in the model can be compared to that estimated from the aquifer test by taking the harmonic mean of the vertical hydraulic conductivity values for model layers 1 through 3, which is 0.017 ft/d, nearly the same as the value of 0.01 determined through analysis of the aquifer test data.

3.5 Simulation Results

The primary method of model calibration was the comparison of simulated hydrographs with observed water levels at 24 observation wells. The simulation results for each of the 24 wells are provided in Appendix C. Some of the calibration locations are described in detail below.

Figure 19 shows the simulated and observed water levels in the vicinity of Hay Ranch for the two shallow cluster wells, RV060 and RV080. At these locations the observed drawdown in model layer 1 is simulated quite well. The simulated rise in water levels from the beginning of the simulation through the early 1970s is from increased recharge from Haiwee Reservoir, while the following drawdown and subsequent recovery is due to the initiation and subsequent cessation of Hay Ranch pumping for irrigated agriculture (Section 2.4). Review of the Hay Ranch production well hydrographs (RV050, North well and RV070, South well) illustrates that the simulated trends in water level recovery from historical pumping are reasonably replicated at these locations, where a longer history of water level observations is available.



Figure 20 also illustrates the simulated and observed water levels for wells RV060 and RV080, but the time axis is for the period 2000 through 2012, and the vertical axis is likewise expanded to provide a more detailed illustration of observed and simulated values. In addition, the simulated water levels are shifted downward in each plot as noted so that a more direct comparison of simulated and observed drawdown can be made. As indicated Figure 20, the simulated drawdown trends are similar; however, as of September 30, 2010 the simulated drawdown at well RV060 is about 0.5 foot greater than the observed value and the simulated drawdown at well RV080 is about 0.2 foot greater than the observed value.

As noted above, the cluster well hydrographs provided in Figures 19 and 20 are for the shallow wells. At each cluster well location, there are two additional deeper wells. These deeper monitor wells are RV061 and RV062 for the north (HR1) cluster well location, and RV081 and RV082 for the south (HR2) cluster well location. At the deeper monitor wells, the simulated drawdown due to Coso pumping is underestimated by a significant amount at each location. A variety of model adjustments were considered in an effort to better match the observed drawdown at these wells, but the final model calibration described in this report is the best that could be achieved taking into account all water level observations and observed aquifer property data.

Figure 21 shows the simulated and observed water levels in the vicinity of Coso Junction at wells RV090 and RV100. The general shape of these hydrographs is similar to that described for the Hay Ranch area, although the simulated historical rises and declines are less pronounced because of the greater distance between these wells and Hay Ranch and Haiwee Reservoir. The historical trend in rising water levels is well replicated in the groundwater model. At each location the apparent initial decline in observed water levels due to Coso pumping is also reasonably simulated.

Figure 22 also illustrates the simulated and observed water levels for wells RV090 and RV100 with axis scales similarly expanded as for the Hay Ranch area wells. In Figure 22, the simulated water levels are shifted upward in each plot as noted so that a more direct comparison of simulated and observed drawdown can be made. As indicated in Figure 22, the simulated drawdown trends are similar, with the final amount of simulated drawdown very close to the observed values. Simulated drawdown at well RV090 is slightly greater than the



observed value, while the simulated drawdown at well RV100 is slightly less than the observed value.

Figure 23 shows the simulated and observed water levels south of Coso Junction at wells RV140 and RV150. The general shape of these hydrographs also mimics that described for the Hay Ranch and Coso Junction areas, although the simulated historical rises and declines are highly subdued relative to the other observation wells discussed. This is because of the even greater distance of these wells from Hay Ranch and Haiwee Reservoir. The historical trend in rising water levels is also well replicated in the groundwater model at these locations. Consistent with the previous hydrographs discussed, more detailed plots for the recent period for wells RV140 and RV150 are provided in Figure 24. The simulated water levels in Figure 24 are not shifted as was done in Figures 20 and 22 because drawdown due to Coso pumping is not yet evident.

In addition to the hydrographs, the historical period model calibration was also evaluated using cross plots of simulated versus observed water levels for December 2009 (prior to the effects of Coso pumping) and September 2010. The results of these comparisons are provided in Figure 25. In Figure 25, the closer the symbols are to the 1:1 line, the more accurate the simulation at that location. In other words, if the model simulated the observed water levels perfectly at each location, the symbols would all fall on the 1:1 line. As indicated in the figure, the simulated water levels are overall in good agreement with the observed water levels, and there is no apparent bias in the calibration results (i.e., the simulated water levels are not consistently higher or lower than the observed water levels).

Also provided in Figure 25 are the calculated mean error (ME) and the root mean squared error (RMSE) for the time periods shown. The ME is the average of the calculated differences (residuals) between the observed and simulated water levels, while the RMSE is the square root of the mean squared residuals. The ME is small for both time periods shown, indicating that on average the difference between simulated and observed heads across the model domain is 0.32 foot for December 2009 and -2.04 feet for September 2010. The fact that the ME for both periods is small indicates that, on average, the simulated water levels are greater than observed water levels by about the same amount that they are lower than observed water levels (i.e., the simulation results are not biased high or low). The ME is higher (and negative) for September



2010 primarily because the model underestimates drawdown in the deeper HR1 and HR2 cluster wells.

The RMSE is 8.42 feet for December 2009 and 11.31 feet for September 2010. The RMSE is always positive because the residuals are squared in the calculation. A common rule of thumb for model calibration is that the RMSE divided by the range in observed water levels across the model domain should be less than 10 percent. This measure is 1.6 percent for December 2009 and 2.2 percent for September 2010, respectively, far below the 10 percent criterion.

The simulated water table as of December 2009 is presented in Figure 26. Note that this map is a composite of the upper three model layers, as there are dry cells (simulated water table is below the base of the cell) along the margins of Rose Valley.

The simulated mass balances for the steady-state simulation and the transient simulation as of December 2009 are provided in Table 1. As indicated in the table, the mass balance error in the simulation is very small, as the total simulated inflows and outflows are nearly identical.

3.6 Sensitivity Analysis

Model sensitivity analysis was conducted for two of the model input parameters that have the greatest effects on simulated changes in water levels—hydraulic conductivity of model layer 1 and specific yield. For hydraulic conductivity, the calibrated values for the three main zones used in model layer 1 were adjusted upward and downward in a successive series of simulations to evaluate the resulting effects on model calibration. The northern zone is the zone of low hydraulic conductivity (3 ft/d) that represents the Dunmovin Hill debris flows. The central zone represents the Hay Ranch and adjoining areas in the central portion of Rose Valley (calibrated hydraulic conductivity of 105 ft/d). The southern Rose Valley zone has a calibrated hydraulic conductivity of 75 ft/d (Figure 14).

Figure 27a illustrates the results of the hydraulic conductivity sensitivity analysis. On the figure, the x-axis value of 100 percent represents the calibrated model value, while other values represent percent increases or decreases relative to the calibrated value. The y-axis of the graph represents the RMSE of each simulation at the end of 2009.



Several observations can be made from Figure 27a. First, the calibrated values of hydraulic conductivity for each zone lead to the best model calibration (i.e., lowest RMSE), with the one exception that the hydraulic conductivity of the northern zone could be reduced by 25 percent and an equally good calibration in terms of RMSE would be obtained. Second, simulation results are most sensitive to changes in the hydraulic conductivity of the southern zone, as indicated by the greatest change in the RMSE.

Sensitivity analysis was also conducted for specific yield, the calibrated value of which is 0.1 except in the narrow alluvial channel that extends south from Haiwee Reservoir. For the sensitivity analysis, the specific yield was increased to 0.2 and decreased to 0.05 for all regions except the alluvial channel noted above. The resulting effects of the changes in specific yield are presented in terms of the simulated water level at well RV080, the HR2 shallow cluster well (Figure 27b). As would be expected, the higher specific yield of 0.2 leads to less simulated drawdown relative to the calibrated model, while the lower specific yield of 0.05 leads to greater simulated drawdown. At well RV080 and overall throughout the model domain, the specific yield of 0.1 used in the calibrated model provides the best correspondence with observed conditions. At some locations, changes in specific yield (higher or lower) could have been applied to marginally improve the historical model calibration, but zones of specific yield were not applied in the model (with the limited exception noted previously) because the potential improvement in model calibration was insufficient to justify the increased number of input parameter zones.

4. Predictive Simulation Results

The updated (current) Rose Valley model was used to reevaluate future Coso pumping amounts that may be implemented as part of the Hay Ranch Water Extraction and Delivery System project without exceeding a 10 percent reduction in groundwater outflow to Little Lake. Simulated reduction in outflow was calculated as a percent reduction from simulated 2009 conditions prior to the initiation of project pumping.

Several methods were considered to evaluate the permit condition that groundwater outflow to Little Lake cannot be decreased at any point in time by more than 10 percent. The method used in the previous evaluation where simulated drawdown at the Little Lake North Dock Well



could not exceed 0.3 foot was considered and rejected. This approach was not favored because (1) the Little Lake North Dock well is in very close proximity to Little Lake, and observed water levels in the well are nearly the same as those in the lake, and (2) the approach of looking at the water level in a single well is not necessarily equivalent to the determination of a reduction in groundwater outflow. The latter point is true because changes in the groundwater flow to Little Lake are dependent upon the vertical and horizontal hydraulic gradient in the vicinity of the lake. The simulated drawdown at a single shallow well may not adequately encompass important changes in both the horizontal and vertical groundwater flow components at the lake.

Two alternative methods of evaluation were considered. The first was evaluation of the change in groundwater flux across model row 107, which is the row that passes immediately south of the Little Lake North well (RV180) location. The idea behind this approach was that any reduction in the amount of groundwater flow crossing this line would represent an equivalent decline in available groundwater resources and outflows in the Little Lake Ranch area, including Little Lake itself. The second approach considered was to evaluate the reduction in simulated outflow to Little Lake based on the simulated efflux at the drain cells used to represent groundwater outflow to Little Lake in the model. This approach is most conceptually appropriate, as groundwater discharge to surface water bodies is not necessarily directly proportional to a reduction in groundwater flow across the entire aquifer thickness at an upstream location. The predictive simulation results described below were evaluated based on each of these approaches, and the drain flow evaluation approach was found to be most conservative (i.e., less pumping led to a 10 percent reduction in drain flow than that which led to a 10 percent reduction in groundwater flow at the Little Lake Ranch North well). The simulation results presented below are based on consideration of the simulated outflow to Little Lake at the drain cells.

Simulated outflow from the ET cells was not considered directly in the predictive simulations because this is a small component of the water budget in the current model. However, in the final predictive scenarios, the maximum reduction in simulated ET is about 8 percent.

The results of three predictive simulations are provided; each simulation includes 3,000 acre-feet (ac-ft) of Coso pumping for the year 2010. The initial year of Coso pumping actually began



on December 25, 2009, and was assumed to be completed as of December 25, 2010. For the final portion of December 2010, 3,000 ac-ft/yr of Coso pumping was also assumed. Pumping for the latter portion of the year (October through December) had to be assumed because the model was being calibrated and updated, and the project schedule could not be met if metered data through the end of the year were incorporated.

The purpose of the three predictive simulation scenarios, designated as A, B and C, are outlined below.

- *Scenario A:* Designed to determine how much water Coso can pump at a continuous annual rate of withdrawal for the remaining 29-year period of the permit and not exceed a 10 percent decline in groundwater flows to Little Lake.
- *Scenario B:* Designed to determine for what length of time Coso can continue to pump 3,000 ac-ft/yr (the 2010 amount) and not exceed a 10 percent decline in groundwater flows to Little Lake.
- *Scenario C:* Designed to determine for what length of time Coso can continue to pump 4,839 ac-ft/yr (the full permit amount) and not exceed a 10 percent decline in groundwater flows to Little Lake.

As in the previous model, maximum hydrologic effects can occur at a time subsequent to the cessation of pumping in each scenario. The results of the three predictive simulation scenarios in terms of simulated drawdown at trigger wells identified in the MMRP are summarized in Table 2. Note that for the HR1 and HR2 cluster wells, drawdown triggers are only provided for the shallowest well at each location (RV060 for the north location and RV080 for the south location). Despite considerable effort expended during the model update and recalibration, the simulated drawdown at the deeper observation wells (i.e., RV061, RV062, RV081, and RV082) does not match observed drawdown sufficiently close to justify using the current model to develop triggers for these wells (Appendix C).

For predictive Scenario A, the simulation results indicate that Coso can pump 790 ac-ft/yr for the next 29 years without exceeding the Little Lake depletion criterion. In this scenario, the



simulated reduction in groundwater flow to Little Lake is 9.8 percent at about 4 years after pumping stops.

For predictive Scenario B, the simulation results indicate that Coso can pump 3,000 ac-ft/yr for the next 4 years and 6 months without exceeding the Little Lake depletion criterion. In this scenario, the simulated reduction in groundwater flow to Little Lake is 9.9 percent at about 8 years and 8 months after pumping stops.

For predictive Scenario C, the simulation results indicate that Coso can pump 4,839 ac-ft/yr for the next 2 years and 8 months without exceeding the Little Lake depletion criterion. In this scenario, the simulated reduction in groundwater flow to Little Lake is 9.7 percent at about 9 years and 2 months after pumping stops.

The simulated change in water levels from December 2009 conditions is plotted in Figures 28, 29, and 30 for predictive scenarios A, B, and C, respectively, for the time that simulated groundwater outflow to Little Lake is at a minimum. For each scenario, the maximum simulated drawdown at Little Lake is less than 1 foot. Also in each scenario, the simulated drawdown in the northern portion of the model domain is a complex composite caused by Coso pumping and a reduction in assumed recharge in the narrows from Haiwee toe-drain flows. The applied recharge in this region for 2009 was 964 ac-ft/yr, while the assumed future recharge is about 563 ac-ft/yr, the average of conditions over the last two decades.

5. Conclusions and Recommendations

The predictive simulations conducted using the updated groundwater flow model indicate that Coso can pump 790 ac-ft/yr for the next 29 years, 3,000 ac-ft/yr for the next 4 years and 6 months, or 4,839 ac-ft/yr (the full permit amount) for the next 2 years and 8 months without exceeding a 10 percent reduction in groundwater flows to Little Lake. These time frames are provided relative to the date January 1, 2011.

Although the current groundwater flow model is a significant update from the previous model, there are still numerous assumptions and uncertainties incorporated in the model that may affect the predictive simulation results. The ability of the model to simulate hydrologic effects



between the Hay Ranch and Little Lake areas can be further validated based on continued monitoring of Rose Valley water levels and comparison of the predictive simulation results (updated for actual metered pumping) to the observed water level responses. DBS&A recommends that such a comparison be conducted annually. Based on the comparison, DBS&A recommends that Inyo County personnel decide whether or not there is a need to develop another updated version of the groundwater model that better simulates observed conditions. Improvement in the predictive capability of the updated models, if any are required, will depend largely on the increased period of water level record available for model calibration. Therefore, the following model updating schedule is recommended, assuming that the existing model does not sufficiently replicate future observed drawdown:

- 5 years for the case where Coso is permitted to continue pumping for the long term (29 years)
- 2 years for the case where Coso is permitted to continue pumping 3,000 ac-ft/yr
- 1 year for the case where Coso is permitted to pump the full permit amount of 4,839 ac-ft/yr

Other predictive scenarios can be examined using the model if required, but the alternative scenarios presented in Section 4 likely provide a sufficient range of results on which to base permit conditions.



References

- Bauer, C.M. 2002. *The hydrogeology of Rose Valley and Little Lake Ranch, Inyo County, California*. M.S. thesis, California State University, Bakersfield. April 2002.
- Brown and Caldwell. 2006. *Rose Valley groundwater model, Coso Operating Company, LLC, Rose Valley, California*. Prepared for Coso Operating Company, LLC, Coso Junction, California. Brown and Caldwell Project Number 129778.001. April 10, 2006.
- Danskin, W.R. 1998. *Evaluation of the hydrologic system and selected water-management alternatives in the Owens Valley, California*. U.S. Geological Survey Water-Supply Paper 2370, Chapter H.
- Doherty, J. 2004. *PEST: Model-independent parameter estimation, User manual: 5th edition*. Watermark Numerical Computing.
- Duffield, W.A. and C.R. Bacon. 1981. *Geologic map of the Coso volcanic field and adjacent areas, Inyo County, California*. U.S. Geological Survey Miscellaneous Investigation Series, Map I-1200.
- Duffield, W.A. and G.I. Smith. 1978. Pleistocene river erosion and intracanyon lava flows near Little Lake, Inyo County, California. In *California Geology* (April 1978).
- Flint, A. and L. Flint. 2007. *Application of the basin characterization model to estimate in-place recharge and runoff potential in the Basin and Range carbonate-rock aquifer system, White Pine County, Nevada, and adjacent areas in Nevada and Utah*. U.S. Geological Survey Scientific Investigations Report 2007-5099.
- GeoTrans, Inc. 2004. *Revised hydrogeologic conceptual model for the Rose Valley, Coso Operating Company, LLC*. Prepared for Coso Operating Company, LLC, Little Lake, California. June 30, 2004.



Los Angeles Department of Water and Power (LADWP). 2009. *Pumping test of well V817 in Rose Valley*. September 2, 2009.

MHA Environmental Consulting (MHA). 2008a. *Coso Operating Company Hay Ranch water extraction and delivery system, Conditional use permit (CUP 2007-003) application, SCH# 2007101002, Draft EIR, Inyo County, California*. Prepared for Inyo County Planning Department, Independence, California. July 2008.

MHA. 2008b. *Coso Operating Company Hay Ranch water extraction and delivery system, Conditional use permit (CUP 2007-003) application, SCH# 2007101002, Final EIR, Inyo County, California*. Prepared for Inyo County Planning Department, Independence, California. December 2008.

Power, W.R. 1958. *Preliminary report on the geology and uranium deposits of Haiwee Ridge, Inyo County, California*. U.S. Atomic Energy Commission Technical Information Service, Salt Lake City, Utah. RME-2066. March 1958.

Rainville, K. 2010. E-mail communication between Keith Rainville, TEAM Engineering and Management Inc., and Neil Blandford, Daniel B. Stephens & Associates, Inc. December 6, 2010

Rockwell International, 1980. *Project: Geology and hydrology technical report on the Coso geothermal study area, In support of: Coso geothermal development environmental statement*. Prepared for the U.S. Bureau of Land Management, Bakersfield, California. Contract No. YA-512-CT8-216. April 1980.

Schaer, D.W. 1981. *A geologic summary of the Owens Valley Drilling Project, Owens and Rose Valleys, Inyo County, California*. Prepared for U.S. Department of Energy, Grand Junction, Colorado. Contract No. DE-AC13-76GJ01664. Bendix Field Engineering Corporation. March 1981.

Sierra Geotechnical Services Inc. (SGSI). 2009. *Summary of well construction operations, [Groundwater monitoring wells HR1A, HR1B, HR1C, HR2A, HR2B, and HR2C], Coso*



Operating Company Hay Ranch property, Rose Valley, Inyo County, California. Prepared for Coso Operating Company, LLC, Inyokern, California. July 11, 2009.

Stinson, M.C. 1977. *Geology of the Haiwee Reservoir 15' quadrangle, Inyo County, California.*

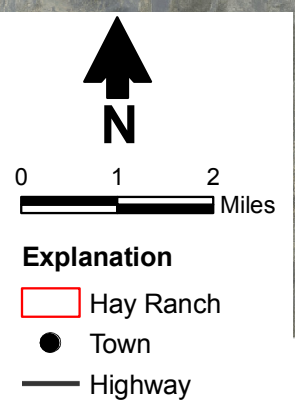
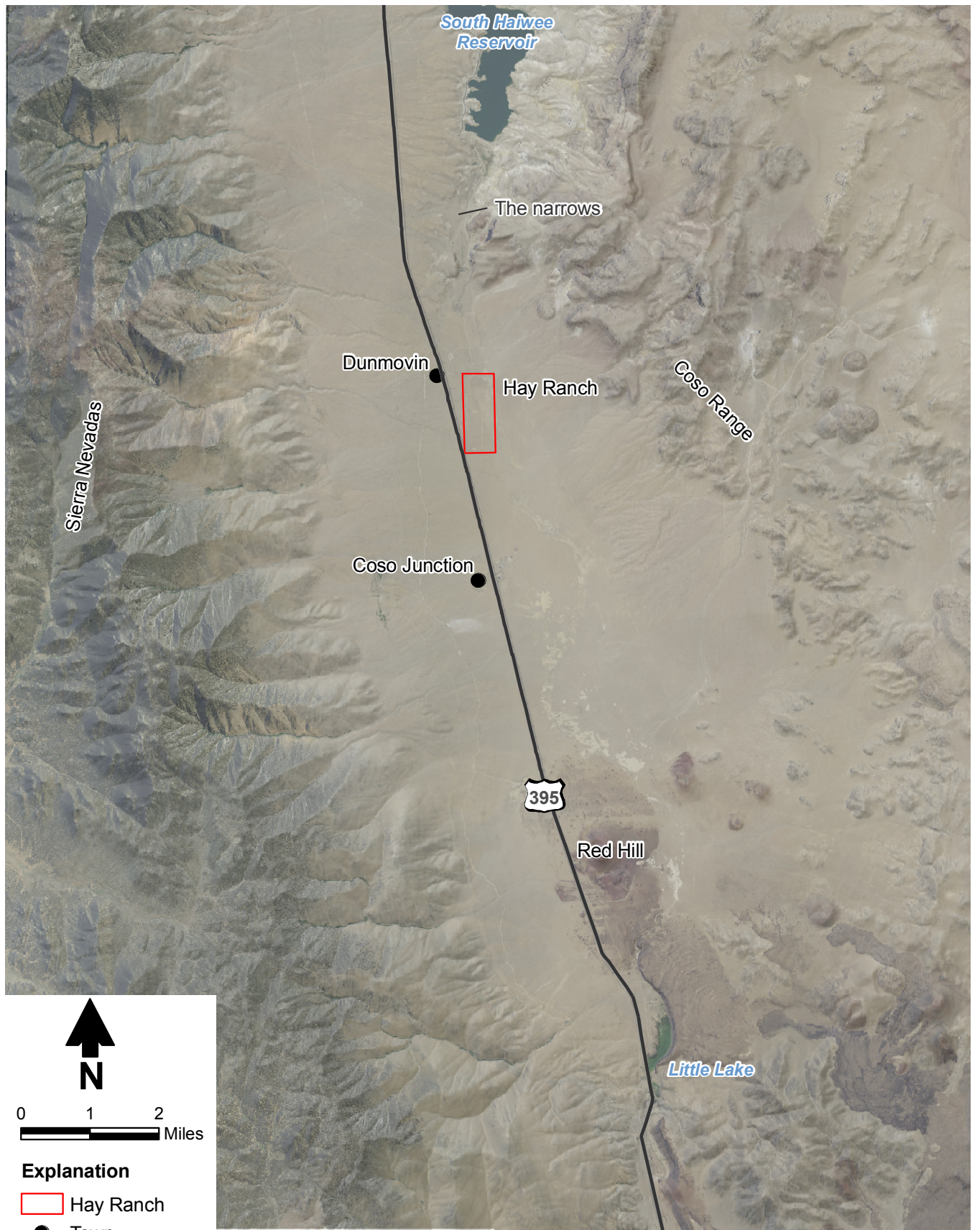
U.S. Geological Survey (USGS). 2009. *Comments on Environmental assessment for the Coso Operating Company Hay Ranch Water Extraction and Delivery System, CA, Bureau of Land Management, December 2008.* Transmitted by letter from James F. Devine to Steve Borchard, Bureau of Land Management, regarding Environmental assessment, Coso Operating Company Hay Ranch Water Extraction and Delivery System Project, CA, December 2008. June 4, 2009.

Whitmarsh, R.S. 1997a. *Geologic map of the Coso Junction 7.5' quadrangle, Inyo County, California.* Scale 1:24,000.

Whitmarsh, R.S. 1997b. *Geologic map of the Little Lake 7.5' quadrangle, Inyo County, California.* Scale 1:24,000.

Figures

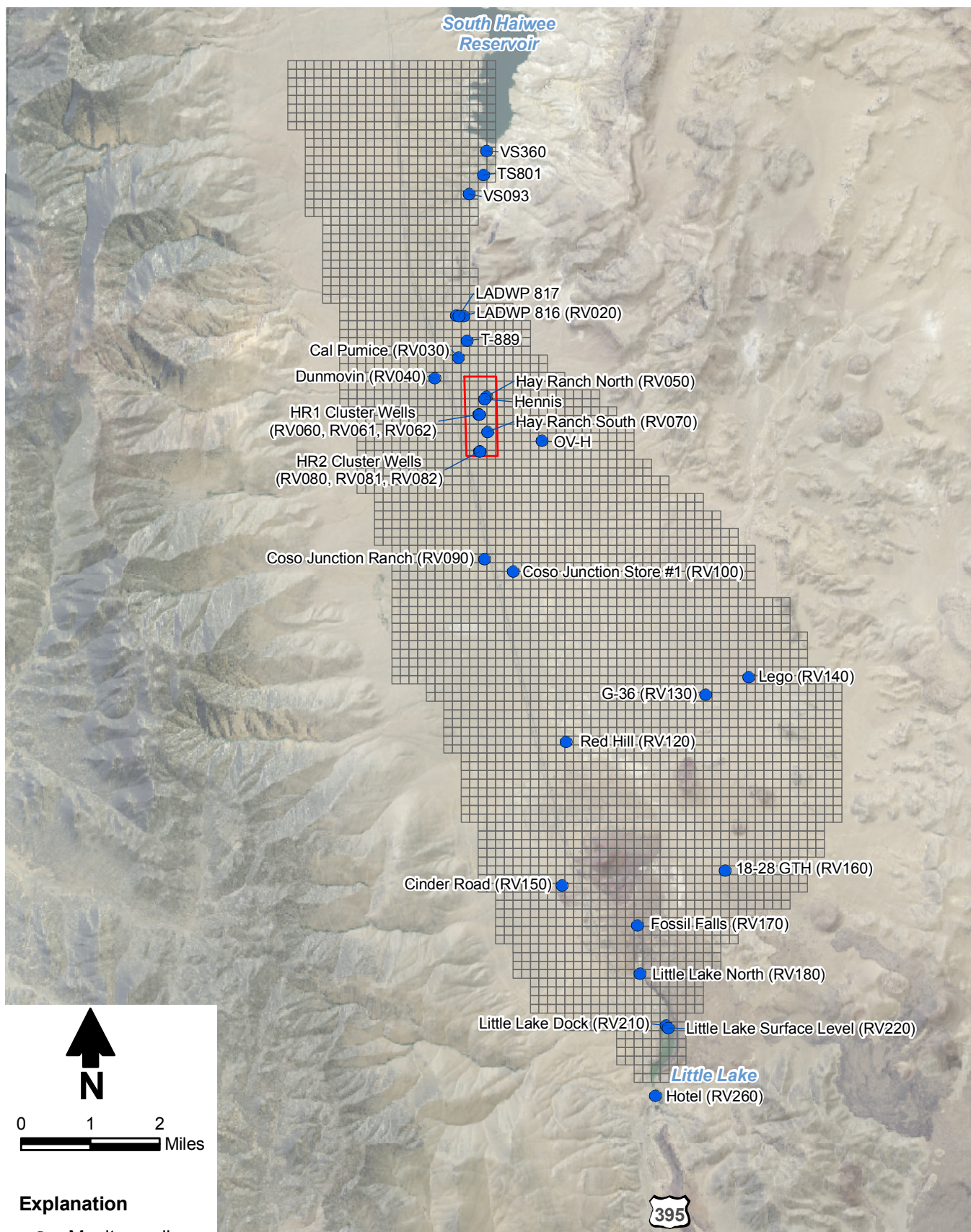
Q:\PROJECTS\LT09.0311_ROSE_VALLEY_MODEL\GIS\MXDS\FIGURES\FIGURE01_BASE_MAP.MXD 112/1



Daniel B. Stephens & Associates, Inc.
1/27/2011 JN LT09.0311

ROSE VALLEY MODEL
Base Map

Figure 1



Explanation

- Monitor well
- Active model cell (layer 1)

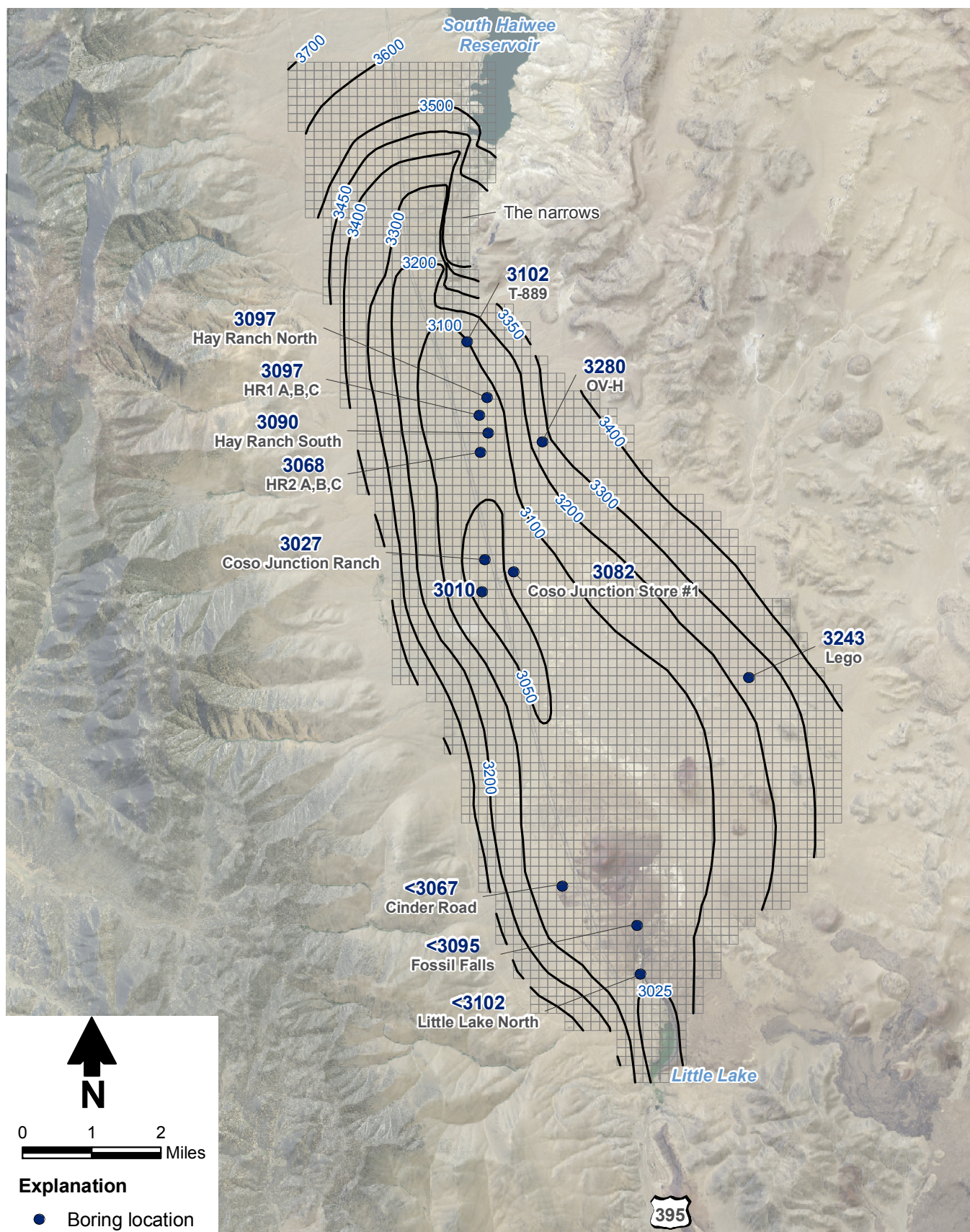


Daniel B. Stephens & Associates, Inc.
1/10/2011 JN LT09.0311

**ROSE VALLEY MODEL
Well Locations**

Figure 2

Q:\PROJECTS\LT09.0311_ROSE_VALLEY_MODEL\GIS\MXDS\FIGURES\FIGURE03_BASE_MODEL_LAYER1.MXD



Explanation

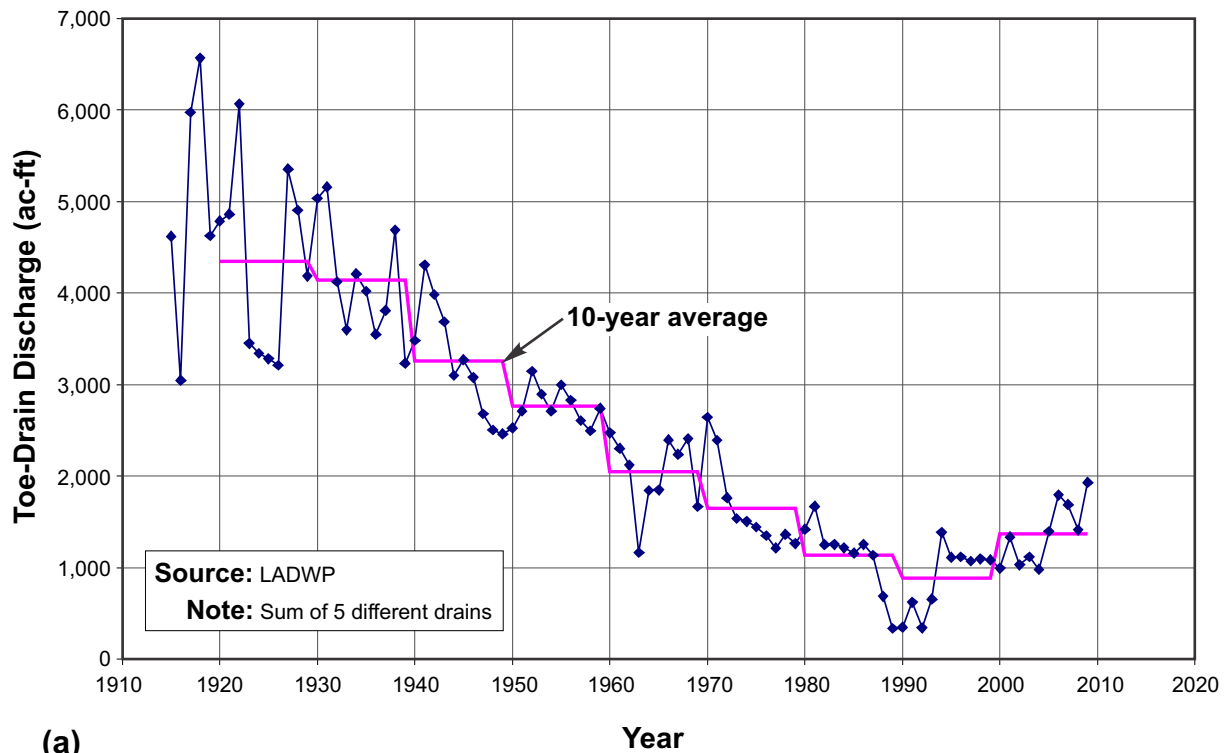
- Boring location
- Elevation of base of model layer 1 (ft msl)
- Active model cell (layer 1)



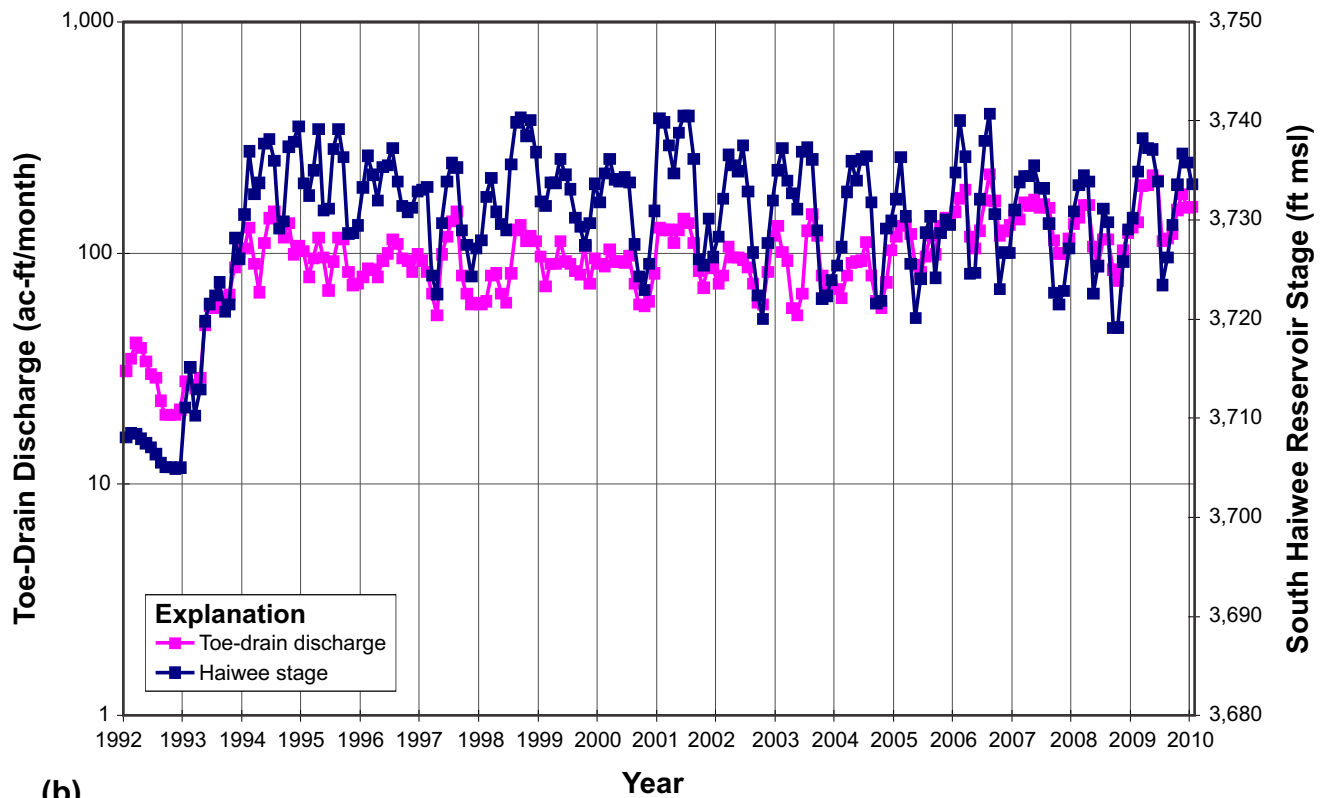
Daniel B. Stephens & Associates, Inc.
1/27/2011 JN LT09.0311

ROSE VALLEY MODEL
Base of Model Layer 1

Figure 3



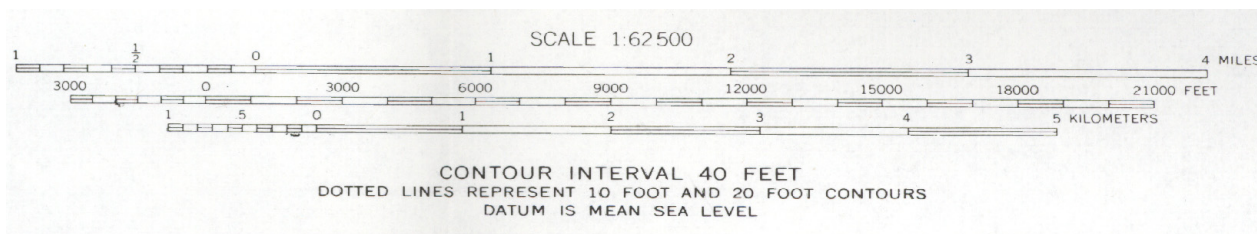
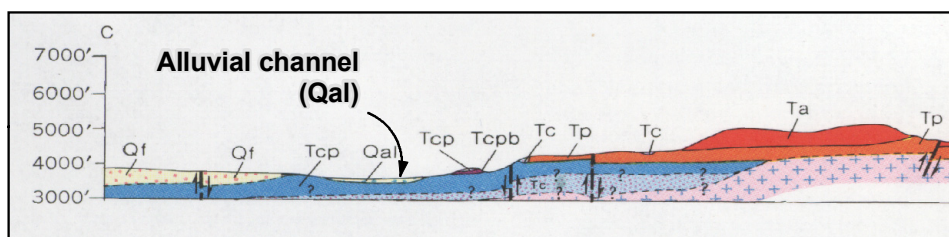
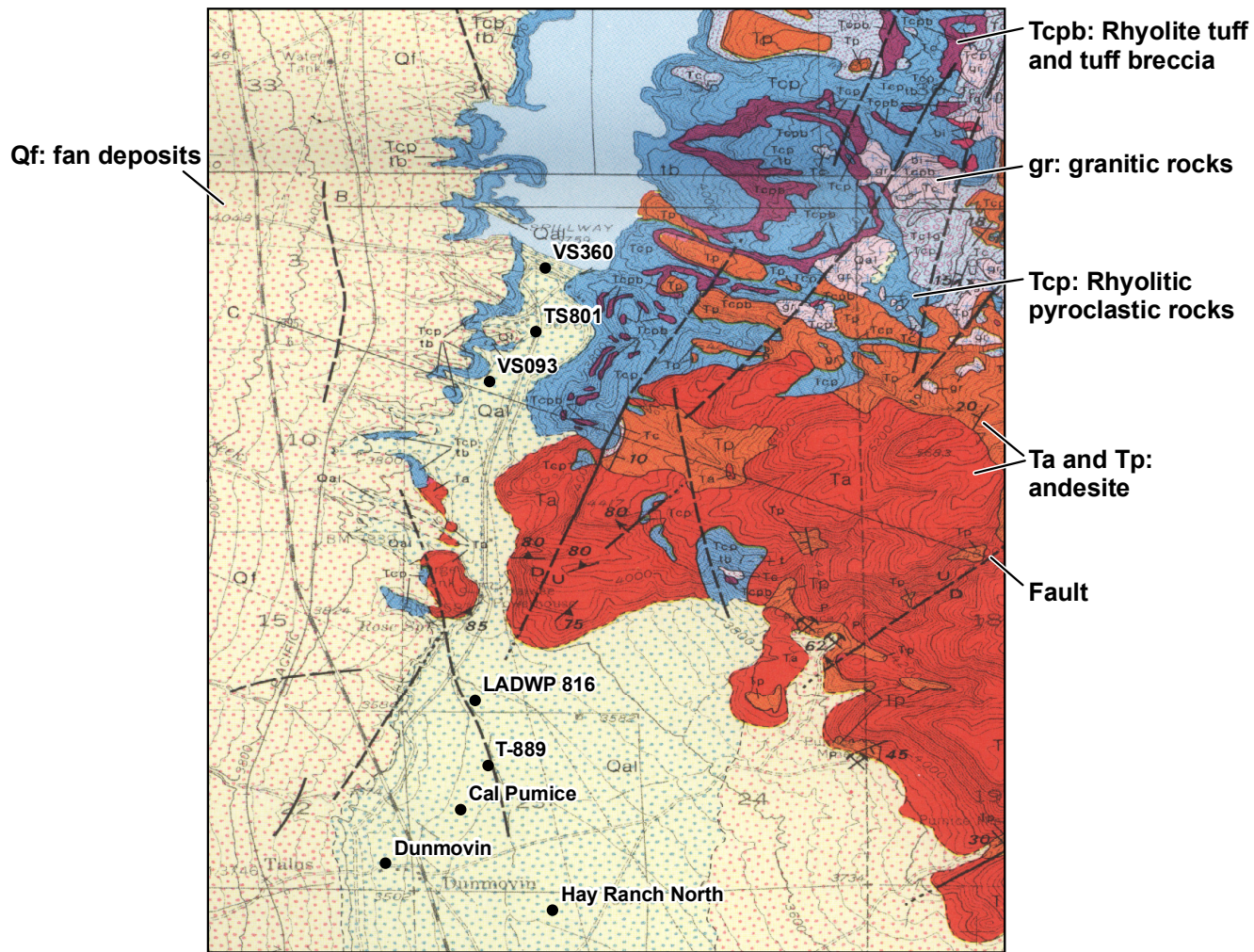
(a)



(b)

ROSE VALLEY MODEL
**Haiwee Reservoir Toe-Drain
 Discharge and Correspondence of
 Toe-Drain Discharge and Reservoir Stage**



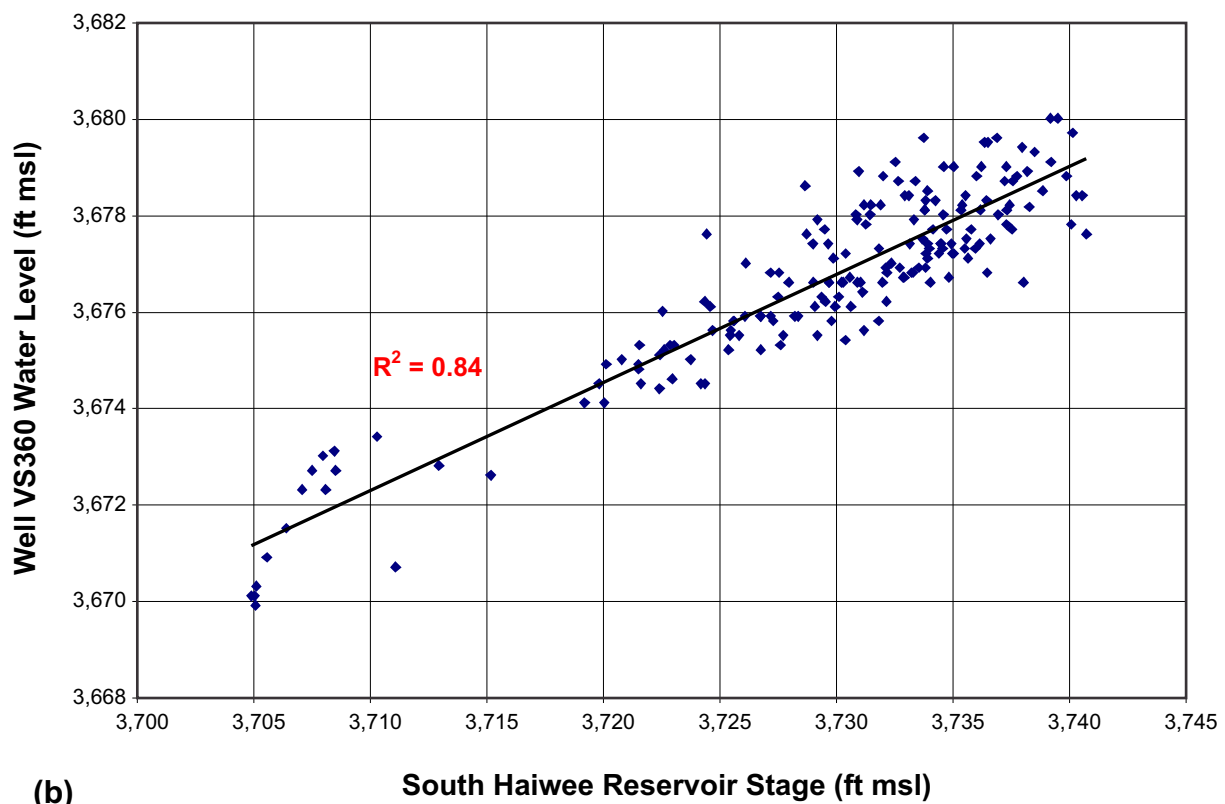
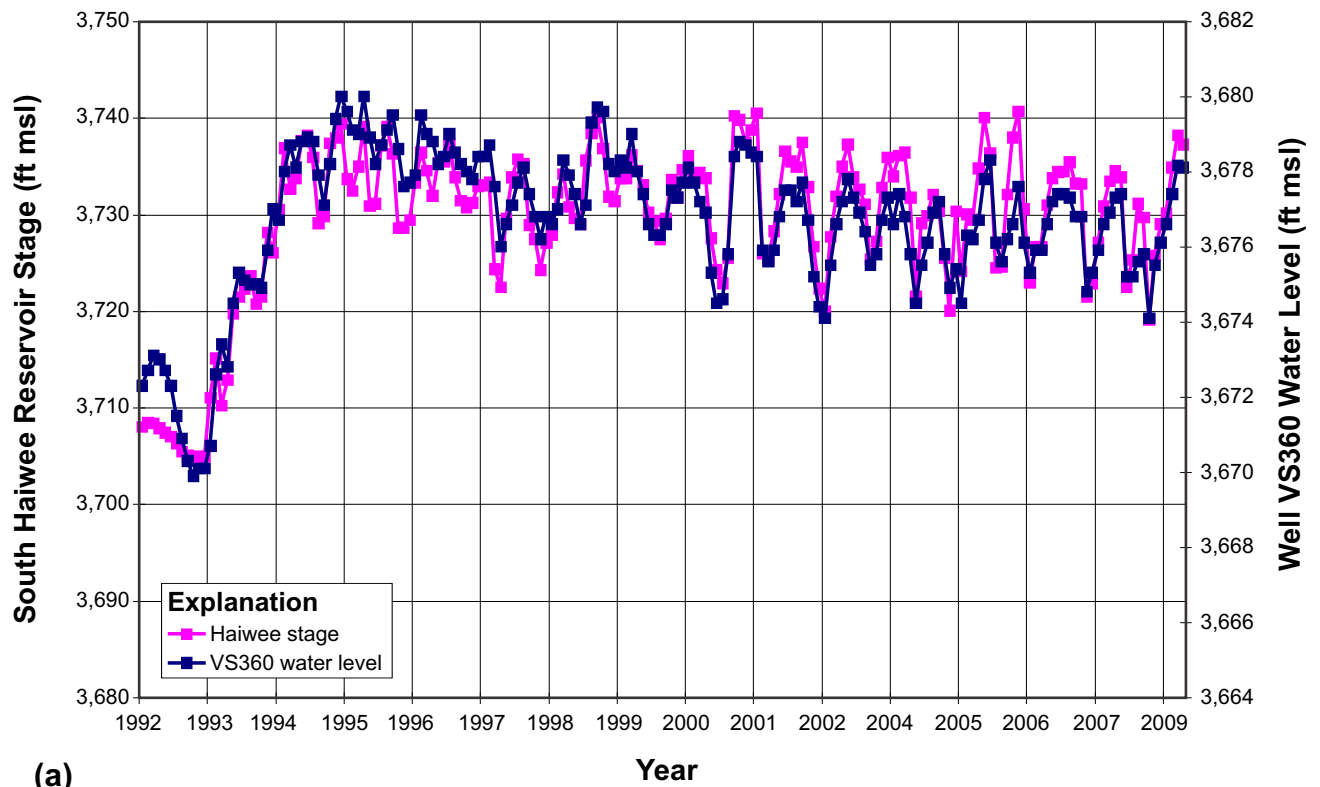


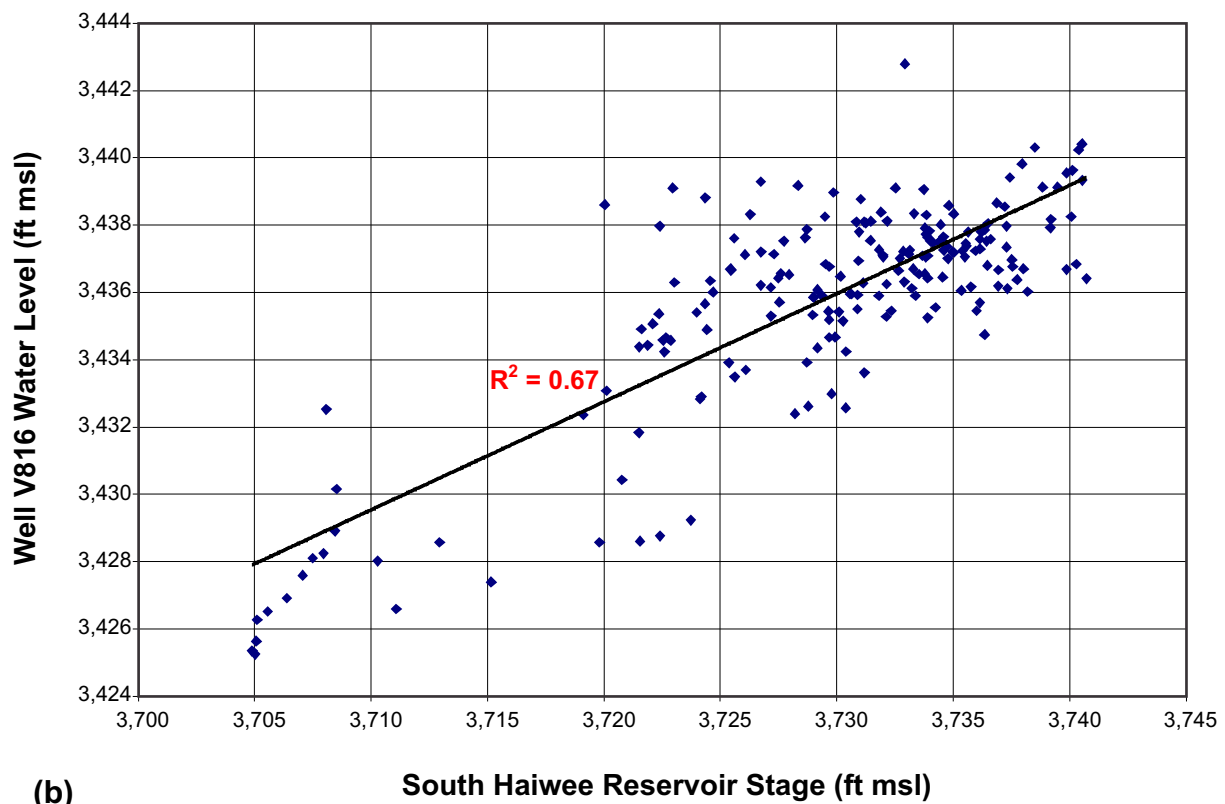
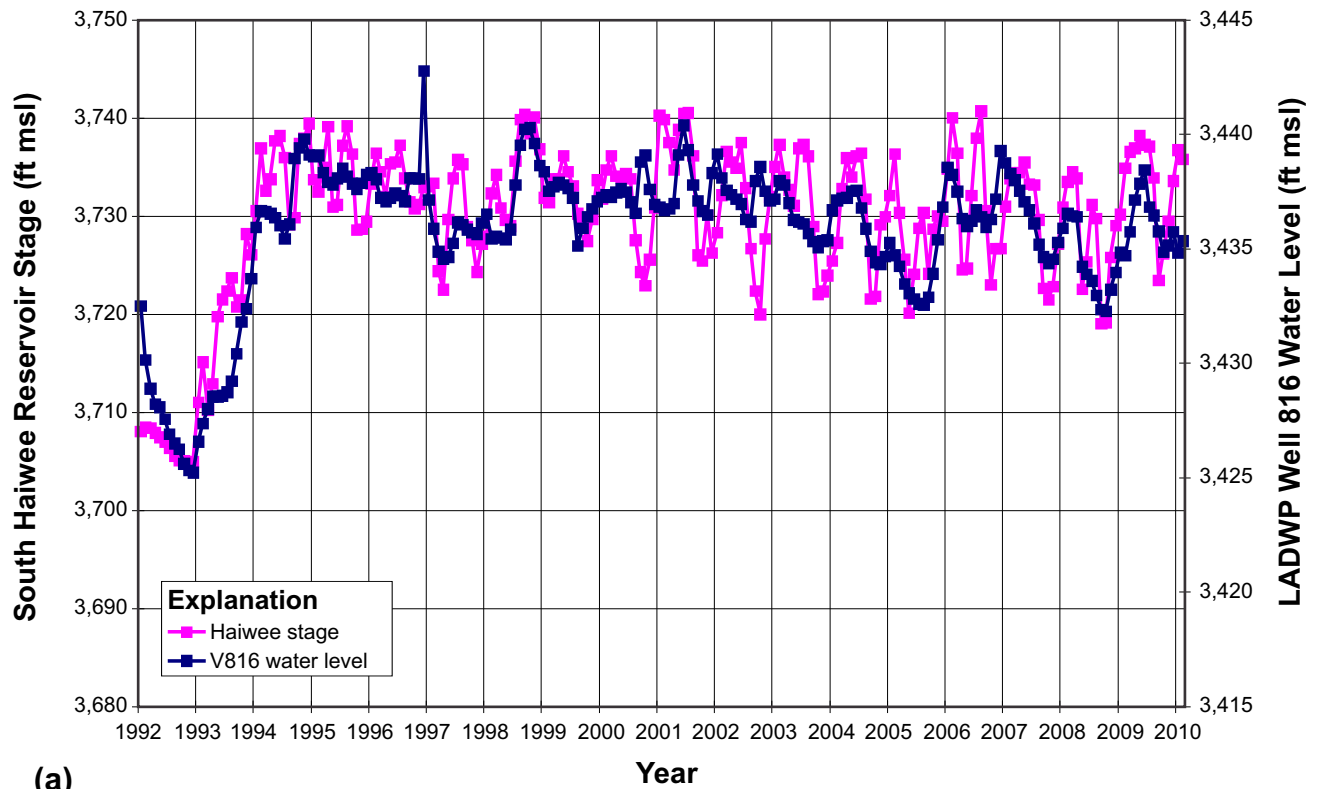
Source: Geologic map and cross section from Stinson (1977)

ROSE VALLEY MODEL Geology and Wells South of Haiwee Reservoir



Daniel B. Stephens & Associates, Inc.
1/24/2011 JN LT09.0311

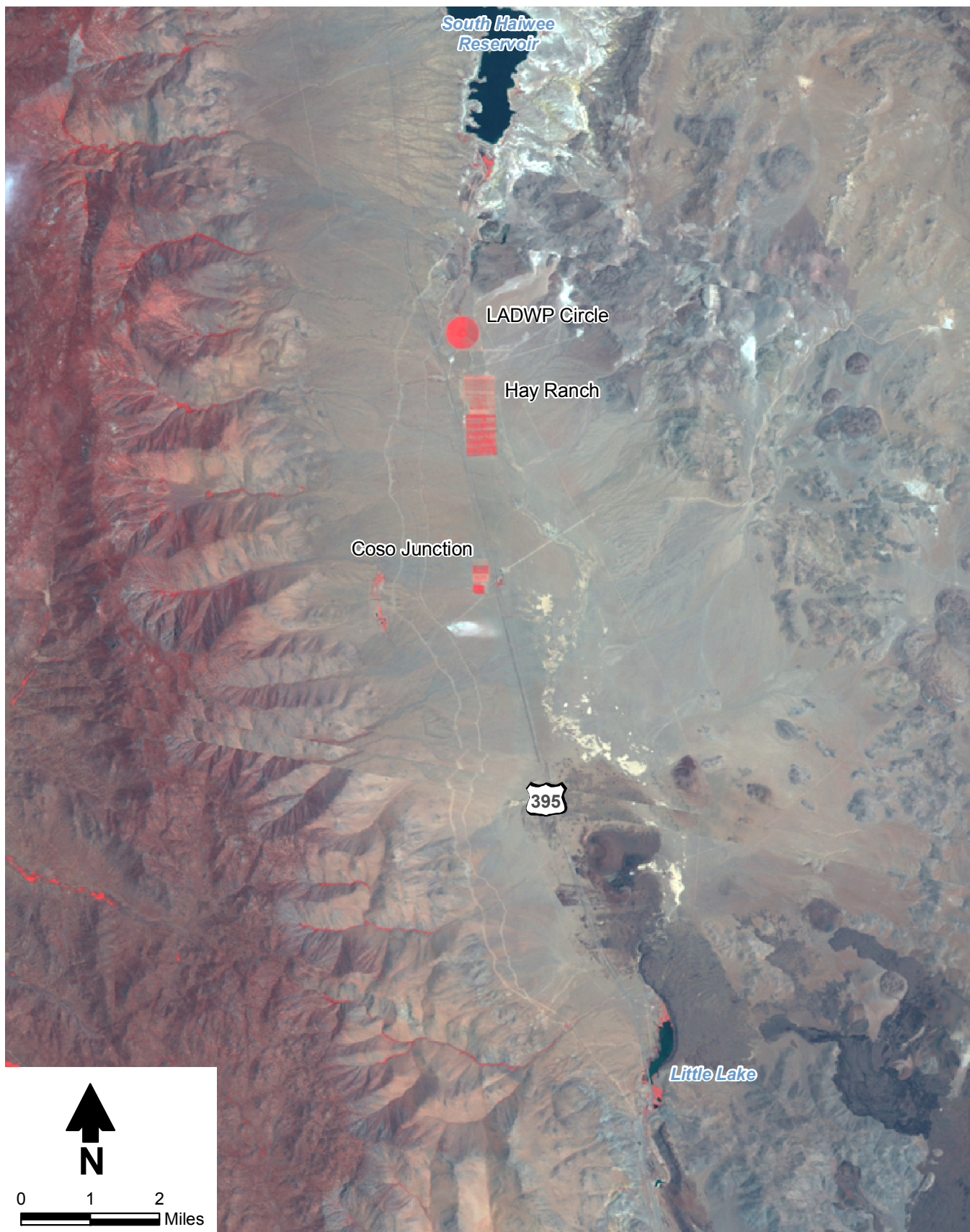




ROSE VALLEY MODEL
**Correspondence of
 LADWP Well 816 Water Levels and
 Haiwee Reservoir Stage, 3-Month Lag**



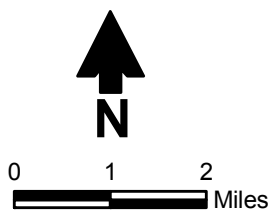
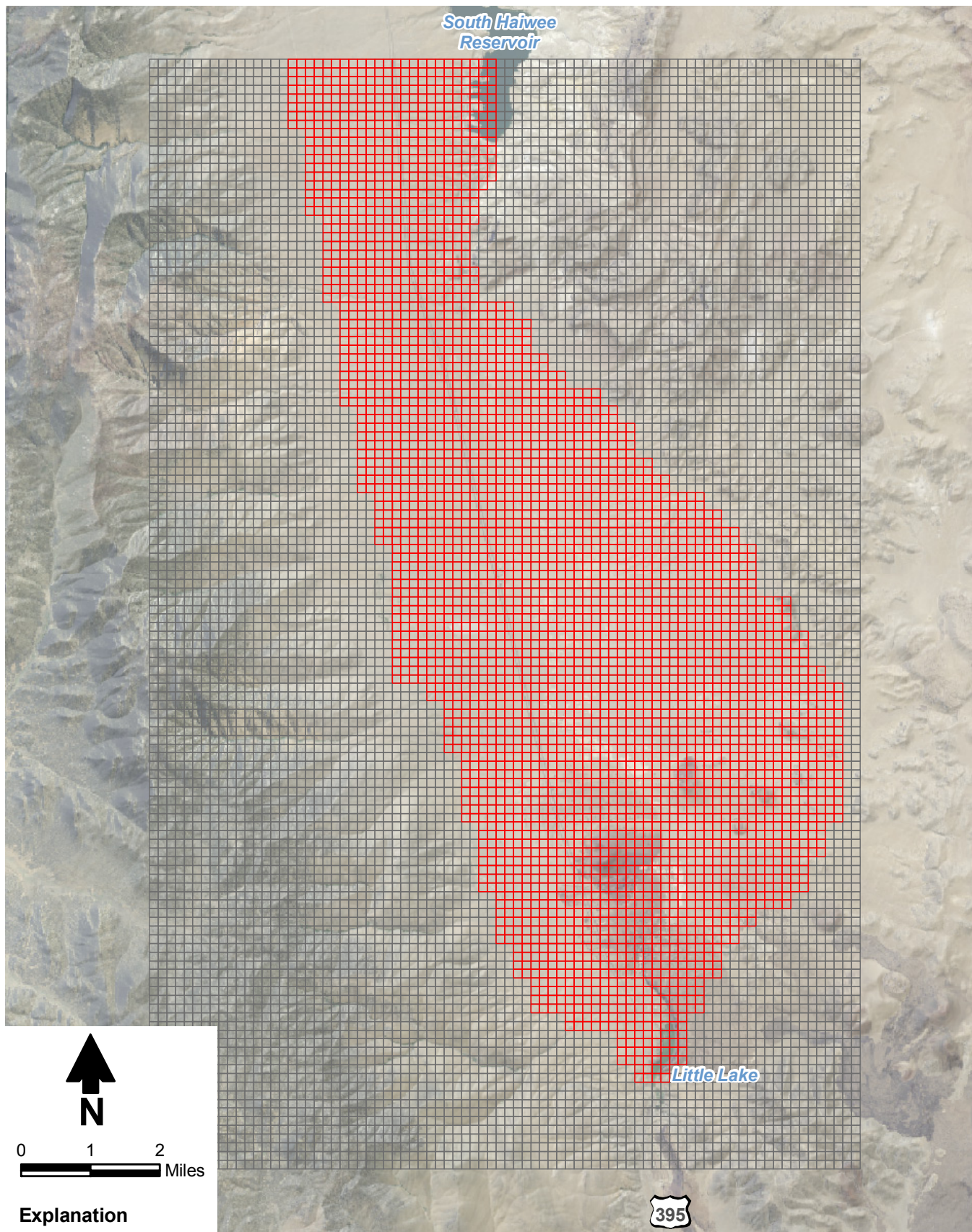
Q:\PROJECTS\LT09.0311_ROSE_VALLEY_MODEL\GIS\MXD\FIGURES\FIGURE08_LANDSAT_JUNE_1985.MXD 112/1





ROSE VALLEY MODEL
LANDSAT Image of Hay Ranch Area
June 17, 1985



Daniel B. Stephens & Associates, Inc.
1/10/2011 JN LT09.0311



Explanation

-  Model grid
-  Active model cell (layer 1)

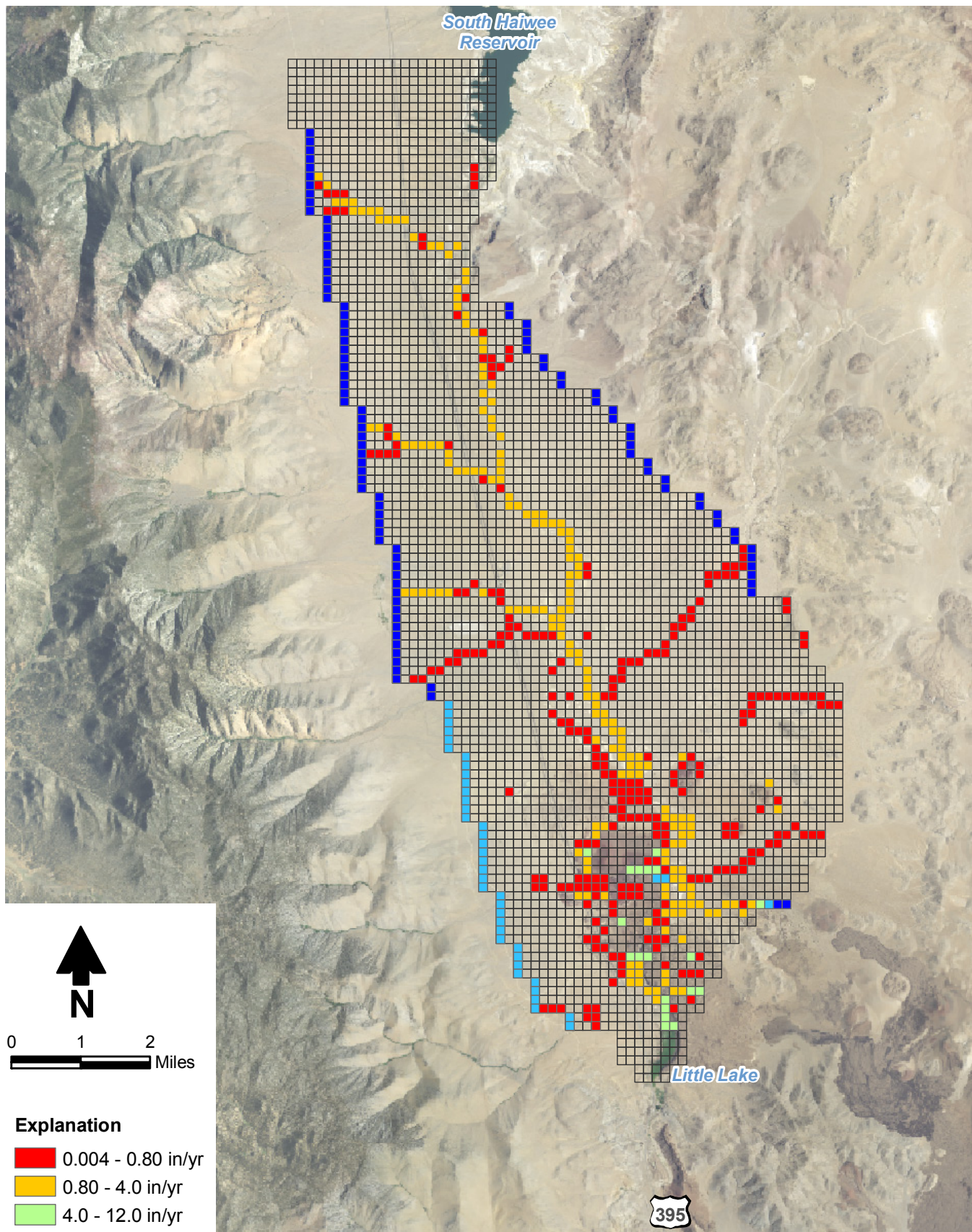


Daniel B. Stephens & Associates, Inc.
1/6/2011 JN LT09.0311

ROSE VALLEY MODEL
Model Grid

Figure 9

Q:\PROJECTS\LT09.0311_ROSE_VALLEY_MODEL\GIS\MXDS\FIGURES\FIGURE10_RECHARGE_LAYER1.MXD 11/2/11



Explanation

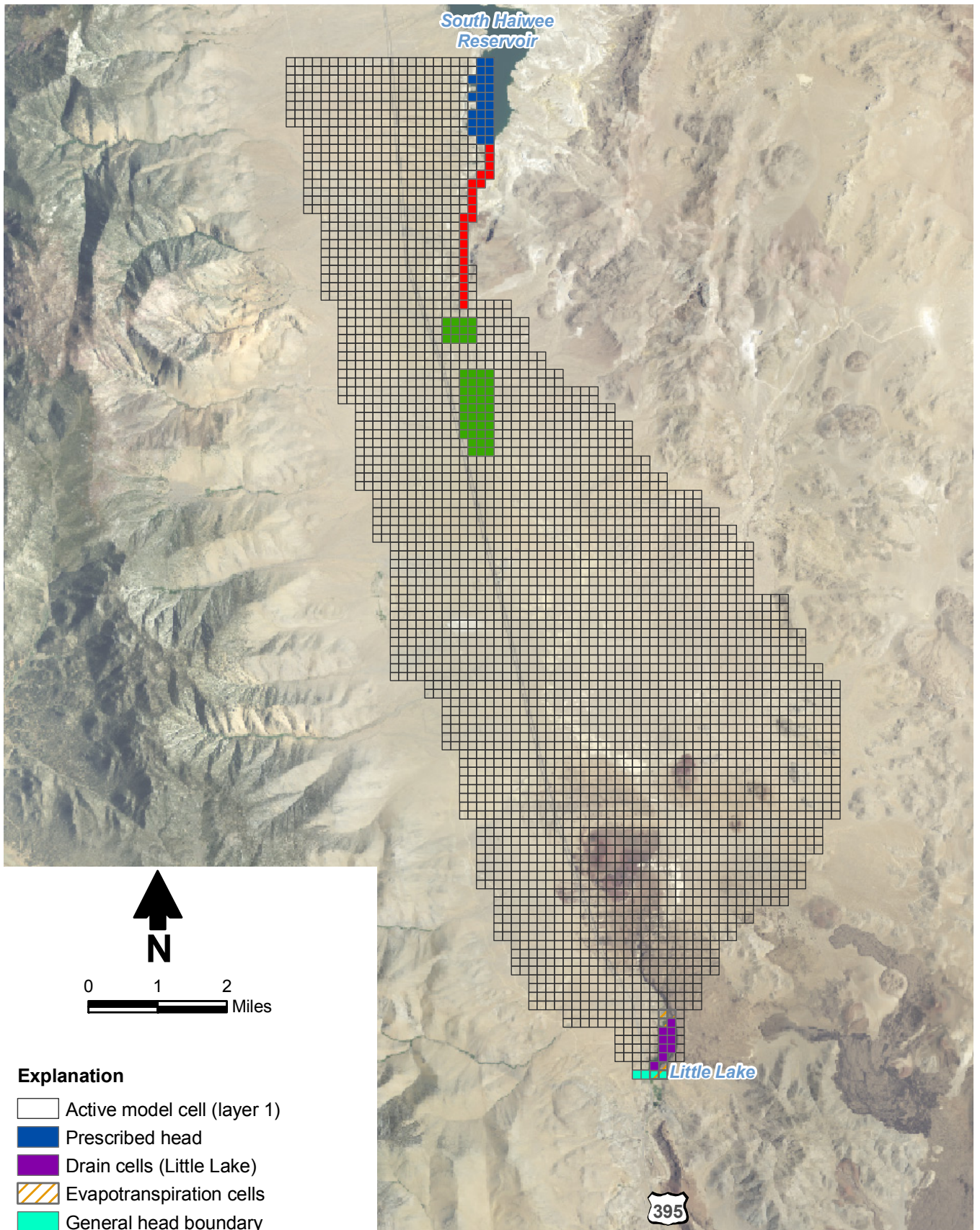
- 0.004 - 0.80 in/yr
- 0.80 - 4.0 in/yr
- 4.0 - 12.0 in/yr
- 12.0 - 30.0 in/yr
- 30.0 - 50.0 in/yr



Daniel B. Stephens & Associates, Inc.
1/6/2011 JN LT09.0311

ROSE VALLEY MODEL
Recharge from Precipitation

Figure 10



Explanation

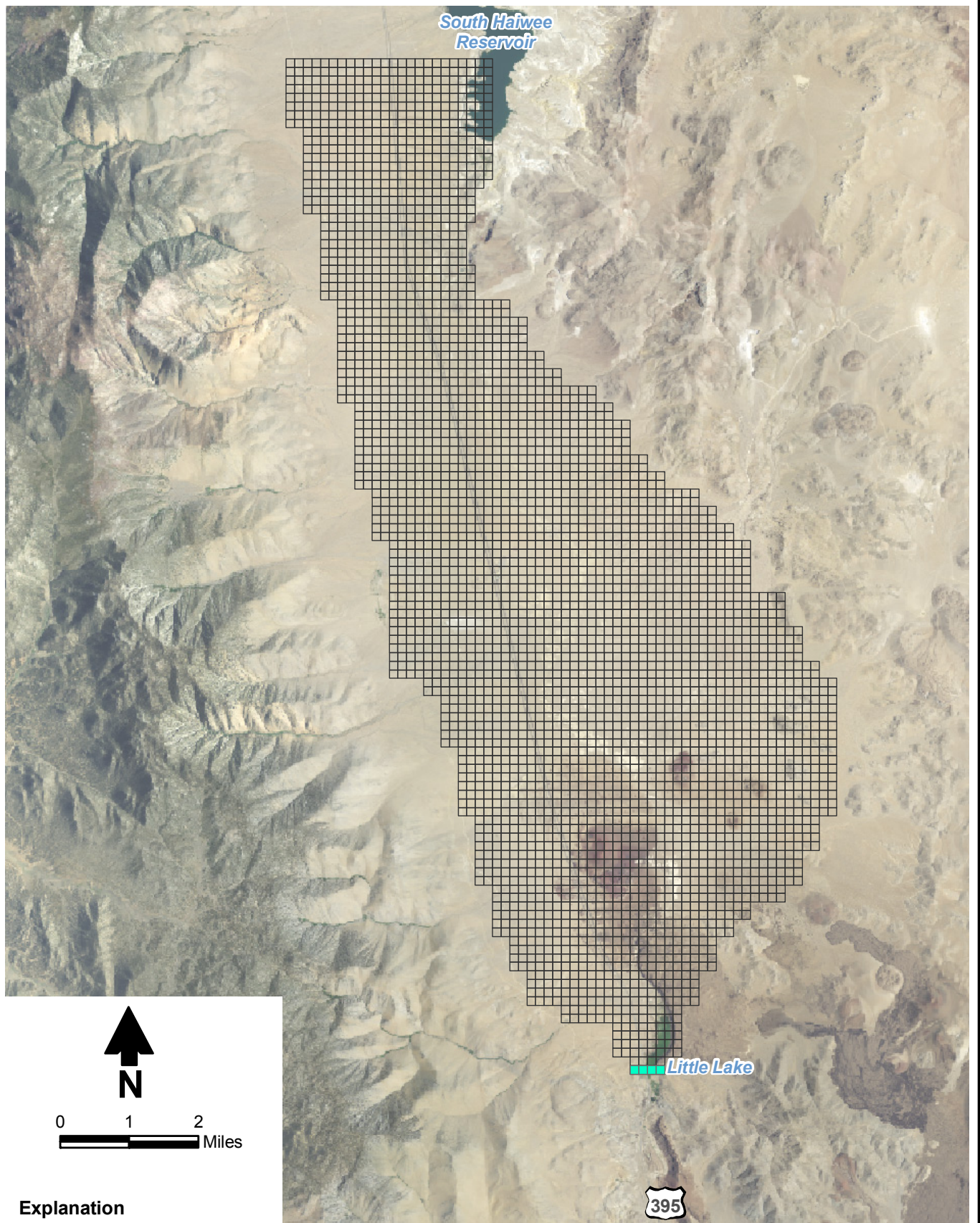
- Active model cell (layer 1)
- Prescribed head
- Drain cells (Little Lake)
- Evapotranspiration cells
- General head boundary
- Recharge from drain water south of Haiwee
- Recharge from irrigation return flow



Daniel B. Stephens & Associates, Inc.
1/7/2011 JN LT09.0311

ROSE VALLEY MODEL Boundary Conditions for Model Layer 1

Figure 11



Explanation

- Active model cell (layer 2)
- General head boundary

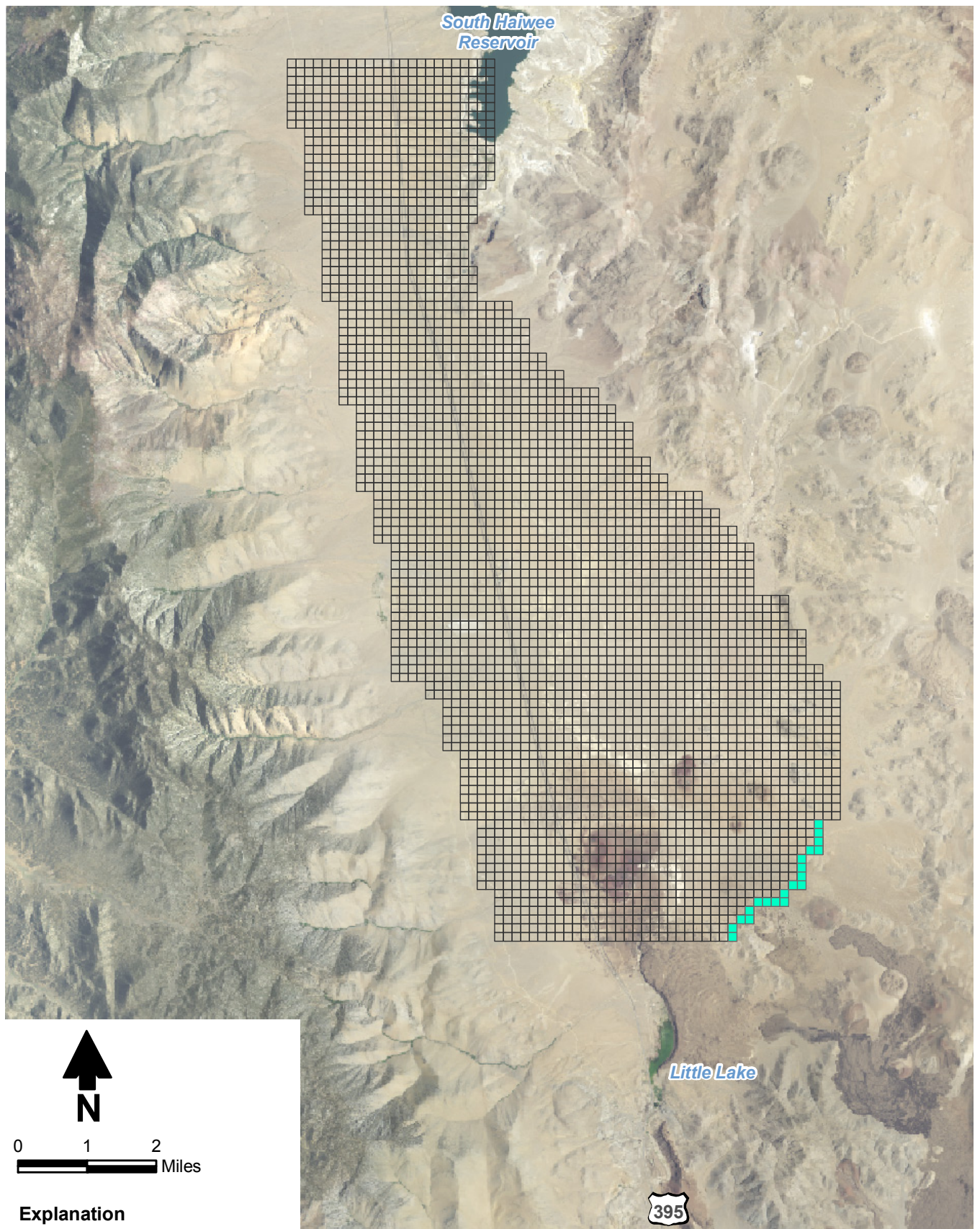


Daniel B. Stephens & Associates, Inc.
1/7/2011 JN LT09.0311



ROSE VALLEY MODEL Boundary Conditions for Model Layer 2

Figure 12

Q:\PROJECTS\LT09.0311_ROSE_VALLEY_MODEL\GIS\MXDS\FIGURES\FIGURE13_BOUNDARY_CONDITIONS_LAYER4_5.MXD 112/1



Explanation

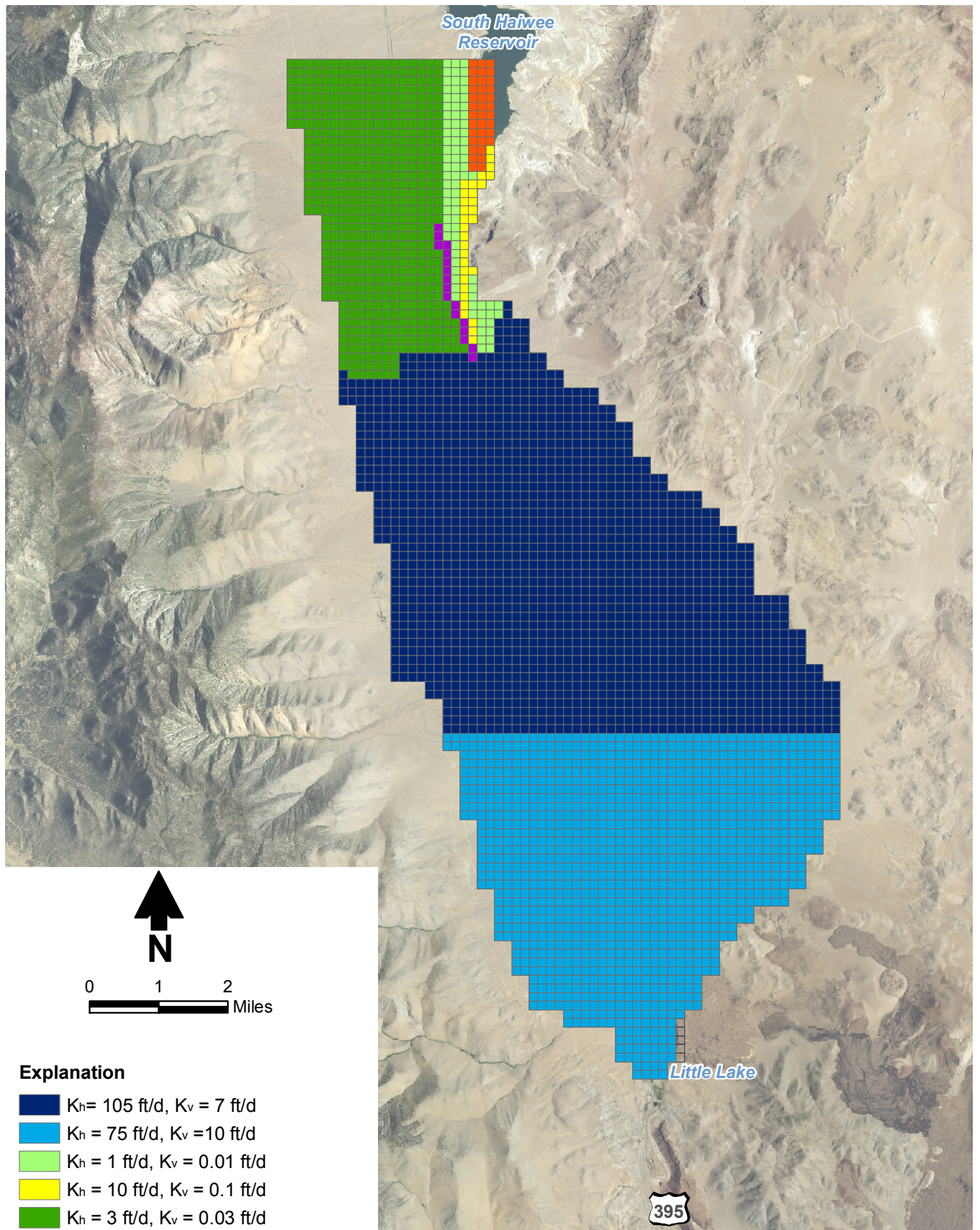
-  Active model cell (layers 4 and 5)
-  General head boundary



Daniel B. Stephens & Associates, Inc.
1/6/2011 JN LT09.0311

ROSE VALLEY MODEL
**Boundary Conditions for
Model Layers 4 and 5**

Figure 13

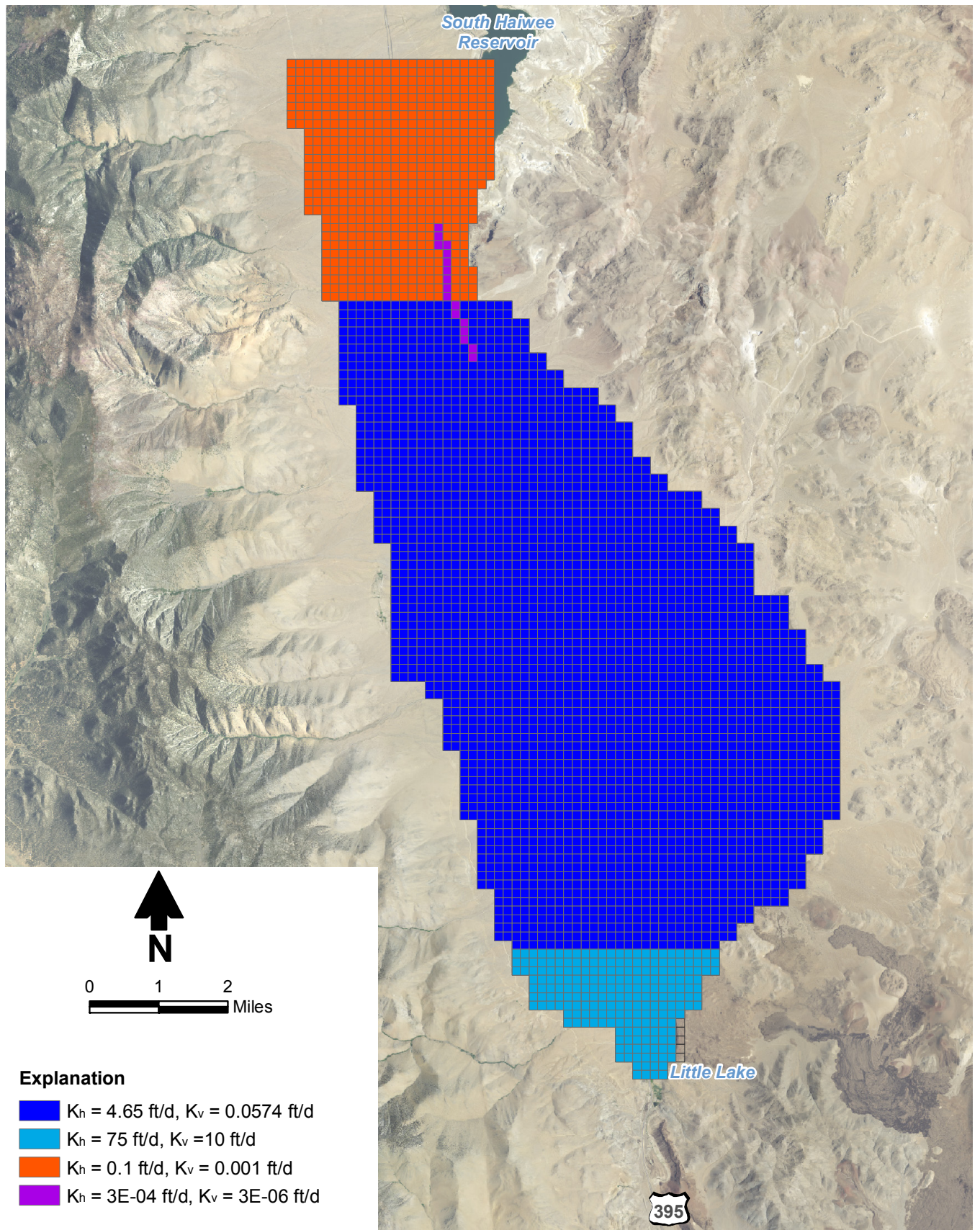


Explanation

- $K_h = 105 \text{ ft/d}$, $K_v = 7 \text{ ft/d}$
- $K_h = 75 \text{ ft/d}$, $K_v = 10 \text{ ft/d}$
- $K_h = 1 \text{ ft/d}$, $K_v = 0.01 \text{ ft/d}$
- $K_h = 10 \text{ ft/d}$, $K_v = 0.1 \text{ ft/d}$
- $K_h = 3 \text{ ft/d}$, $K_v = 0.03 \text{ ft/d}$
- $K_h = 0.1 \text{ ft/d}$, $K_v = 0.001 \text{ ft/d}$
- $K_h = 3\text{E-}04 \text{ ft/d}$, $K_v = 3\text{E-}06 \text{ ft/d}$

ROSE VALLEY MODEL
Horizontal and Vertical Hydraulic Conductivity
Model Layer 1

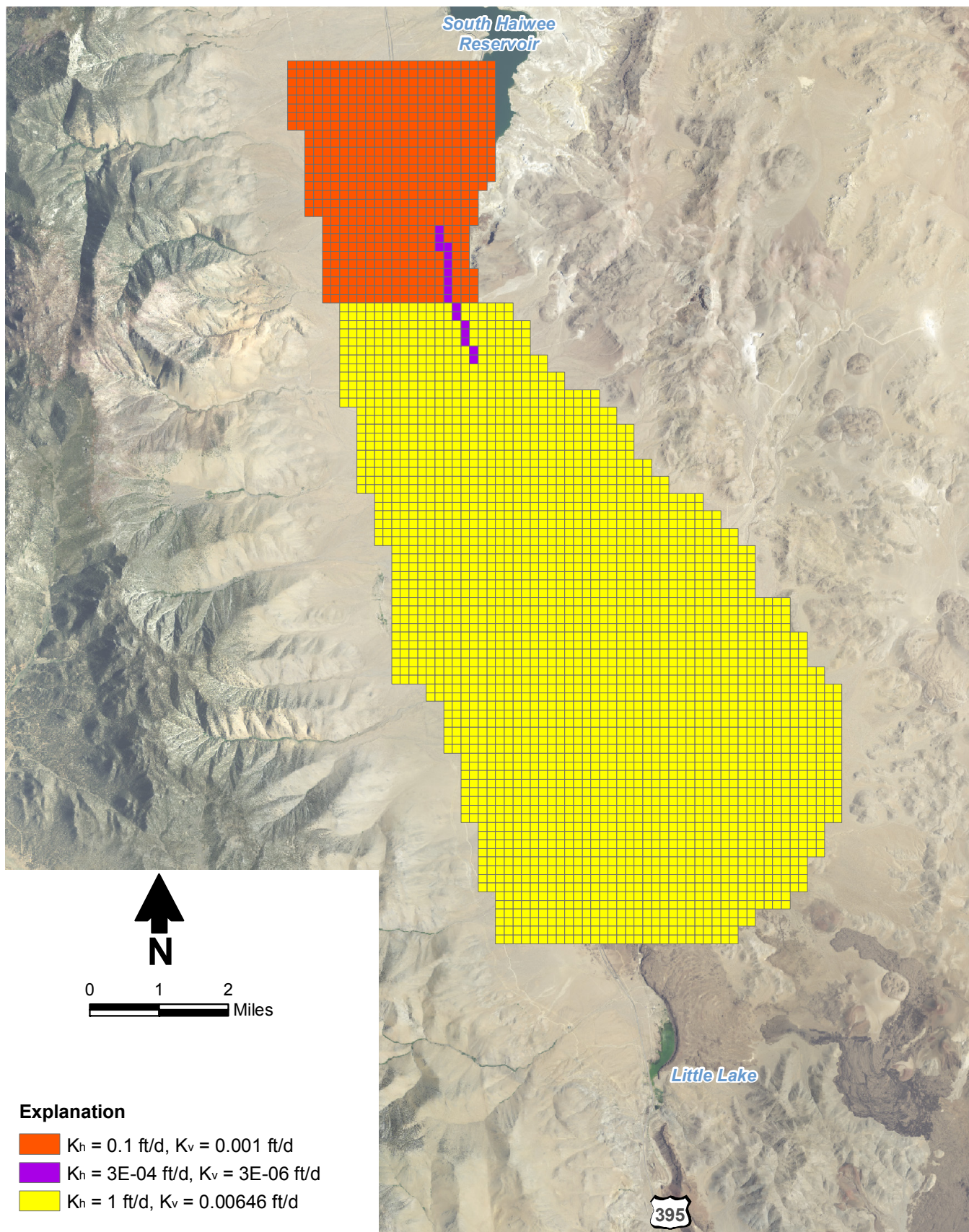




ROSE VALLEY MODEL
Horizontal and Vertical Hydraulic Conductivity
Model Layer 2



Q:\PROJECTS\LT09.0311_ROSE_VALLEY_MODEL\GIS\XDS\FIGURES\FIGURE16_HYDRAULIC_CONDUCTIVITY_LAYER3.MXD

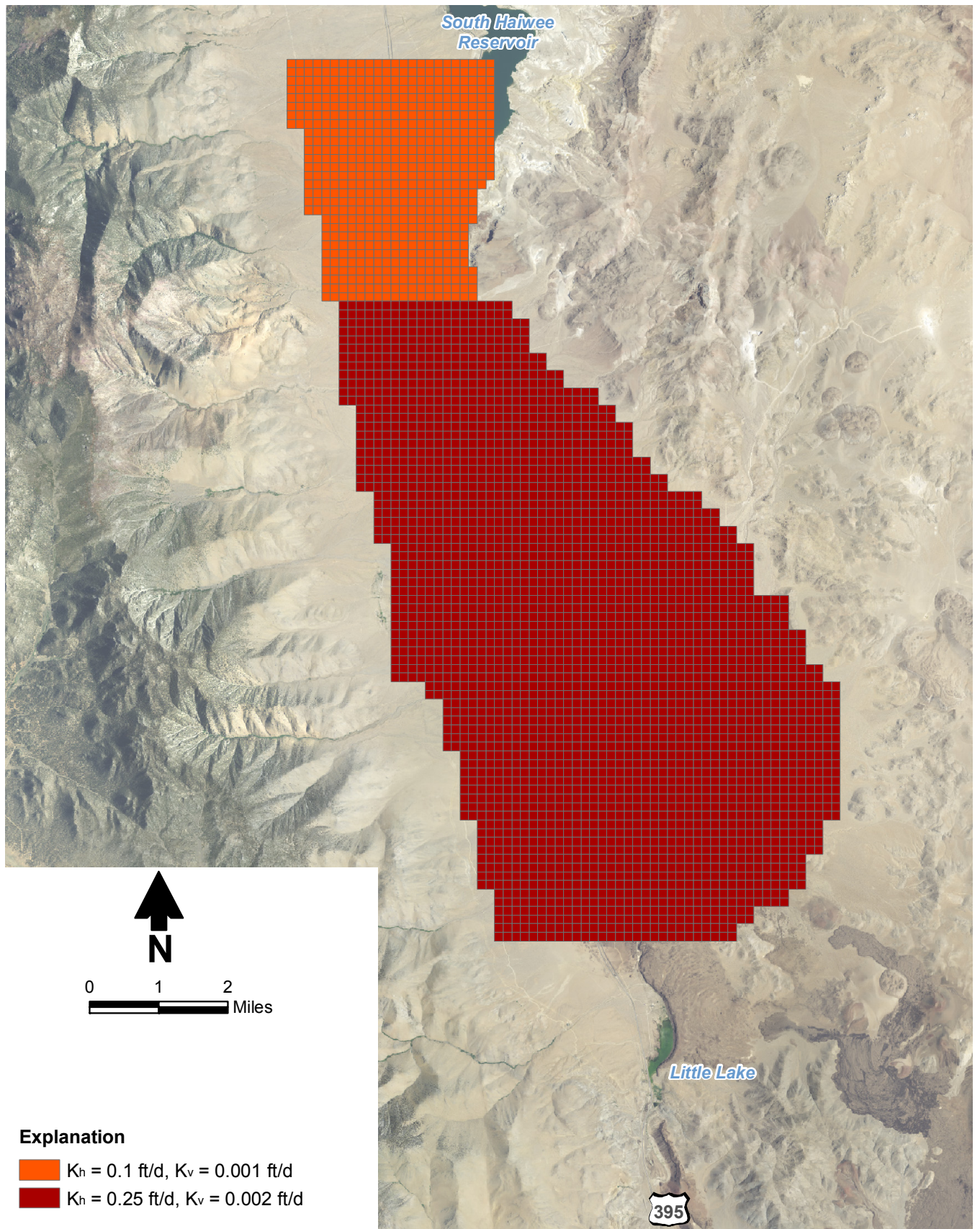


ROSE VALLEY MODEL
Horizontal and Vertical Hydraulic Conductivity
Model Layer 3



Daniel B. Stephens & Associates, Inc.
1/10/2011 JN LT09.0311

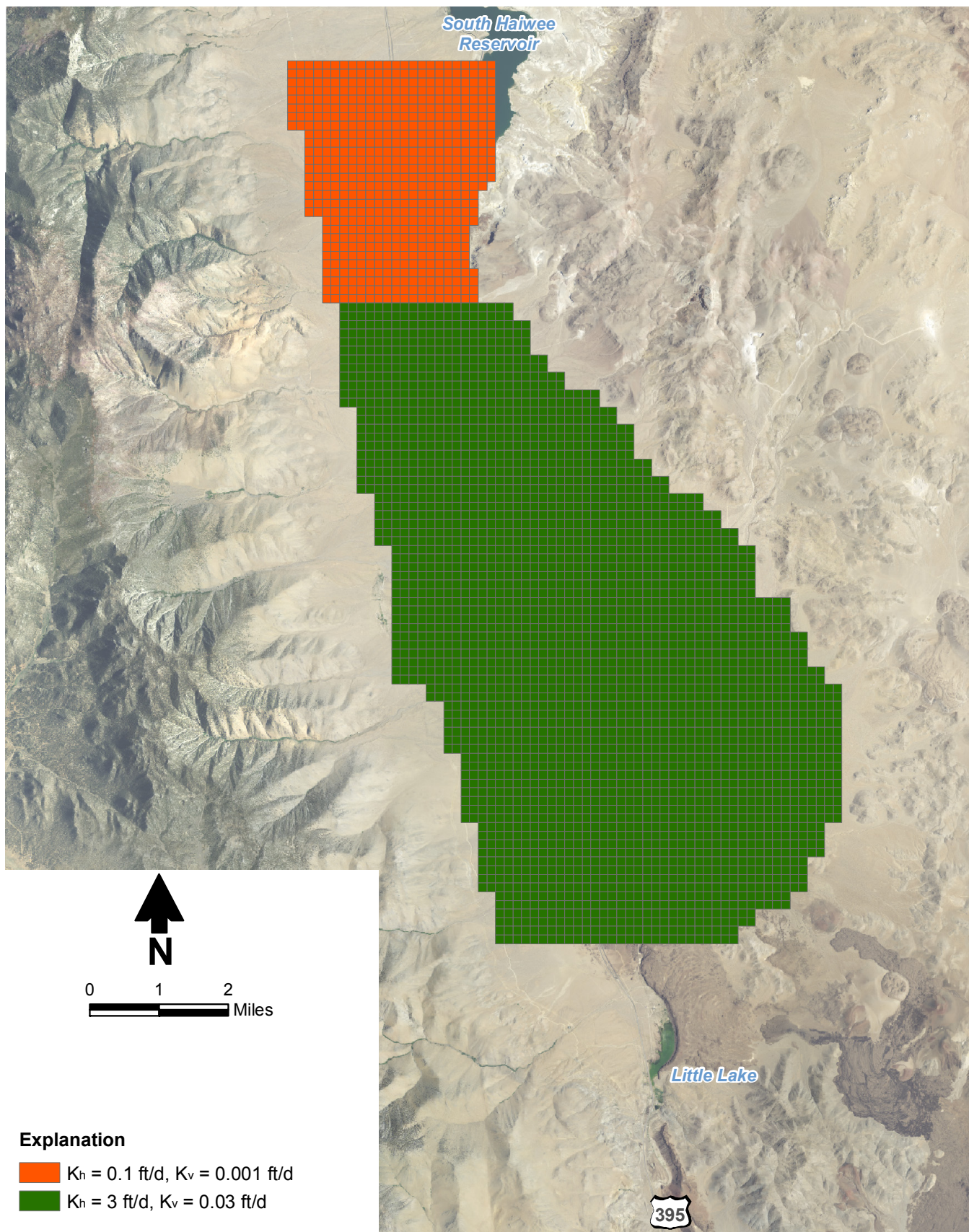
Figure 16



ROSE VALLEY MODEL
Horizontal and Vertical Hydraulic Conductivity
Model Layer 4



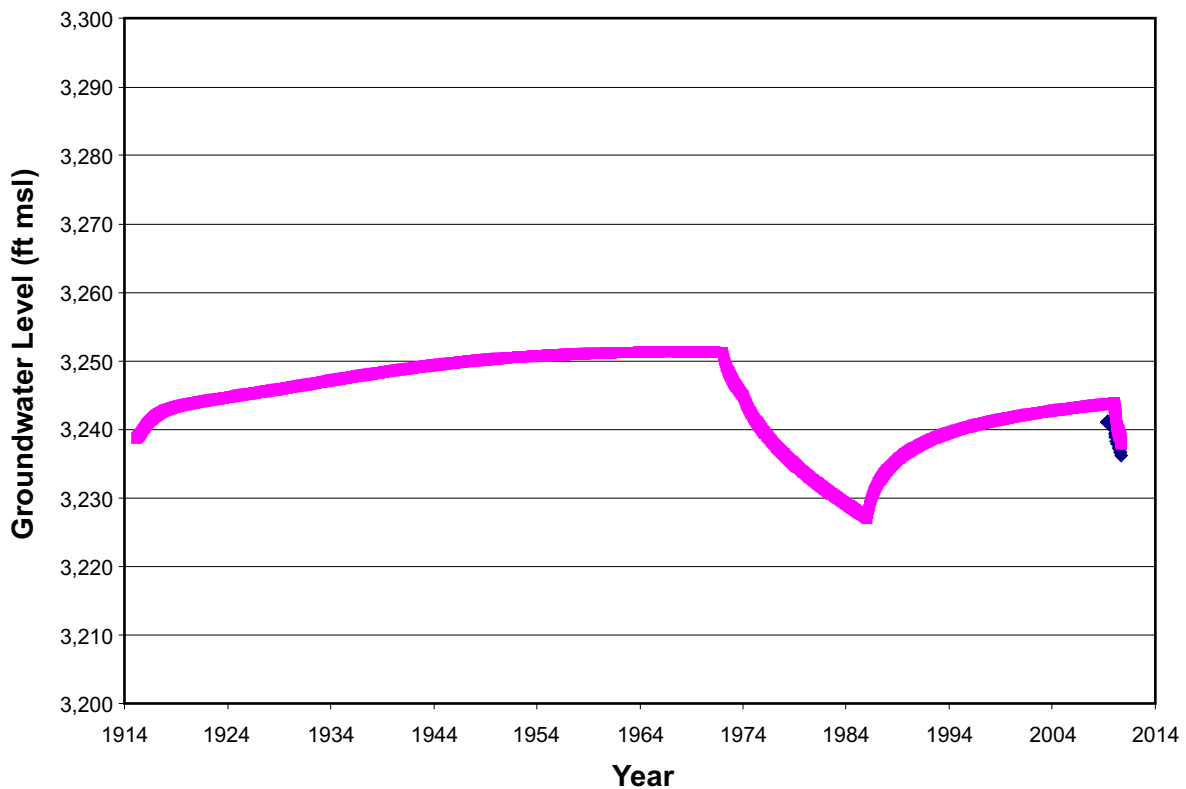
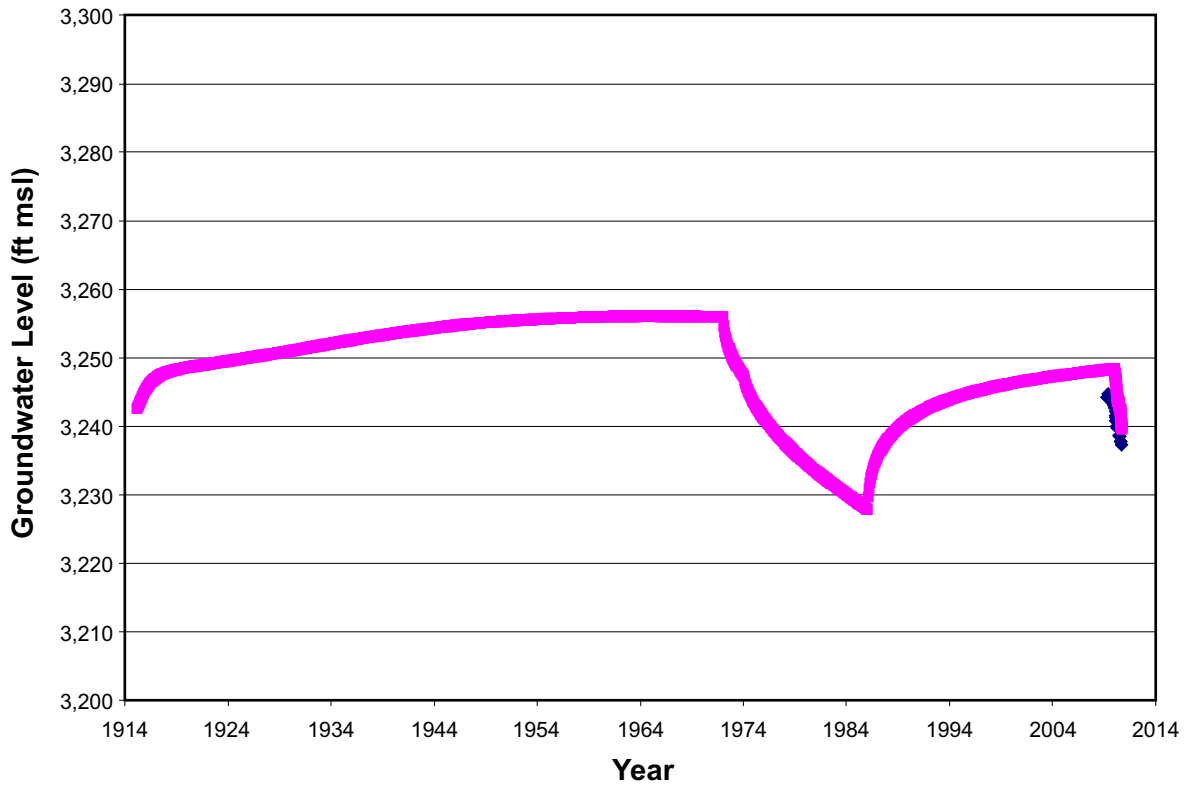
Q:\PROJECTS\LT09.0311_ROSE_VALLEY_MODEL\GIS\XDS\FIGURES\FIGURE18_HYDRAULIC_CONDUCTIVITY_LAYERS.MXD



ROSE VALLEY MODEL
Horizontal and Vertical Hydraulic Conductivity
Model Layer 5



Daniel B. Stephens & Associates, Inc.
1/10/2011 JN LT09.0311



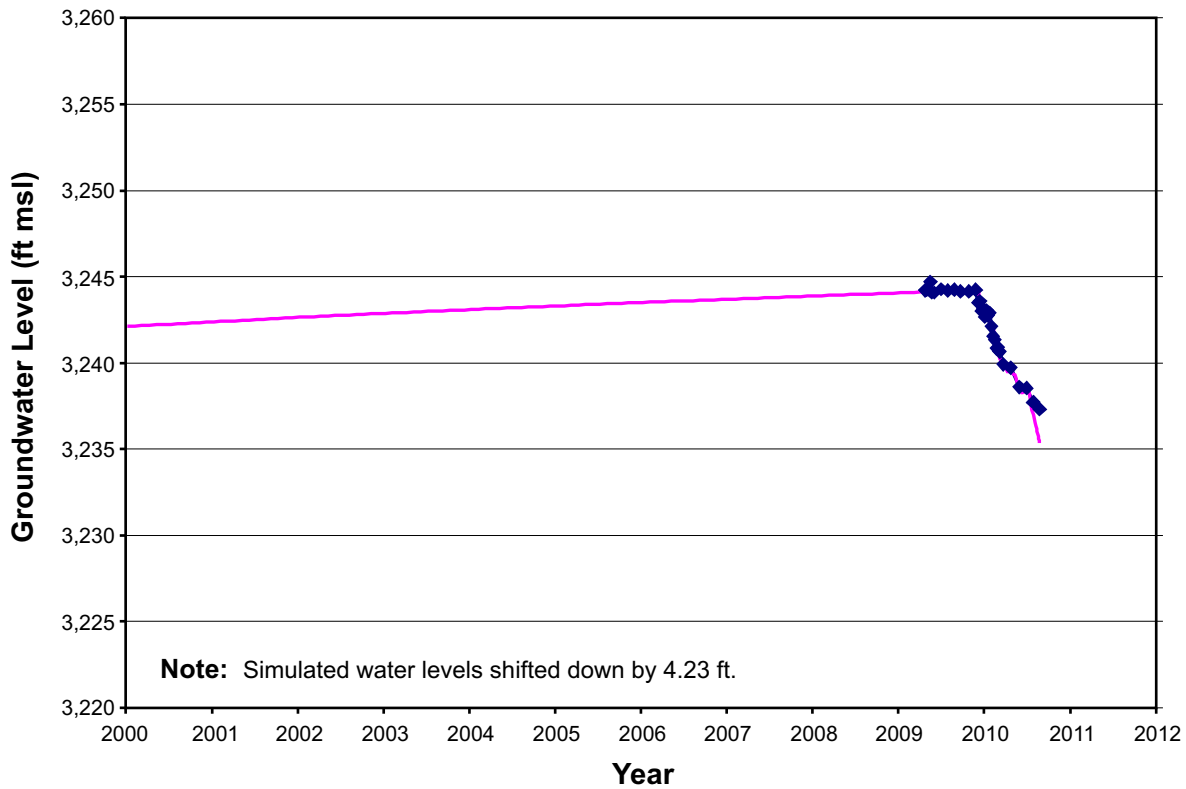
Explanation

- Simulated model layer 1 water level
- ◆ Observed water level

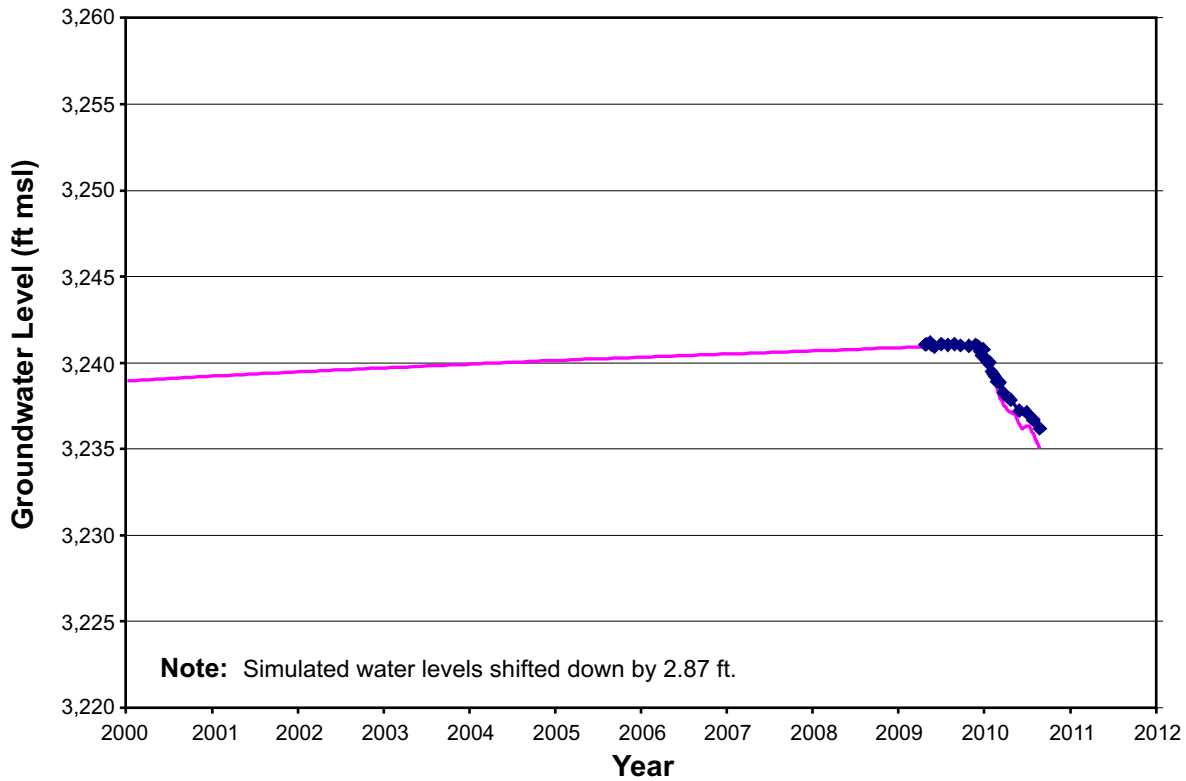
ROSE VALLEY MODEL

**Simulated and Observed Water Levels at
HR1 and HR2 Shallow Cluster Wells**





(a) Well RV060 - HR1 Shallow Cluster Well



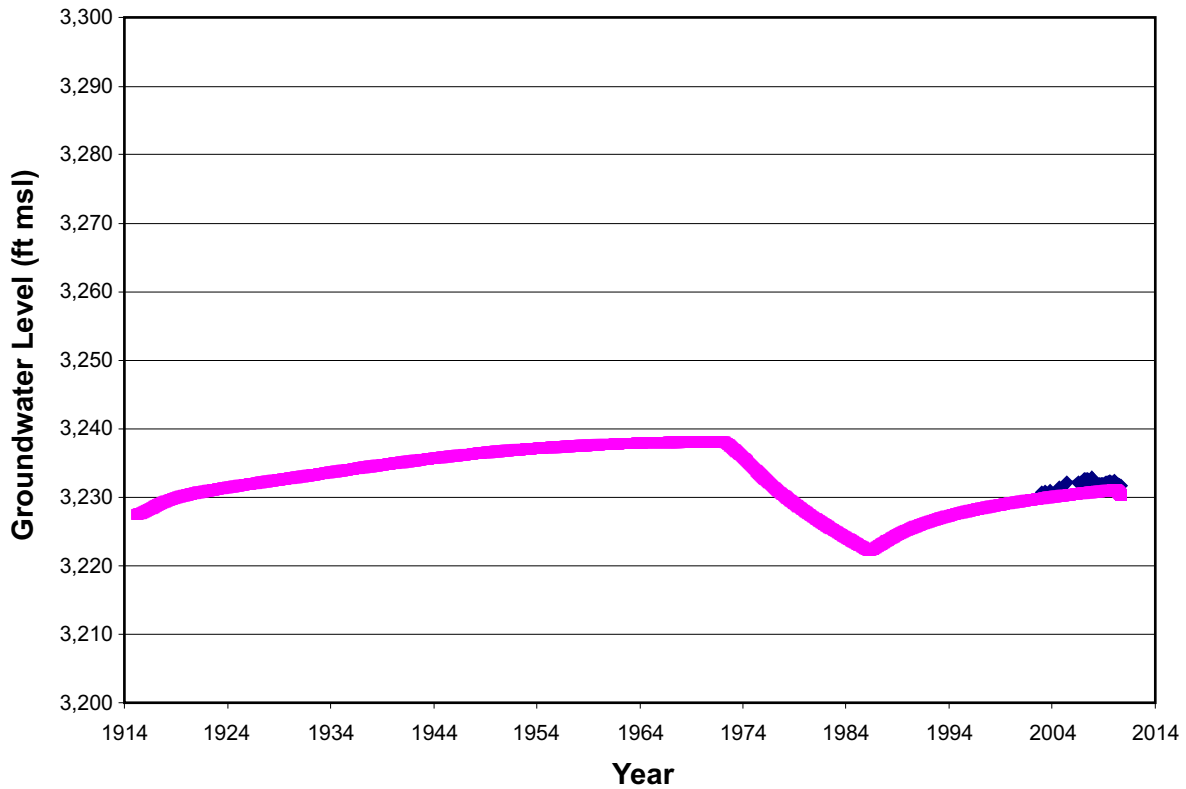
(b) Well RV080 - HR2 Shallow Cluster Well

Explanation

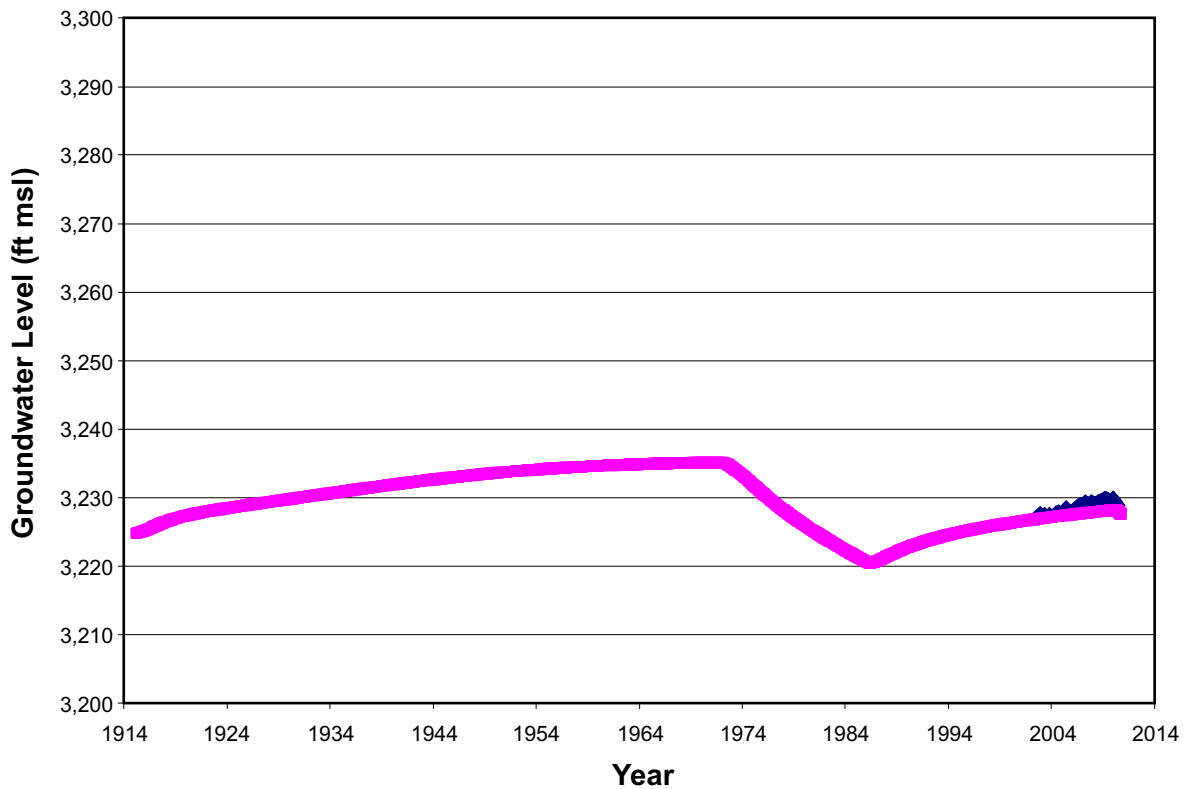
- Simulated model layer 1 water level
- ◆◆ Observed water level

ROSE VALLEY MODEL
Recent Period Simulated and
Observed Water Levels at
HR1 and HR2 Shallow Cluster Wells





(a) Well RV090 - Coso Junction Ranch



(b) Well RV100 - Coso Junction Store

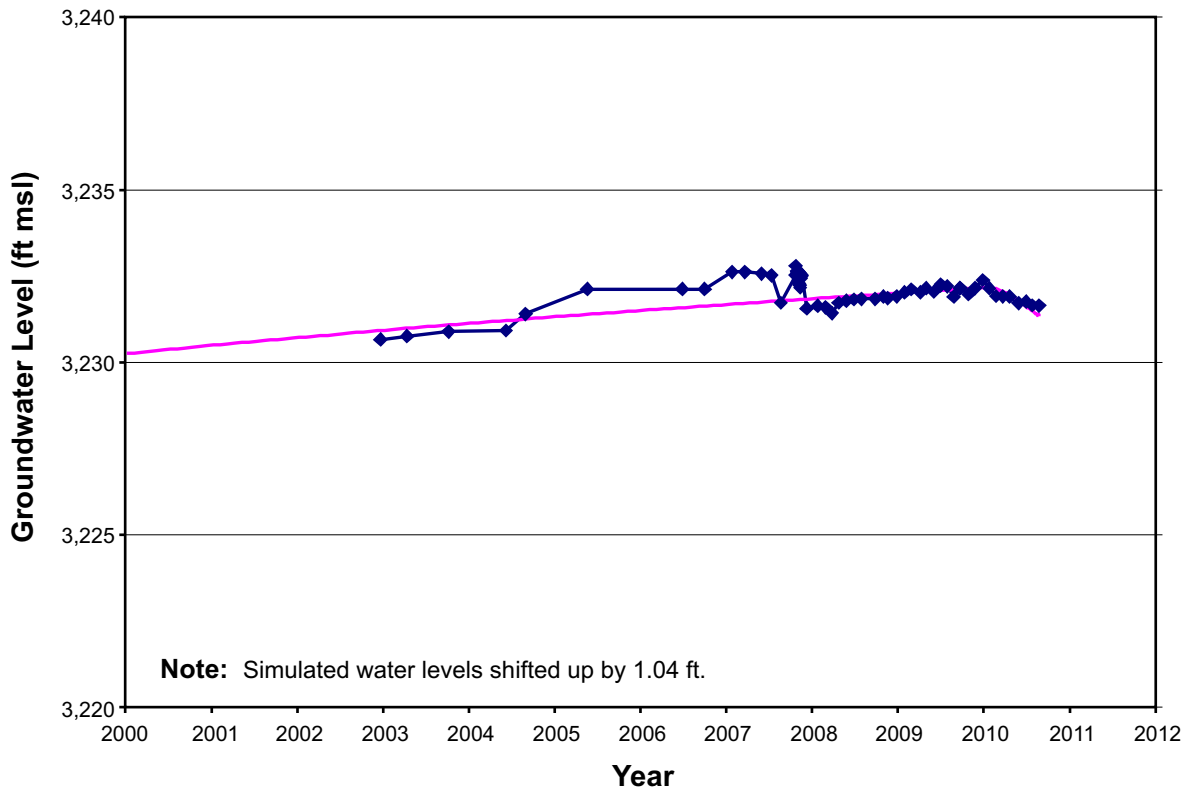
Explanation

- Simulated model layer 1 water level
- ◆ Observed water level

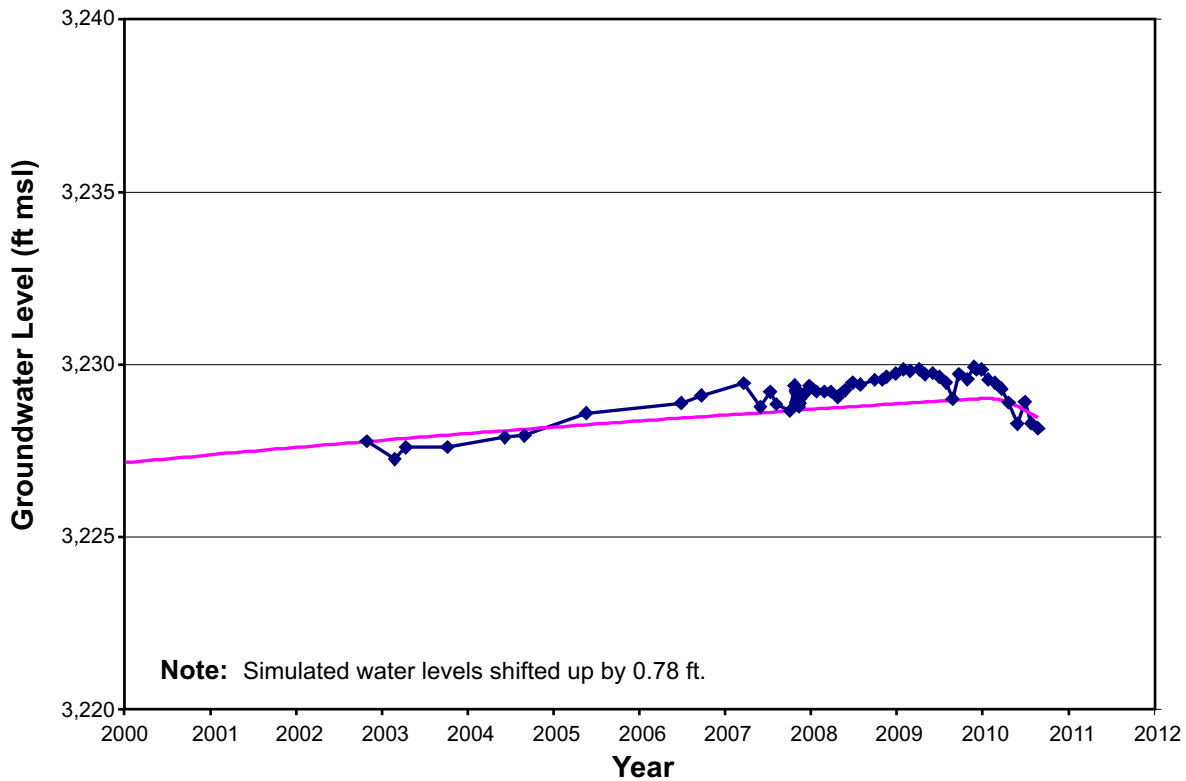
ROSE VALLEY MODEL

**Simulated and Observed Water Levels at
Wells RV090 and RV100 South of Hay Ranch**





(a) Well RV090 - Coso Junction Ranch



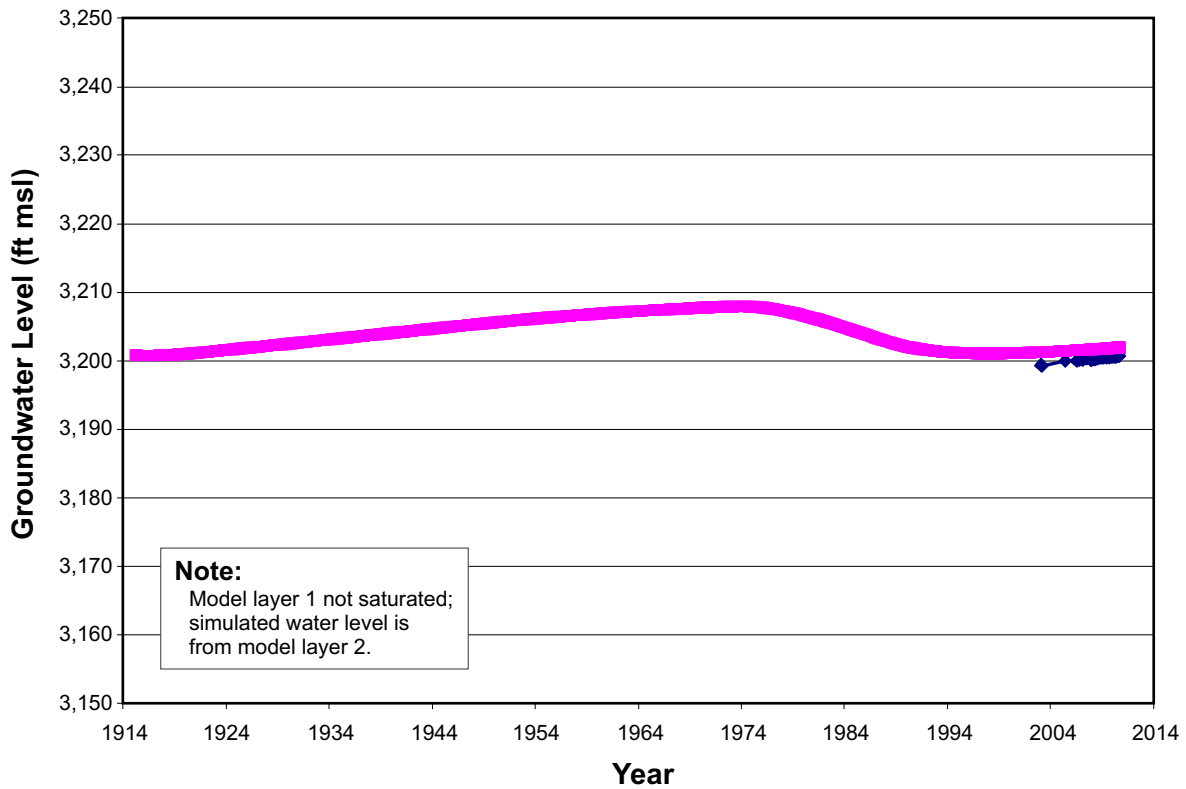
(b) Well RV100 - Coso Junction Store

Explanation

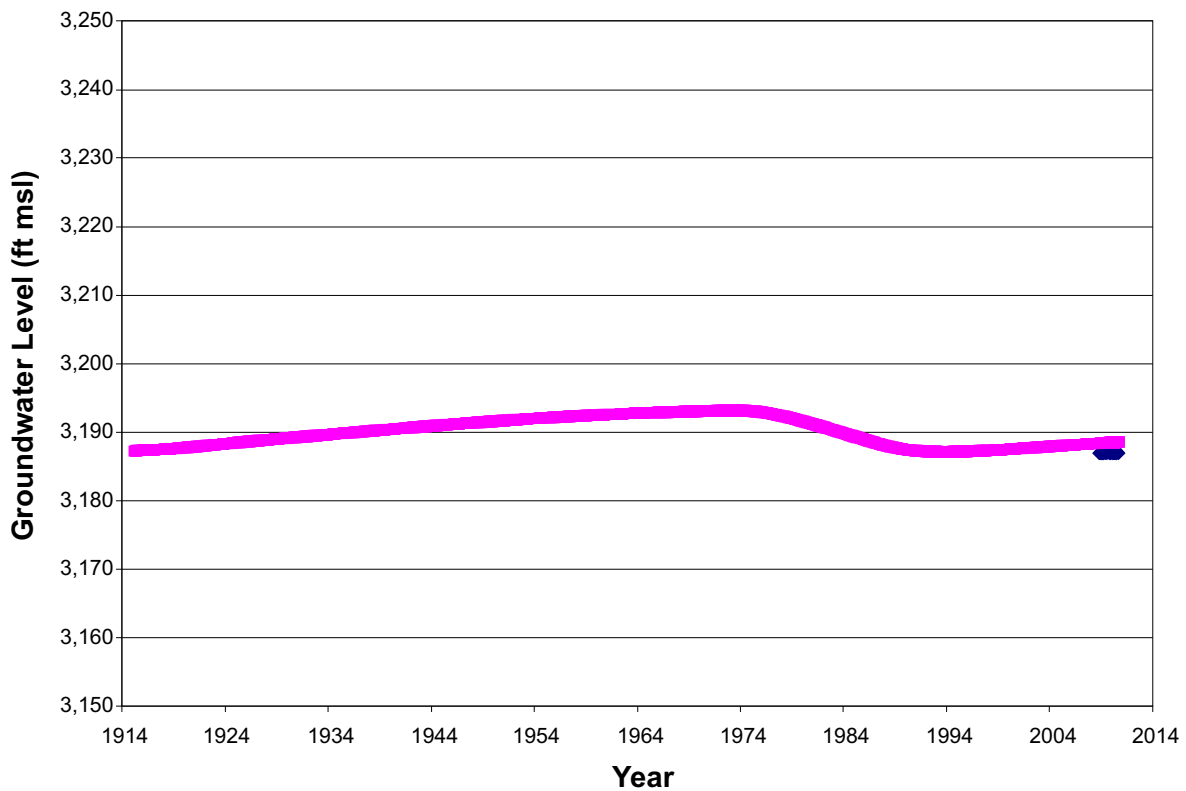
- Simulated model layer 1 water level
- ◆◆ Observed water level

ROSE VALLEY MODEL
Recent Period Simulated and
Observed Water Levels at
Wells RV090 and RV100 South of Hay Ranch





(a) Well RV140 - Lego



(b) Well RV150 - Cinder Road

Explanation

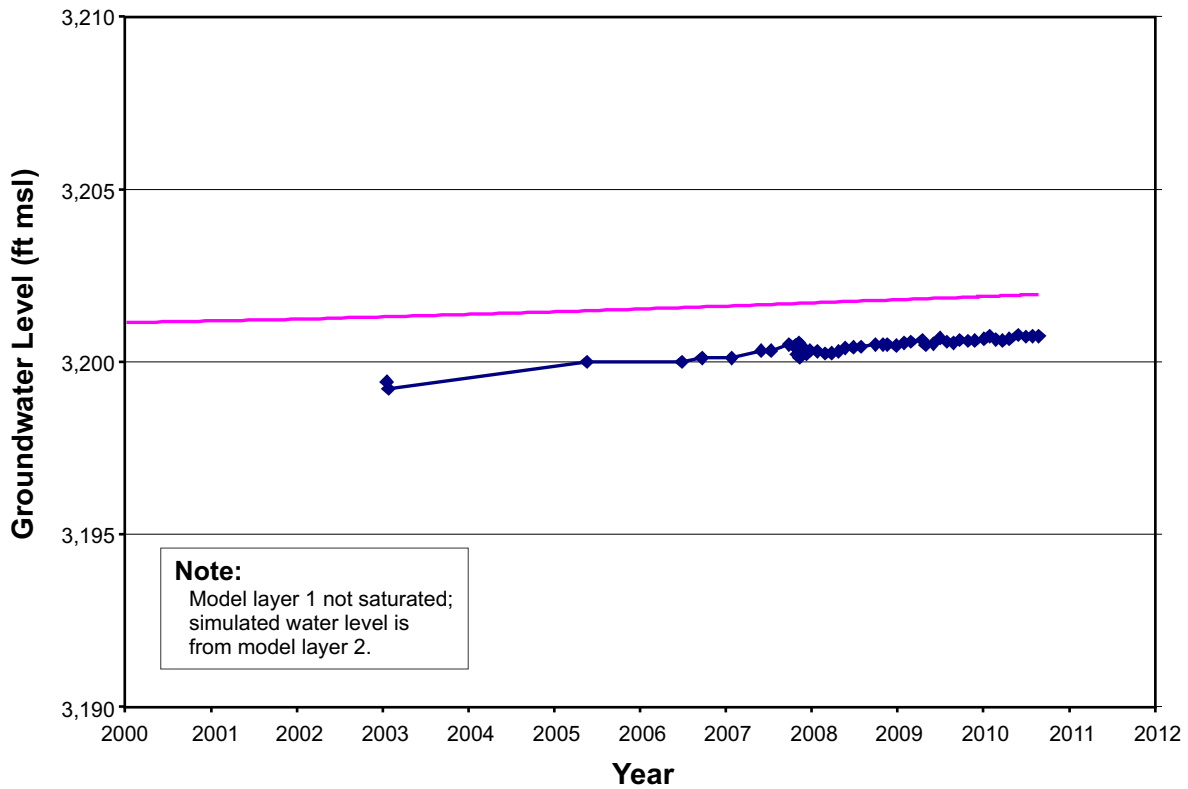
- █ Simulated model layer 1 water level
(unless otherwise noted)
- ◆◆ Observed water level

ROSE VALLEY MODEL

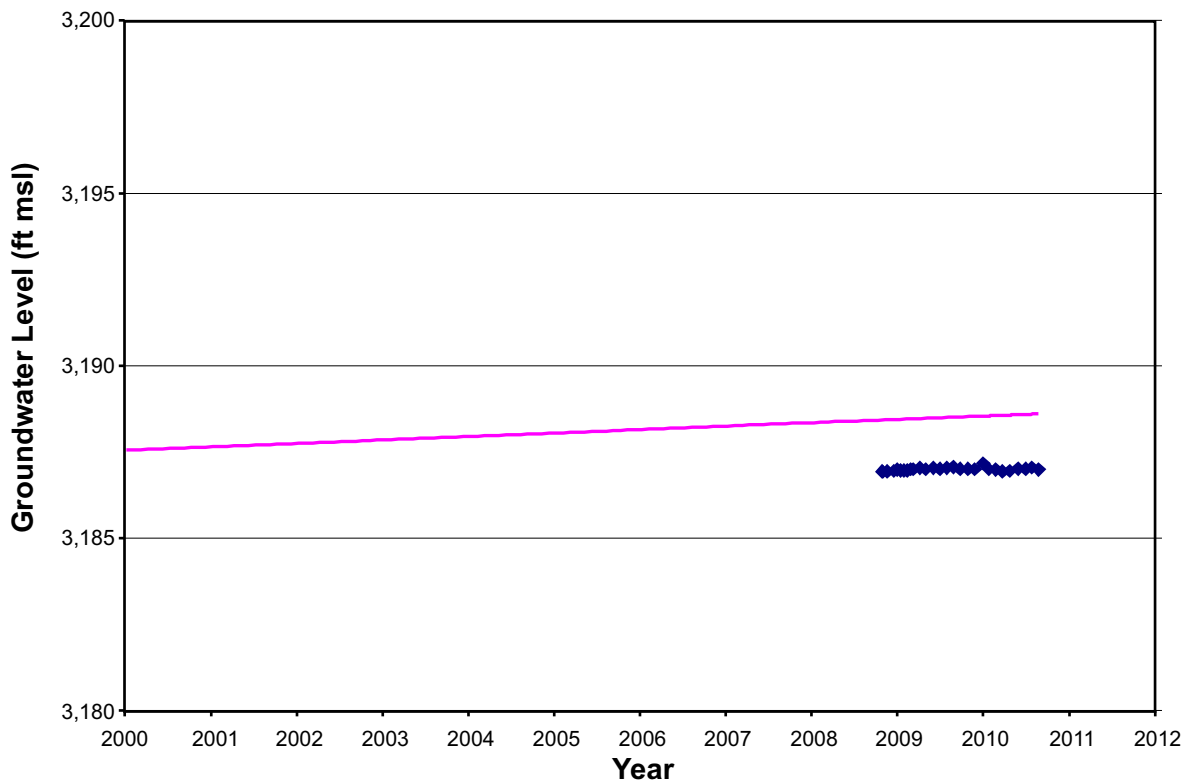
**Simulated and Observed Water Levels at
Wells RV140 and RV150 South of Coso Junction**



Q:\PROJECTS\LT09.0311_ROSE_VALLEY_MODEL\VR_DRAWINGS\LT09.0311_08W_SIM_AND_OBSER_WLS_2000-2012.CDR (PG. 3 OF 3)



(a) Well RV140 - Lego



(b) Well RV150 - Cinder Road

Explanation

- Simulated model layer 1 water level
(unless otherwise noted)
- ◆◆◆ Observed water level

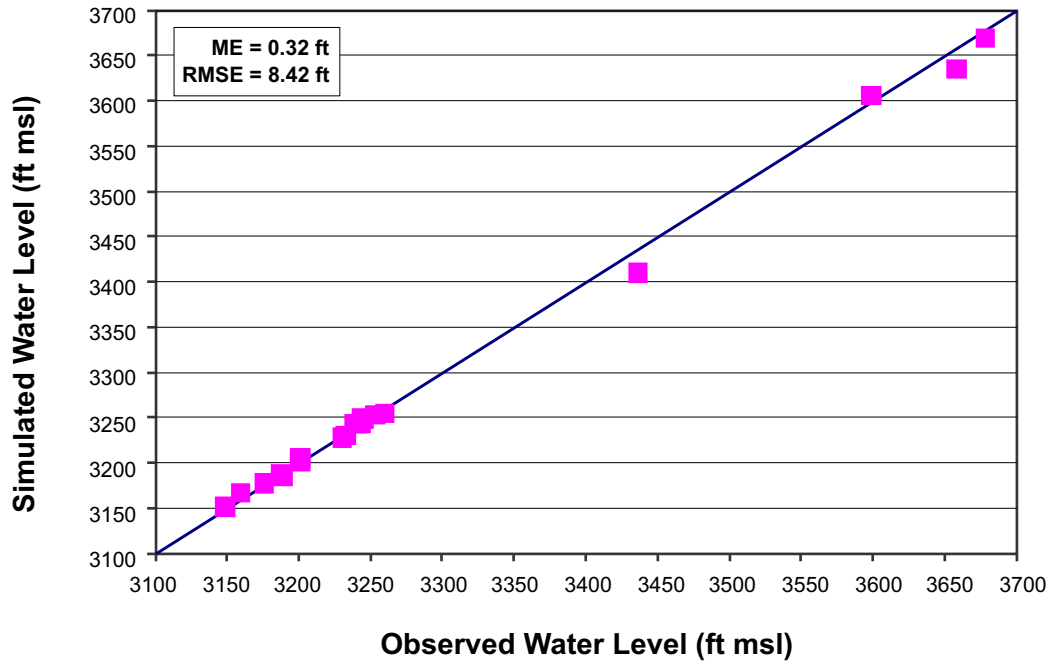
ROSE VALLEY MODEL

**Recent Period Simulated and
Observed Water Levels at**

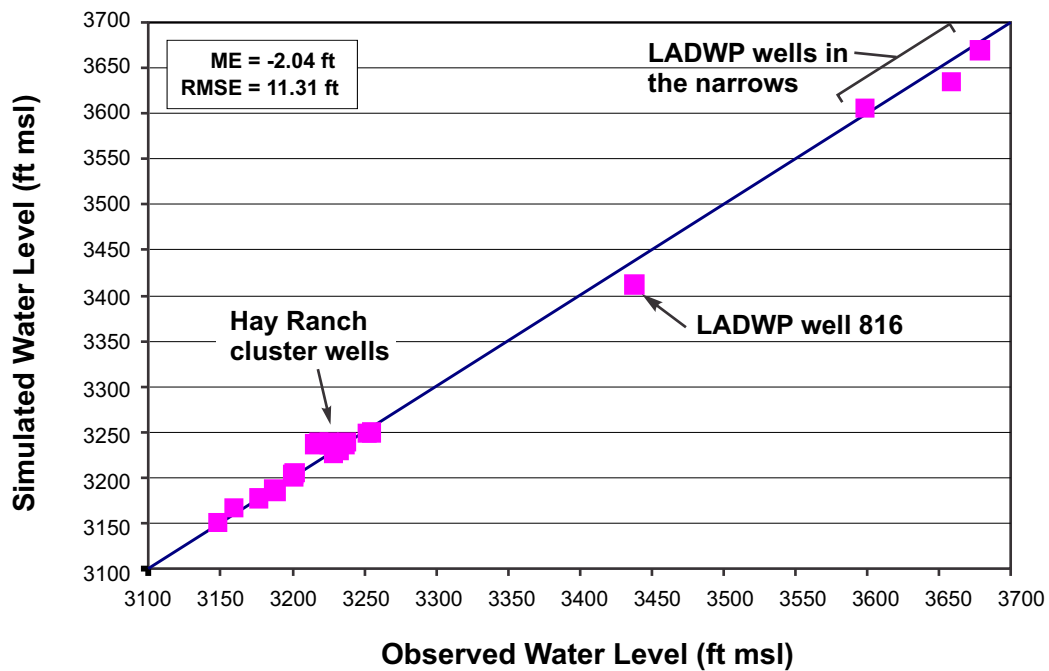
Wells RV140 and RV150 South of Coso Junction



Q:\PROJECTS\LT09.0311_ROSE_VALLEY_MODEL\DRAWINGS\LT09.0311_04W_SIM_AND_OBSER_WLS_dec2009_SEPT_2010.CDR



(a) December 2009



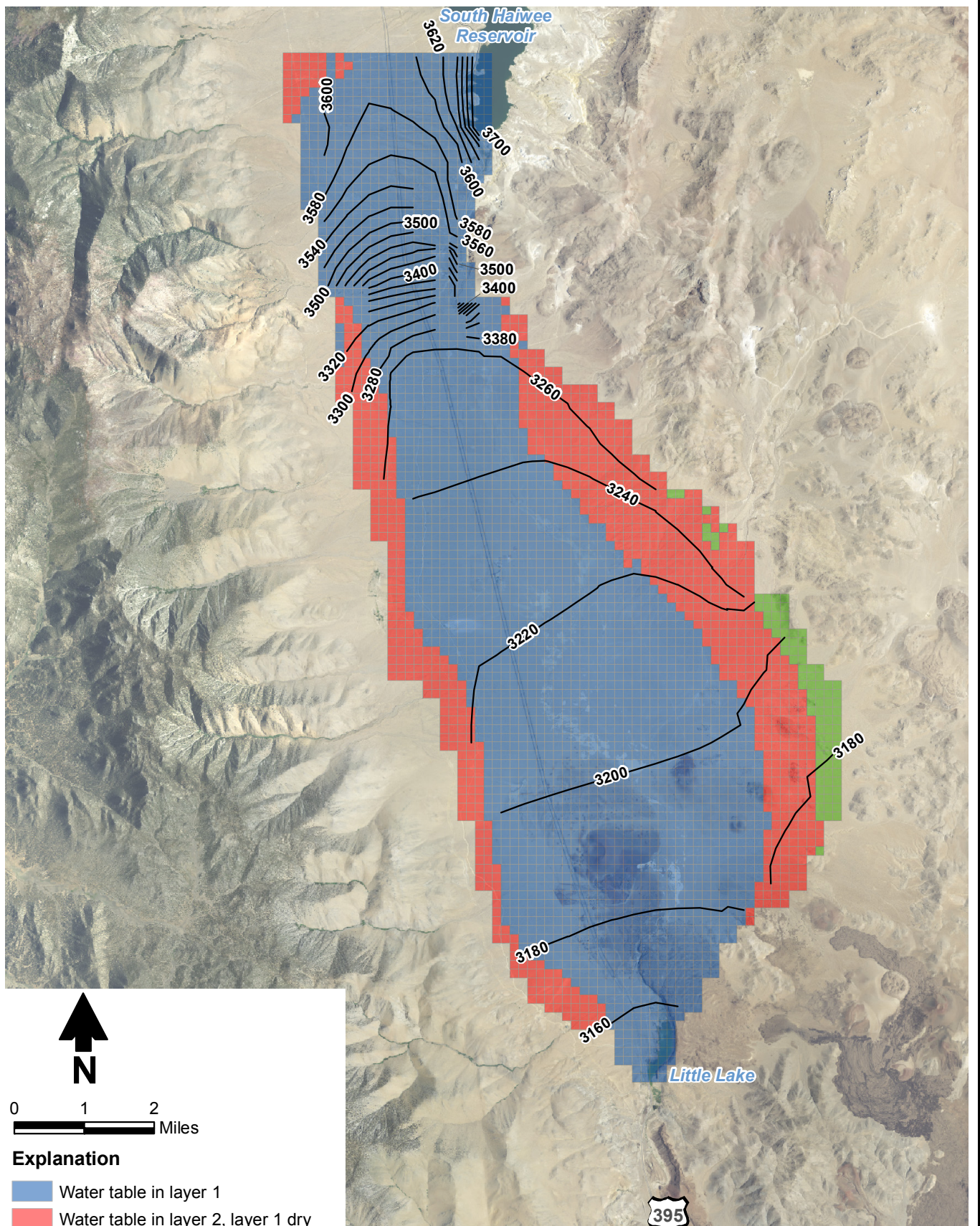
(b) September 2010

Notes:

ME = Mean error
RMSE = Root mean squared error



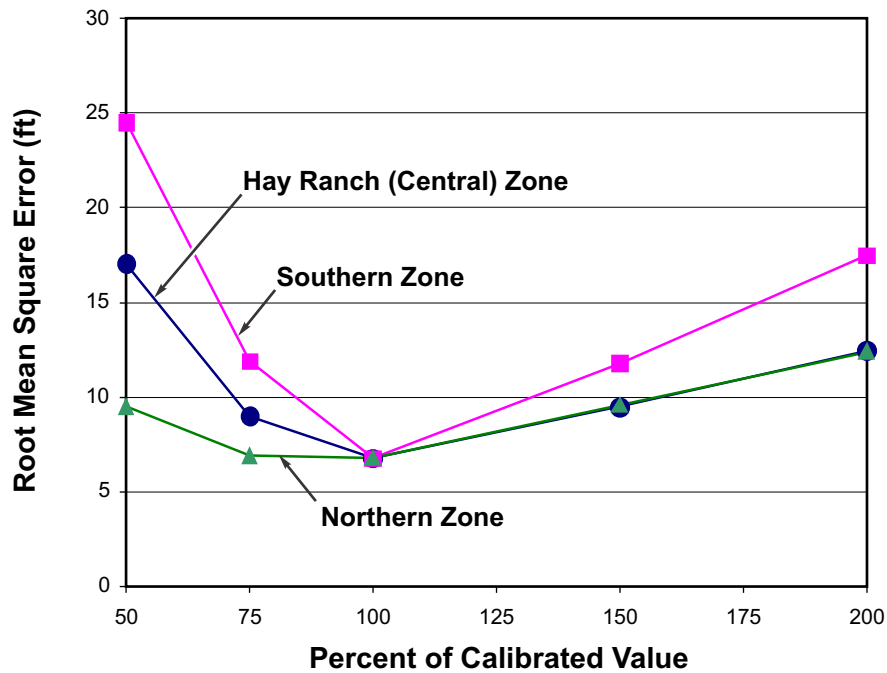
Q:\PROJECTS\LT09.0311_ROSE_VALLEY_MODEL\GIS\MXDS\FIGURES\FIGURE26_WLE_2009.MXD



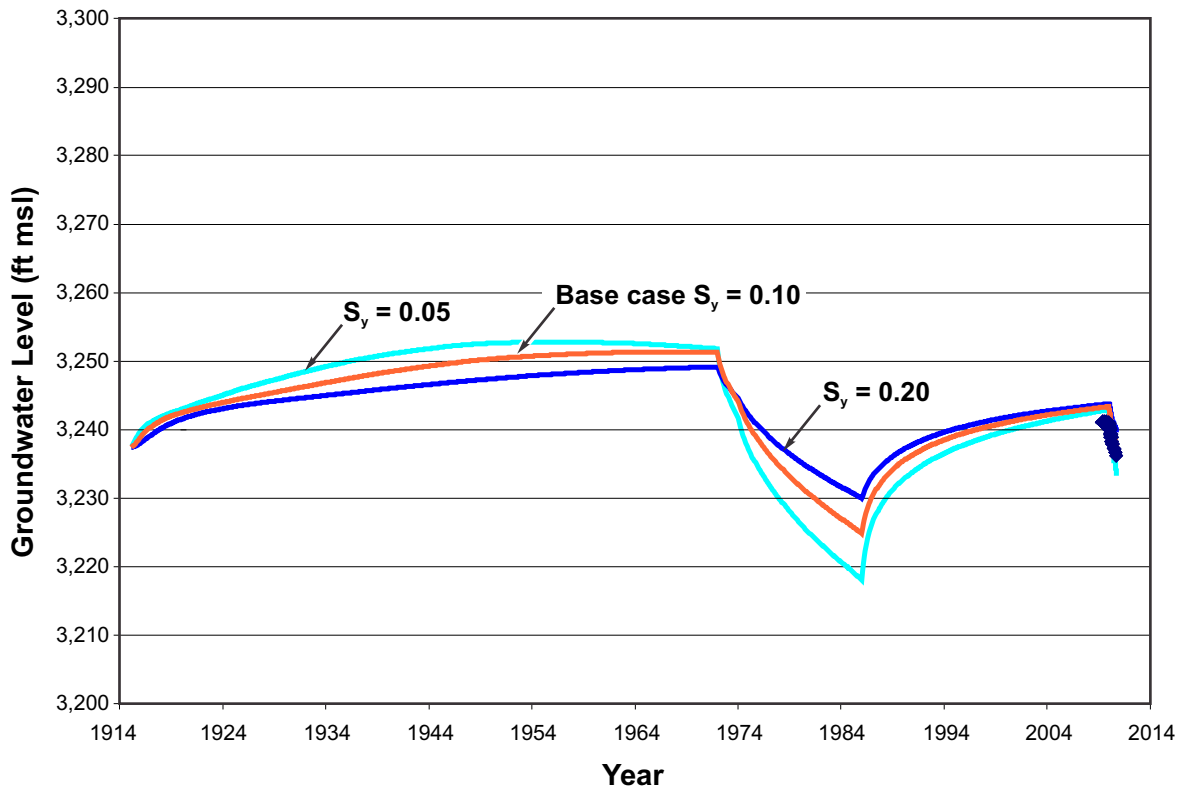
Daniel B. Stephens & Associates, Inc.
1/27/2011 JN LT09.0311

ROSE VALLEY MODEL
Simulated December 2009 Water Table

Figure 26



(a) Hydraulic Conductivity



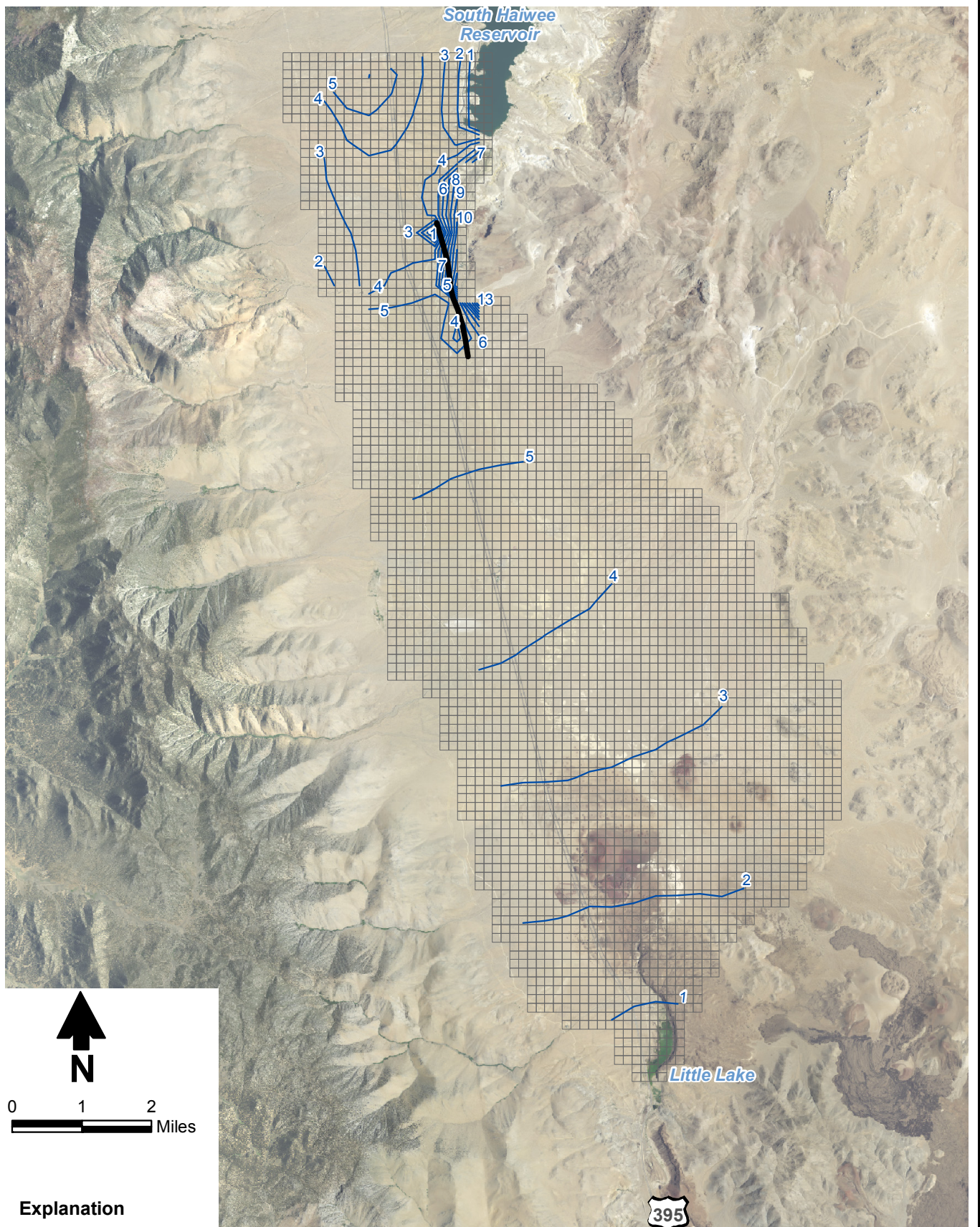
(b) Simulated Water Level at Well RV080 for Specific Yield Sensitivity Analysis

Explanation

◆◆ Observed water level



Q:\PROJECTS\LT09.0311_ROSE_VALLEY_MODEL\GIS\MXDS\FIGURES\FIGURE28_PREDICTIVE_DRAWDOWN_SCENARIO-A.MXD



Explanation

- Fault
- Layer 1 drawdown (ft)

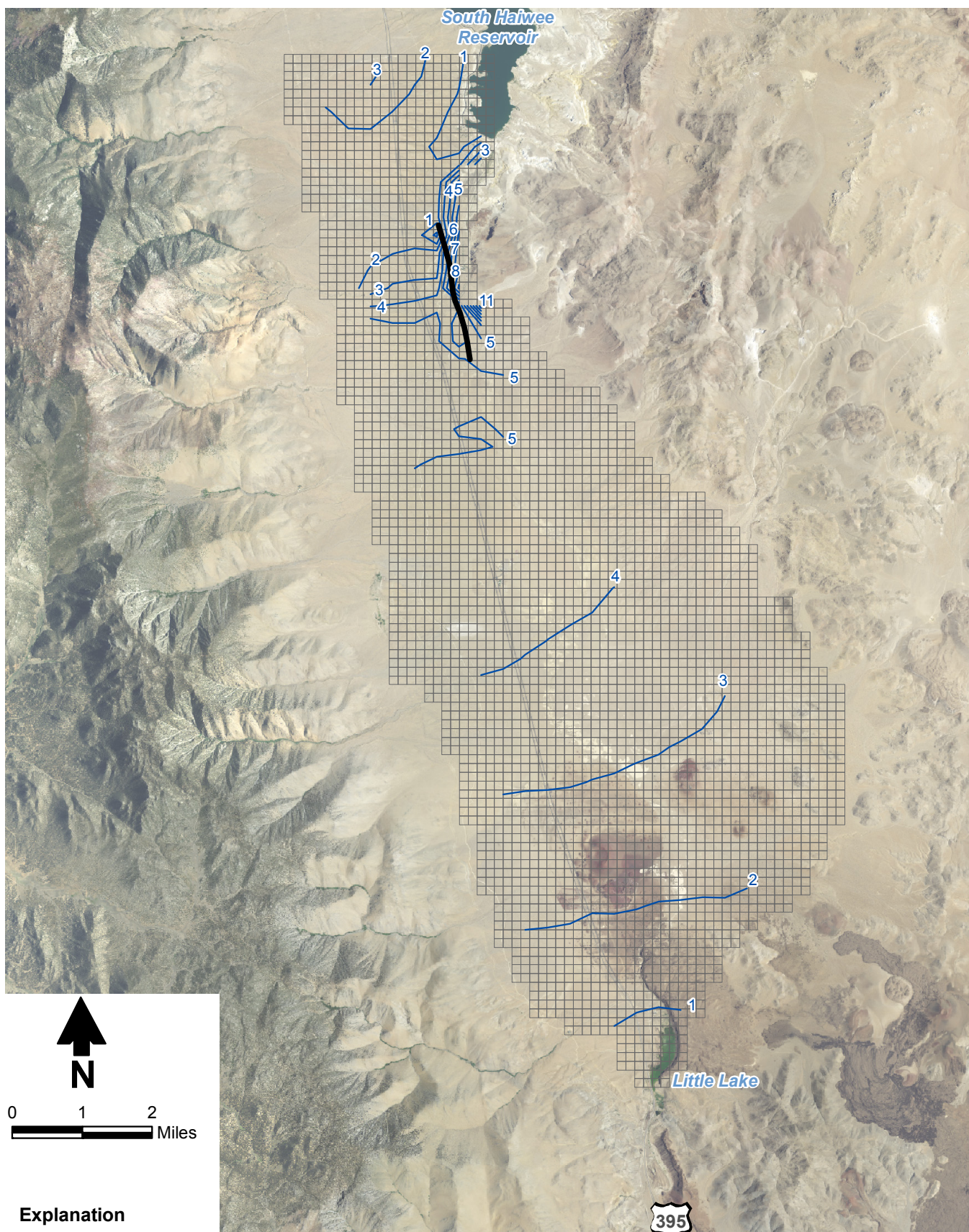


Daniel B. Stephens & Associates, Inc.
1/10/2011 JN LT09.0311

ROSE VALLEY MODEL
**Simulated Drawdown from 2009 Conditions at
Time of Minimum Flow to Little Lake (Scenario A)**

Figure 28

Q:\PROJECTS\LT09.0311_ROSE_VALLEY_MODEL\GIS\MXDS\FIGURES\FIGURE29_PREDICTIVE_DRAWDOWN_SCENARIO-B.MXD



Explanation

— Fault

— Layer 1 drawdown (ft)



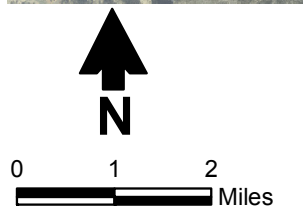
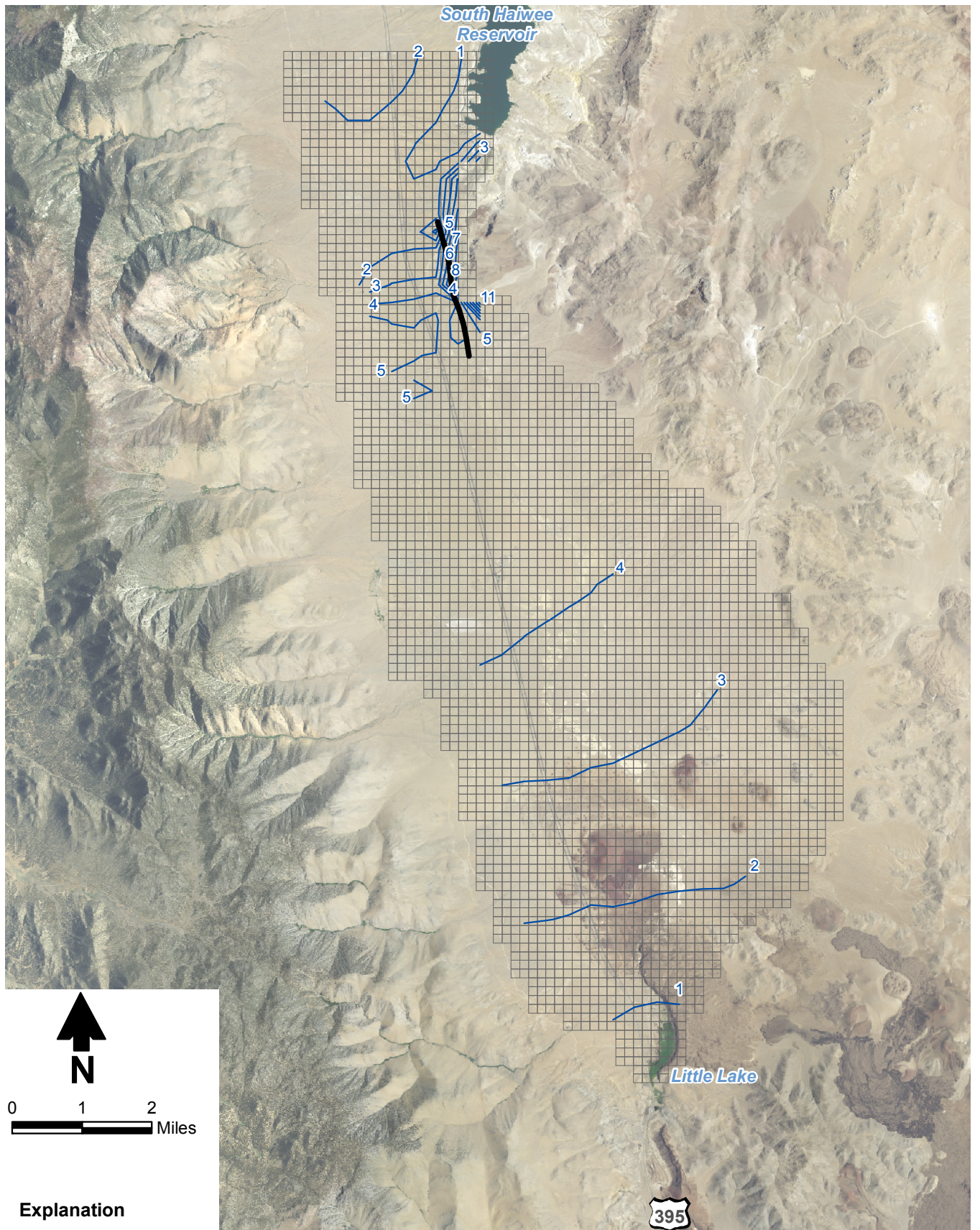
Daniel B. Stephens & Associates, Inc.
1/27/2011 JN LT09.0311

ROSE VALLEY MODEL

**Simulated Drawdown from 2009 Conditions at
Time of Minimum Flow to Little Lake (Scenario B)**

Figure 29

Q:\PROJECTS\LT09.0311_ROSE_VALLEY_MODEL\GIS\MXDS\FIGURES\FIGURE30_PREDICTIVE_DRAWDOWN_SCENARIO-C.MXD



Explanation

- Fault
- Layer 1 drawdown (ft)



Daniel B. Stephens & Associates, Inc.
1/27/2011 JN LT09.0311

ROSE VALLEY MODEL
**Simulated Drawdown from 2009 Conditions at
Time of Minimum Flow to Little Lake (Scenario C)**

Tables



Daniel B. Stephens & Associates, Inc.

Table 1. Simulation Mass Balance for Steady-State and Transient (1985 and 2009) Simulations

Source	Inflow/Outflow (acre-feet/year)			Notes
	Steady-State	1985	2009	
Groundwater Inflows				
Water released from storage due to declining hydraulic head	0	2,448	66	
Prescribed head boundaries	462	285	291	Portion of northern boundary (15 cells) in steady-state model; Haiwee Reservoir in transient model.
Recharge from toe-drain flows in The Narrows	0	1,712	964	Implemented using the well package
Recharge from precipitation	4,455	4,455	4,455	Implemented using the recharge package
Total inflows	4,917	8,898	5,777	
Groundwater Outflows				
Water that enters into storage due to increasing hydraulic head	0	41	727	
Groundwater pumping, non-Hay Ranch	0	597	34	Pumping for small Rose Valley users and LADWP (1985)
Hay Ranch groundwater pumping	0	3,216	0	Multi-node well package
Groundwater outflow to Little Lake	1,017	1,223	1,121	Drain package. Bauer (2002) estimated groundwater outflow to Little Lake to be 1,233 ac-ft/yr.
Evapotranspiration	21	337	23	Evapotranspiration package
General head boundaries	3,878	3,485	3,868	General head boundary package
Total outflows	4,917	8,899	5,772	



Daniel B. Stephens & Associates, Inc.

Table 2. Predictive Simulation Results

Monitor Well	Scenario A			Scenario B			Scenario C		
	Maximum Acceptable Drawdown (feet)	Time to Maximum Acceptable Drawdown (years since pumping began)	Drawdown at Cessation of Pumping (feet)	Maximum Acceptable Drawdown (feet)	Time to Maximum Acceptable Drawdown (years since pumping began)	Drawdown at Cessation of Pumping (feet)	Maximum Acceptable Drawdown (feet)	Time to Maximum Acceptable Drawdown (years since pumping began)	Drawdown at Cessation of Pumping (feet)
Dunmovin Well (RV040)	9.2	30.0	9.2	18.9	5.5	18.9	23.3	3.8	23.2
Cal Pumice Well (RV030)	9.2	30.0	9.2	18.9	5.5	18.9	23.3	3.8	23.2
HR1 Shallow Cluster Well (RV060)	11.8	1.0	10.0	23.5	5.5	23.5	31.3	3.7	31.3
HR2 Shallow Cluster Well (RV080)	9.9	1.0	9.5	21.2	5.5	21.2	27.6	3.7	27.6
Coso Junction Ranch Well (RV090)	6.6	30.1	6.6	10.7	5.8	10.5	11.7	4.0	11.3
Coso Junction Store #1 Well (RV100)	6.1	30.1	6.1	9.5	5.8	9.2	10.1	4.2	9.5
Red Hill Well (RV120)	3.6	31.3	3.5	3.9	9.0	2.6	3.9	7.8	1.8
Well G36 (RV130)	3.3	31.9	3.2	3.4	10.3	1.8	3.4	9.2	1
Lego Well (RV140)	2.5	34.2	2.3	2.3	14.5	0.4	2.3	13.5	0
Cinder Road Well (RV150)	2.2	33.2	2.1	2.3	12.4	0.6	2.3	11.4	0.2
Well 18-28 GTH (RV160)	2.2	33.7	2.0	2.1	13.5	0.4	2.1	12.5	0
Little Lake North Well (RV180)	1.3	33.9	1.2	1.4	13.5	0.2	1.3	12.5	0

Note: Scenario A: 3,000 acre-feet per year (ac-ft/yr) in 2010 followed by 790 ac-ft/yr for the next 29 years

Scenario B: 3,000 ac-ft/yr in 2010 followed by 3,000 ac-ft/yr for 4 years and 6 months

Scenario C: 3,000 ac-ft/yr in 2010 followed by 4,839 ac-ft/yr for 2 years and 8 months

Appendix A

Recharge Modeling Analysis for Rose Valley

Appendix A: Recharge Modeling Analysis for Rose Valley

January 28, 2011



Daniel B. Stephens & Associates, Inc.

6020 Academy NE, Suite 100 • Albuquerque, New Mexico 87109



Table of Contents

Section	Page
1. Introduction	A-1
1.1 Location, Physiography, and Climate	A-1
1.2 Surface Drainage.....	A-2
1.3 Vegetation	A-2
1.4 Geology	A-3
2. Recharge Processes.....	A-4
3. Previous Rose Valley Basin Recharge Estimates.....	A-6
4. Water Balance Modeling	A-7
4.1 Model Calculations	A-7
4.1.1 Precipitation	A-8
4.1.2 Water Transport and Storage	A-9
4.1.3 Runoff and Runon	A-11
4.1.4 Evapotranspiration	A-11
4.1.5 Net Infiltration (Recharge).....	A-18
4.2 Input Data	A-18
4.2.1 Climate.....	A-18
4.2.2 Soils	A-19
4.2.3 Bedrock.....	A-20
4.2.4 Vegetation.....	A-20
4.2.5 Topography.....	A-21
5. Results	A-22
References.....	A-24



List of Figures

Figure

- A-1 Location and Physiography of Rose Valley Basin
- A-2 Distribution of Vegetation in DPWM
- A-3 Distribution of Bedrock in DPWM
- A-4 Schematic of Water Balance Components and Computational Nodes Present in a Single Model Cell
- A-5 DPWM Area
- A-6 RAW Station in the Vicinity of Rose Valley Basin
- A-7 Total Annual Precipitation for Water Years 2000 to 2009
- A-8 Distribution of Soil Type in DPWM
- A-9 Distribution of Soil Depth in DPWM
- A-10 Mean Annual Net Infiltration Simulated by DPWM



List of Tables

Table

- A-1 Estimated recharge to Rose Valley Groundwater Basin from Precipitation
- A-2 Summary of General DPWM Input Values
- A-3 Soil Data for the Rose Valley Basin
- A-4 Geology and Saturated Hydraulic Conductivity
- A-5 Mean Maximum Rooting Depths and Plant Heights
- A-6 DPWM Simulated Annual Water Balance Budget



1. Introduction

One of the tasks that Daniel B. Stephens & Associates, Inc. (DBS&A) completed for Inyo County as part of the evaluation and update of the Rose Valley groundwater model is an independent estimate of natural recharge to groundwater within the Rose Valley Basin, Inyo County, California (Figure A-1). Brown and Caldwell (2006) estimated the recharge to the Rose Valley Groundwater Basin as 4,200 acre-feet per year (ac-ft/yr) and applied this value to develop a groundwater model. This quantity of recharge was also used in subsequent models developed for the draft and final EIRs (MHA, 2008a and 2008b). The U.S. Geological Survey (USGS) (2009) commented on the uncertainties in the estimation of recharge and the resulting effects of those uncertainties on the groundwater system, and recommended that recharge be reevaluated. Others (e.g., GEOSCIENCE, 2009) commented that the amount of recharge considered is conservative (smaller than would be expected).

The objective of this work is to estimate the amount of natural recharge that occurs to groundwater within the basin using the distributed parameter watershed model (DPWM) developed by DBS&A. This model is a “bucket” type soil-water-balance model, which evaluates precipitation, evapotranspiration, and resultant percolation through the soil column. The modeling approach includes some of the same methods applied in similar basin and range locations by the USGS (e.g., Flint and Flint, 2007). Although there are insufficient data to determine highly accurate or precise estimates of recharge to the Rose Valley aquifer, application of the DPWM allows for quantitative estimates based on site-specific climatological, geologic, soils, and vegetation factors.

1.1 Location, Physiography, and Climate

The Rose Valley Groundwater Basin consists of unconsolidated alluvial sediments underlying a north-south trending valley in southwest Inyo County and is bounded by the consolidated rocks of the Sierra Nevada on the west, the Coso Range on the east, and Little Lake Gap on the south. Merging alluvial fans descending from the Sierra Nevada on the west and the Coso Range on the east form the northern boundary of the basin. The area contributing recharge to the groundwater basin was defined for this study as the surface water watershed (watershed)



that includes the peaks of the Sierra Nevada with elevations of more than 9,000 feet above mean sea level (feet msl) and those in the Coso Range exceeding 6,000 feet msl (Figure A-1). The 37,000-acre watershed is 15 miles long oriented roughly north-south, and is about 4 miles wide.

The Rose Valley climate is arid, with hot dry summers and relatively cold dry winters. In general, precipitation increases with elevation while temperature decreases with elevation. In the winter, the precipitation falls as snow generally above 5,000 feet msl and as rain below this elevation. Precipitation also decreases from west to east, with higher precipitation on the western flanks of the Sierra Nevada just west of the watershed and lower precipitation in the rain shadow of the Sierra Nevada in the Rose Valley and the Coso Range. The average annual precipitation in the Rose Valley ranges from 5 to 7 inches, and occurs primarily in the late fall and winter months from November to March (CDWR, 1975, as cited by Bauer, 2002). Localized summer thunderstorms occur between July and September (Bauer, 2002).

1.2 Surface Drainage

There are many primary and secondary washes in the basin that are dry for the majority of the year and flow only in response to rapid rainfall or snowmelt. Ephemeral springs and channel flow can occur infrequently and in very small amounts elsewhere in the basin. The surface flow and the majority of the subsurface flow from the basin discharge into the Little Lake Ranch area, and from this area surface water and groundwater discharge through the Little Lake Gap into the Indian Wells Valley (Bauer, 2002; Williams, 2004).

1.3 Vegetation

Vegetation types vary considerably within the Rose Valley Basin watershed, from desert scrub at the lowest elevations to evergreen forests at the highest elevations. The distribution of vegetation types in the Rose Valley Basin used in the DPWM (Figure A-2) was obtained from digital land cover datasets provided by the California Gap land cover mapping project (Lennartz et al., 2008).



1.4 Geology

Rose Valley is within the Basin and Range physiographic province and is a graben between the Sierra Nevada to the west and the Coso Range to the east. The surface geology of Rose Valley consists primarily of alluvial sediments with significant areas of basalt flows in the south. The Sierra Nevada are primarily granodiorite, while the Coso Range consists primarily of rhyolite, granodiorite, and basalt. Figure A-3 shows the distribution of bedrock used in the DPWM.



2. Recharge Processes

For the purposes of this work, recharge is defined as atmospheric water that falls to the ground surface and reaches the regional water table within the Rose Valley Basin watershed boundaries. The recharge potential depends on a variety of factors, including the amount and duration of precipitation, surficial and bedrock geology, soil depth and permeability, land surface slope and orientation, and vegetation. Although potential evapotranspiration may exceed precipitation on an annualized basis over a basin, during winter or early spring months or during brief and intense summer storms, potential evapotranspiration can be less than precipitation, and it is at these times where the greatest potential for recharge exists.

For recharge to occur, precipitation must rapidly pass through the soil column or it will be removed through evapotranspiration. In order for this to happen, the amount of water available for infiltration in a given location must exceed the rate of evapotranspiration and the storage capacity of the soil column. In a climate such as that of Rose Valley, this condition occurs as focused recharge, such as collection of water in a depression or in a stream channel, or broad recharge on the thin soils of the mountain block. In the Rose Valley Basin there are four general types of recharge that are likely to occur: mountain block recharge, mountain front recharge, local recharge, and diffuse recharge. Each of these types of recharge is discussed below.

In the more mountainous terrain where bedrock is exposed, mountain block recharge occurs because there is little to no soil and bare rock is exposed at the surface, and vegetation is sparse because there is little potential for the storage of moisture for subsequent use by plants during dry periods. The potential for water to infiltrate is highest where the bedrock is permeable or highly fractured. The greatest amount of recharge is usually expected to occur at the higher elevations where precipitation is greater, soils are thinner, and the bedrock is permeable.

Some of the precipitation that falls on the mountain terrain runs off in ephemeral washes and becomes recharge in the transition zone between the mountain block and the valley floor. This recharge process is termed mountain front recharge (e.g., Wilson and Guan, 2004). The



mountain front recharge receives contributions from major washes and perhaps hundreds of other minor washes that collect water as it runs off of the mountain block.

Local recharge may occur in places such as along unvegetated sandy drainages in the interior of the basin or where water may temporarily pond. At these places, focused infiltration and deep percolation from the infrequent storms can lead to recharge.

Precipitation that infiltrates on the broad lowland areas between washes percolates through surficial soils and is stored as soil moisture. The vast majority of this soil water is captured by desert vegetation and becomes evapotranspiration. However, what is not captured may migrate downward toward the water table, especially at the higher elevations of the valley floor or where there are deep fissures or macropores. This type of recharge is called diffuse recharge, and is generally very small in desert basins.



3. Previous Rose Valley Basin Recharge Estimates

Rose Valley Groundwater Basin recharge estimates from previous studies are summarized in Table A-1; they range from 611 to 4,700 ac-ft/yr.

National Weapons Center (U.S. NWC, 1978, as cited by Rockwell International, 1980) estimated 611 ac-ft/yr of recharge. Rockwell International (1980) concluded that the recharge estimates are rough approximations at best, and estimated a range of 1,900 to 3,000 ac-ft/yr. Williams (2004) reports that Saint-Amand (1986) estimated the basin recharge at 800 ac-ft/yr. Brown and Caldwell (2006) estimated the recharge by assuming 10 percent of the total precipitation occurring above an elevation of 4,500 feet msl. They estimate a range of potential values from 1,348 to 6,705 ac-ft/yr, but select 4,191 ac-ft/yr as a reasonable estimate. Williams (2004) estimated 4,000 ac-ft/yr based on a relative comparison of recharge estimated to originate from the Sierra Nevada west of Rose Valley and adjacent to Indian Wells Valley. Williams (2004) states that his estimate may be low for recharge from the Sierra Nevada adjacent to Rose Valley, and his estimate does not include any recharge from the Coso Range.

The USGS (2009), in comments on the draft EIR (MHA, 2008a), provide 2,350 to 4,700 ac-ft/yr as the likely range of natural recharge from precipitation. This estimate is based on the regional basin characterization model (BCM) and also accounts for uncertainties in the BCM estimates. The USGS also estimated the approximate contribution from the Sierra Nevada as 2,040 to 4,070 ac-ft/yr, and from the Coso Range as 310 to 630 ac-ft/yr. Although the BCM and DPWM are similar in many respects, the BCM does not route surface water runoff within the watershed; rather, the contribution to recharge from runoff is an assumed percentage for the region (Flint et al., 2004).



4. Water Balance Modeling

DBS&A developed a DPWM based on the MASSIF model developed by Sandia National Laboratory (2007) for Yucca Mountain. The DPWM is similar in concept to water balance models used by the USGS (e.g., PRMS [Leavesley et al., 1983]; INFIL [Hevesi et al., 2003]; BCM [Flint and Flint, 2007]). The DPWM uses a daily time step over variable grid cell sizes that range up to 8,100 square meters (m^2) (90 meters by 90 meters). The model generally relies on the widely accepted FAO-56 procedure for computing actual evapotranspiration (AET) from the reference evapotranspiration (ET_0) estimated with the Penman-Monteith method (Allen et al., 1998 and 2005). Water budget components accounted for in the model include precipitation, bare soil evaporation, transpiration, runoff, runoff, snow accumulation, snowmelt, snow sublimation, soil water storage, and net infiltration. A bedrock boundary is placed at the bottom of DPWM model cells with shallow soil depths; this boundary will restrict infiltration when the saturated hydraulic conductivity of the bedrock is less than that of the soil. Unlike the USGS BCM, DPWM accounts for the routing of runoff through the watershed and, unlike the MASSIF model, the DPWM accounts for focused flow in washes using a mass balance approach and variable cell sizes.

4.1 Model Calculations

To conduct the water balance, the model domain for the area of interest was divided into a grid consisting of 89,324 cells, ranging in size from 2,900 square feet up to 87,188 square feet (2 acres). Note that this model grid is not the same as the groundwater (MODFLOW) model grid. The watershed contributing to the Rose Valley groundwater system is a subset (43,182 cells) of the DPWM domain. In each cell, the soil profile is divided into three layers with four nodes (Figure A-4). The upper layer (Layer 1) has bare soil evaporation and transpiration, and its thickness is based on the maximum depth of bare soil evaporation ("evaporation layer depth" [Z_e] in FAO-56 [Allen et al., 1998]). Layer 1 is divided into two nodes (Nodes 1 and 2). Node 1 is the bare soil fraction of the cell where evaporation is dominant, and Node 2 is the fraction of the cell surface covered by vegetation canopy where transpiration is dominant. Bare soil evaporation does not occur in Node 2, but transpiration occurs to some degree in both Nodes 1



and 2. The areas of Nodes 1 and 2 are adjusted over the year as the vegetation grows, peaks, and then declines based on the basal transpiration coefficient (K_{cb}).

The second layer (Layer 2 and Node 3) represents the remainder of the root zone for the vegetation type; its thickness is the maximum rooting depth minus the thickness of Layer 1. Transpiration is dominant in Layer 2, but some diffuse evaporation also occurs.

The final layer (Layer 3) represents the thickness of soil below the root zone and allows no transpiration or evaporation. The thickness of Layer 3 is the depth to bedrock minus the thicknesses of Layers 1 and 2. In cells with deep alluvium, the thickness is limited to 20 meters minus the root layer thicknesses. Drainage from Layer 3 is limited by the bedrock saturated hydraulic conductivity when it is less than the soil saturated hydraulic conductivity.

4.1.1 Precipitation

Daily precipitation is provided as input to the model using the Five Mile California RAWS data, and the daily data are spatially distributed over the watershed based on the parameter-elevation regressions on independent slopes model (PRISM) estimate of the normal mean precipitation for the period 1971-2000 (Daly et al., 1994). PRISM provides annual average and monthly precipitation data developed from multiple weather station locations located throughout the region. PRISM data vary precipitation by elevation and account for orographic effects (e.g., rain shadows). When precipitation occurs in a given day in the RAWS data, it is assumed that it occurs over the entire modeled watershed domain.

4.1.1.1 Duration of Precipitation Events

Each daily time step of the water balance model is divided into two steps when precipitation occurs: (1) the water balance for the duration of precipitation event and (2) the water balance for the remainder of the day. The duration of each precipitation event was assumed to be 12 hours except during the months of July through September, when the storm duration was assumed to be 2 hours. In the case of a day with snowmelt, the duration of precipitation is assumed to be 12 hours.



4.1.1.2 Snow

When the daily average temperature is below 32°F and precipitation occurs, the precipitation occurs as snow. Precipitation may occur as both rain and snow on a given day in the watershed because air temperature varies with elevation. The snow is stored as an equivalent depth of water in the model. In the time step with snow accumulation, a specified fraction of the snow is removed by sublimation that represents the entire sublimation for the water year. This approach accurately simulates the annual quantity of sublimation but does not necessarily accurately reproduce daily sublimation rates. However, this simplification is not expected to significantly influence the estimate of net infiltration. The model uses a sublimation rate of 15 percent of the snowpack based on research conducted in the Colorado Front Range (Hood et al., 1999).

When snowpack is present and the average daily temperature is above 32°F, the snow melts at the snowmelt rate specified in the input files. The rate of snowmelt varies from 2.0 millimeters per day per degree Celsius (mm/d/°C) on December 21 to 5.2 mm/d/°C on June 21 using the methodology in the HELP model (Schroeder et al., 1994).

4.1.2 Water Transport and Storage

The DPWM routes soil-water in the subsurface using a field capacity approach similar to other water balance models such as MASSIF, HELP, INFIL, and BCM. The field capacity approach, also referred to as a bucket model, allows instant drainage of all water that exceeds the field capacity of the soil, which is typically equivalent to the water content of a given soil at 1/10 or 1/3 bar. The field capacity approach computes downward drainage from the evaporative layer (Layer 1) to the root zone layer (Layer 2) to the sediments between the root zone and bedrock (Layer 3). Water is routed downward at a rate that is limited by the hydraulic conductivity of the layer or, where the layer is overlying bedrock, by the saturated hydraulic conductivity of the bedrock. Once net infiltration has been computed from the bottom layer, any water that exceeds the maximum holding capacity of the layer is passed back up. If water in the uppermost layer exceeds the maximum holding capacity, then the water is passed to the downstream cell as runoff.



Water is accounted for in the DPWM cell nodes as an equivalent depth of water in the node per unit area, termed “water level”. Water level is related to the average volumetric water content (θ) in a node, as follows:

$$\text{Water level (mm)} = \theta \text{ (m}^3/\text{m}^3) \cdot \text{node thickness (mm)} \quad (\text{Eq. 4-1})$$

Similarly, the maximum water level, field capacity water level, and wilting point water levels are computed as follows:

$$\text{Field capacity water level (mm)} = \theta_{fc} \text{ (m}^3/\text{m}^3) \cdot \text{node thickness (mm)} \quad (\text{Eq. 4-2})$$

$$\text{Maximum water level (mm)} = \theta_s \text{ (m}^3/\text{m}^3) \cdot \text{node thickness (mm)} \quad (\text{Eq. 4-3})$$

$$\text{Wilting point water level (mm)} = \theta_{wp} \text{ (m}^3/\text{m}^3) \cdot \text{node thickness (mm)} \quad (\text{Eq. 4-4})$$

The field capacity and wilting point water contents are computed from the capillary pressure head provided by the user as model input using the van Genuchten parameters (van Genuchten, 1980). The model used a field capacity of $-1/10$ bar and a wilting point of -60 bars. The wilting point is much greater than the typical -15 -bar limit found for agricultural vegetation because desert vegetation can extract water at much greater capillary pressures than agricultural crops.

Drainage is assumed to be dominant during the period when precipitation is applied. Most storms occur over a period less than the duration of the daily model time step. To better simulate processes during partial-day events, the hydraulic conductivity of the soil or rock is adjusted downward in proportion to the percentage of the day over which the storm occurs. The saturated or unsaturated hydraulic conductivity is modified for the duration of the precipitation or non-precipitation event, as follows:

$$K_{\text{modified}} \text{ (mm/d)} = K \text{ (mm/d)} \cdot (\text{duration (hrs)} / 24 \text{ hrs}) \quad (\text{Eq. 4-5})$$

If there is snowmelt, the duration is set to 12 hours. This modification also applies to the bedrock saturated hydraulic conductivity.



4.1.3 Runoff and Runon

Runoff occurs in a cell when the upper model layer (Layer 1) exceeds saturation or the rate of water application over the storm fraction of the day exceeds the saturated hydraulic conductivity of the soil or rock. Runoff is routed to the lowest adjacent grid cell elevation based on the 90-meter digital elevation model (DEM). A cell can receive runoff from up to seven adjacent cells, but provides runoff to only one downstream cell. All surface water is routed through the model in one day.

Cells that contain washes are divided into two cells based on the active area of wash within the cell. The total active area of wash is calculated as the length of the wash within the cell times the width of the wash. Washes were classified into three types of widths: (1) major washes with a width of 10 meters, (2) intermediate washes with a width of 5 meters, and (3) minor washes with a width of 3 meters. The major, minor, and intermediate washes were classified from the DEM based on the flow accumulation of cells upstream. The total active wash area defines the size of the new grid cell within the standard model grid cell of 90 meters by 90 meters (8,100 m²). The remaining area becomes an interwash cell. The routed runoff in washes remains within the wash until it completely infiltrates, reaches the basin exit, or, in some minor cases, when the wash channel simply dumps out onto an area of the basin. The soil properties of the wash soils are specified separately from other soils in the DPWM input files. The soil depth of the wash cell is the same as that of the interwash cell.

4.1.4 Evapotranspiration

For evapotranspiration, the model relies on the widely accepted FAO-56 procedure for computing actual evapotranspiration (AET) from the reference evapotranspiration (ET₀) estimated with the Penman-Monteith method (Allen et al., 1998). The FAO-56 method (Allen et al., 1998) computes a reference evapotranspiration value using the Penman-Monteith equation that represents evapotranspiration from an extensive surface of green grass of uniform height, actively growing and adequately watered. The reference evapotranspiration is modified for any agricultural or natural vegetation type using crop coefficients (K_{cb}). A coefficient of 1.0 represents the reference grass vegetation. Coefficients less than 1 represent less dense



vegetation, while coefficients greater than 1 represent dense vegetation. The FAO-56 method supplies equations for computing crop coefficients for natural vegetation using site-specific climate data and a measure of the vegetation density such as the leaf area index (LAI). The Penman-Monteith evapotranspiration computation in FAO-56 includes adjustments for cloud cover when precipitation occurs and adjustments for sky clearness. The general horizontal solar radiation for the basin is modified for each model cell based on the slope and aspect of the land surface.

Evapotranspiration is computed after the computation of infiltration and runoff. The actual total evapotranspiration for a cell on a given day is calculated as follows:

$$ET = ET_0 (K_r K_e + K_s \cdot K_{cb}) \quad (\text{Eq. 4-6})$$

where ET_0 = the reference evapotranspiration based on climate parameters

K_r = the evaporation reduction coefficient

K_e = the soil evaporation coefficient

K_s = the water stress coefficient

K_{cb} = the basal transpiration coefficient

4.1.4.1 Reference Evapotranspiration (ET_0)

The reference evapotranspiration represents the evapotranspiration from a reference crop without any water limitations. The reference crop used in DPWM is the standard FAO-56 short crop that closely resembles an extensive surface of green grass of uniform height, actively growing, completely shading the ground and with adequate water (Allen et al., 1998). The equation for ET_0 is as follows:

$$ET_0 = \frac{0.408\Delta(R_n - G) + \gamma \frac{900}{T + 273} U_2 (e_s - e_a)}{\Delta + \gamma(1 + 0.34U_2)} \quad (\text{Eq. 4-7})$$

where: ET_0 = reference crop evapotranspiration (mm/d)

R_n = solar radiation at crop surface ($\text{MJ m}^{-2}/\text{d}$)

G = soil heat flux density ($\text{MJ m}^{-2} \text{d}^{-1}$)



- T = mean daily air temperature at 2-meter height ($^{\circ}\text{C}$)
 e_s = saturated vapor pressure (kPa)
 e_a = actual vapor pressure (kPa)
 U_2 = mean daily wind speed at 2-meter height (m/s)
 Δ = slope of the vapor pressure curve (kPa/ $^{\circ}\text{C}$)
 γ = psychrometric constant (kPa/ $^{\circ}\text{C}$)

The methods used to determine each term in the equation and to calculate ET_0 are documented by Allen et al. (1998). Some model-specific calculations and adjustments are described below.

4.1.4.1.1 Vapor Pressure Deficit. The influence of humidity on the reference evapotranspiration is based on the vapor pressure deficit that is the difference between the cell saturation vapor pressure (e_s) and the basin actual vapor pressure (e_a). The vapor pressure deficit represents the pressure gradient driving transpiration. The saturation vapor pressure (e_s) is calculated for each cell based on the minimum and maximum air temperatures. The actual saturation vapor pressure (e_a) is generalized for the basin based on the dewpoint temperature at the average basin elevation. The dewpoint temperature is estimated from the minimum daily temperature at the reference weather station that is lapse corrected to the basin average elevation, and then an additional correction factor, the dewpoint offset, is subtracted from the minimum daily temperature to account for the aridity of the basin. The dewpoint offset typically ranges from 2 to 4 degrees and should be limited to a maximum value of about 5 degrees as ET_0 is the estimate of evapotranspiration for the reference grass surface, which is more humid than the native vegetation (Allen, 2010).

4.1.4.1.2 Hargreaves' Adjustment Coefficient for Solar Radiation. The Hargreaves' equation allows for the estimation of incoming solar radiation based on the difference between the maximum and minimum air temperatures, extraterrestrial radiation, and the Hargreaves' adjustment coefficient (K_{rs}). The K_{rs} typically ranges from 0.16 to 0.19 and can be obtained by calibration to measured solar radiation on clear sky days. The value of 0.19 represents nearly clear sky, which is expected of the Rose Valley Basin. The incoming horizontal solar radiation is generalized for the basin based on the average elevation and latitude. The horizontal incoming solar radiation is then adjusted for the slope and azimuth of the model cell.



4.1.4.1.3 Adjustment of Solar Radiation for Precipitable Water, Sun Angle, Atmospheric Thickness, and Turbidity. The FAO-56 method provides adjustments for solar radiation based on the average angle of the sun for the time of year, turbidity in the atmosphere, atmospheric thickness, and precipitable water (Allen et al., 1998; Allen et al., 2005, Equation D-2). The adjustment for turbidity ranges from 0.5 or less for extremely turbid, dusty, or polluted air up to 1.0 for clean air. As recommended by Allen et al. (2005) for routine prediction of solar radiation and based on the calibrated sky clearness index, a value of 1.0 was used for the turbidity coefficient for the Rose Valley. The average sun angle for the day of the year was computed using Equation D-5 in Allen et al. (2005). The amount of precipitable water in the atmosphere was generally estimated for the basin based on the vapor pressure and average basin elevation (Allen et al., 2005, Equation D-3). The adjustment for atmospheric thickness is simply based on the atmospheric pressure at the cell estimated from elevation (Allen et al., 2005, Equation 3).

4.1.4.1.4 Adjustment of Solar Radiation for Slope and Azimuth. The author of the FAO-56 method, Dr. Richard Allen, along with other collaborators, developed a method to adjust the daily solar radiation for slope and azimuth (Trezza and Allen, 2006). The translation procedure for slope and azimuth follows the methods published by Reindel et al. (1990) and Duffie and Beckman (1980 and 1991).

4.1.4.2 Actual Evapotranspiration

Actual evapotranspiration (AET) is computed from the reference evapotranspiration based on the relative fractions of bare soil evaporation and transpiration. Without any water limitations, the actual evapotranspiration will be equivalent to crop evapotranspiration (ET_c), as follows (Allen et al., 1998, Equation 69):

$$ET_c = (K_{cb} + K_e) ET_0 \quad (\text{Eq. 4-8})$$

where ET_c = the crop evapotranspiration

K_{cb} = the basal crop coefficient (e.g., transpiration component of ET_c)

K_e = the surface evaporation coefficient

ET_0 = the reference evapotranspiration based on climate parameters



The sum of K_{cb} and K_e is the crop coefficient K_c , and can never exceed a maximum value (K_{cmax}) based on the available energy from the sun. As water is depleted from the root zone, the values of K_e and K_{cb} are reduced using the evaporation reduction coefficient (K_r) and the water stress coefficient (K_s), respectively. The relative proportion of surface evaporation is also controlled by the fraction of ground covered by the vegetation canopy. Surface evaporation is only dominant in the uncovered or bare soil fraction (Node 1 of Layer 1 in the model). The basal crop coefficient includes a small fraction of diffuse evaporation from beneath the vegetation canopy but is dominated by the transpiration. Transpiration occurs from Node 2 of Layer 1 and all of Layer 2 (Node 3) in the model.

Transpiration is zero ($K_{cb} = 0$) when the average air temperature for the day is less than 5°C (41°F) based on observations of transpiration in Juniper trees (Bedell et al., 1993). Evaporation from the upper soil layer may still occur when K_{cb} is zero because the evaporation coefficient (K_e) is equal to $K_{cmax} - K_{cb}$.

4.1.4.2.1 Evaporation Reduction Coefficient (K_r). As the depth of water stored in the soil is depleted below field capacity (termed the depletion level [D_e]), the rate of evaporation and transpiration can decrease from the maximum. There are several variables computed in the FAO-56 method based on field capacity, wilting point, and soil texture (Allen et al., 1998). Evaporation is only computed for Node 1 in Layer 1.

The total evaporable water (TEW) is the total amount of water available for evaporation and is computed in the FAO-56 method as follows:

$$TEW = (\Theta_{fc} - 0.5\Theta_{wp}) Z_e \quad (\text{Eq. 4-9})$$

where Z_e = the thickness of layer (typical range is 0.1 to 0.15 meter)

Θ_{fc} = the field capacity

Θ_{wp} = the wilting point

The term $0.5\Theta_{wp}$ implies that the water content can be reduced with evaporation below a level that can be removed by transpiration. The Z_e was conservatively set to the upper end of the



range recommended in FAO-56 (0.15 meter); the greater depth of the evaporative layer allows for more water to be stored and depleted by evaporation.

The amount of water that is readily evaporable (REW) is determined from soil texture (Allen et al., 1998, Table 19), and ranges from 2 to 7 millimeters (mm) for sand up to 8 to 12 mm for clay. A value of 8 mm was selected for the model based on the predominance of loamy soils found in the basin).

TEW and REW are used to determine the reduction in evaporation rate (K_r , ranges from 0 to 1) (Allen et al., 1998, p. 145), as follows:

$$K_r = \frac{TEW - D_e}{TEW - REW} \quad (\text{Eq. 4-10})$$

4.1.4.2.2 Water Stress Coefficient (K_s). The water stress coefficient is based on the total amount of water available for transpiration (TAW), defined in FAO-56 (Allen et al., 1998) as follows:

$$TAW \text{ (mm)} = \frac{1,000 \text{ mm}}{m} (\Theta_{fc} - \Theta_{wp}) Z_r \text{ (m)} \quad (\text{Eq. 4-11})$$

where Θ_{fc} = the field capacity water content
 Θ_{wp} = the wilting point water content
 Z_r = the mean maximum rooting depth

At first, as the water level is reduced below field capacity, there is no water stress reduction in transpiration (i.e., $K_s = 1$). This fraction of TAW that is readily available for transpiration (RAW) is computed as follows:

$$RAW \text{ (mm)} = p \cdot TAW \text{ (mm)} \quad (\text{Eq. 4-12})$$

where p is the average fraction of total available soil water (TAW) that can be depleted from the root zone before moisture stress occurs (ranges from 0 to 1) (Allen et al., 1998, p. 162). This



depletion factor (p) depends on the evapotranspiration rate and the rooting depth of the plants. Where daily evapotranspiration is high (greater than 8 millimeters per day [mm/d]) and plant roots are shallow, p is typically 0.3. Where daily evapotranspiration is low (less than 3 mm/d) and plant roots are deep, p is typically 0.7. Typically a value of 0.5 is chosen (Allen et al., 1998) and a uniform value of 0.5 was used for Rose Valley Basin.

The transpiration reduction factor (K_s) is computed from TAW, root zone depletion (D_r = field capacity water level – root zone water level), and RAW, as follows:

$$K_s = \frac{TAW - D_r}{TAW - RAW} \quad (\text{Eq. 4-13})$$

4.1.4.2.3 Canopy Coefficients. As plant growth increases, the fraction of ground covered by the plant canopy (f_c) increases. Bare soil evaporation does not take place under the canopy, leaving more water for transpiration. As plants begin to decline and enter a dormant phase, the plant canopy decreases. This change is modeled using the equation recommended by the FAO-56 method (Allen et al., 1998, Equation 76), as follows:

$$f_c = \left(\frac{K_{cb} - K_{cmin}}{K_{cmax} - K_{cmin}} \right)^{\left(1 + \frac{1}{2}h_{plant}\right)} \quad (\text{Eq. 4-14})$$

where K_{cb} = the basal crop coefficient

K_{cmax} = the maximum crop coefficient based on available energy

K_{cmin} = the minimum crop coefficient

h_{plant} = the mean maximum plant height

The canopy coefficient defines the relative fractions of Nodes 1 and 2 in each cell. As f_c changes and the sizes of Nodes 1 and 2 change, water is appropriately transferred between Nodes 1 and 2 to maintain the water balance.



4.1.5 Net Infiltration (Recharge)

After evaluating precipitation, water storage, and surface runoff for each daily time step, the model calculates net infiltration or recharge. Net infiltration is the quantity of water that passes below the root zone using the field capacity method, where downward drainage ceases below the field capacity pressure point and upward movement of soil-water does not occur. The field capacity method is a simplification of soil-water movement, but is a valid approach for watershed-scale simulations. The net infiltration is potential recharge that often reaches the water table but may be intercepted by perched zones and discharged at springs. Depending on the depth to groundwater and infiltration rate, the net infiltration may take years, decades, or possibly even centuries to reach groundwater. However, the average quantity of net infiltration below the root zone is similar to the average quantity of groundwater recharge as the dry, average, and wet pulses average out in the vadose zone. Although it may take a long time to reach the regional water table, the net infiltration is considered to represent recharge at the time it passes below the root zone. The assumption is made that over time this water will continue to migrate downward to the regional water table and will not be lost to evapotranspiration, permanent storage in the vadose zone, or discharge to surface water such as seeps and springs.

4.2 Input Data

Data were collected from weather stations operated by a variety of entities, site-specific literature sources, general literature sources, and/or were estimated from other properties. General model parameters including average latitude and elevation within the basin are summarized in Table A-2. The model domain is the Rose Valley Basin watershed (Figure A-5).

4.2.1 Climate

Direct climate inputs to the DPWM include daily total precipitation, maximum daily air temperature, minimum daily air temperature, and average daily wind speed. Climate data for calibration of the water balance model used the observed data collected at the Five Mile California RAWS adjacent to the Rose Valley Basin (Figure A-6). Based on the period of data



availability from the Five Mile California RAWs, the Rose Valley water balance was simulated for the 10-year period 2000 to 2009. Figure A-7 shows the total annual precipitation for water years 2000 to 2009.

Reference air temperature data were obtained from Five Mile California RAWs and were lapse corrected for elevation based on the mean annual maximum temperature predicted by PRISM for the 1971–2000 normal period. The lapse rate is -7.8 degrees Celsius per kilometer ($^{\circ}\text{C}/\text{km}$). Wind speed data are obtained from the Five Mile California RAWs at an elevation of 4,150 feet msl.

4.2.2 Soils

Soils data were obtained from the USDA STATSGO database, which contains electronic data from field surveys conducted by the USDA in Inyo County including the Rose Valley Basin. More detailed SSURGO data were available on only a limited basis for Inyo County; consequently, this dataset was not applied. Soil type and depth data are presented on Figures A-8 and A-9, respectively. Tabular soil data are presented on Table A-3.

The USDA databases provide texture data (percent sand, silt, and clay), saturated hydraulic conductivity, dry bulk density, saturated water content, and water contents at 1/3 bar and 15 bars for each soil horizon. A weighted average is computed for each soil map unit based on the volume represented by the soil horizon (horizon layer thickness x fraction of map surface area). The water retention characteristics were estimated using the Rawls and Brakensiek (1985) method (Table A-3) with the soil texture data, water contents, and bulk densities obtained from the USDA database. The USDA reports depth to bedrock ranges for depths shallower than 5 feet. For soils specified as greater than 5 feet in thickness by the USDA, the soil depths were assumed to be far greater than the maximum rooting depth of any vegetation association (20 meters).



4.2.3 Bedrock

Bedrock underlying the soils of the Rose Valley Basin may restrict net infiltration when the saturated hydraulic conductivity of the bedrock is less than the infiltration rate and soils are shallow. The distribution of bedrock types was obtained from geologic maps of California (Ludington et al., 2007). The saturated hydraulic conductivities were estimated from literature sources as shown in Table A-4.

4.2.4 Vegetation

The spatial distribution of the vegetation in the Rose Valley Basin is shown in Figure A-2. The valley floor and the lower elevations of the Sierra Nevada are predominantly desert shrub and scrub, while the higher elevations of the Sierra Nevada are primarily evergreen forest.

4.2.4.1 Rooting Depths of Vegetation Associations

Table A-5 summarizes the rooting depths assigned to each vegetation association in DPWM simulations. Most roots were assumed to be 2 meters in depth, with the exception of grasslands at 1 meter and trees (both riparian woodlands and evergreen forests) at 3.3 meters. The rooting depth determines the total thickness of Layers 1 and 2 unless bedrock is present at a shallower depth. It is assumed that rooting density in bedrock is not significant.

4.2.4.2 Mean Maximum Plant Height

Table A-5 summarizes the mean maximum plant height for vegetations associations in the Rose Valley Basin. Plant heights greater than 2 meters are treated as 2 meters in the FAO-56 method (Allen et al., 1998), and the plant height generally has little influence on the estimation of net infiltration. Plant heights range from 0.3 meter for grasslands up to 12 meters for evergreen forests.

4.2.4.3 Leaf Area Index and Phenology

LAI is the ratio of one-sided leaf area over the total land area (L^2/L^2). Values of LAI were obtained from datasets published by the National Aeronautics and Space Administration (NASA) from the MODIS satellites (USGS, 2010) on a monthly basis for the very wet water year



of 2005 (October 2004 through September 2005). The pattern of LAI measured by MODIS was also used to determine the phenology for the vegetation associations (initiation of leaves, peak growing season, decline in growth, and dormant season) on a monthly basis. The scale of the MODIS is coarse at 1-km grid cell sizes, but represents measurements of actual vegetation within the Rose Valley.

4.2.5 Topography

Topography in the model was derived from USGS DEMs at 90-meter grid scales. The DPWM grids used the slope, azimuth and elevation, and the routing of flow as predicted by the 90-meter DEM and the geographic information system (GIS) delineated washes.



5. Results

Water balance components were determined for the water years 2000 to 2009 and are provided in Table A-6. The estimated mean precipitation within the watershed boundary is about 54,000 acre-feet. The DPWM simulated 9 percent of the estimated precipitation (4,900 acre-feet) as the net mean recharge to the Rose Valley groundwater system. The distribution of mean annual net infiltration for the DPWM simulation is presented in Figure A-10.

The majority of the simulated recharge occurs in the Sierra Nevada and through the beds of the washes that originate from the Sierra Nevada. There is negligible diffuse natural recharge simulated between the washes on the Rose Valley floor, a result that is consistent with the observations in previous studies (e.g., Phillips, 1994). The simulated mean runoff that exits the watershed boundary is about 600 ac-ft/yr, and ranges from 7 to 2,300 ac-ft/yr. This estimate of runoff must be considered highly approximate due to the limited nature of the flow routing algorithms employed in the DPWM.

The final recharge used in the groundwater model is slightly different than that estimated using DPWM. The total estimated mountain front recharge from the Sierra Nevada was reduced by 5 percent, from 3,246 ac-ft/yr to 3,084 ac-ft/yr, as a rough approximation to account for recharge that occurs in the mountain block but reemerges as spring flow outside the groundwater model domain. This spring flow is assumed to be lost to evapotranspiration. In addition, 206 ac-ft/yr of recharge estimated to occur in the Coso Range at the southern and southeastern ends of Rose Valley is excluded from the groundwater model, as groundwater flow beneath the Coso Range in this area is believed to be south or southeast toward the Indian Wells Valley, rather than north or northwest toward Rose Valley. The estimated Rose Valley recharge from precipitation implemented in the groundwater model, is therefore 4,493 ac-ft/yr, distributed as follows:

- Mountain block and mountain front recharge from the Sierra Nevada: 3,084 ac-ft/yr
- Mountain block and mountain front recharge from the Coso Range: 918 ac-ft/yr
- Focused recharge along drainages within the MODFLOW model domain: 491 ac-ft/yr



In the final groundwater model, the actual recharge is slightly less than the total noted above (4,455 ac-ft/yr) due to some simulated dry cells along the mountain front at the southern end of the model domain.

The calculated mean annual recharge is applied for each simulation period (steady-state, historical, and predictive) in the model. Although it is possible that cyclical drought and wet periods may lead to corresponding changes in water levels, such changes are not discernable based on the observed water level dataset for Rose Valley. Furthermore, the effects on water levels of variable amounts of recharge that may occur from year to year will tend to be muted as the recharge moves through the fractured rocks and shallow alluvium of the mountain fronts toward the basin-fill sediments of Rose Valley that constitute the primary aquifer system. Water levels in wells close to drainages that are sources of significant recharge may respond to specific periods of higher and lower recharge, although this recharge mechanism is calculated to represent only 11 percent of the total mean annual value. The simulation approach of applying calculated mean annual recharge may warrant reconsideration in future work as additional data become available.



References

- Allen, R.G. 2010. E-mail communication from Richard G. Allen to Todd Umstot, Daniel B. Stephens & Associates, Inc., and Jan Hendrickx regarding A dewpoint offset question. March 22, 2010.
- Allen, R.G., L.S. Pereira, D. Raes, and M. Smith. 1998. *Crop evapotranspiration guidelines for computing crop water requirements*. FAO Irrigation and Drainage Paper 56, Rome, Italy.
- Allen, R.G., I.A. Walter, R.L. Elliott, T. Howell, D. Itenfisu, and M. Jensen. 2005. *The ASCE standardized reference evapotranspiration equation*. American Society of Civil Engineers, Reston, Virginia.
- Bauer, C.M. 2002. *The hydrogeology of Rose Valley and Little Lake Ranch, Inyo County, California*. M.S. thesis, California State University, Bakersfield. April 2002.
- Brown and Caldwell. 2006. *Rose Valley groundwater model, Coso Operating Company, LLC, Rose Valley, California*. Prepared for COSO Operating Company, LLC, Coso Junction, California. Brown and Caldwell Project Number 129778.001. April 10, 2006.
- California Department of Water Resources (CDWR). 1975. *Vegetative water use in California*. Bulletin No. 113-3, Sacramento, California.
- Carsel, R.F. and R.S. Parrish. 1988. Developing joint probability distributions of soil water retention characteristics. *Water Resources Research* 24(5):755-769.
- Daly, C., R.P. Neilson, and D.L. Phillips. 1994. A statistical-topographic model for mapping climatological precipitation over mountain terrain. *Journal of Applied Meteorology* 33(2):140-158.
- Duffie, J.A. and W.A. Beckman. 1980. *Solar engineering of thermal processes*. John Wiley & Sons, New York.



Duffie, J.A. and W.A. Beckman. 1991. *Solar engineering of thermal processes*, Second Edition. Wiley Interscience, New York.

Flint, A.L., L.E. Flint, J.A. Hevesi, and J.M. Blainey. 2004. Fundamental concepts of recharge in the desert southwest: A regional modeling perspective. pp. 159-184 in Hogan, J.F., F.M. Philips, and B.R. Scanlon (eds.), *Groundwater recharge in a desert environment: the southwestern United States*. Water Science and Applications Series, Vol. 9. American Geophysical Union, Washington, D.C.

Flint, A. and L. Flint. 2007. *Application of the basin characterization model to estimate in-place recharge and runoff potential in the Basin and Range carbonate-rock aquifer system, White Pine County, Nevada, and adjacent areas in Nevada and Utah*. USGS Scientific Investigations Report 2007-5099.

GEOSCIENCE Support Services, Inc. (GEOSCIENCE). 2009. Technical memorandum from Dennis E. Williams to Charity B. Schiller, Best, Best, and Krieger, LLC, regarding Geohydrologic opinion regarding the Hay Ranch Water Extraction and Delivery System conditional use permit application FEIR. March 3, 2009.

GeoTrans, Inc. 2003. *Results of aquifer tests, Hay Ranch production wells, Rose Valley, Coso Junction, California*. Prepared for Coso Operating Company, LLC, Little Lake, California. October 13, 2003.

Hevesi, J.A., A.L. Flint, and L.E. Flint. 2003. *Simulation of net infiltration and potential recharge using a distributed-parameter watershed model of the Death Valley Region, Nevada and California*. USGS Water-Resources Investigations Report 03-4090.

Hood, E., M. Williams, and D. Cline. 1999. Sublimation from a seasonal snowpack at a continental, mid-latitude alpine site. *Hydrologic Processes* 13:1781-1797.



- Leavesley, G.H., R.W. Lichty, B.M. Troutman, and L.G. Saindon. 1983. *Precipitation-runoff modeling system: User's manual*. USGS Water-Resources Investigations Report 83-4238, 207 p.
- Lennartz, S., T. Bax, J. Aycrigg, A. Davidson, M. Reid, and R. Congalton. 2008. *Final report on land cover mapping methods for California map zones 3, 4, 5, 6, 12, and 13*. Available online at <<http://gap.uidaho.edu/index.php/gap-home/california-land-cover>>.
- Ludington, S., B.C. Moring, R.J. Miller, P.A. Stone, A.A. Bookstrom, D.R. Bedford, J.G. Evans, G.A. Haxel, C.J. Nutt, K.S. Flynn, and M.J. Hopkins. 2007. *Preliminary integrated geologic map databases for the United States, Western states: California, Nevada, Arizona, Washington, Oregon, Idaho, and Utah, Version 1.3*. U.S. Geological Survey Open-File Report 2005-1305. Available at <<http://pubs.usgs.gov/of/2005/1305/>>.
- MHA Environmental Consulting (MHA). 2008a. *Coso Operating Company Hay Ranch water extraction and delivery system, Conditional use permit (CUP 2007-003) application, SCH# 2007101002, Draft EIR, Inyo County, California*. Prepared for Inyo County Planning Department, Independence, California. July 2008.
- MHA. 2008b. *Coso Operating Company Hay Ranch water extraction and delivery system, Conditional use permit (CUP 2007-003) application, SCH# 2007101002, Final EIR, Inyo County, California*. Prepared for Inyo County Planning Department, Independence, California. December 2008.
- Phillips, F.M. 1994. Environmental tracers for water movement in desert soils of the American southwest. *Soil Sci. Soc. Am. J.* 58:14–24.
- Reindel, D.T., W.A. Beckman, and J.A. Duffie. 1990. Diffuse fraction correlations. *Solar Energy* 45(1):1-7.
- Rawls, W.J. and D.L. Brakensiek. 1985. Prediction of soil water properties for hydrologic modeling. pp. 293-299 in Jones, E.B. and T.J. Ward (eds.), *Watershed management in the*



eighties. Proceedings of the symposium, ASCE convention in Denver, Colorado, April 30–May 1, 1985.

Rockwell International, 1980. *Project: Geology and hydrology technical report on the Coso geothermal study area, In support of: Coso geothermal development environmental statement*. Prepared for the U.S. Bureau of Land Management, Bakersfield, California. Contract No. YA-512-CT8-216. April 1980.

Saint-Amand, P. 1986. *Water supply of Indian Wells Valley, California*. Naval Weapons Center Technical Publication 6404.

Sandia National Laboratory. 2007. *Simulation of net infiltration for present-day and potential future climates, Yucca Mountain Project*. MDL-NBS-HS-000023 REV 01. May 2007.

Schroeder, P.R., T.S. Dozier, P.A. Zappi, B.M. McEnroe, J.W. Sjoström, and R.L. Peyton. 1994. *The hydrologic evaluation of landfill performance (HELP) model: Engineering documentation for version 3*. U.S. Environmental Protection Agency Office of Research and Development, Washington, DC. September 1994. EPA/600/R-94/168b.

Trezza, R. and Allen, R.G. 2006. *Procedure and calculation steps for solar radiation and reference evapotranspiration (ET_0) on inclined surfaces*.

U.S. Geological Survey (USGS). 2009. Comments on Environmental assessment for the Coso Operating Company Hay Ranch Water Extraction and Delivery System, CA, Bureau of Land Management, December 2008. June 4, 2009.

USGS. 2010. MODIS datasets accessed December 2010 through the USGS Global Visualization Viewer, “MODIS Terra” collection and the “MOD15A2 LAI” images. <<http://glovis.usgs.gov/>>.

U.S. Naval Weapons Center (NWC). 1978. *Draft environmental impact statement for the Navy Coso Geothermal Development Program, Vol. 1*. Technical Publication No. TS-78-59.



van Genuchten, M.Th. 1980. A closed-form equation for predicting the hydraulic conductivity of unsaturated soils. *Soil Science Society of America Journal* 44:892-898.

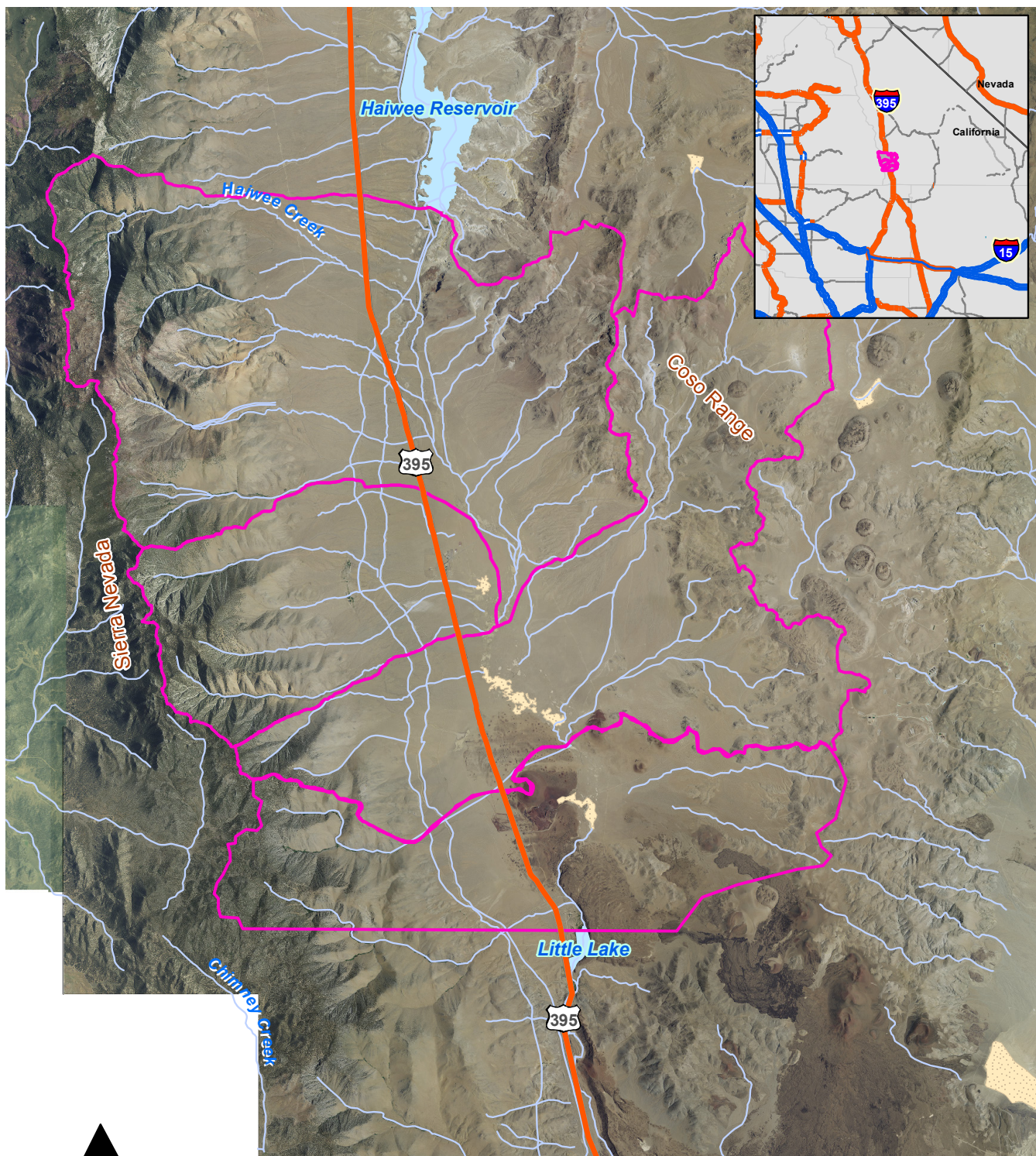
Welch, A.H. and D.J. Bright (eds.). 2007. *Water resources of the Basin and Range carbonate-rock aquifer system, White Pine County, Nevada, and adjacent areas in Nevada and Utah—Draft report*. USGS Open-File Report 2007-1156.

Williams, D.V. 2004. *Hydrogeologic and hydrochemical framework of Indian Wells Valley, California: Evidence for interbasin flow in the southern Sierra Nevada*. M.S. thesis, Colorado School of Mines, Golden, Colorado.

Wilson, J.L. and H. Guan. 2004. Mountain-block hydrology and mountain-front recharge. In Hogan, J.F., F.M. Philips, and B.R. Scanlon (eds.), *Groundwater recharge in a desert environment: the southwestern United States*. Water Science and Applications Series, Vol. 9. American Geophysical Union, Washington, D.C.

Figures

Q:\PROJECTS\LT09.0311_ROSE_VALLEY_MODEL\GIS\MXD\FIGURES\FIGURE-A-1_LOCATION_AND_PHYSIOGRAPHY.MXD



0 1.5 3
Miles

Explanation

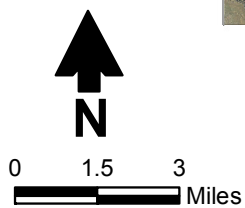
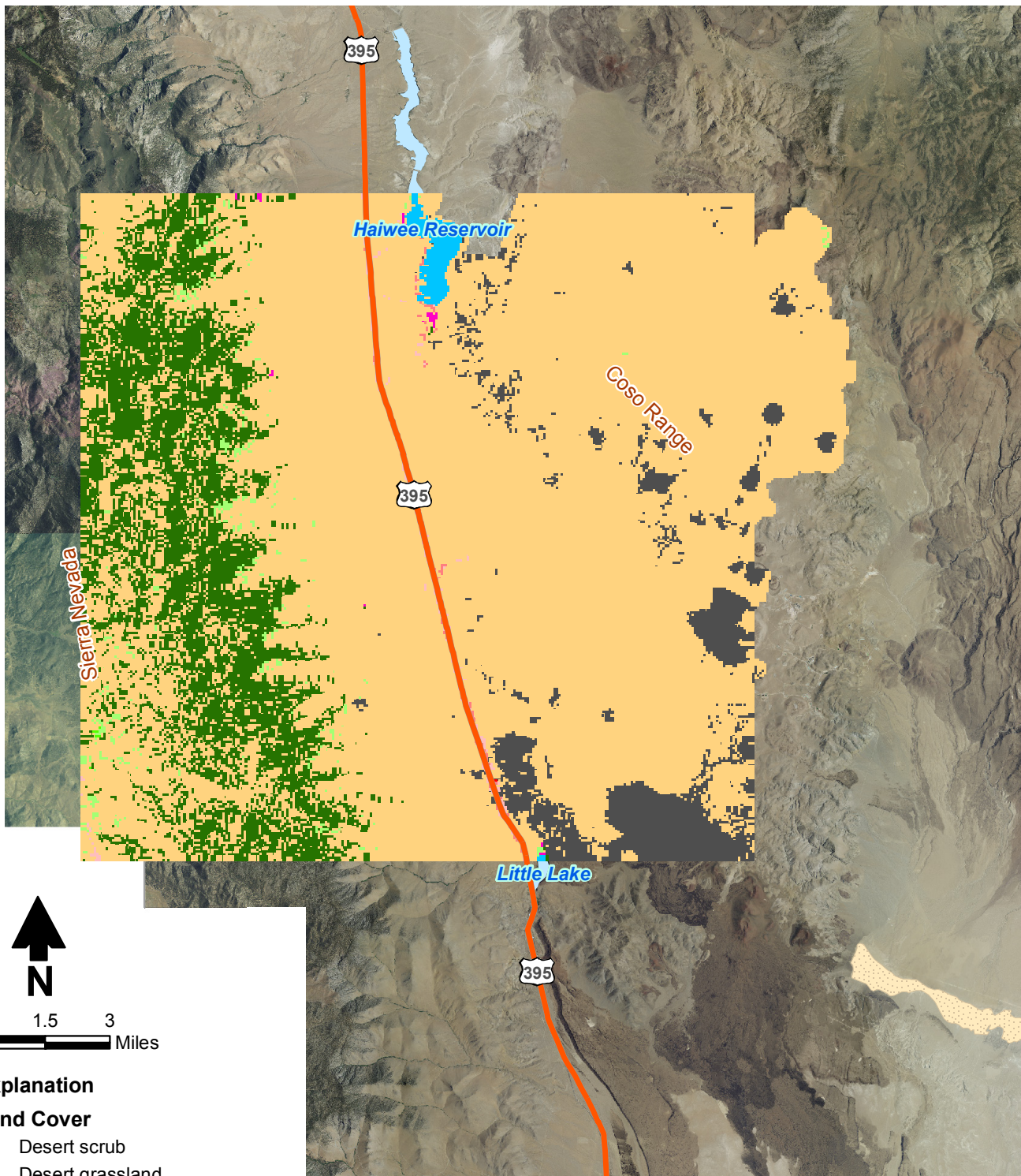
- Watershed boundary
- Stream/river



Daniel B. Stephens & Associates, Inc.
1/11/2011 JN LT09.0311

ROSE VALLEY MODEL
Location and Physiography of Rose Valley

Figure A-1



Explanation

Land Cover

- Desert scrub
- Desert grassland
- Developed, open space
- Developed, low intensity
- Developed, medium intensity
- Evergreen forest
- Woody wetlands
- Emergent herbaceous wetlands
- Bare rock
- Open water

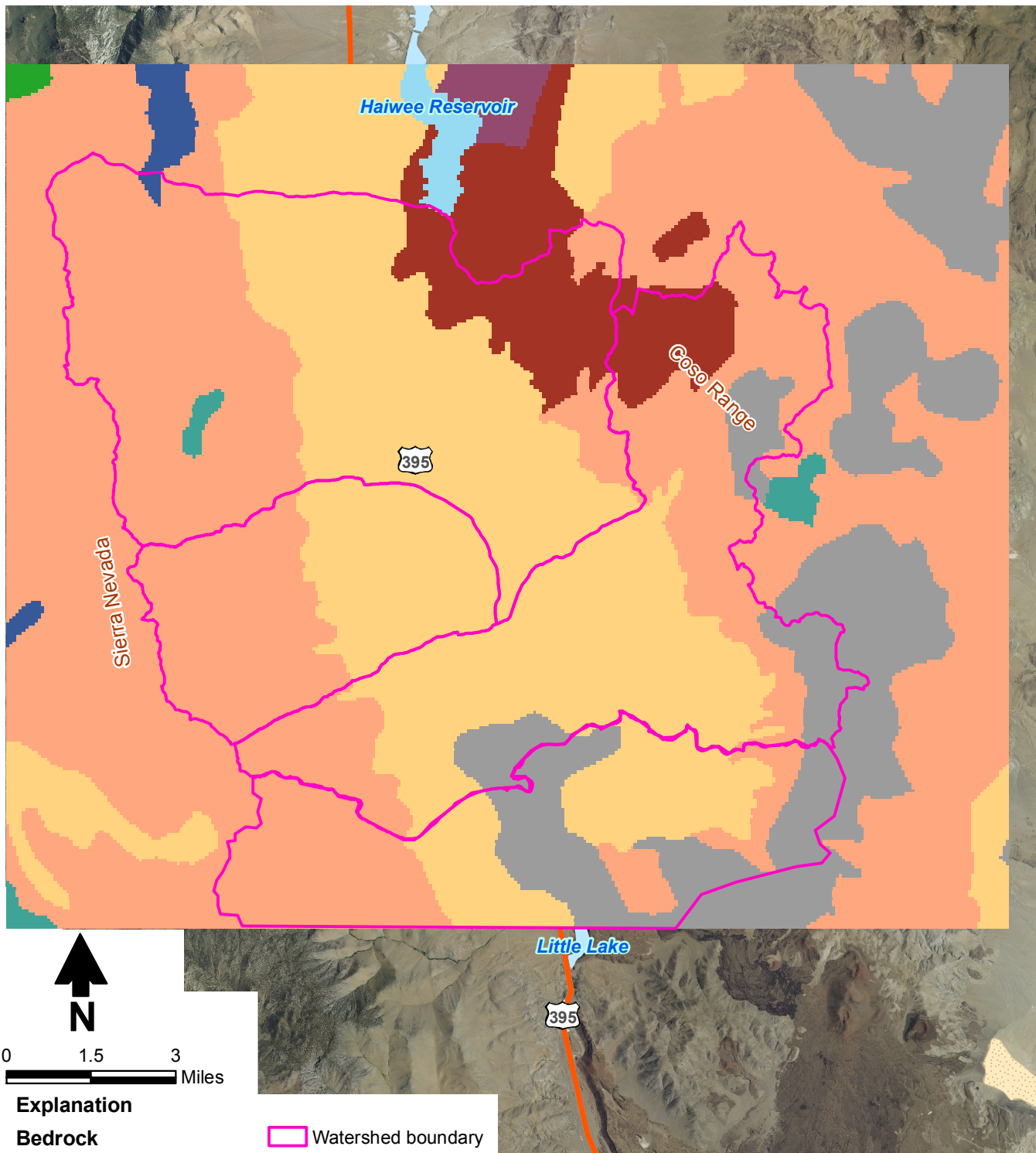


Daniel B. Stephens & Associates, Inc.
1/11/2011 JN LT09.0311

ROSE VALLEY MODEL
**Distribution of Vegetation and
Landcover in DPWM**

Figure A-2

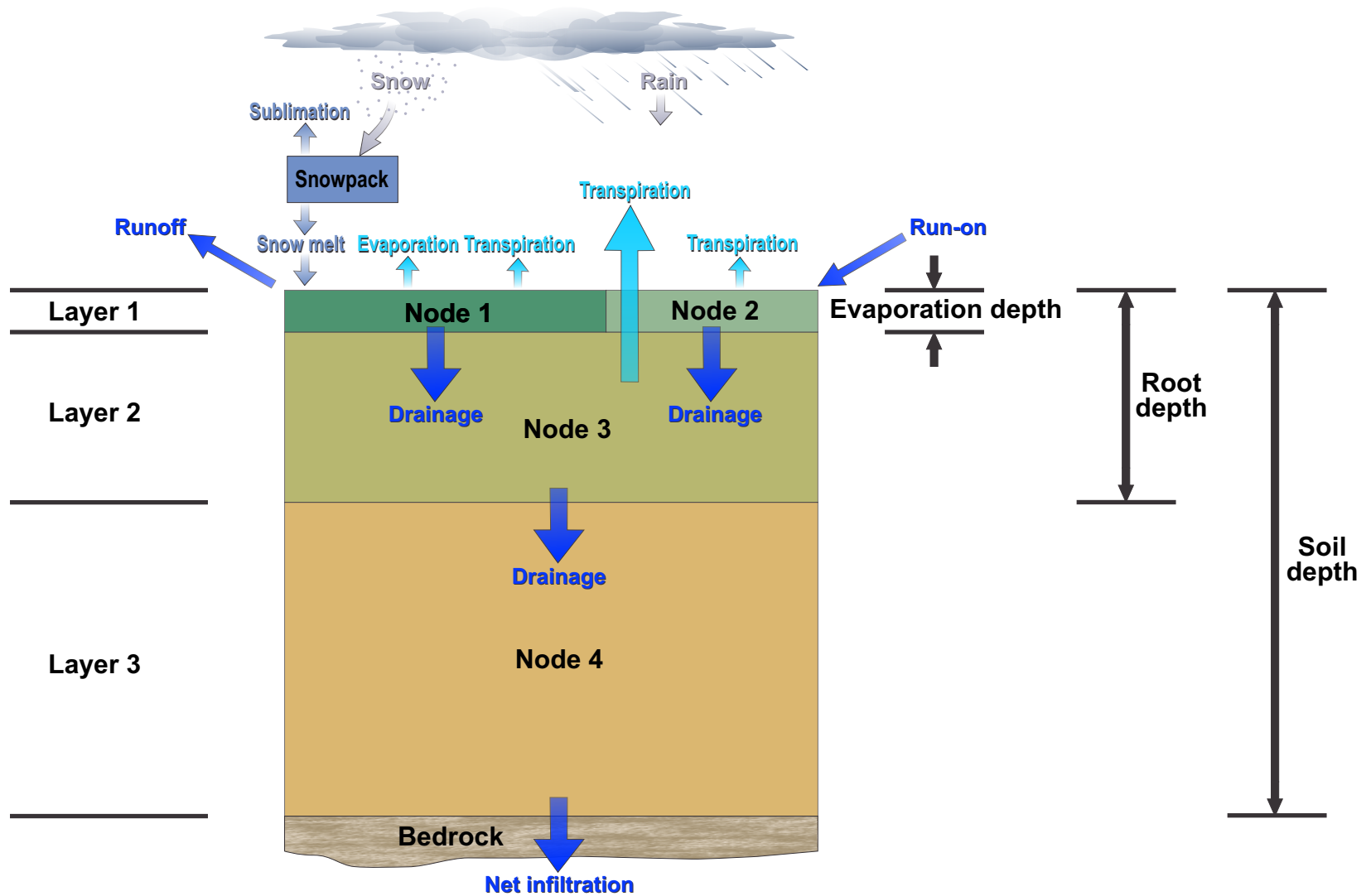
Q:\PROJECTS\LT09.0311_ROSE_VALLEY_MODEL\GIS\MXDS\FIGURES\FIGURE-A-3_BEDROCK.MXD



Daniel B. Stephens & Associates, Inc.
1/11/2011 JN LT09.0311

ROSE VALLEY MODEL
Distribution of Bedrock in DPWM

Figure A-3



Notes:

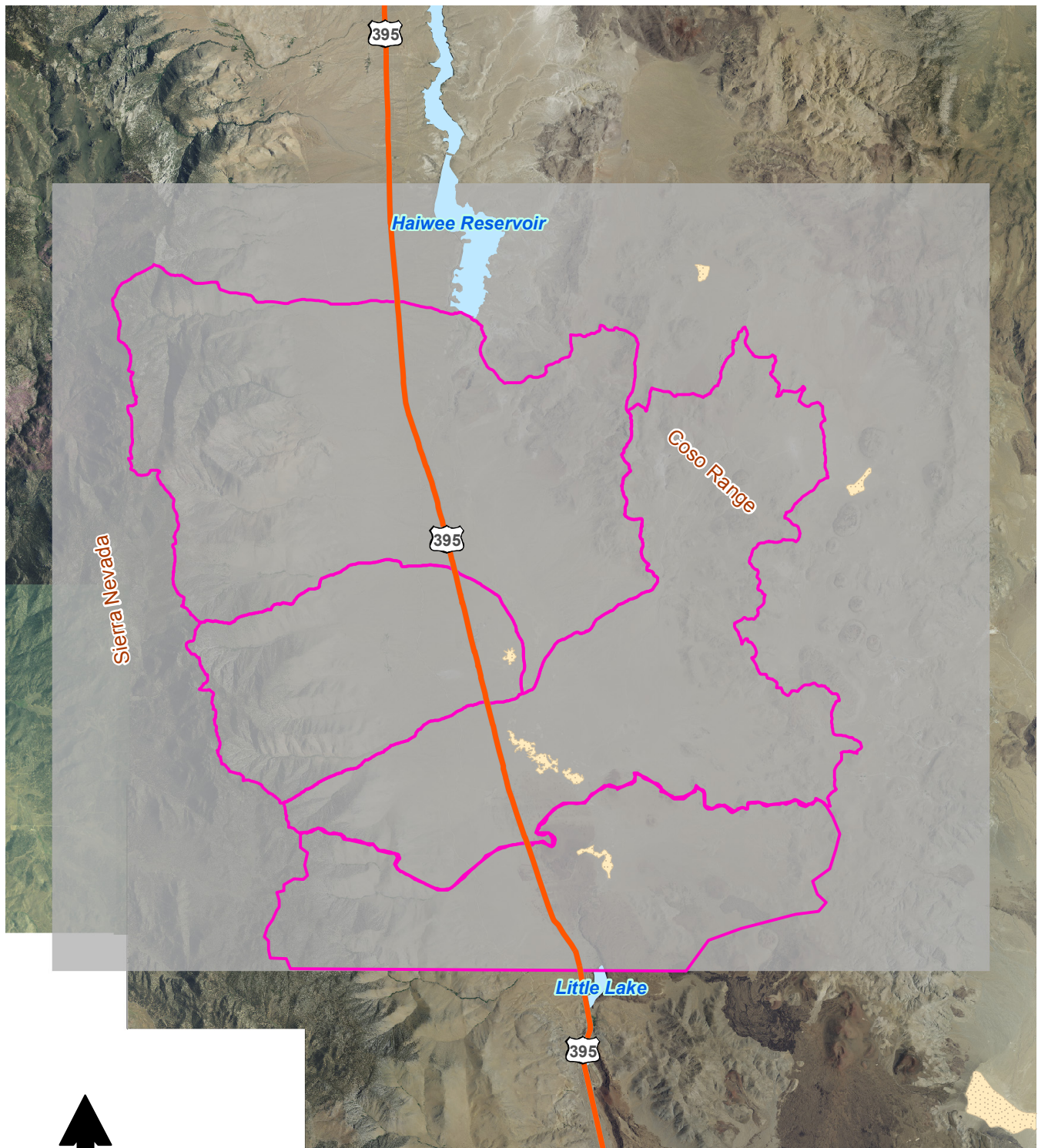
- Node 1** = fraction exposed and wetted (f_{ew})
- Node 2** = fraction covered by vegetation canopy (f_c)

ROSE VALLEY MODEL

**Schematic of Water Balance Components and
Computational Nodes Present in a Single Model Cell**



Q:\PROJECTS\LT09.0311_ROSE_VALLEY_MODEL\GIS\MXDS\FIGURES\FIGURE-A-5_MODEL.GRID.MXD



0 1.5 3
Miles

Explanation

- Model area
- Watershed boundary

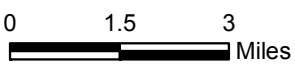
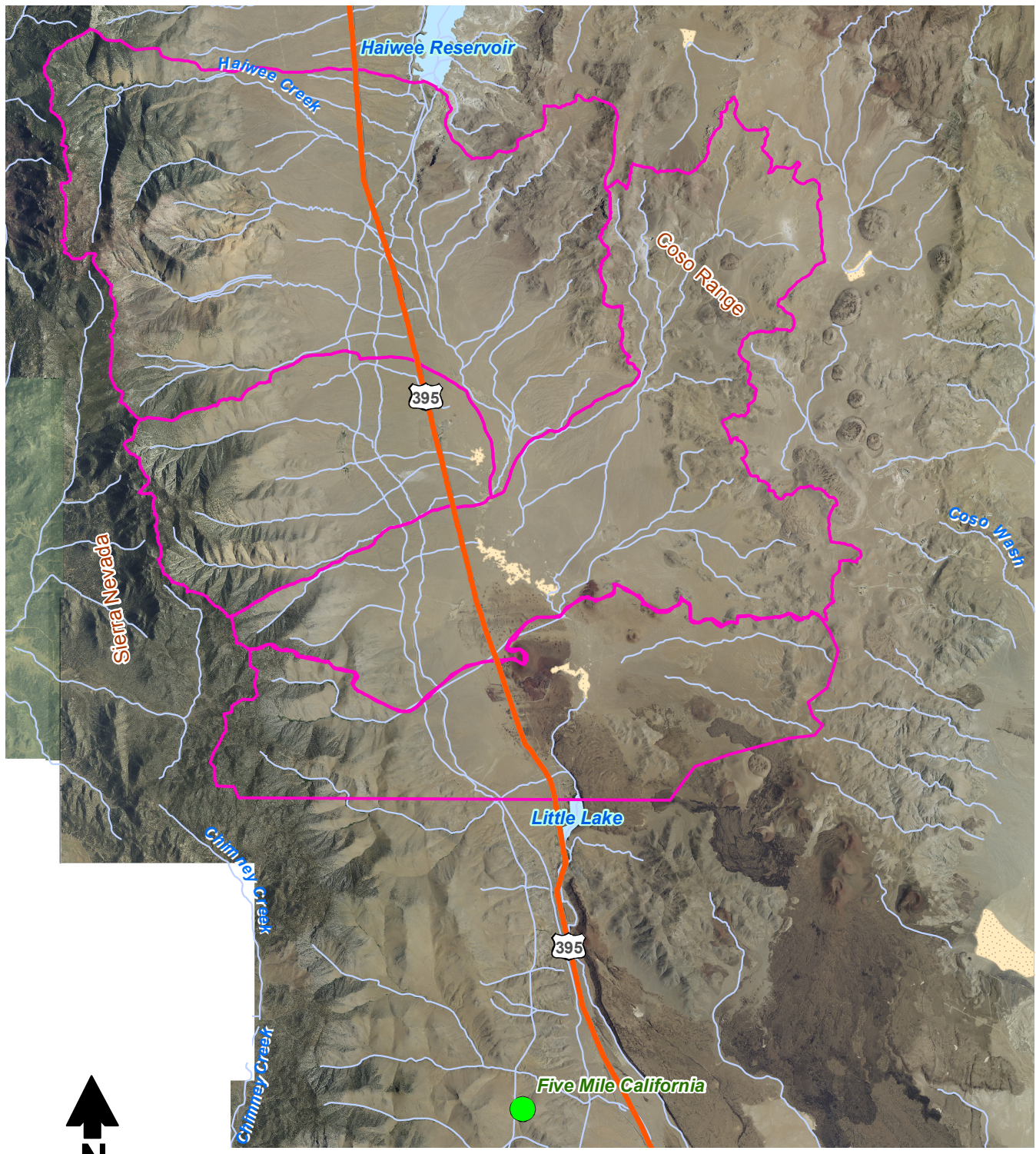


Daniel B. Stephens & Associates, Inc.
1/11/2011 JN LT09.0311




ROSE VALLEY MODEL
DPWM Area

Figure A-5

Q:\PROJECTS\LT09.0311_ROSE_VALLEY_MODEL\GIS\MXDS\FIGURES\FIGUREA-6_RAWSSTATIONS.MXD



Explanation

-  RAWS
-  Watershed boundary
-  Stream/river



Daniel B. Stephens & Associates, Inc.
1/11/2011 JN LT09.0311

ROSE VALLEY MODEL
RAW Station in the Vicinity of Rose Valley

Figure A-6

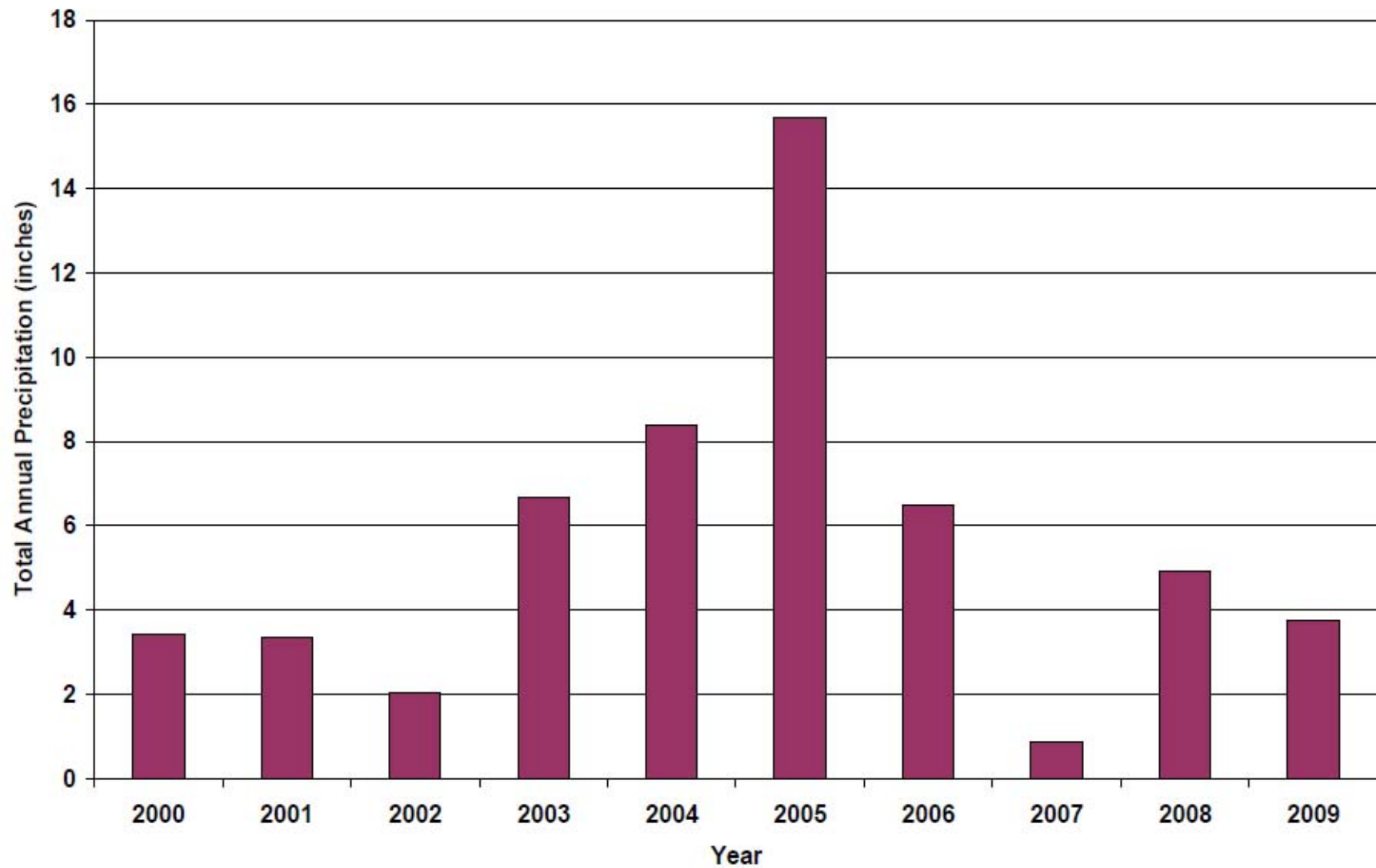


Figure A-7

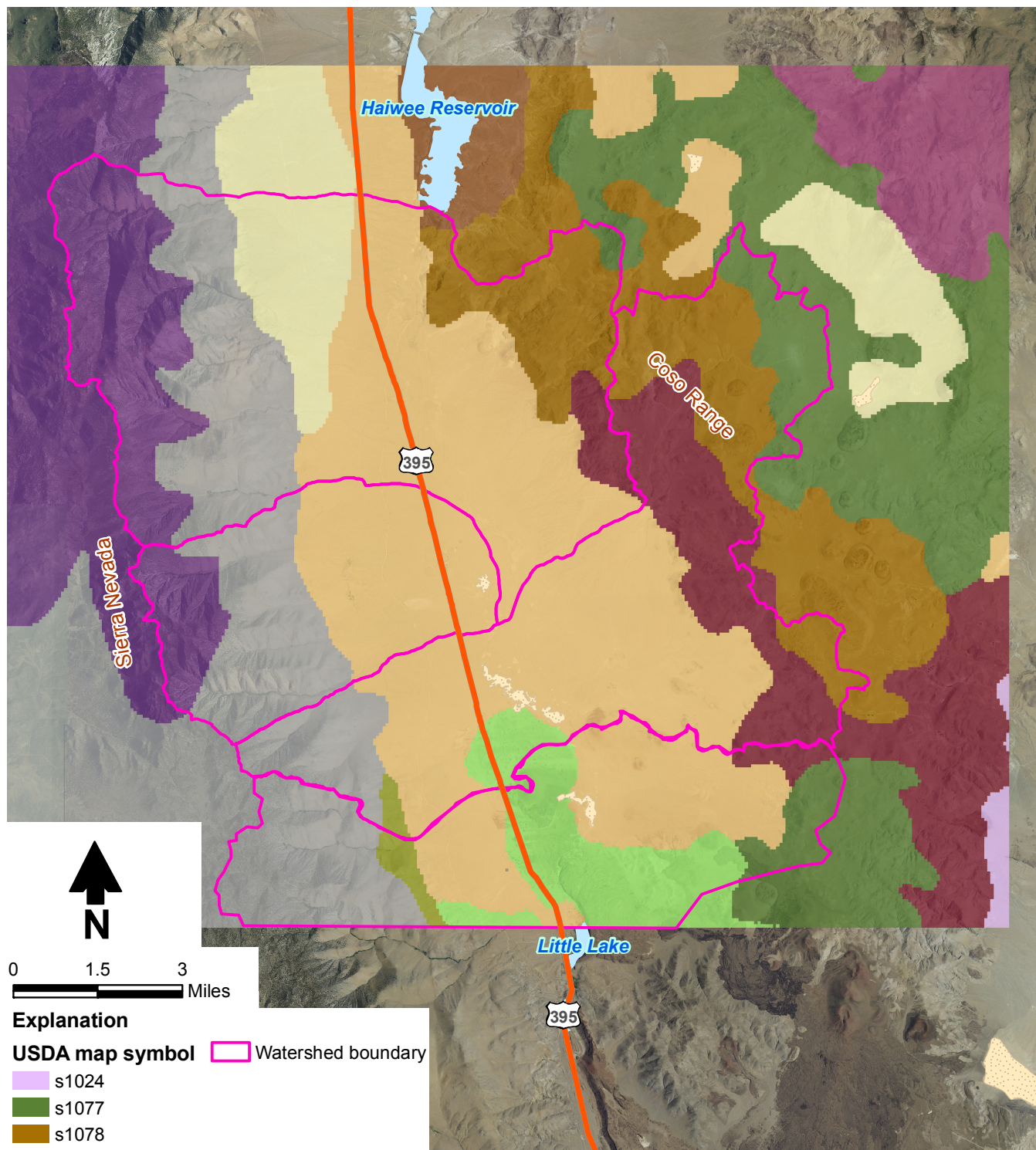


Daniel B. Stephens & Associates, Inc.

1/11/11

ROSE VALLEY MODEL
Total Annual Precipitation
Five Mile California RAWS

Q:\PROJECTS\LT09.0311_ROSE_VALLEY_MODEL\GIS\MXDS\FIGURES\FIGURE-A-8_DISTRIBUTION_OF_SOIL_TYPE.MXD

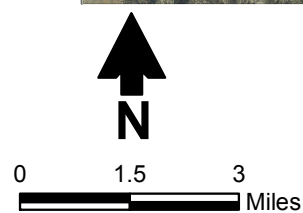
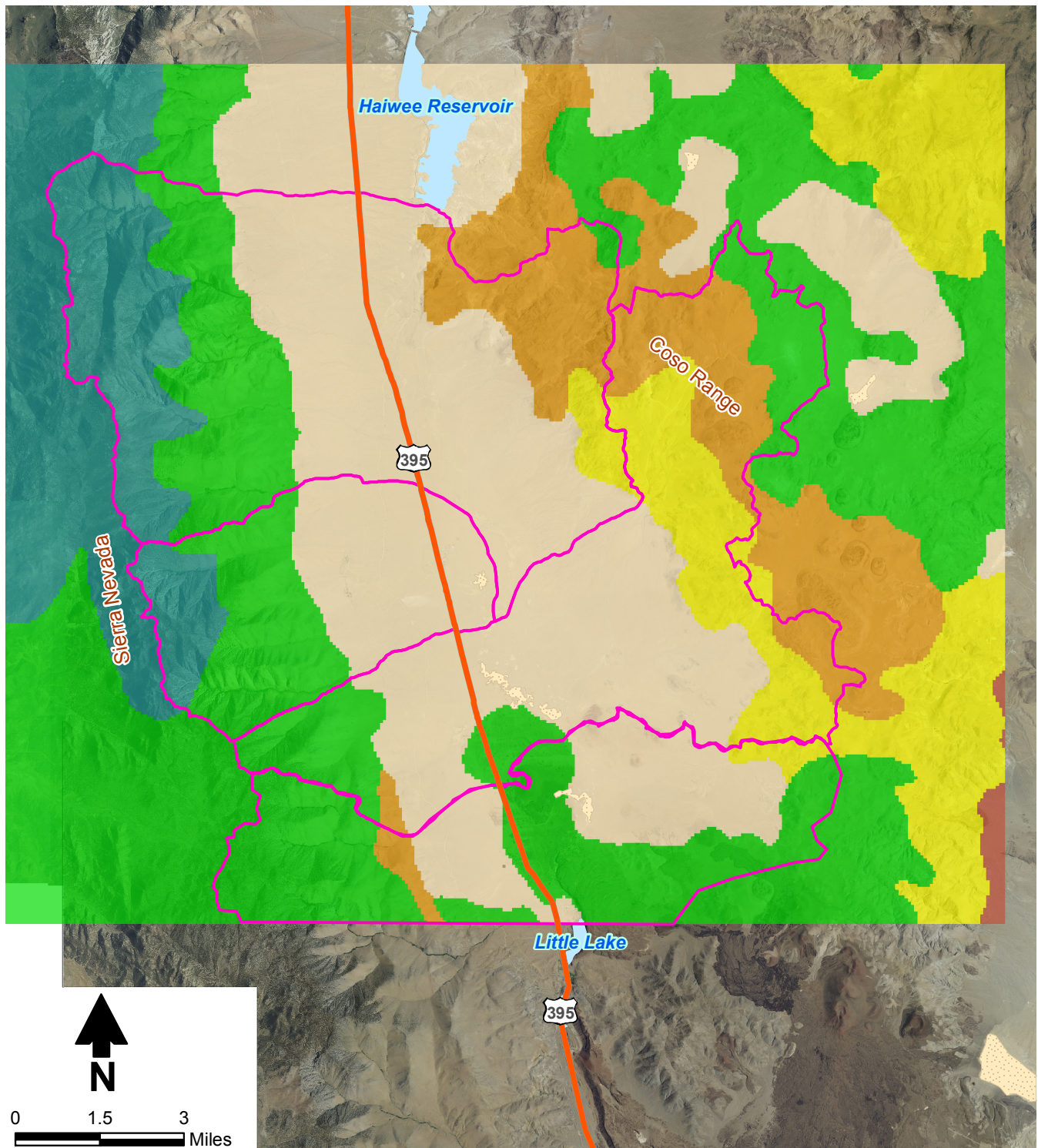


Daniel B. Stephens & Associates, Inc.
1/24/2011 JN LT09.0311

ROSE VALLEY MODEL
Distribution of Soil Type in DPWM

Figure A-8

Q:\PROJECTS\LT09.0311_ROSE_VALLEY_MODEL\GIS\MXDS\FIGURES\FIGUREA-9_DISTRIBUTION_OF_SOIL_DEPTH.MXD



Explanation

- Soil depth (feet)**
- 0 - 1
 - 1 - 2
 - 2 - 3
 - 4 - 5
 - 5 - 6
 - > 5 feet
- Watershed boundary

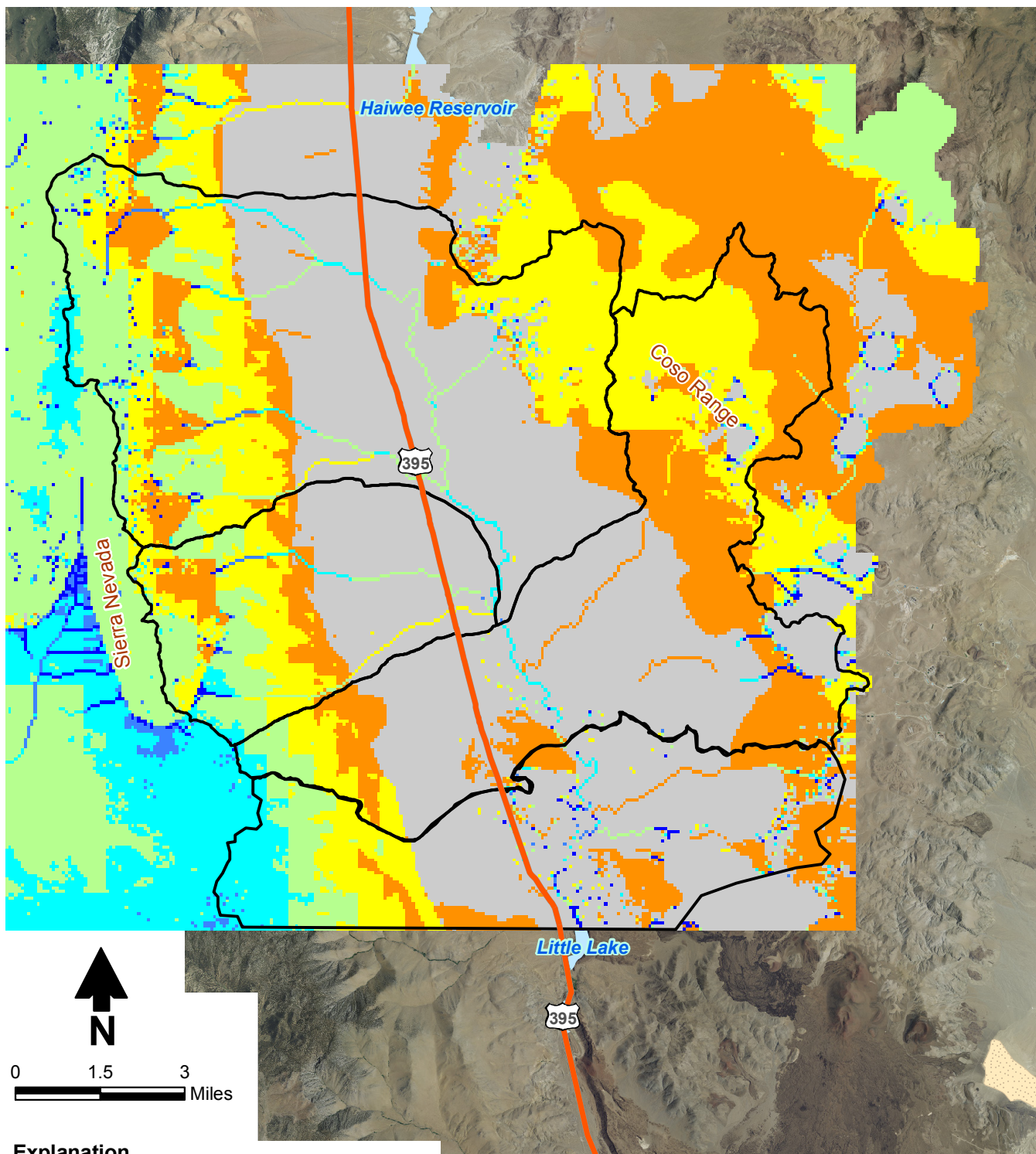


Daniel B. Stephens & Associates, Inc.
1/11/2011 JN LT09.0311

ROSE VALLEY MODEL
Distribution of Soil Depth in DPWM

Figure A-9

Q:\PROJECTS\LT09.0311_ROSE_VALLEY_MODEL\GIS\MXDS\FIGURES\FIGUREA10_MEDIAN_RECHARGE.MXD



Explanation

Mean net infiltration Watershed boundary

- None
- < 0.5 in/yr
- 0.5 - 1.0 in/yr
- 1 - 3 in/yr
- 3 - 5 in/yr
- 5 - 7 in/yr
- > 7 in/yr



Daniel B. Stephens & Associates, Inc.
1/11/2011 JN LT09.0311

ROSE VALLEY MODEL
Mean Net Infiltration
Simulated by DPWM

Figure A-10

Tables



Table A-1. Estimated Recharge to Rose Valley Groundwater Basin from Precipitation

Estimated Recharge (ac-ft /yr)	Source and Comments
611	U.S. Naval Weapons Center (1979) as cited by Rockwell International (1980)
1,900 to 3,000	Rockwell International (1980)
800	Saint-Amand (1986) as cited by Williams (2004)
4,191	Brown and Caldwell (2006). Estimate is for Sierra Nevada only; recharge from the Coso Range is assumed to be zero.
4,000	Williams (2004). Estimate is for Sierra Nevada only, and actual recharge may be higher.
2,350 to 4,700	USGS (2009)



Daniel B. Stephens & Associates, Inc.

Table A-2. Summary of General DPWM Input Values

Parameter	Variable	Value	Units	Comment
Field capacity	head_fc	102	cm	1/10 bar
Wilting point	head_wp	61,293	cm	60 bar
Elevation of lower reference weather station	elevref1	4,150	ft msl	Five Mile California Weather Station
Lapse rate for air temperature (dry adiabatic lapse rate)	CTcor	-7.8	°C/km	PRISM mean annual maximum air temperatures for 1971-2000 Normal period
Average elevation for basin	elevavg	5,446	ft msl	Average of USGS DEM cells in the basin
Average latitude for basin	Latavg	36	degrees	Approximate basin midpoint
Adjustment coefficient in Hargreaves' radiation formula	Krs	0.19	°C – 0.5	
Evaporation layer depth	Ze	0.15	meters	Depth of the surface soil layer that is subject to drying by way of evaporation. Upper end of range in Allen et al., 1998, p. 144 (ranges 0.10 to 0.15 meters)
Readily evaporable water	REW	8	mm	Upper end of range for loamy sand (Allen et al., 1998, Table 19)
Initial capillary head node 1	IC1	61,293	cm	Set to wilting point (60 bar)
Initial capillary head node 2	IC2	61,293	cm	Set to wilting point (60 bar)
Initial capillary head node 3	IC3	61,293	cm	Set to wilting point (60 bar)
Initial capillary head node 4	IC4	102	cm	Set to field capacity (1/10 bar)
Depletion factor	p	0.5	—	Varies 0 to 1 but typically ranges from 0.30 for shallow rooted plants at high values of ET_c (>8 mm/d) to 0.70 for deep rooted plants at low values of ET_c (<3 mm/d) with 0.5 in common use.
Fraction of snowfall that sublimates	Csublime	0.15	—	Hood et al., 1999, p. 1794
Minimum snow melt factor	MFMIN	2	mm/d/°C	Minimum expected to occur on December 21 (Schroeder et al., 1994)
Maximum snow melt factor	MFMAX	5.2	mm/d/°C	Maximum expected to occur on June 21 (Schroeder et al., 1994)
Minimum transpiration coefficient (K_c) for dry surface soil (upper 0.10 to 0.15 meter) with no vegetation cover	Kc_min	0	—	0 recommended by Allen et al. (1998) for arid environments

cm = Centimeters
ft msl = Feet above mean sea level

DEM = Digital elevation model
mm = Millimeters

ET_c = Crop evapotranspiration
mm/d/°C = Millimeters per day per degree Celsius



Table A-3. Soil Data

Map Unit Key / ID	USDA Database Source	Weighted Average Soil Properties ^a (% by weight ^b)				Modeled					
		Sand	Silt	Clay	Dry Bulk Density (g/cm ³)	Saturated Hydraulic Conductivity (m/s)	Van Genuchten alpha (1/cm)	Van Genuchten n	Saturated Water Content (cm ³ /cm ³)	Residual Water Content (cm ³ /cm ³)	Depth (meters)
s5668	STATSGO	59.0	23.4	17.6	1.59	3.70×10^{-6}	6.32×10^{-2}	1.34	0.40	0.09	0.62
s1077	STATSGO	62.2	23.3	14.5	1.61	4.89×10^{-6}	6.73×10^{-2}	1.37	0.39	0.08	1.08
s1104	STATSGO	53.6	27.5	19.0	1.70	9.5×10^{-7}	3.66×10^{-2}	1.33	0.36	0.09	1.35
s764	STATSGO	77.9	14.8	7.3	1.57	2.4×10^{-5}	1.13×10^{-1}	1.44	0.41	0.06	1.01
s1087	STATSGO	76.0	14.9	9.1	1.50	3.18×10^{-5}	1.31×10^{-1}	1.41	0.44	0.06	20.00
s1086	STATSGO	77.0	13.3	9.8	1.56	2.59×10^{-5}	1.26×10^{-1}	1.41	0.41	0.07	20.00
s1090	STATSGO	83.6	10.5	5.9	1.39	3.42×10^{-5}	1.15×10^{-1}	1.42	0.48	0.05	20.00
s1078	STATSGO	61.5	25.5	13.1	1.26	2.74×10^{-5}	1.20×10^{-1}	1.35	0.53	0.07	0.53
s1130	STATSGO	69.9	19.2	10.9	1.59	1.17×10^{-5}	9.14×10^{-2}	1.40	0.40	0.07	0.84
s1127	STATSGO	68.5	18.7	12.8	1.12	7.38×10^{-5}	1.80×10^{-1}	1.35	0.58	0.07	1.04
s812	STATSGO	85.9	9.3	4.8	1.15	1.40×10^{-4}	1.79×10^{-1}	1.42	0.57	0.04	0.51
Wash ^c	NA	NA	NA	NA	NA	8.26×10^{-5}	1.45×10^{-1}	1.46	0.43	0.05	NA

^a From USDA soil database

^b Unless otherwise noted

^c Wash properties are based on Carsel and Parrish (1988) for sand except for van Genuchten n

g/cm³ = Grams per cubic centimeter

m/s = Meters per second

cm³/cm³ = Cubic centimeters per cubic centimeter

NA = Not available



Table A-4 Geology and Saturated Hydraulic Conductivity

Primary Rock Type	Saturated Hydraulic Conductivity (m/s)	Source
Alluvium	8.26×10^{-5}	GeoTrans, 2003
Basalt	1.41×10^{-7}	Welch and Bright, 2007
Gabbro	1.41×10^{-7}	Welch and Bright, 2007
Granodiorite	1.41×10^{-7}	Welch and Bright, 2007
Plutonic	1.41×10^{-7}	Welch and Bright, 2007
Rhyolite	1.41×10^{-7}	Welch and Bright, 2007
Schist	1.41×10^{-7}	Welch and Bright, 2007

m/s = Meters per second



Table A-5. Mean Maximum Rooting Depths and Plant Height

Vegetation Association	Mean Maximum Rooting Depth (meters)	Mean Maximum Plant Height (meters)
Desert scrub	2	0.5
Desert grassland	1	0.3
Developed open space	2	0.5
Developed low intensity	2	0.5
Evergreen forest	3.3	12
Woody wetlands	3.3	12
Developed medium intensity	2	0.5
Emergent herbaceous wetlands	2	0.5



Daniel B. Stephens & Associates, Inc.

Table A-6. DPWM Simulated Annual Water Balance Budget

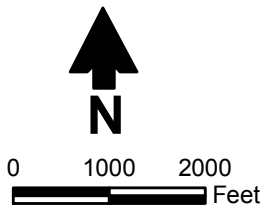
Water Year	Parameter Value (acre-feet)					
	Precipitation	Recharge	Actual ET	Runoff	Sublimation	Change in Storage
2000	37,263	1,878	34,981	25	1,368	-922
2001	36,727	1,893	32,959	20	1,947	-38
2002	26,618	591	24,591	505	665	308
2003	62,153	4,556	56,161	264	1,156	220
2004	75,094	7,804	63,750	2,318	1,229	286
2005	130,922	24,037	99,653	1,079	3,227	3,370
2006	60,698	2,316	57,850	1,200	781	-1,197
2007	17,655	821	18,975	7	448	-2,577
2008	48,520	3,463	42,867	579	1,753	-19
2009	39,638	1,285	37,320	54	1,323	-283
Average	53,529	4,864	46,911	605	1,390	-85

ET = Evapotranspiration

Appendix B

LANDSAT Images of Historical Irrigated Acreage

Q:\PROJECTS\LT09.0311_ROSE_VALLEY_MODEL\GIS\MXDS\FIGURES\LANDSAT_FIGURES\LANDSAT_1972_AUG_10.MXD 010321



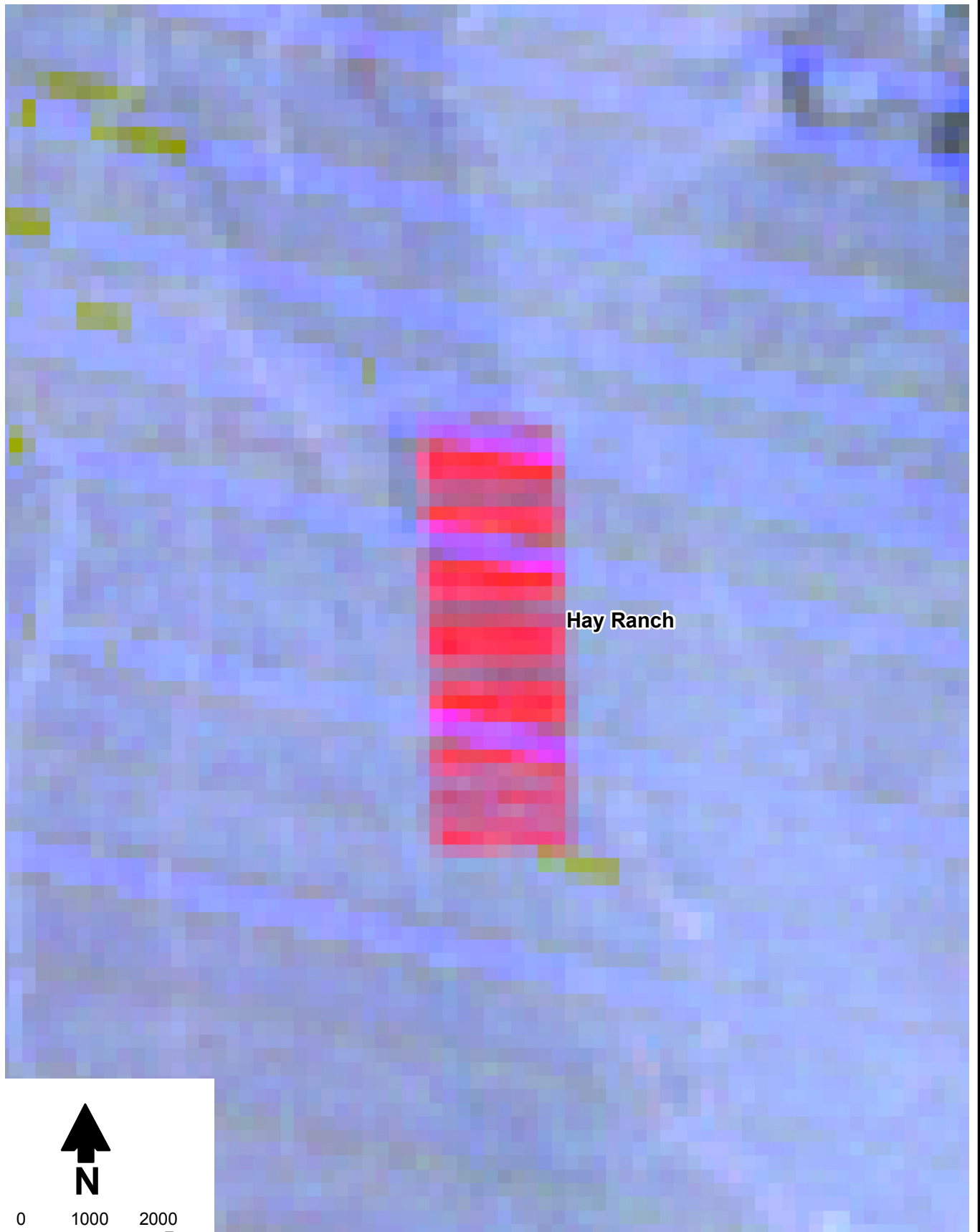
ROSE VALLEY MODEL

**LANDSAT Image of Hay Ranch Area,
August 10, 1972**



Daniel B. Stephens & Associates, Inc.
12/30/2010 JN LT09.0311

Q:\PROJECTS\LT09.0311_ROSE_VALLEY_MODEL\GIS\MXDS\FIGURES\LANDSAT_1974_JULY_31.MXD 010321



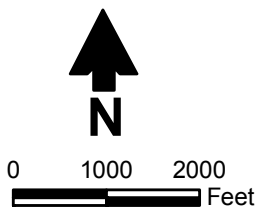
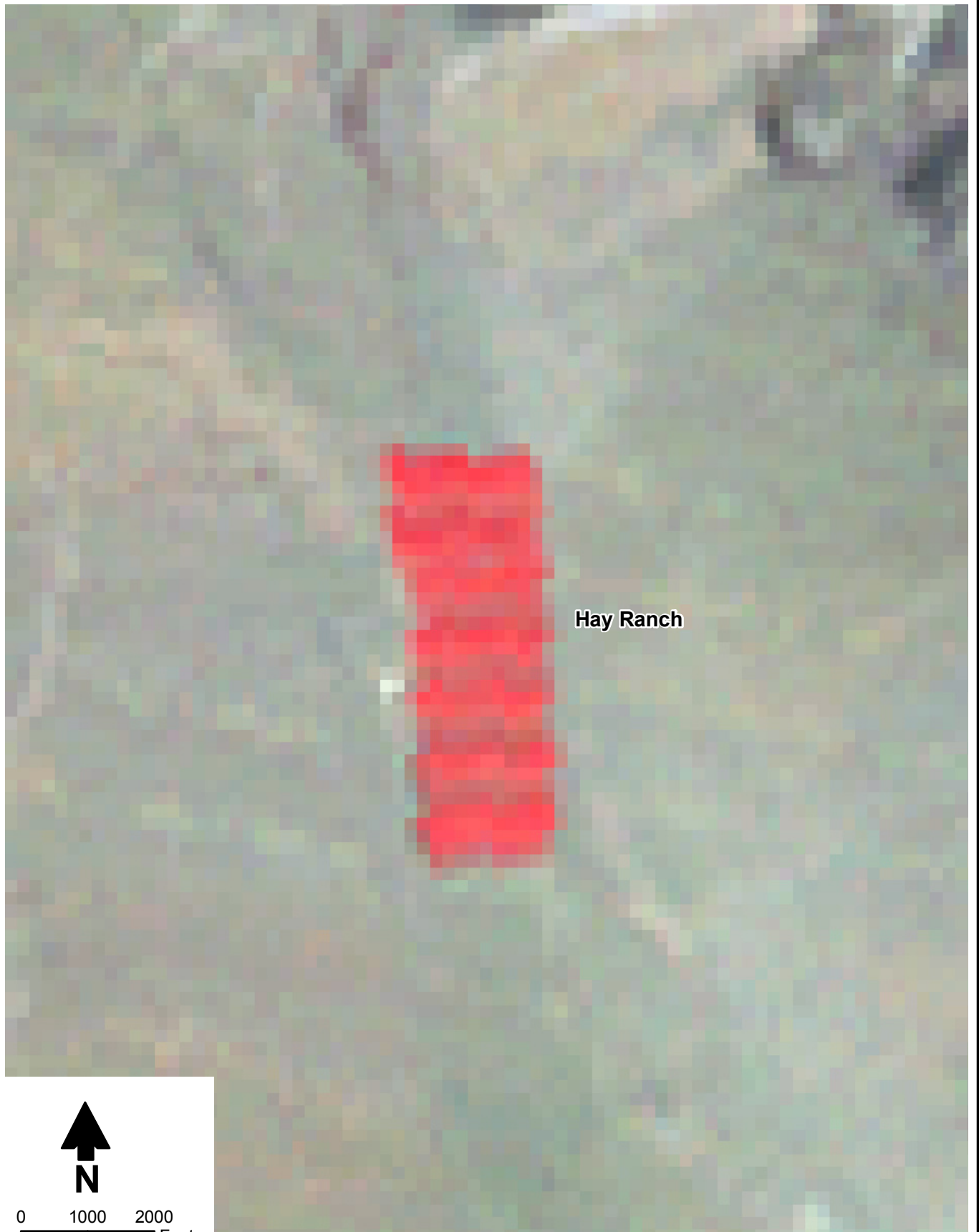
ROSE VALLEY MODEL

**LANDSAT Image of Hay Ranch Area,
July 31, 1974**



Daniel B. Stephens & Associates, Inc.
12/30/2010 JN LT09.0311

Q:\PROJECTS\LT09.0311_ROSE_VALLEY_MODEL\GIS\MXDS\FIGURES\LANDSAT_FIGURES\LANDSAT_1977_MAY_31.MXD 010321



ROSE VALLEY MODEL

**LANDSAT Image of Hay Ranch Area,
May 31, 1977**

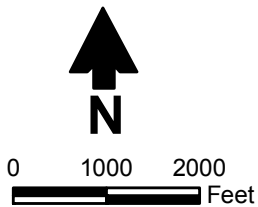


Daniel B. Stephens & Associates, Inc.
12/30/2010 JN LT09.0311

Q:\PROJECTS\LT09.0311_ROSE_VALLEY_MODEL\GIS\MXDS\FIGURES\LANDSAT_FIGURES\LANDSAT_1979_APRIL_15.MXD 010321



Hay Ranch



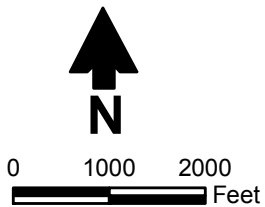
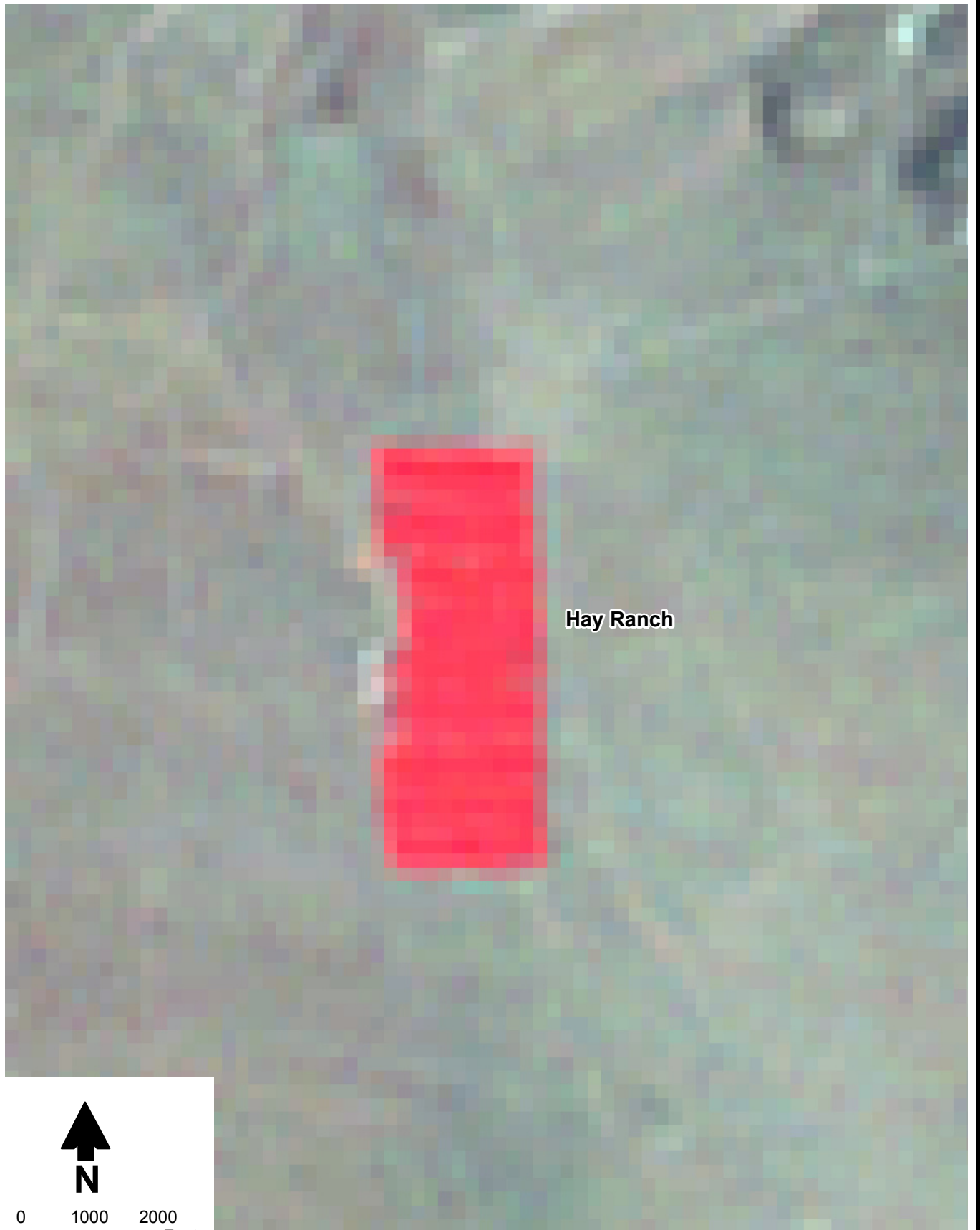
ROSE VALLEY MODEL

**LANDSAT Image of Hay Ranch Area,
April 15, 1979**



Daniel B. Stephens & Associates, Inc.
12/30/2010 JN LT09.0311

Q:\PROJECTS\LT09.0311_ROSE_VALLEY_MODEL\GIS\MXDS\FIGURES\LANDSAT_FIGURES\LANDSAT_1980_JULY_26.MXD 010321



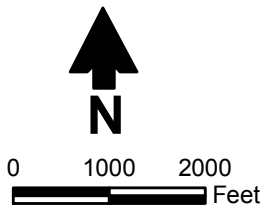
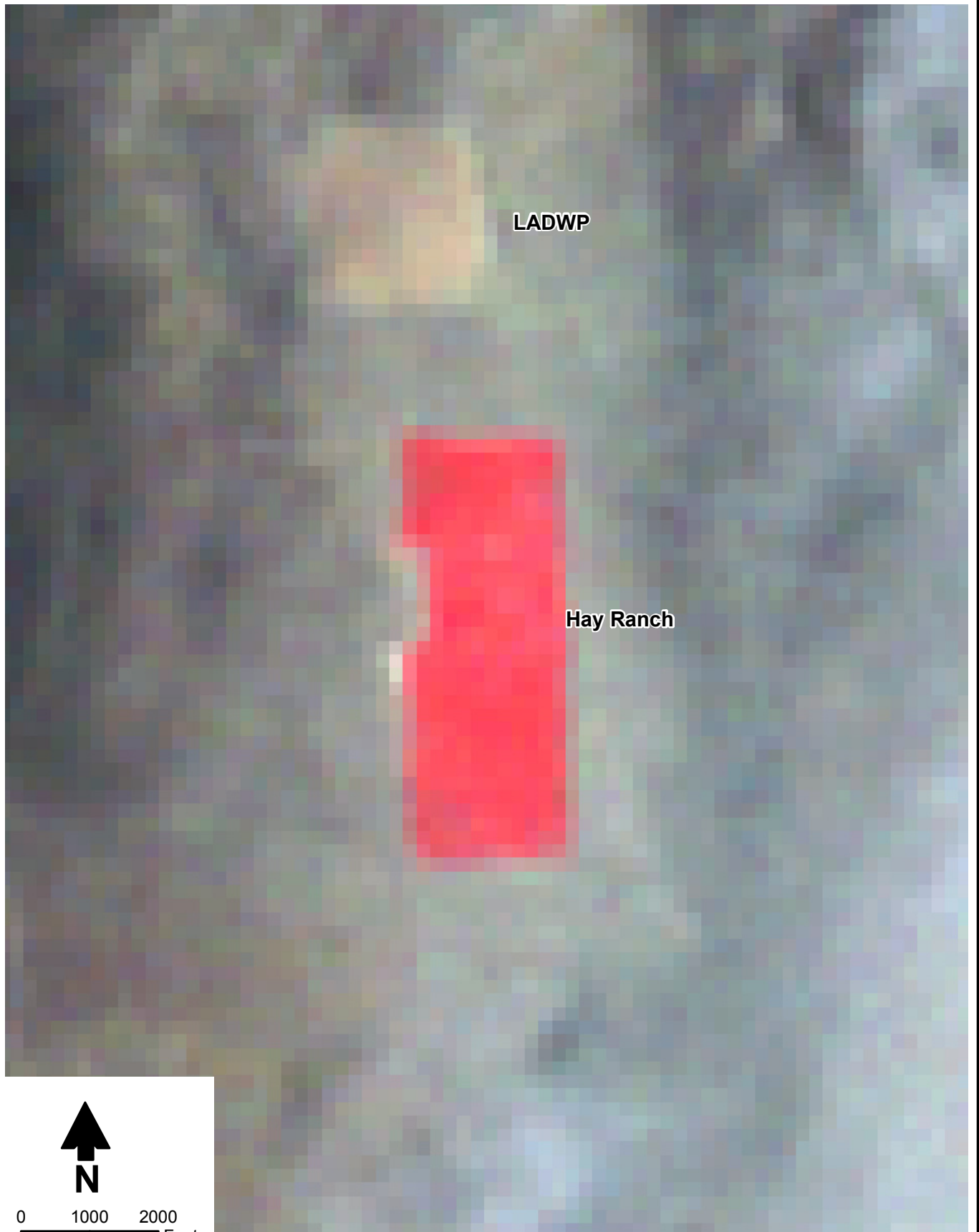
ROSE VALLEY MODEL

**LANDSAT Image of Hay Ranch Area,
July 26, 1980**



Daniel B. Stephens & Associates, Inc.
12/30/2010 JN LT09.0311

Q:\PROJECTS\LT09.0311_ROSE_VALLEY_MODEL\GIS\MXDS\FIGURES\LANDSAT_FIGURES\LANDSAT_1981_JULY_21.MXD 010321



ROSE VALLEY MODEL

**LANDSAT Image of Hay Ranch Area,
July 21, 1981**



Daniel B. Stephens & Associates, Inc.
12/30/2010 JN LT09.0311

Q:\PROJECTS\LT09.0311_ROSE_VALLEY_MODEL\GIS\XDS\FIGURES\LANDSAT_FIGURES\LANDSAT_1982_JULY_25.MXD 010321



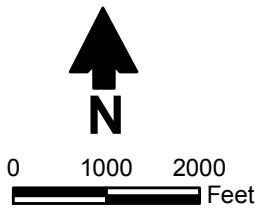
ROSE VALLEY MODEL

**LANDSAT Image of Hay Ranch Area,
July 25, 1982**



Daniel B. Stephens & Associates, Inc.
12/30/2010 JN LT09.0311

Q:\PROJECTS\LT09.0311_ROSE_VALLEY_MODEL\GIS\MXDS\FIGURES\LANDSAT_FIGURES\LANDSAT_1983_MAY_19.MXD 010321



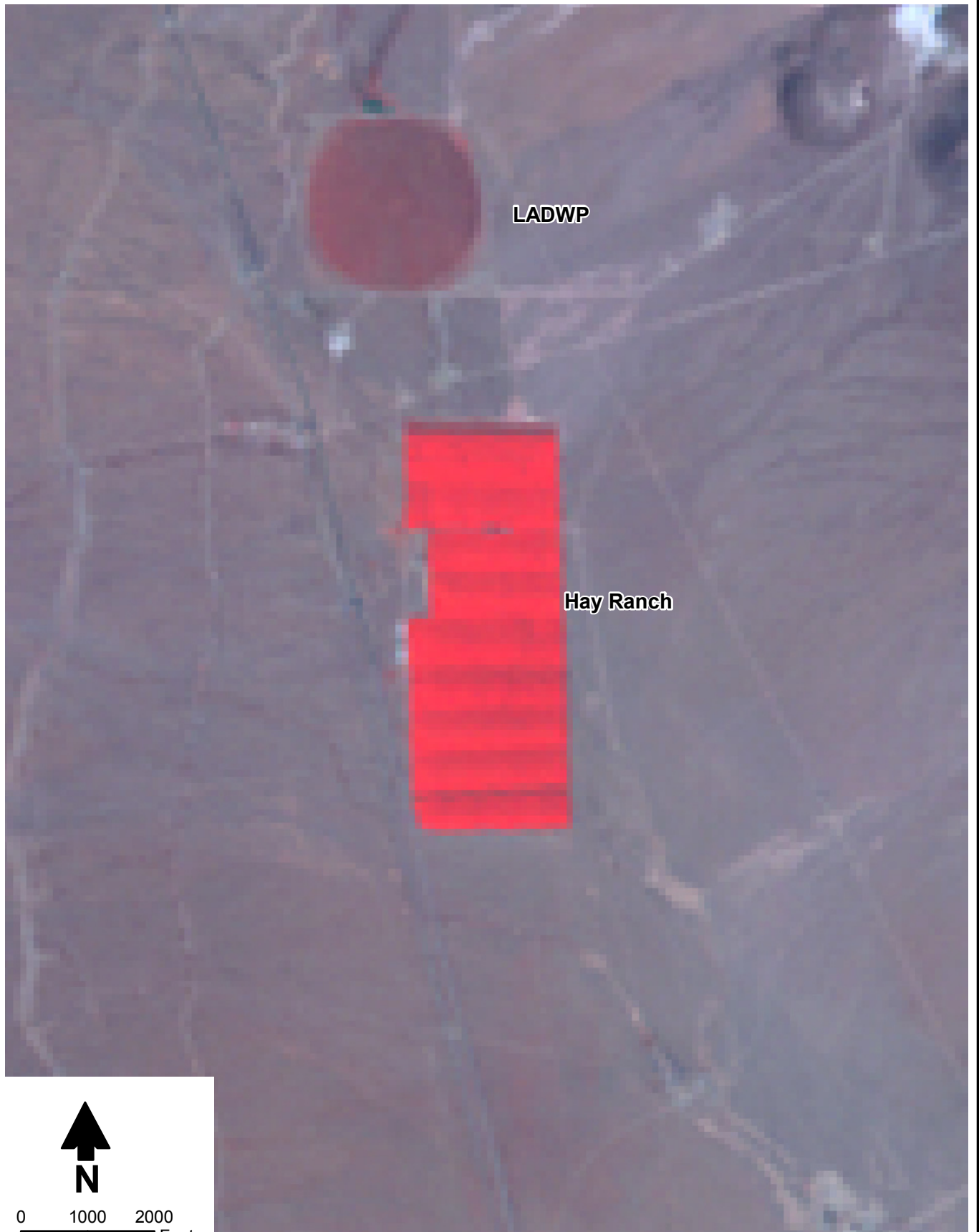
ROSE VALLEY MODEL

**LANDSAT Image of Hay Ranch Area,
May 19, 1983**



Daniel B. Stephens & Associates, Inc.
12/30/2010 JN LT09.0311

Q:\PROJECTS\LT09.0311_ROSE_VALLEY_MODEL\GIS\MXDS\FIGURES\LANDSAT_FIGURES\LANDSAT_1984_AUGUST_1.MXD 010321



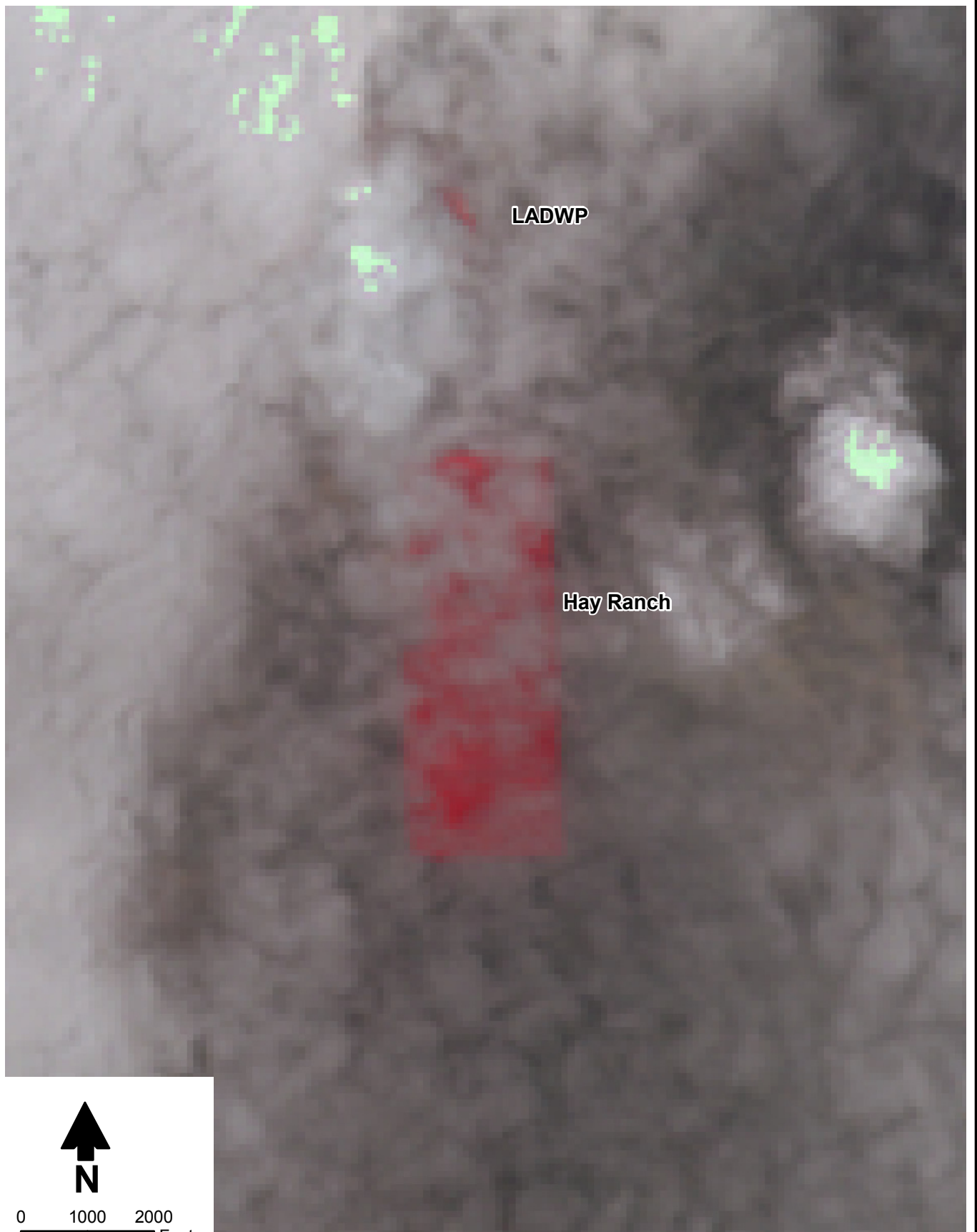
ROSE VALLEY MODEL

**LANDSAT Image of Hay Ranch Area,
August 1, 1984**



Daniel B. Stephens & Associates, Inc.
12/30/2010 JN LT09.0311

Q:\PROJECTS\LT09.0311_ROSE_VALLEY_MODEL\GIS\MXDS\FIGURES\LANDSAT_FIGURES\LANDSAT_1984_JULY_16.MXD 010321



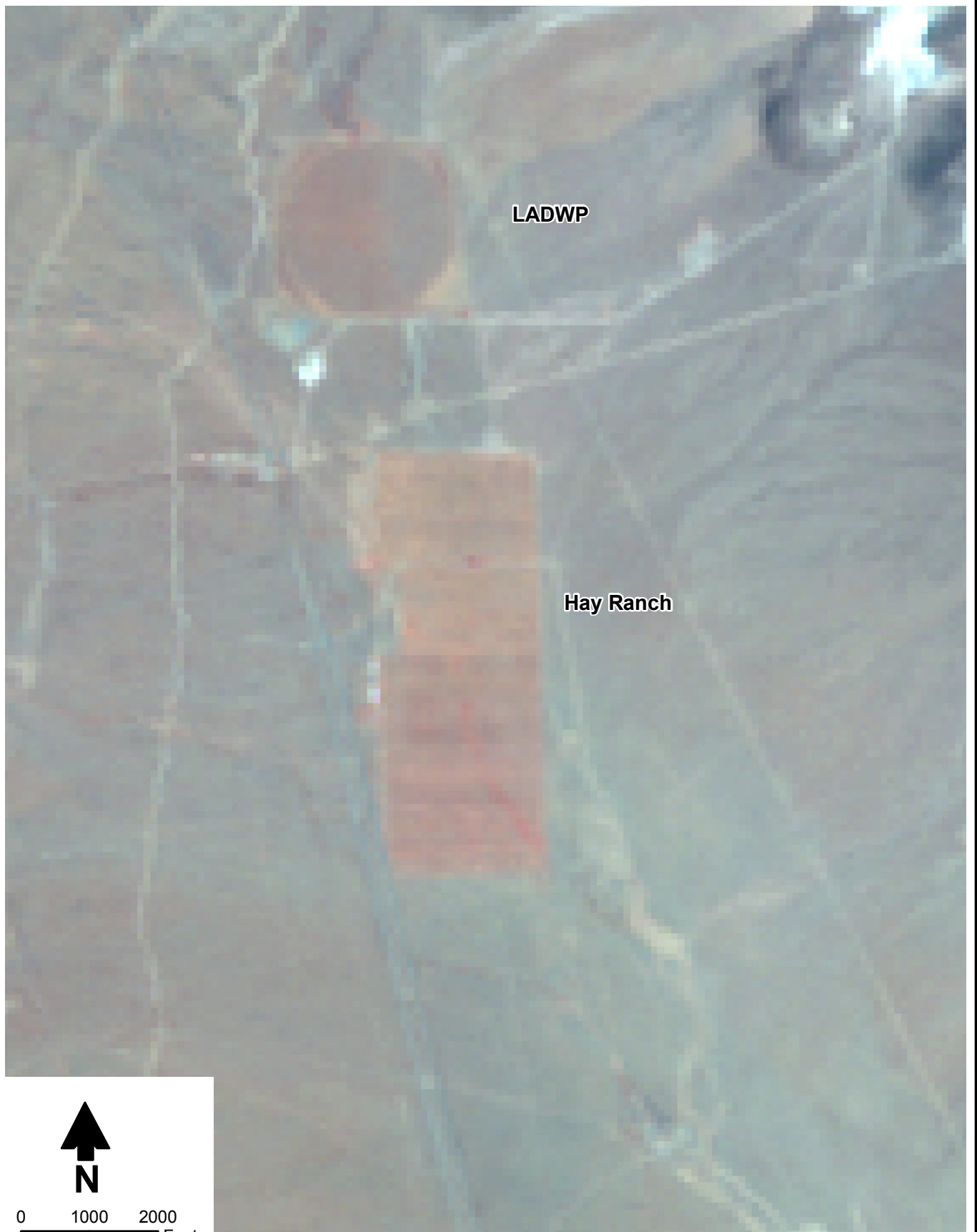
ROSE VALLEY MODEL

**LANDSAT Image of Hay Ranch Area,
July 16, 1984**



Daniel B. Stephens & Associates, Inc.
12/30/2010 JN LT09.0311

Q:\PROJECTS\LT09.0311_ROSE_VALLEY_MODEL\GIS\MXDS\FIGURES\LANDSAT_FIGURES\LANDSAT_1985_JULY_3.MXD 010321



ROSE VALLEY MODEL

**LANDSAT Image of Hay Ranch Area,
July 3, 1985**



Daniel B. Stephens & Associates, Inc.
12/30/2010 JN LT09.0311

Q:\PROJECTS\LT09.0311_ROSE_VALLEY_MODEL\GIS\MXDS\FIGURES\LANDSAT_FIGURES\LANDSAT_1985_JUNE_17.MXD 01 0321



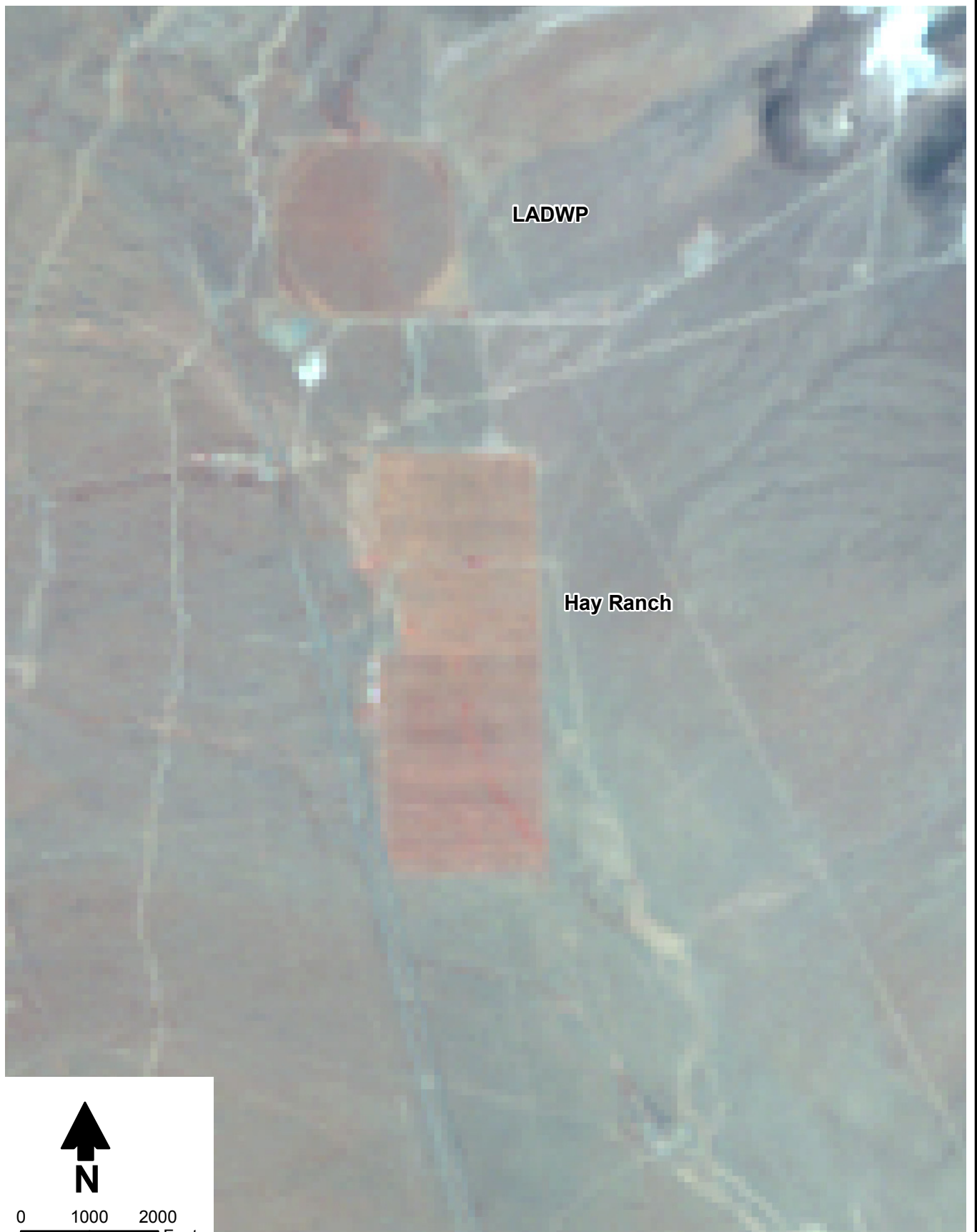
ROSE VALLEY MODEL

**LANDSAT Image of Hay Ranch Area,
June 17, 1985**



Daniel B. Stephens & Associates, Inc.
12/30/2010 JN LT09.0311

Q:\PROJECTS\LT09.0311_ROSE_VALLEY_MODEL\GIS\MXDS\FIGURES\LANDSAT_FIGURES\LANDSAT_1986_AUGUST_7.MXD 010321



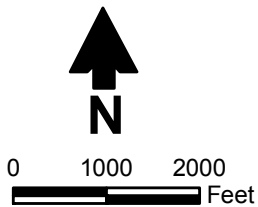
ROSE VALLEY MODEL

**LANDSAT Image of Hay Ranch Area,
August 7, 1986**



Daniel B. Stephens & Associates, Inc.
12/30/2010 JN LT09.0311

Q:\PROJECTS\LT09.0311_ROSE_VALLEY_MODEL\GIS\MXDS\FIGURES\LANDSAT_FIGURES\LANDSAT_1987_APRIL_20.MXD 010321



ROSE VALLEY MODEL

**LANDSAT Image of Hay Ranch Area,
April 20, 1987**



Daniel B. Stephens & Associates, Inc.
12/30/2010 JN LT09.0311

Q:\PROJECTS\LT09.0311_ROSE_VALLEY_MODEL\GIS\MXDS\FIGURES\LANDSAT_FIGURES\LANDSAT_1987_JULY_25.MXD 010321



ROSE VALLEY MODEL

**LANDSAT Image of Hay Ranch Area,
July 25, 1987**



Daniel B. Stephens & Associates, Inc.
12/30/2010 JN LT09.0311

Q:\PROJECTS\LT09.0311_ROSE_VALLEY_MODEL\GIS\MXDS\FIGURES\LANDSAT_FIGURES\LANDSAT_1988_JULY_27.MXD 010321



0 1000 2000
Feet

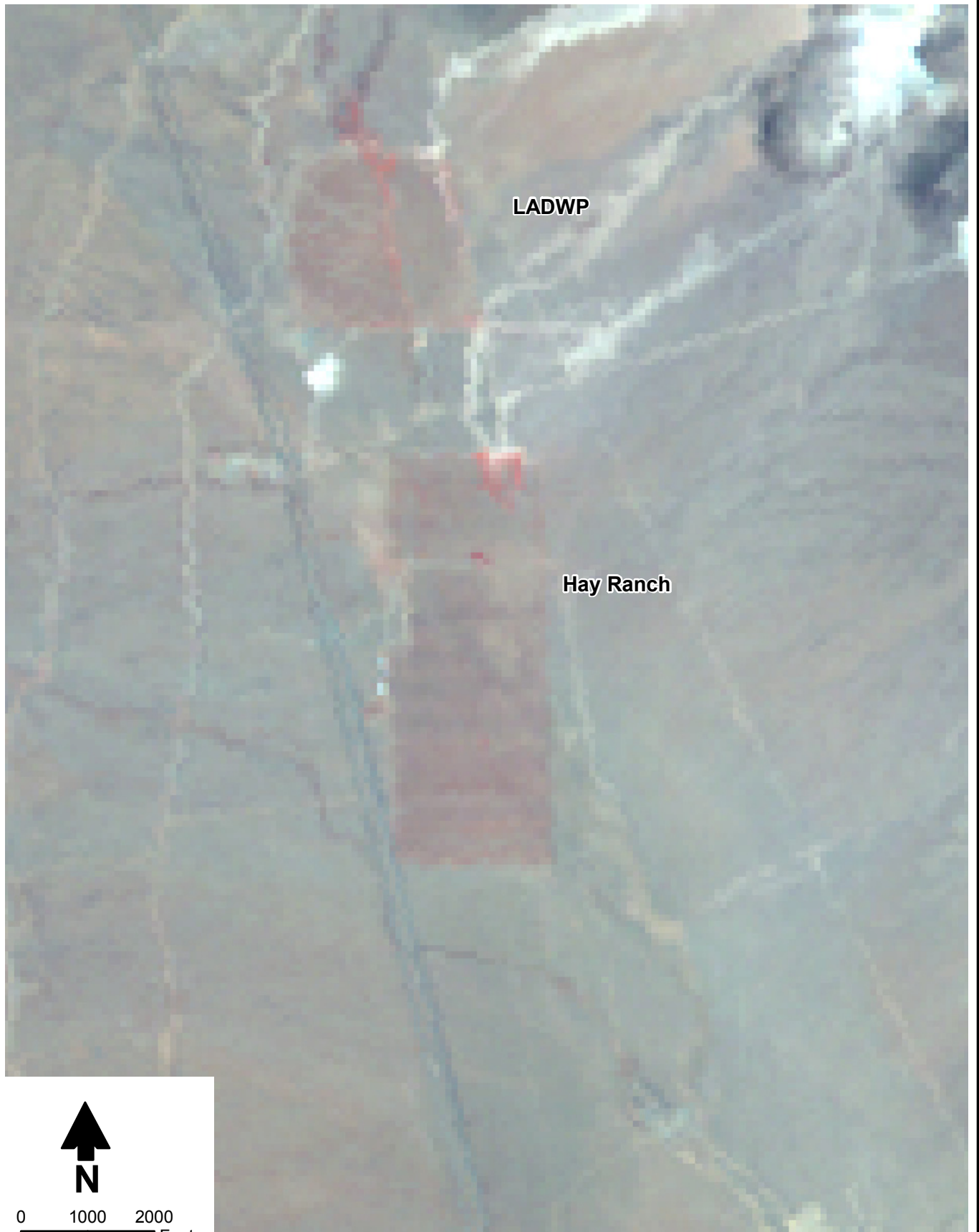
ROSE VALLEY MODEL

**LANDSAT Image of Hay Ranch Area,
July 27, 1988**



Daniel B. Stephens & Associates, Inc.
12/30/2010 JN LT09.0311

Q:\PROJECTS\LT09.0311_ROSE_VALLEY_MODEL\GIS\MXDS\FIGURES\LANDSAT_FIGURES\LANDSAT_1989_JUNE_28.MXD 01 0321



ROSE VALLEY MODEL

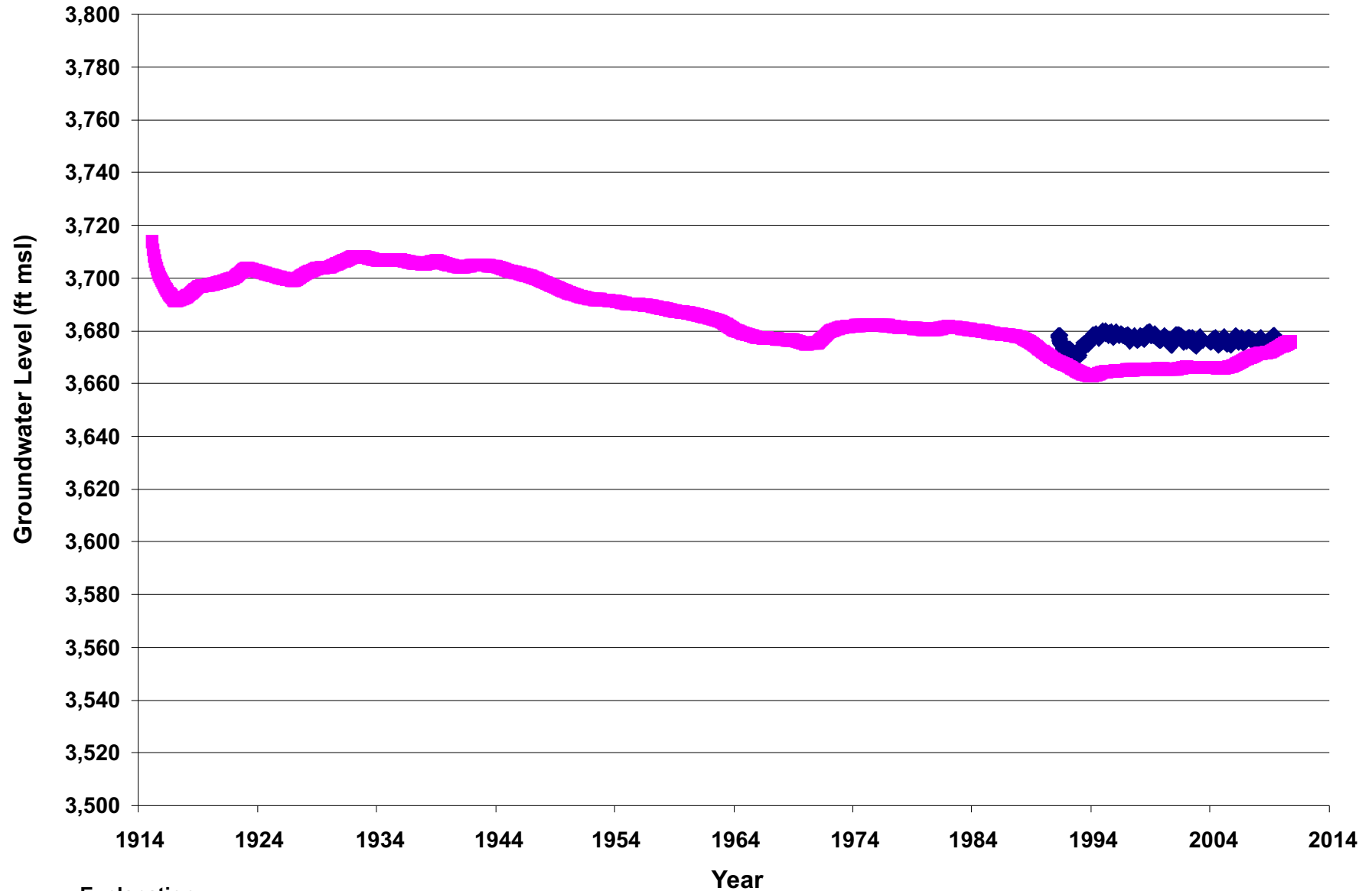
**LANDSAT Image of Hay Ranch Area,
June 28, 1989**

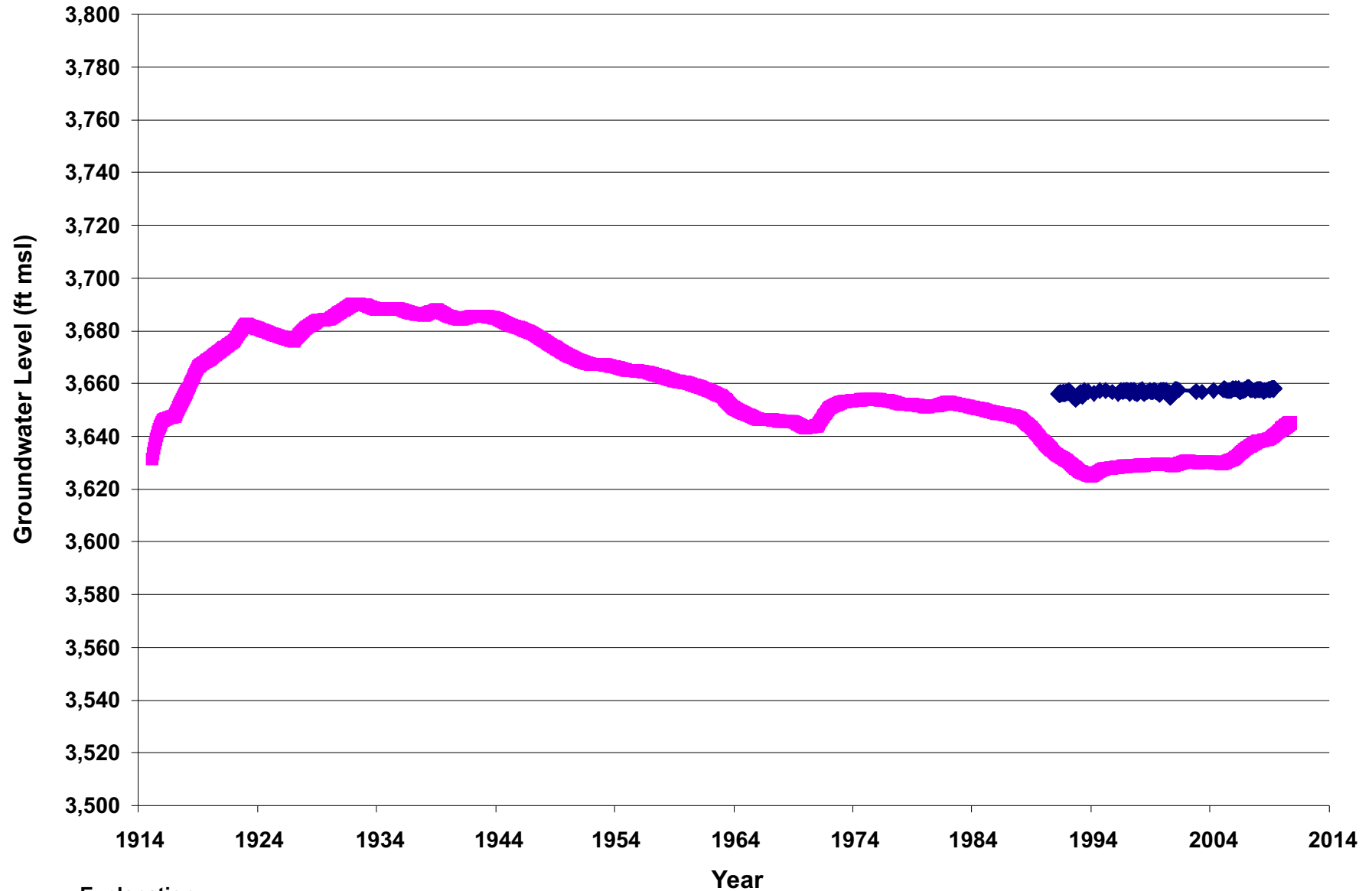


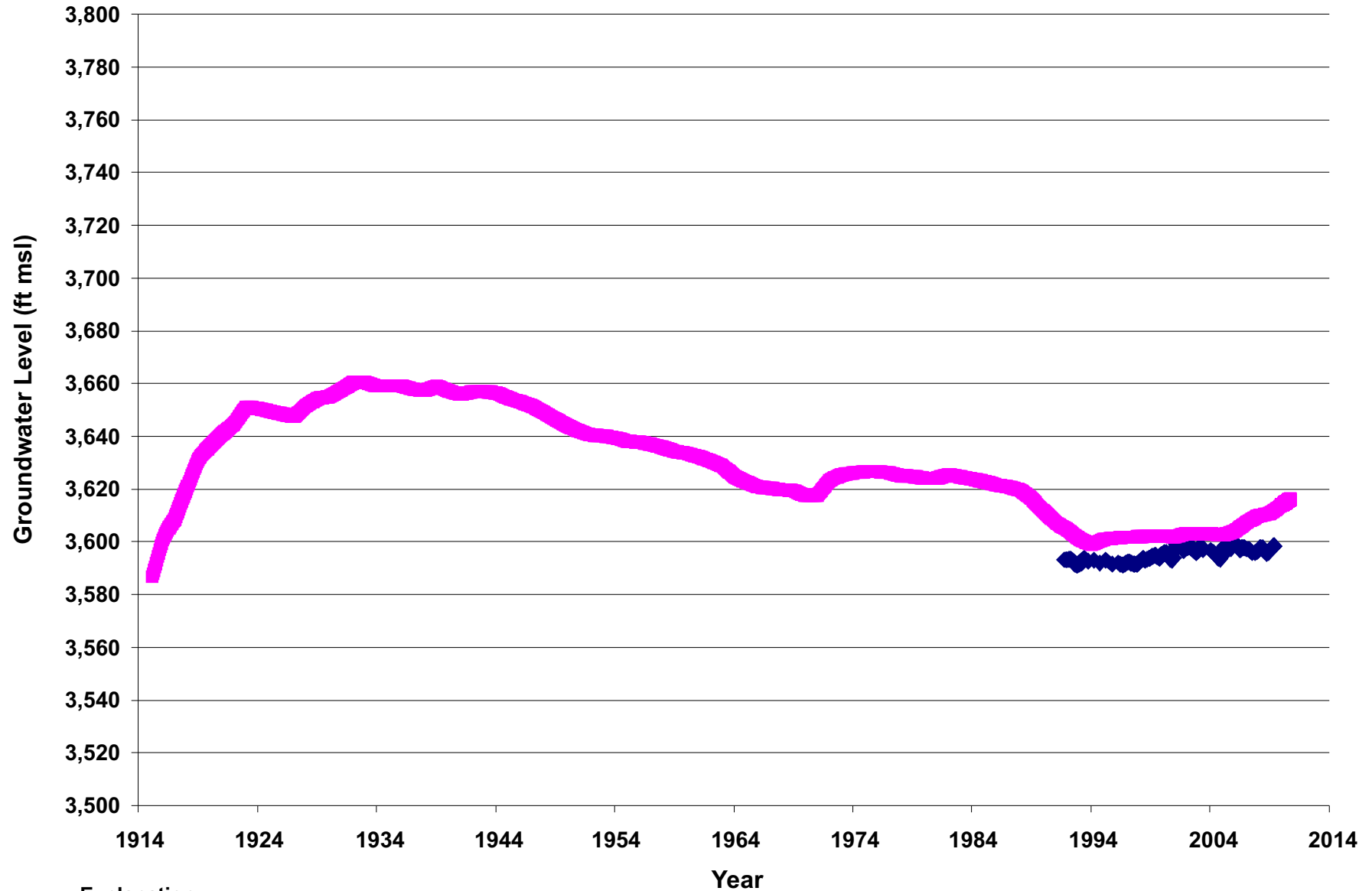
Daniel B. Stephens & Associates, Inc.
12/30/2010 JN LT09.0311

Appendix C

Simulated and Observed Water Levels



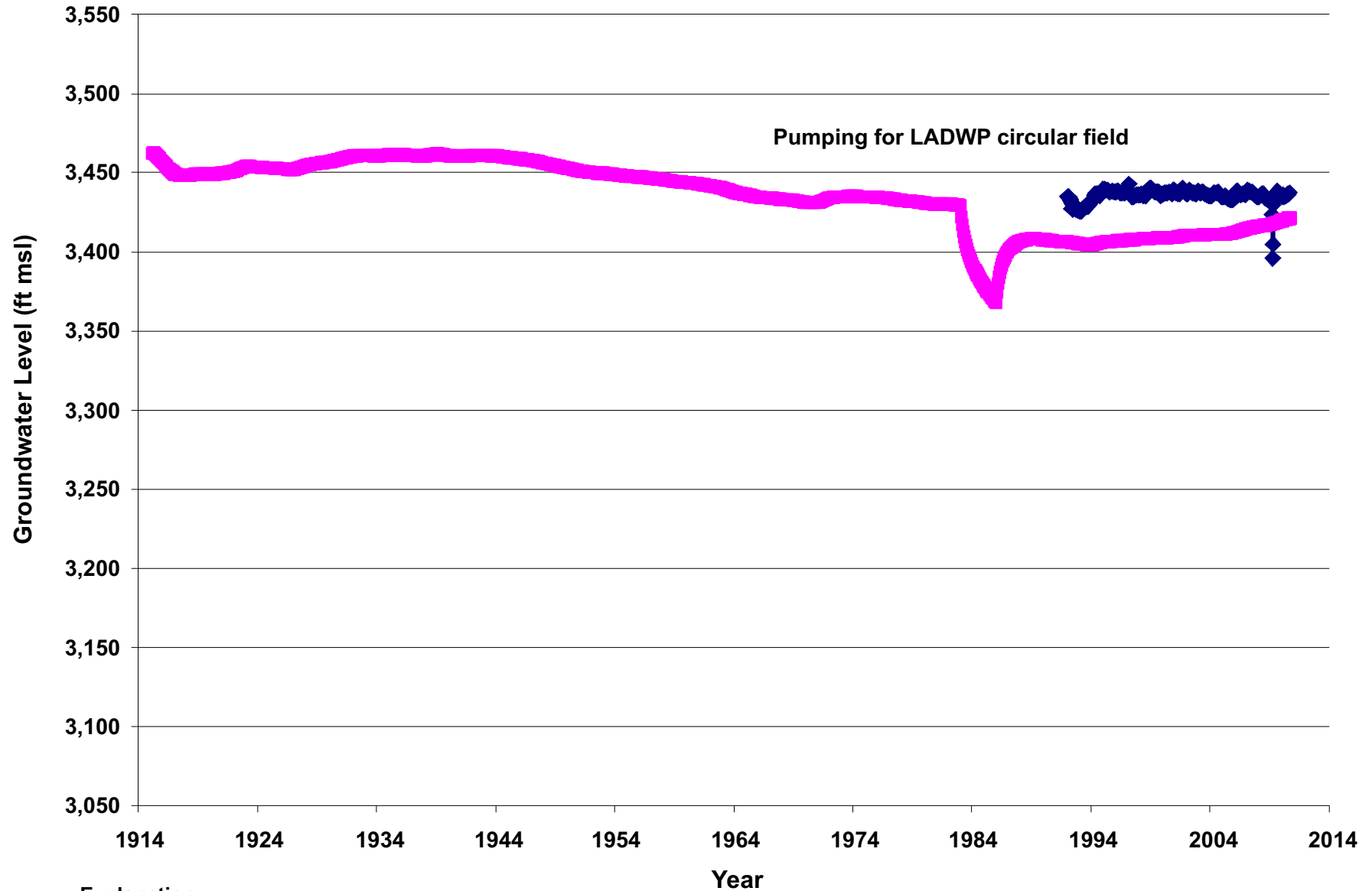




Explanation

- Simulated water level
- Observed water level

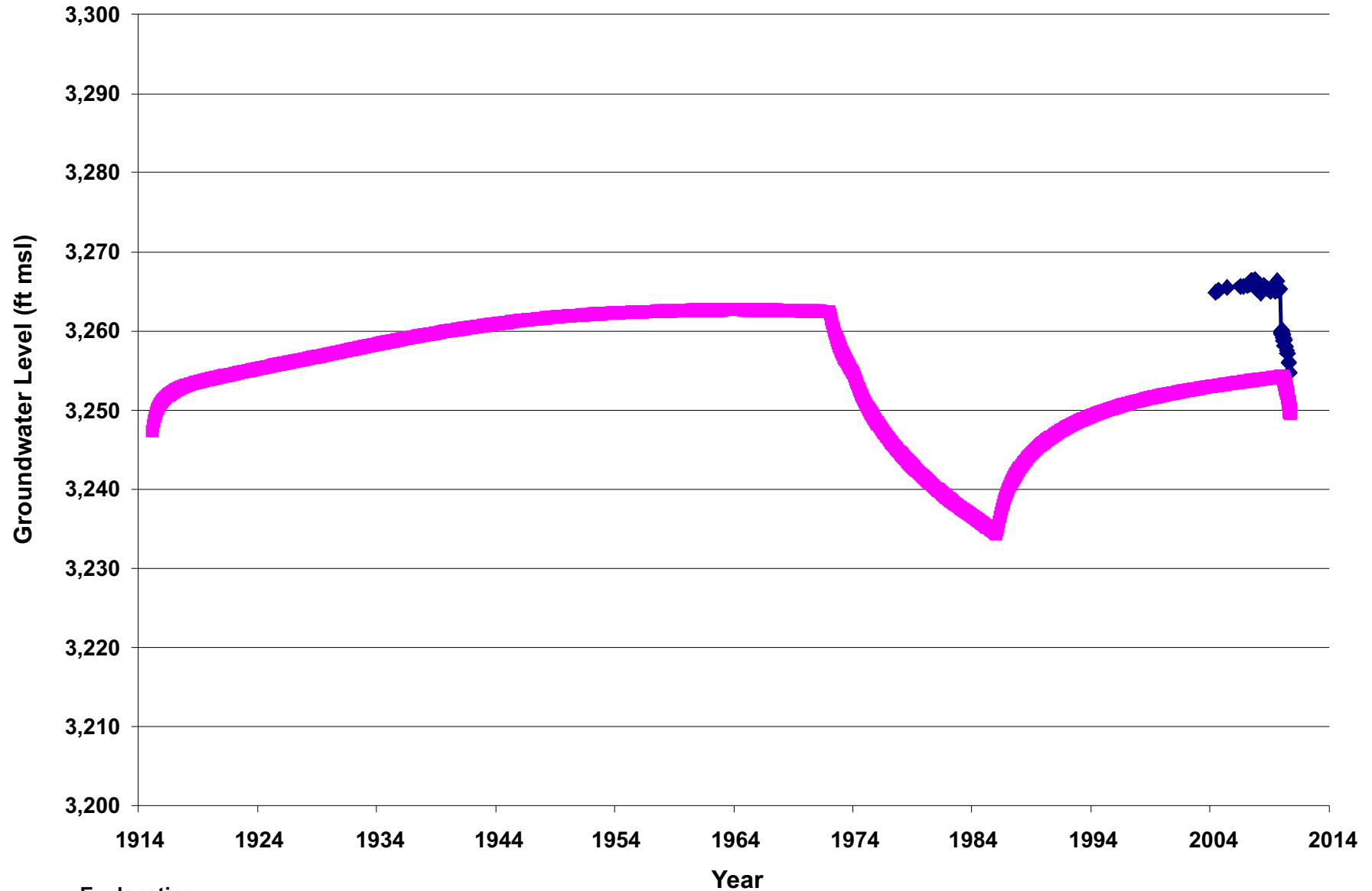




Explanation

- Simulated water level
- Observed water level





Explanation

- Simulated water level
- Observed water level

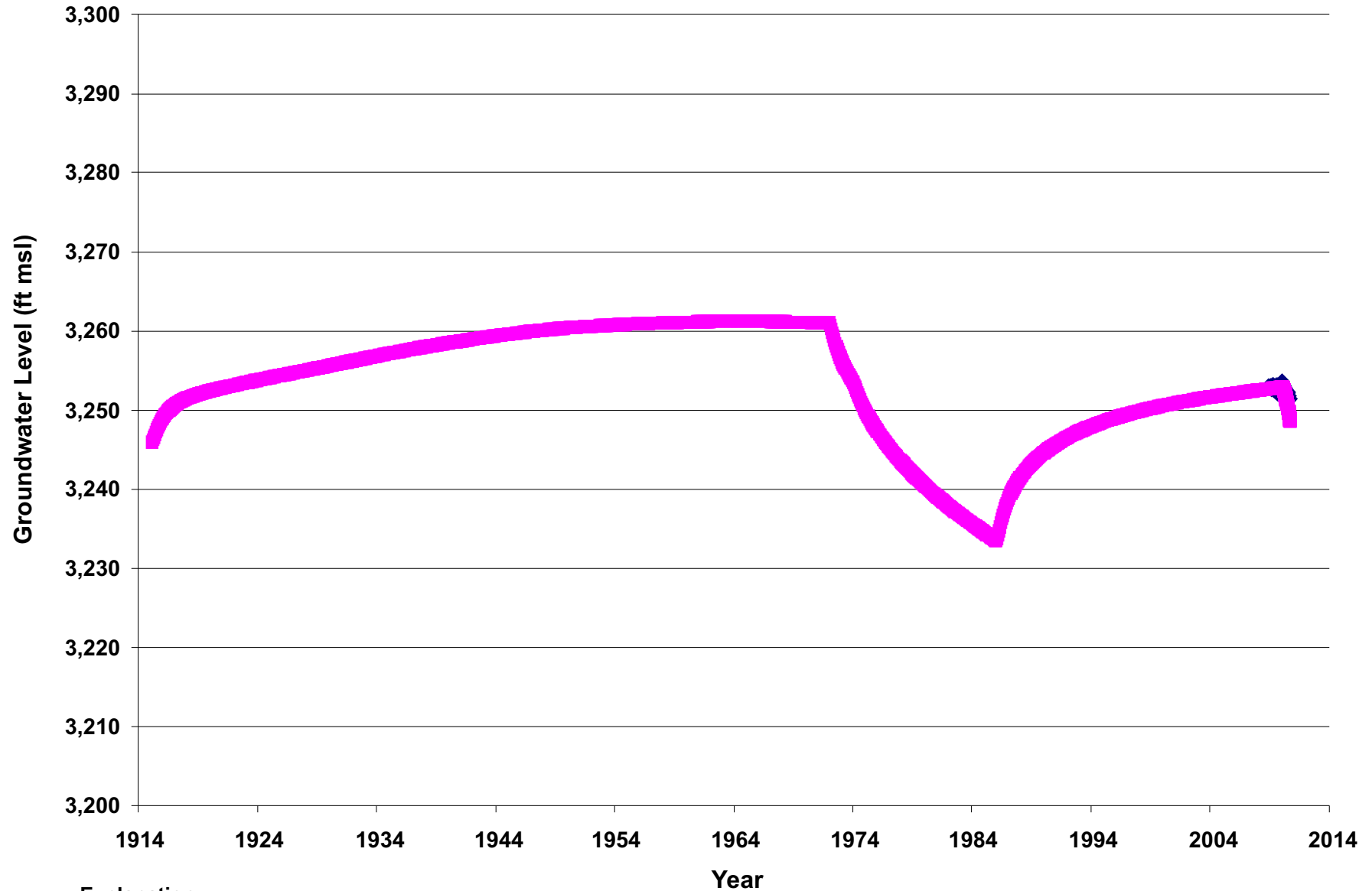


Daniel B. Stephens & Associates, Inc.

1-4-11

JN LT09.0311

ROSE VALLEY MODEL
Well RV030 Hydrograph



Explanation

- Simulated water level
- Observed water level

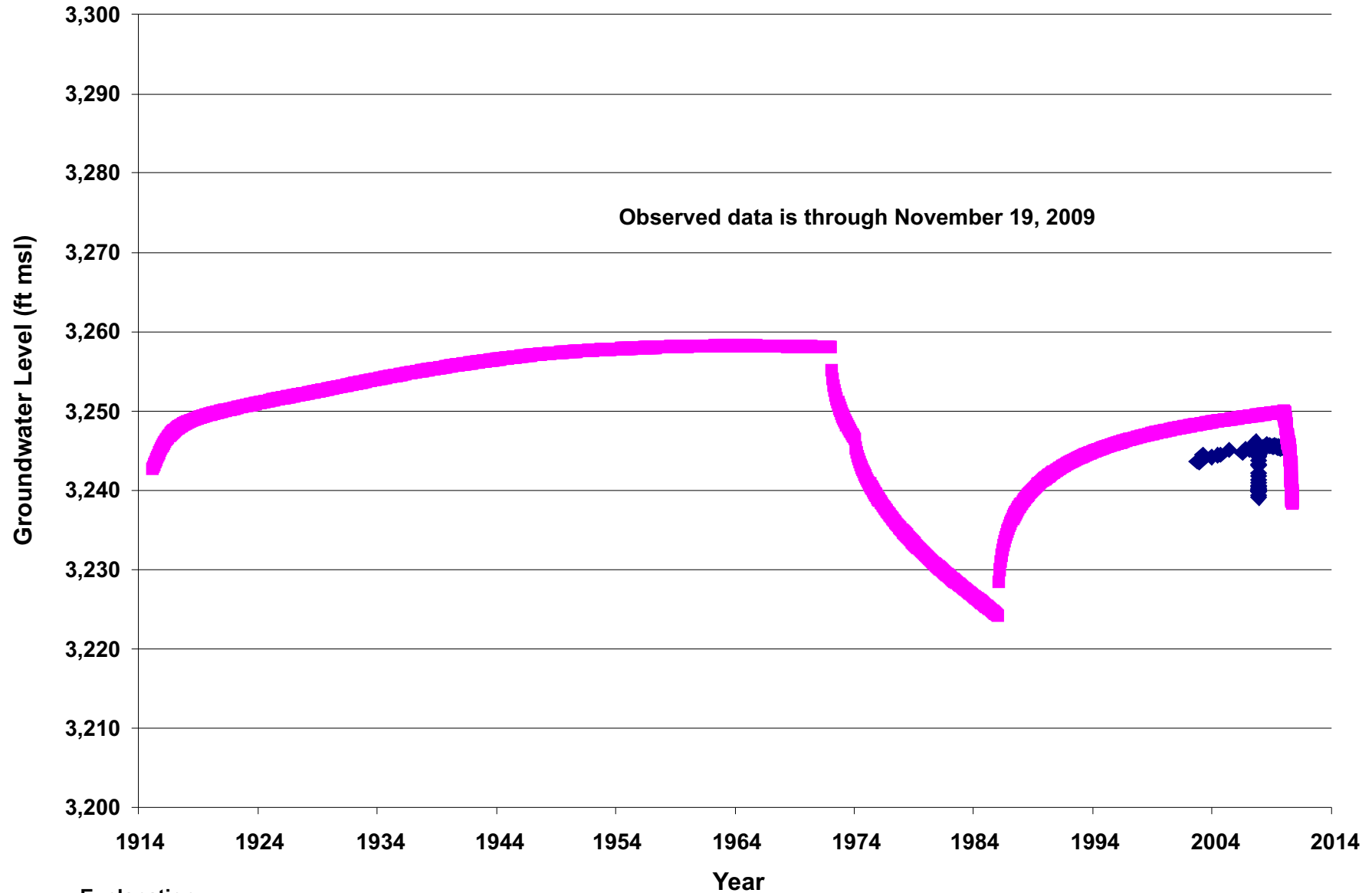


Daniel B. Stephens & Associates, Inc.

1-4-11

JN LT09.0311

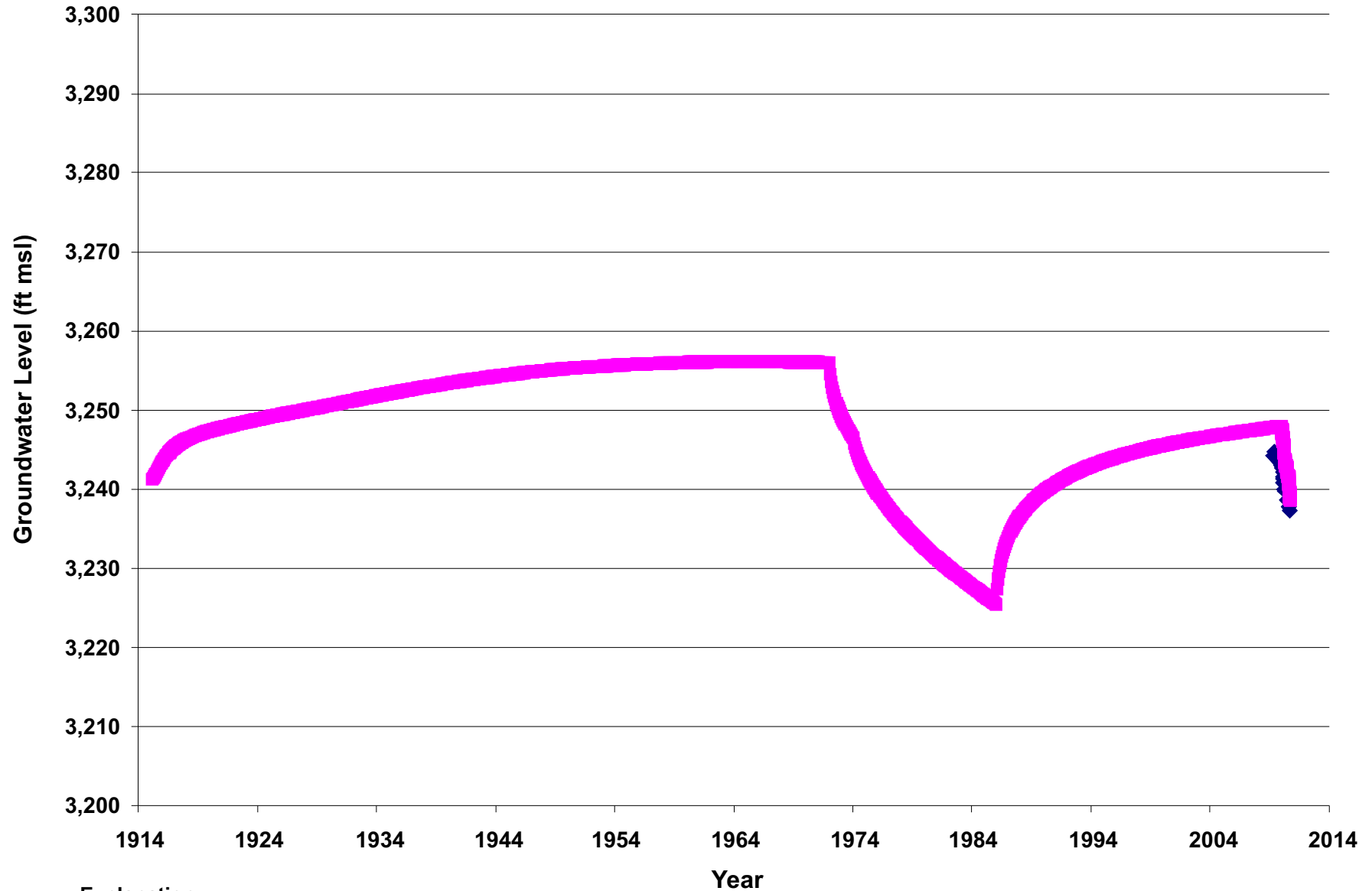
ROSE VALLEY MODEL
Well RV040 Hydrograph



Explanation

- Simulated water level
- Observed water level





Explanation

- Simulated water level
- Observed water level

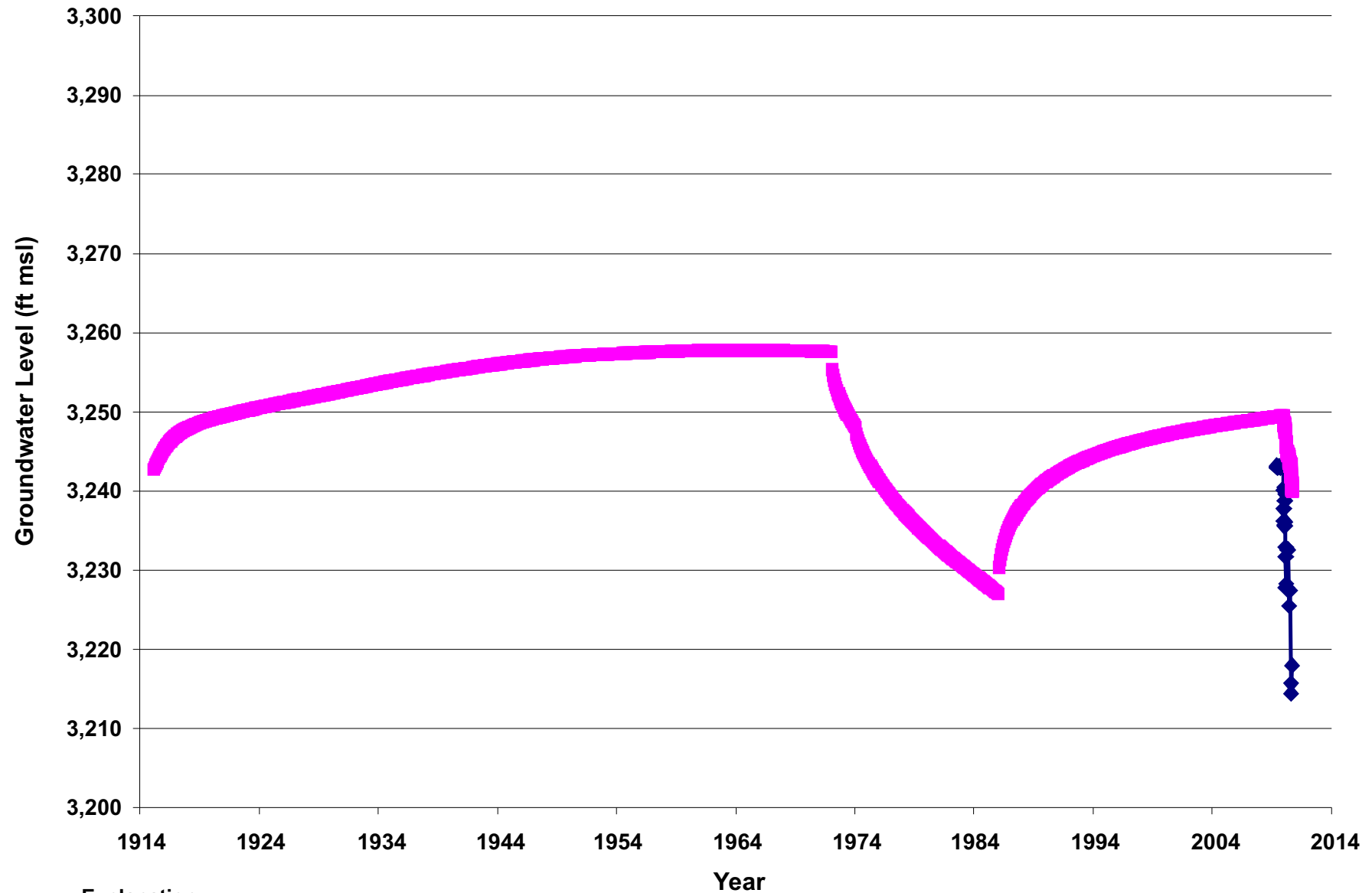


Daniel B. Stephens & Associates, Inc.

1-4-11

JN LT09.0311

ROSE VALLEY MODEL
Well RV060 Hydrograph



Explanation

- Simulated water level
- Observed water level

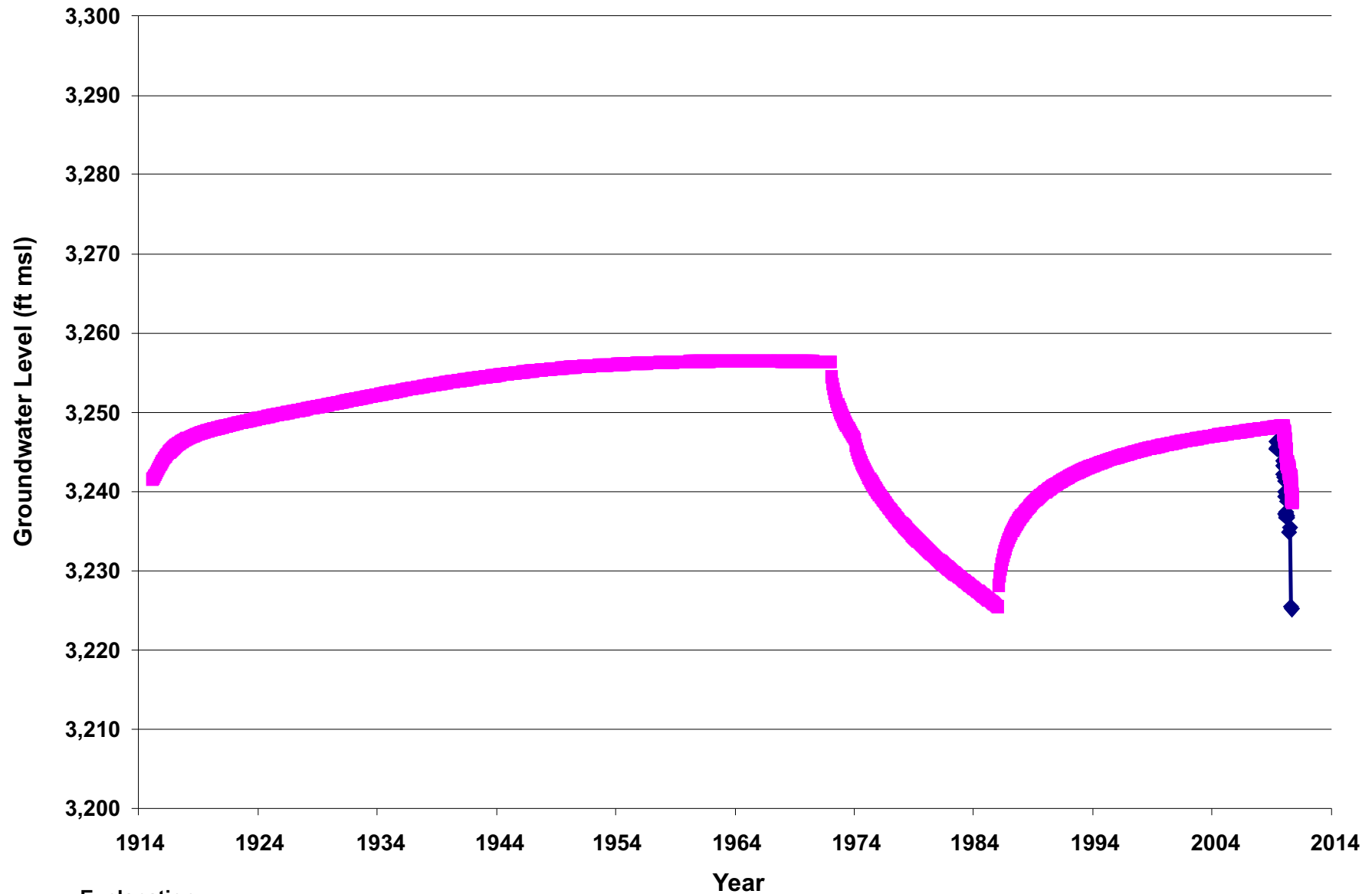


Daniel B. Stephens & Associates, Inc.

1-4-11

JN LT09.0311

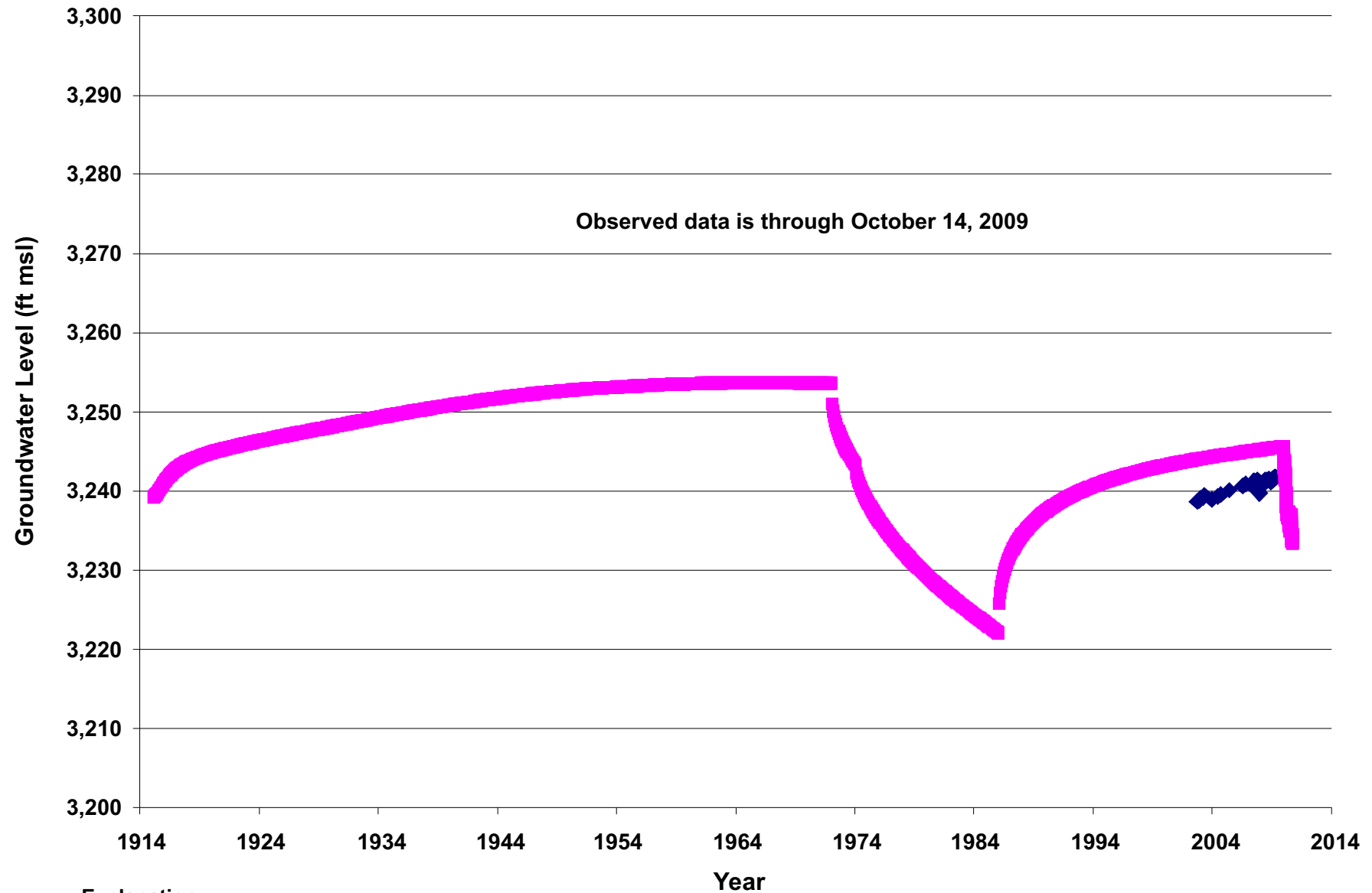
ROSE VALLEY MODEL
Well RV061 Hydrograph



Explanation

- Simulated water level
- Observed water level

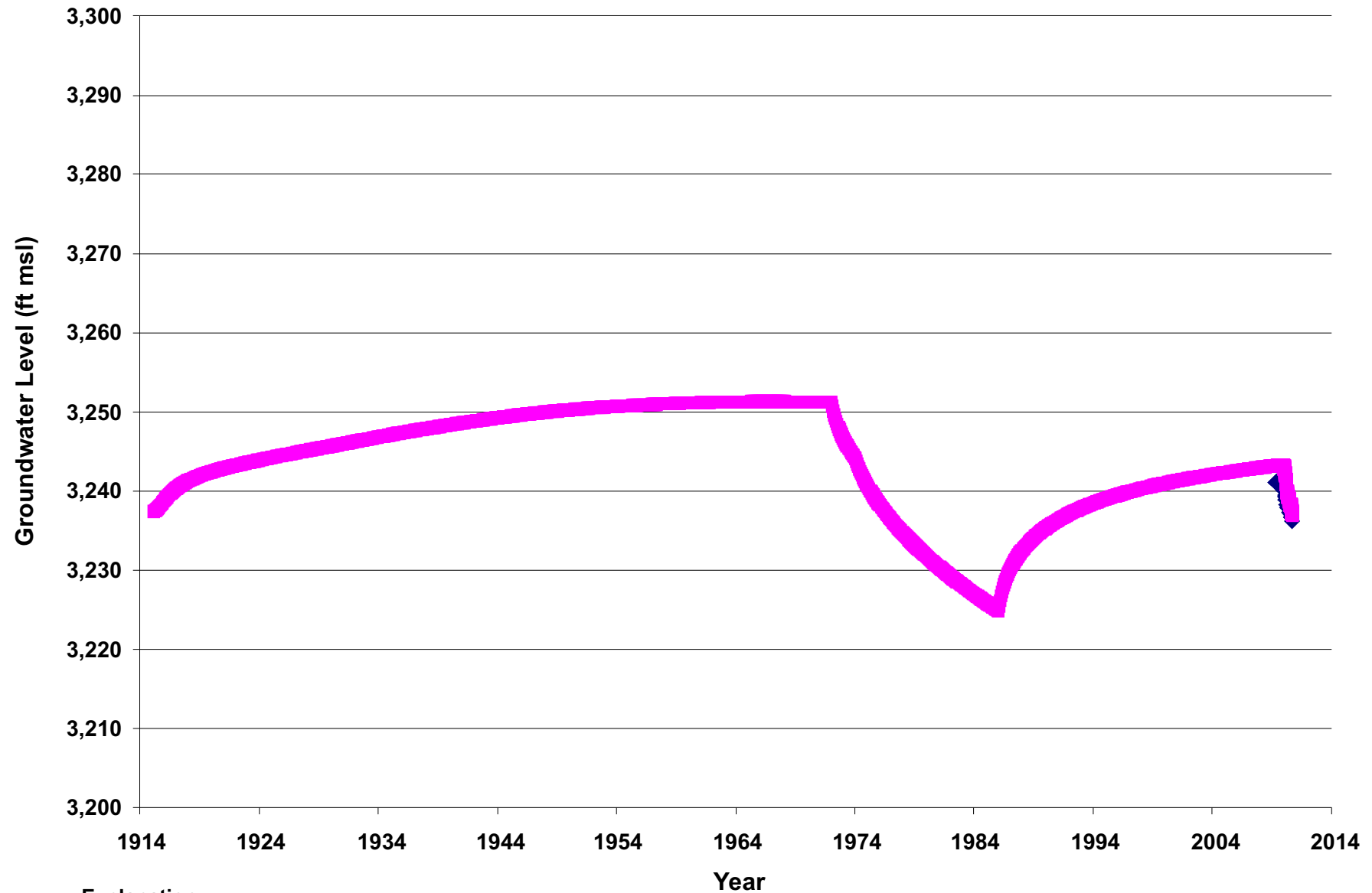




Explanation

- Simulated water level
- Observed water level

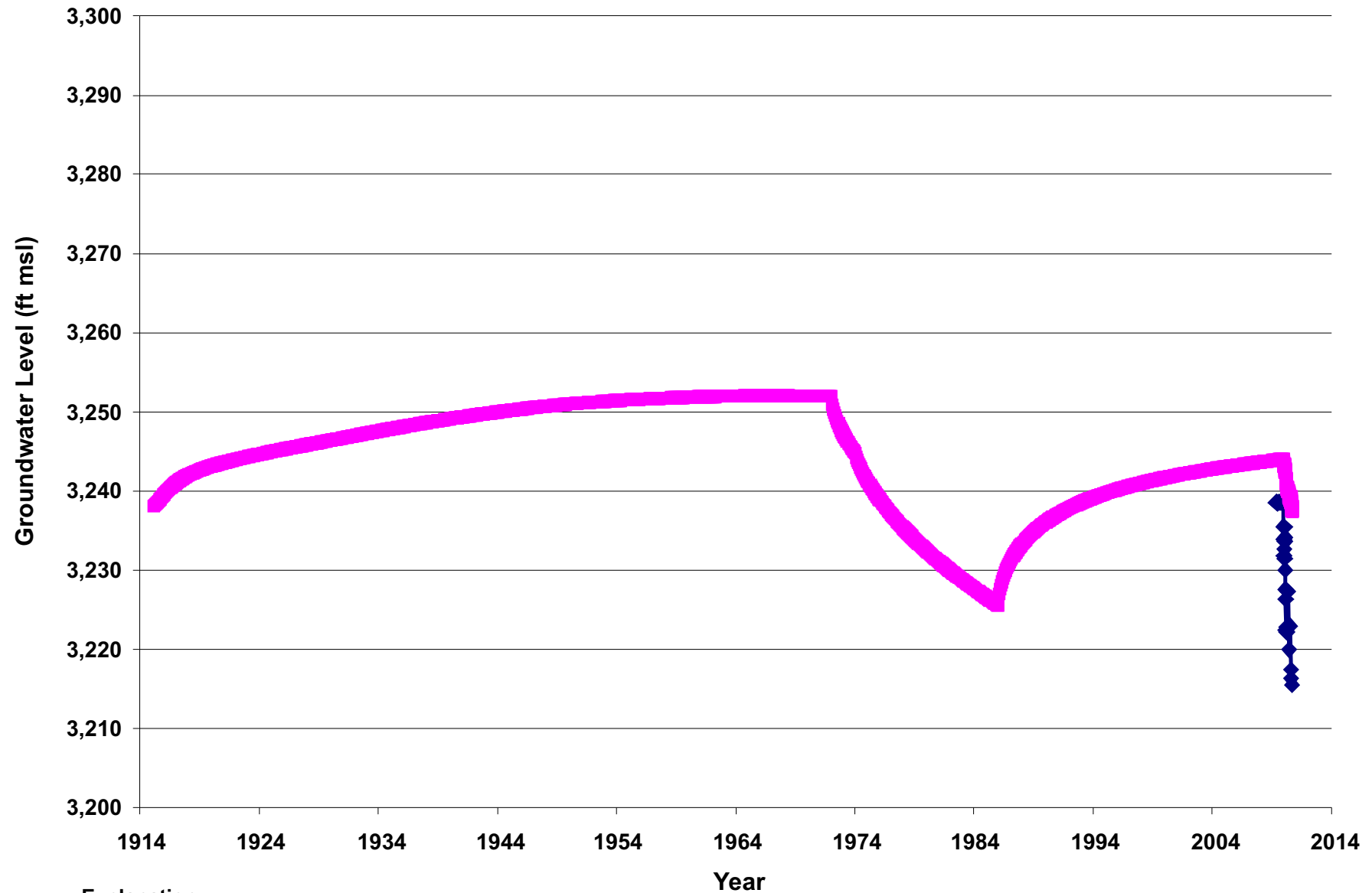




Explanation

- Simulated water level
- Observed water level

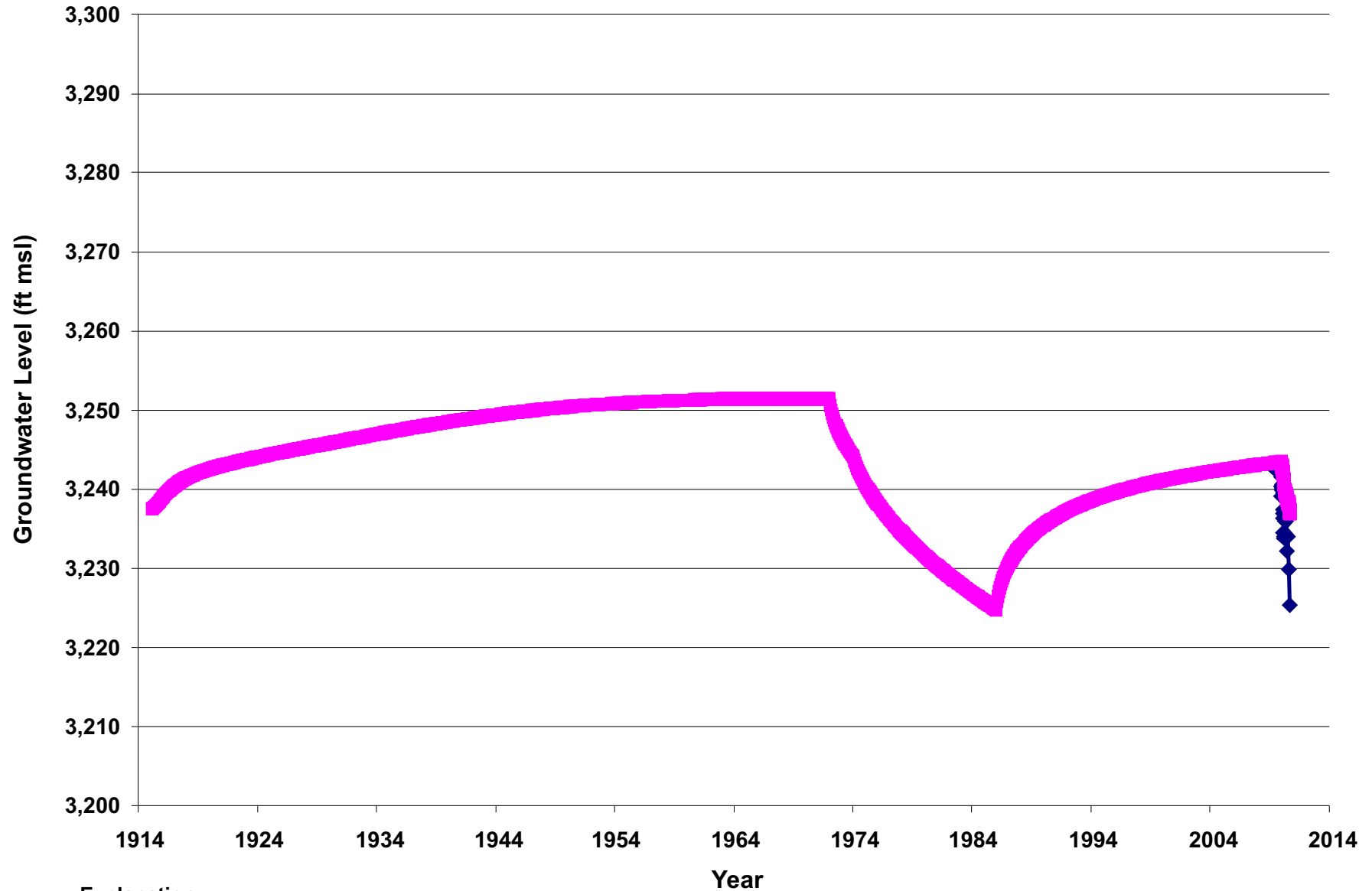




Explanation

- Simulated water level
- Observed water level

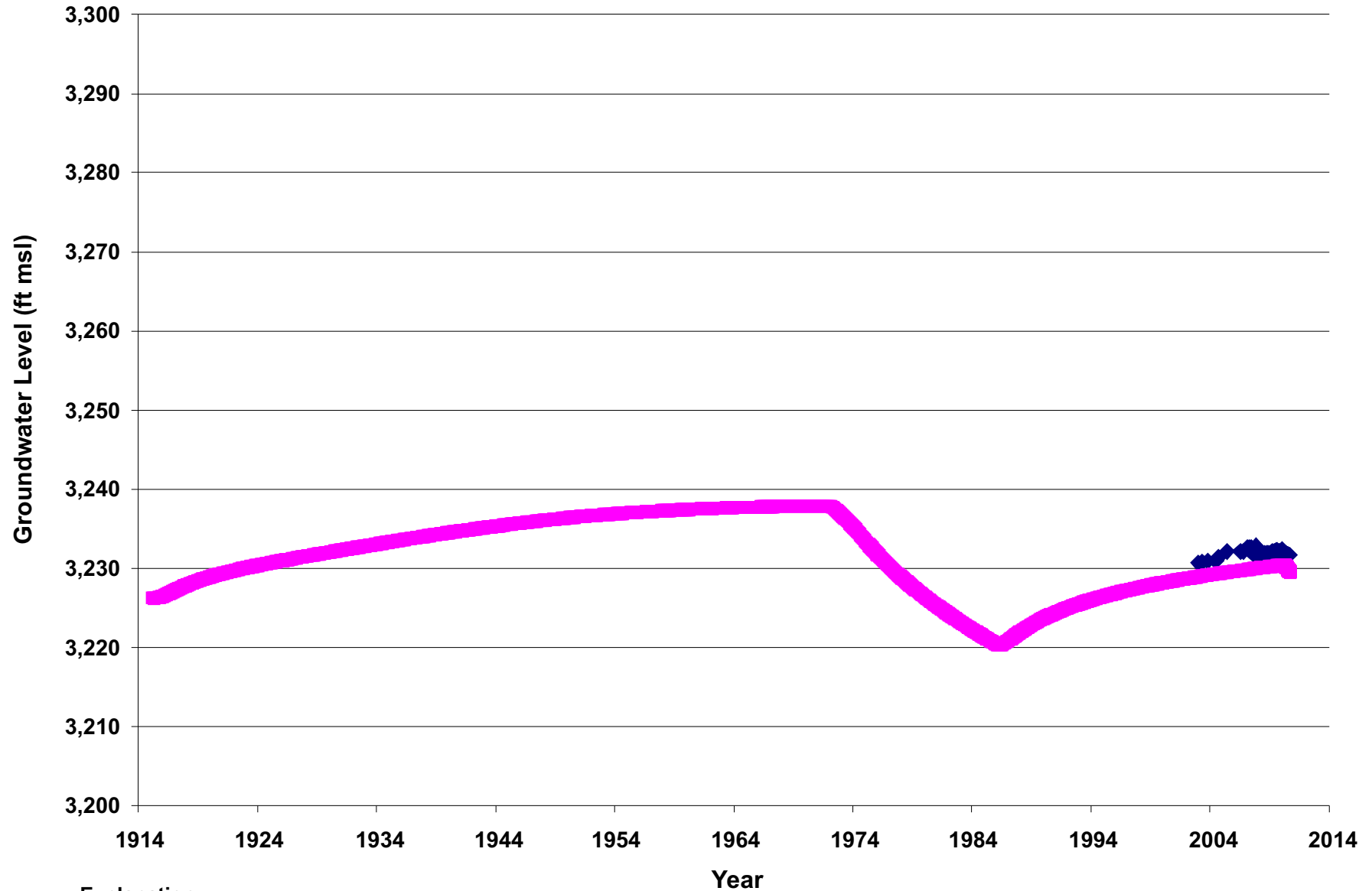




Explanation

- Simulated water level
- Observed water level

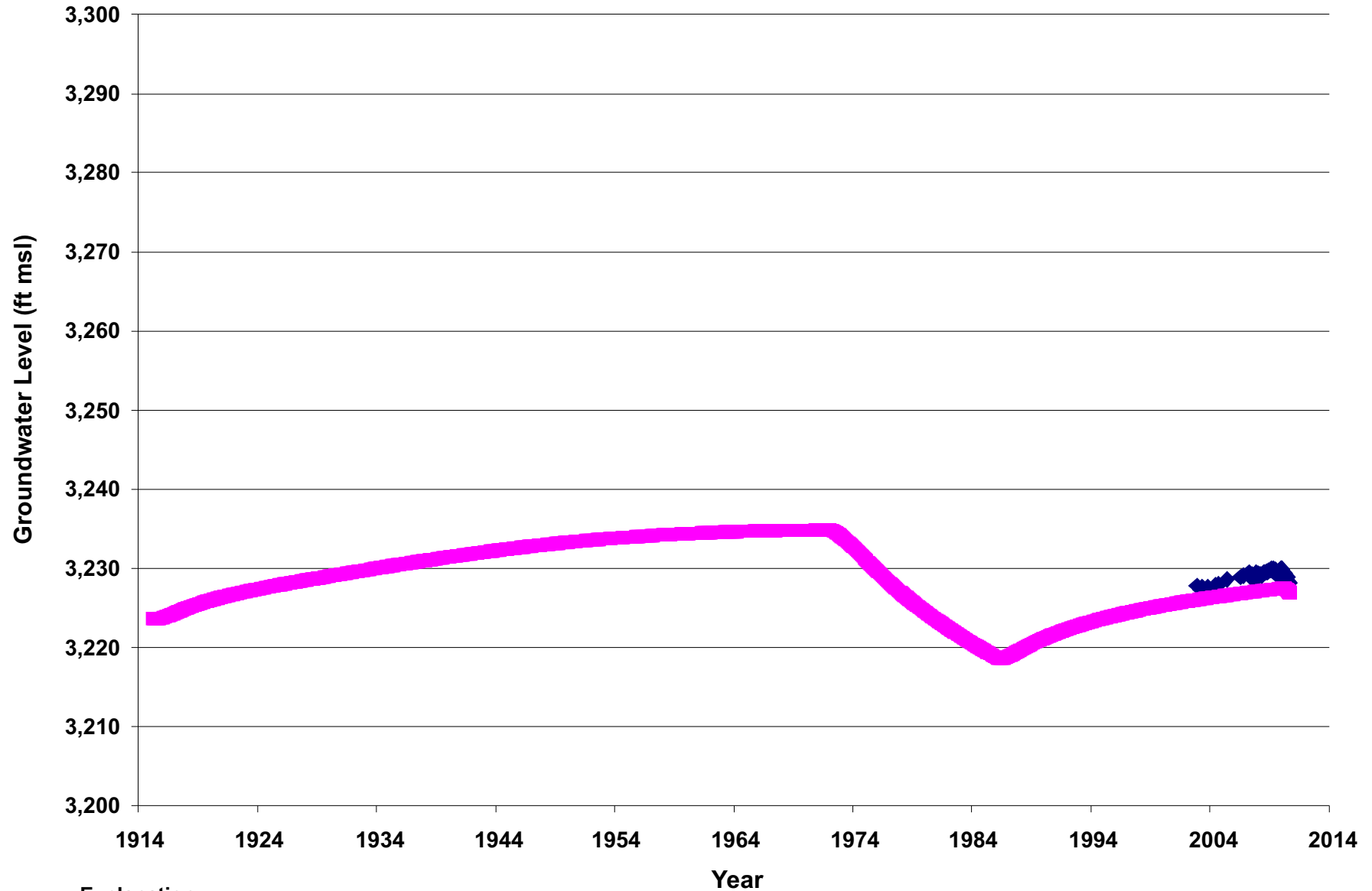




Explanation

- Simulated water level
- Observed water level





Explanation

- Simulated water level
- Observed water level

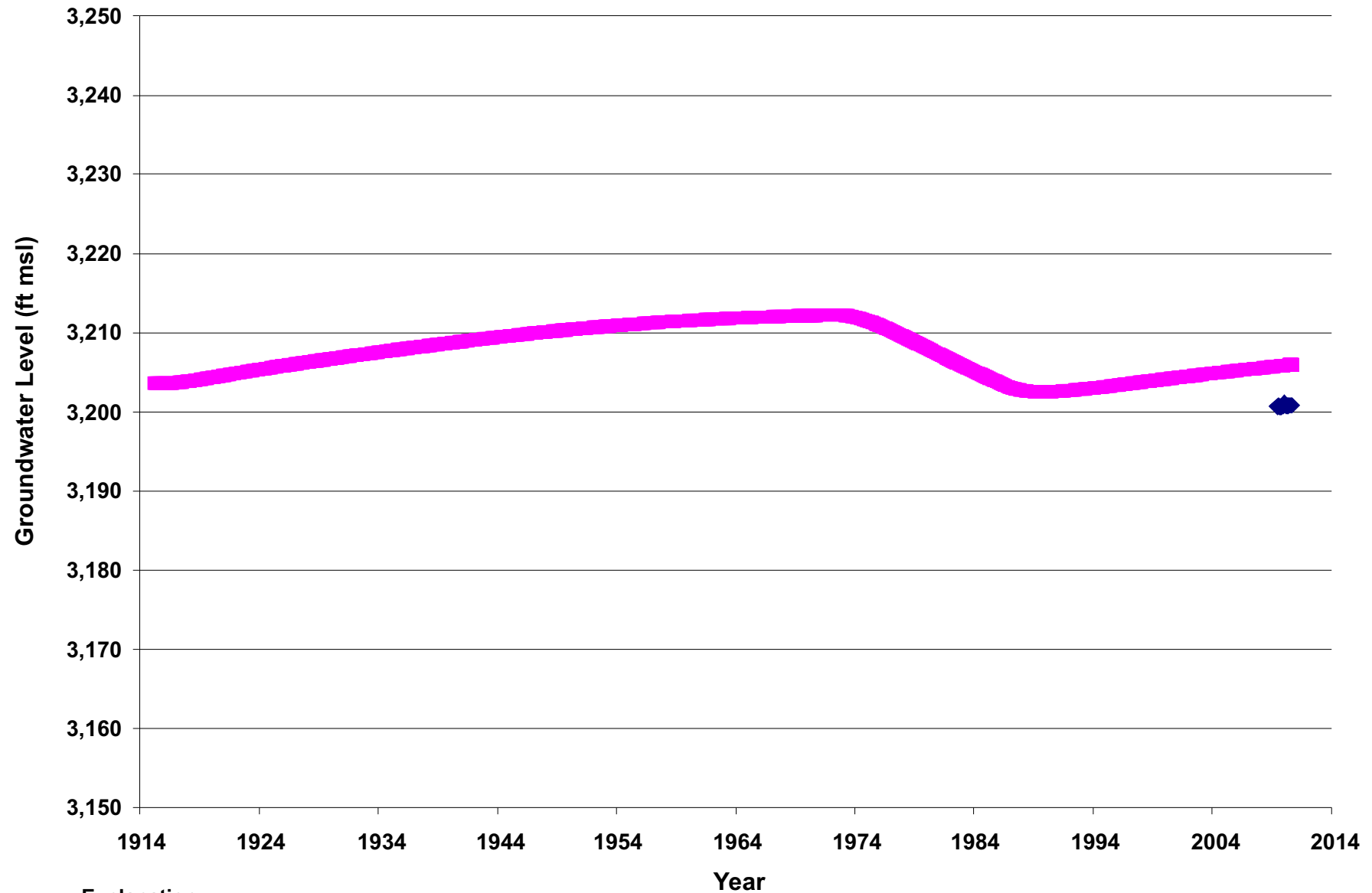


Daniel B. Stephens & Associates, Inc.

1-4-11

JN LT09.0311

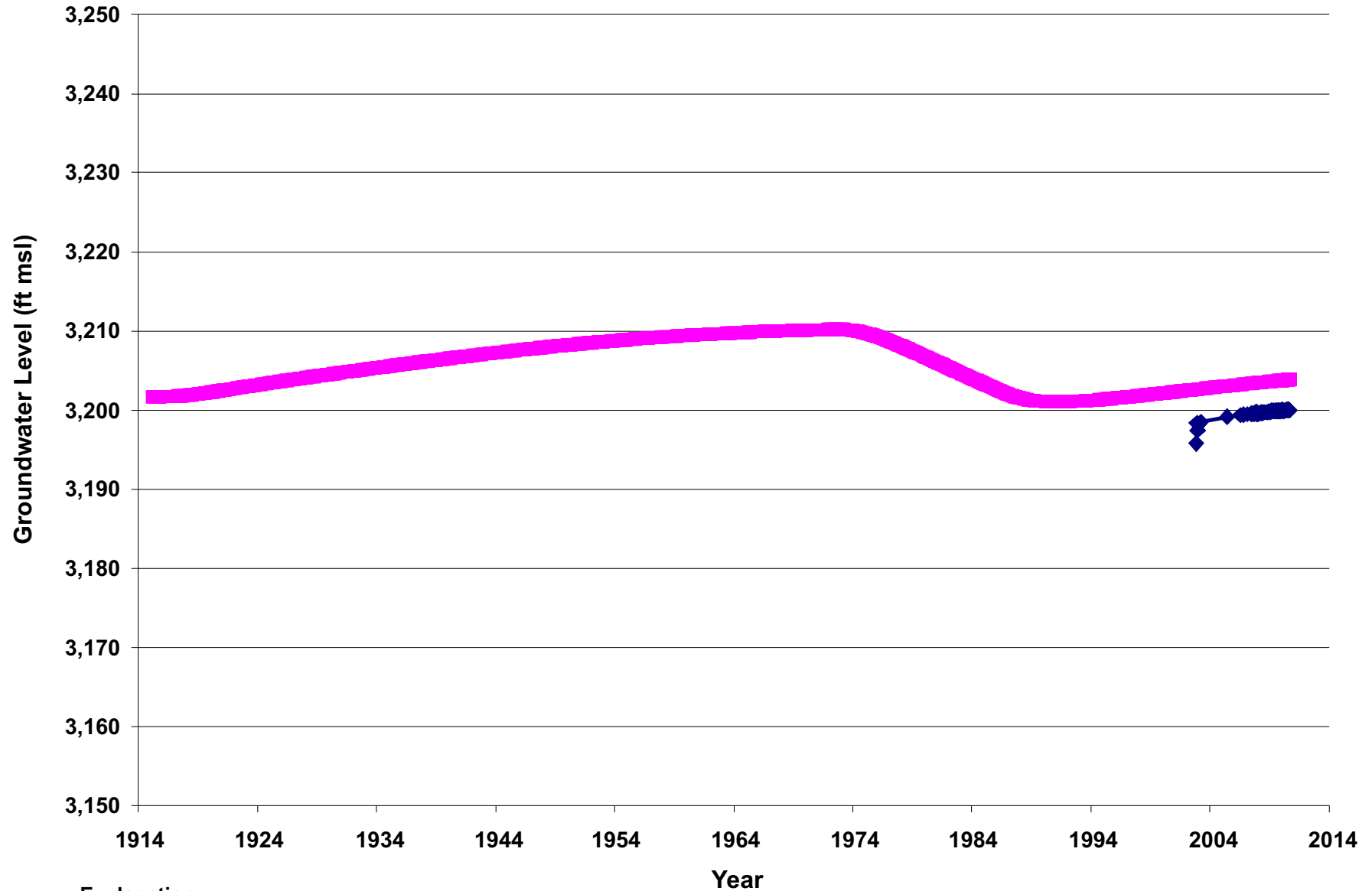
ROSE VALLEY MODEL
Well RV100 Hydrograph



Explanation

- Simulated water level
- Observed water level

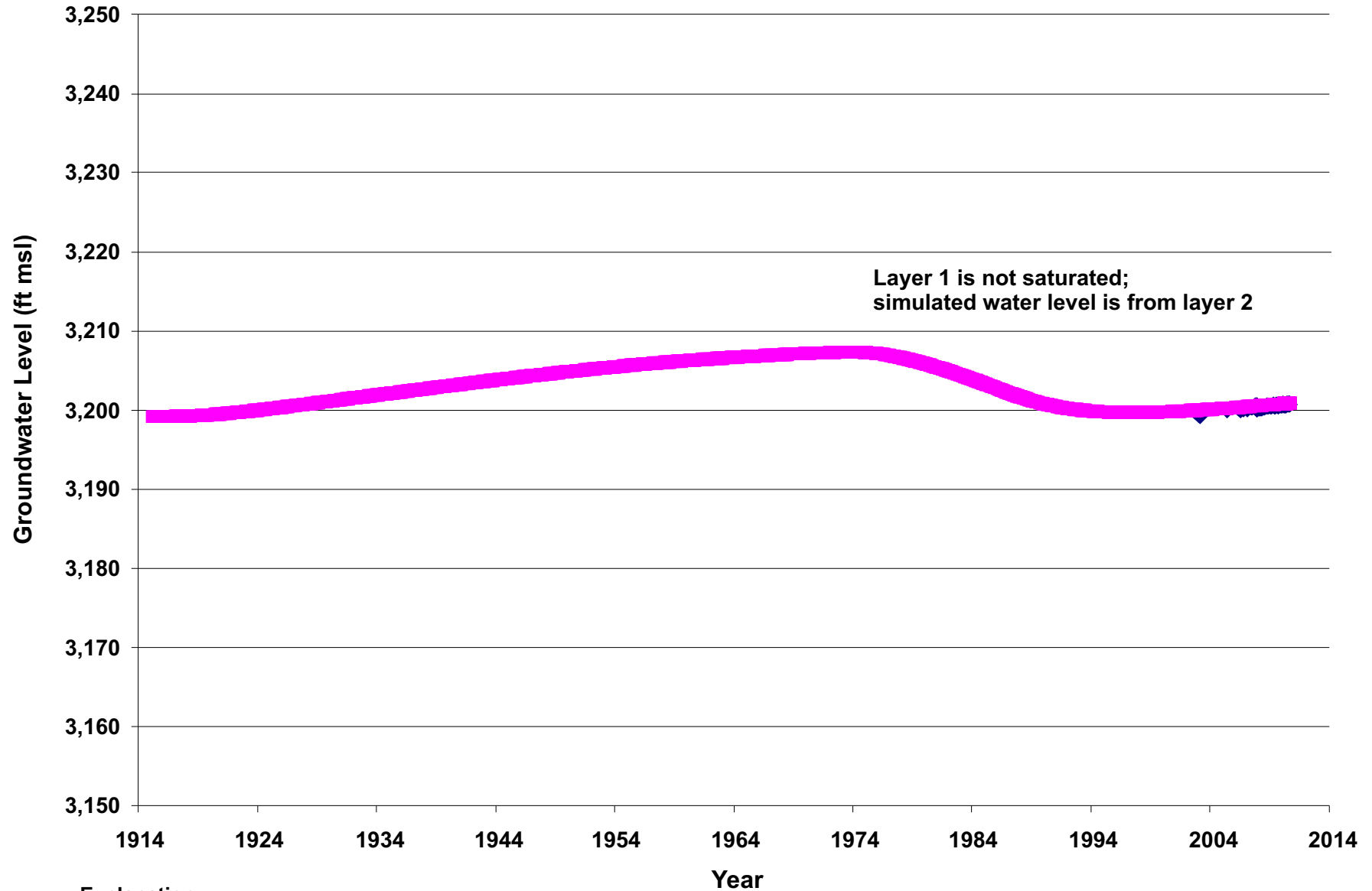




Explanation

- Simulated water level
- Observed water level

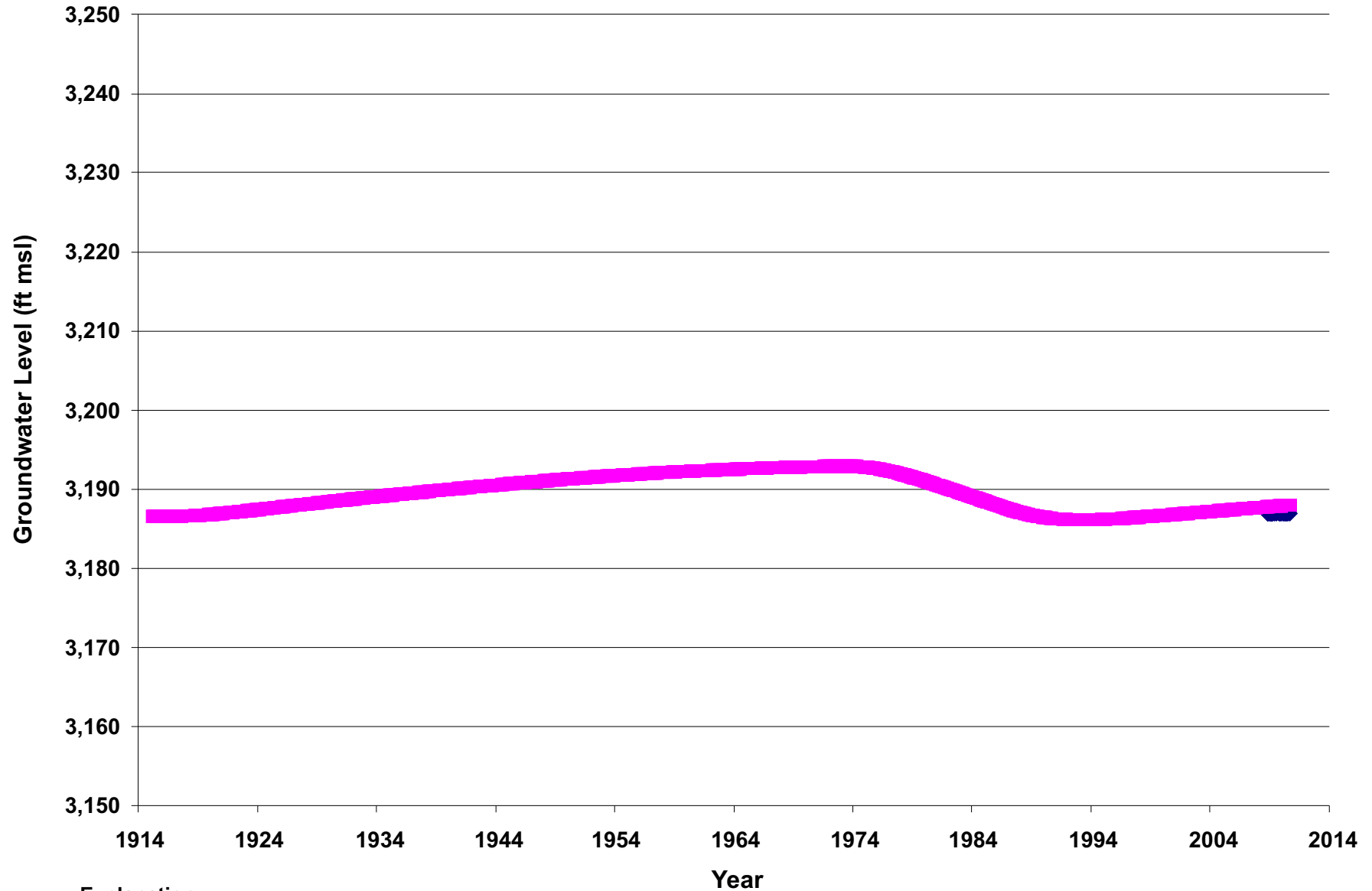




Explanation

- Simulated water level
- Observed water level

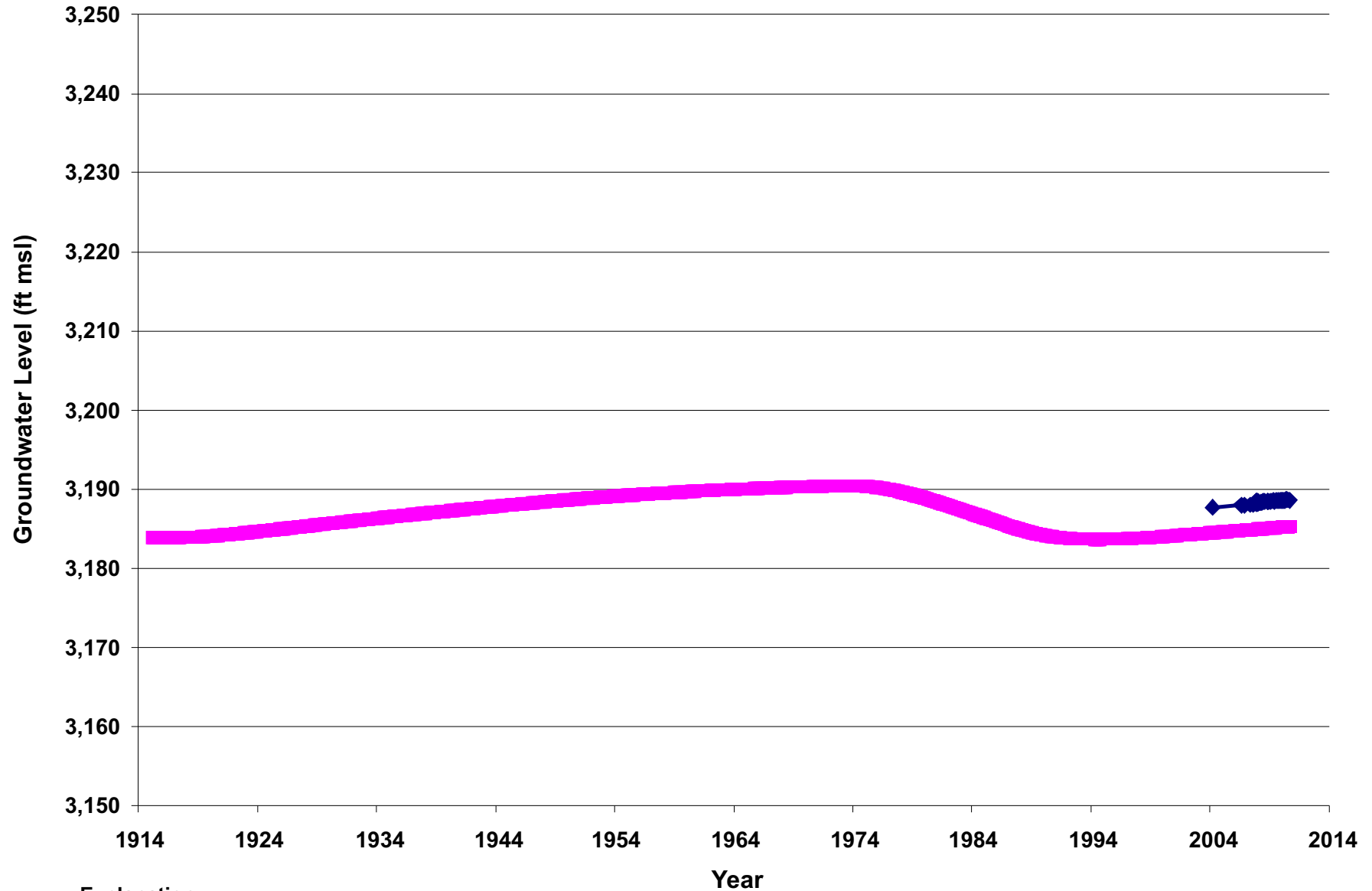




Explanation

- Simulated water level
- Observed water level

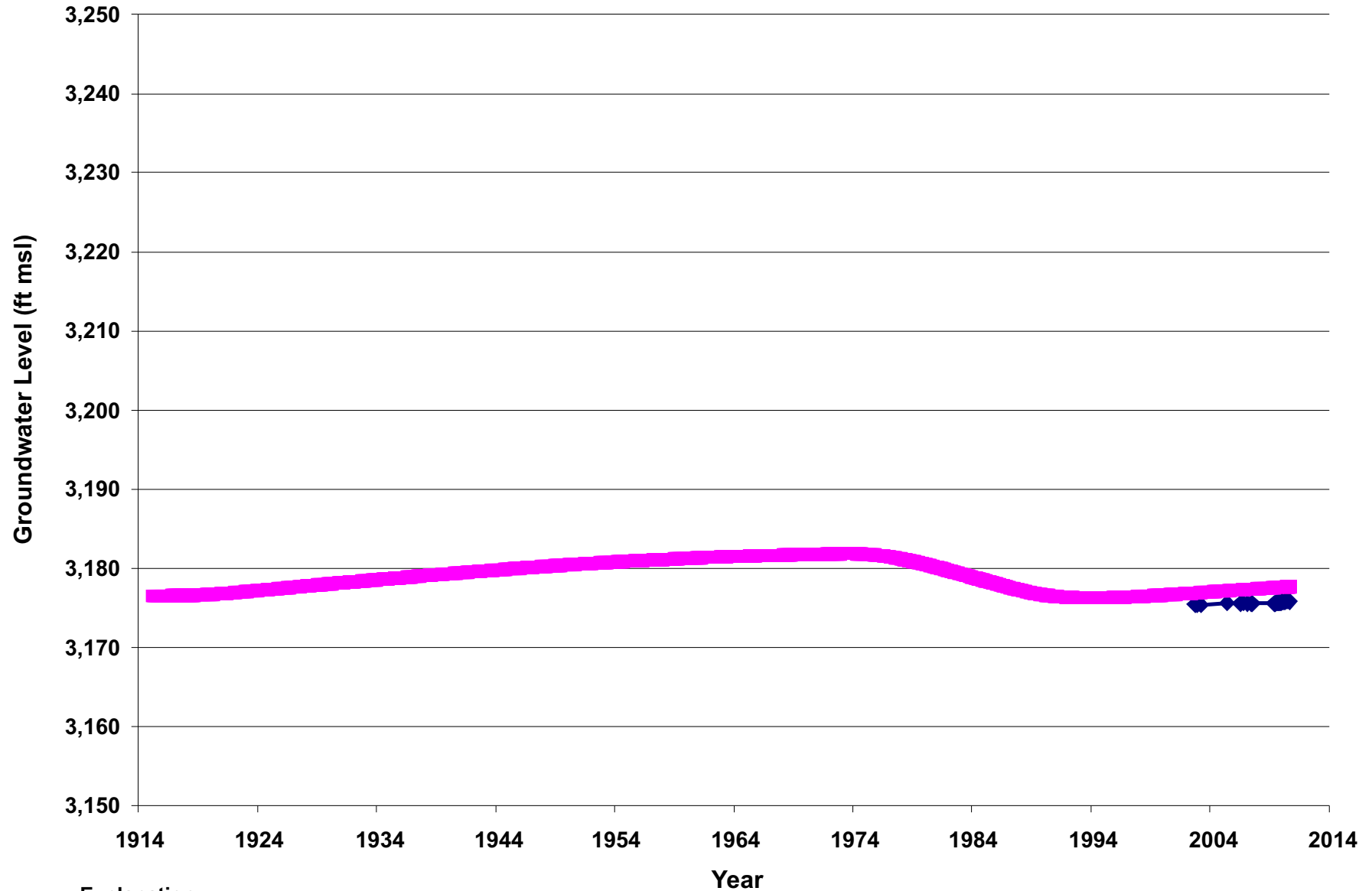




Explanation

- Simulated water level
- Observed water level

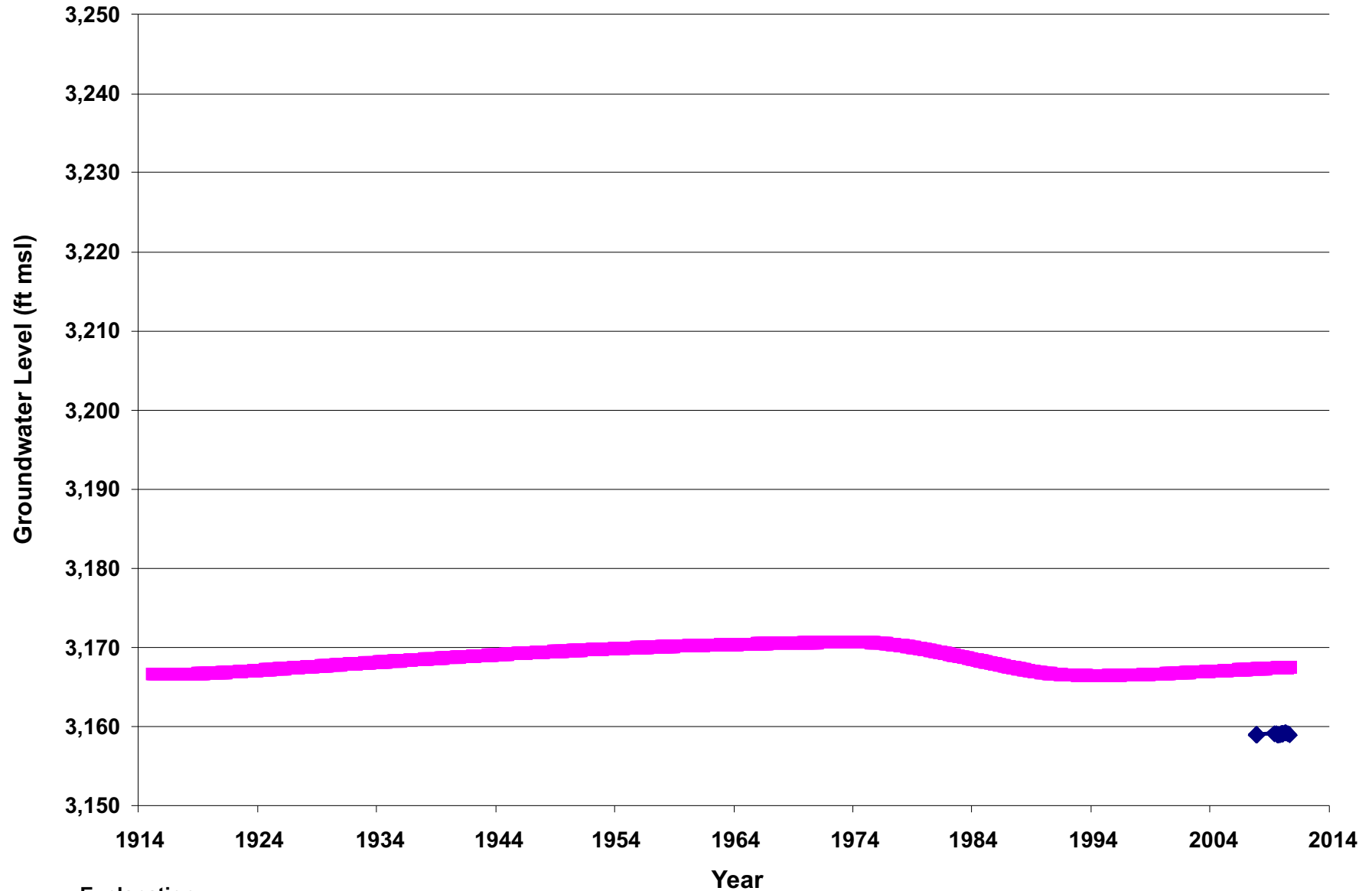




Explanation

- Simulated water level
- Observed water level





Explanation

- Simulated water level
- Observed water level

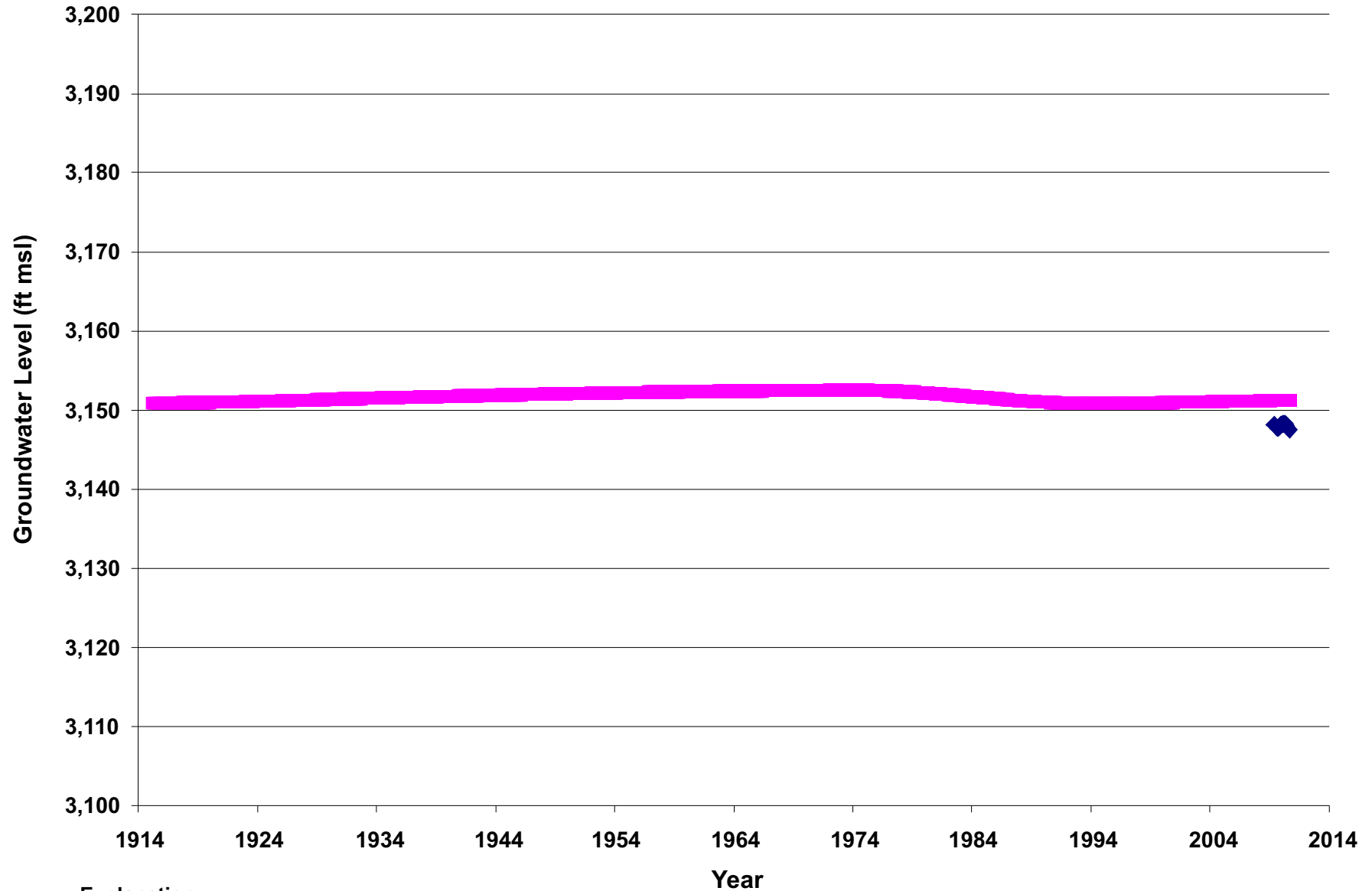


Daniel B. Stephens & Associates, Inc.

1-4-11

JN LT09.0311

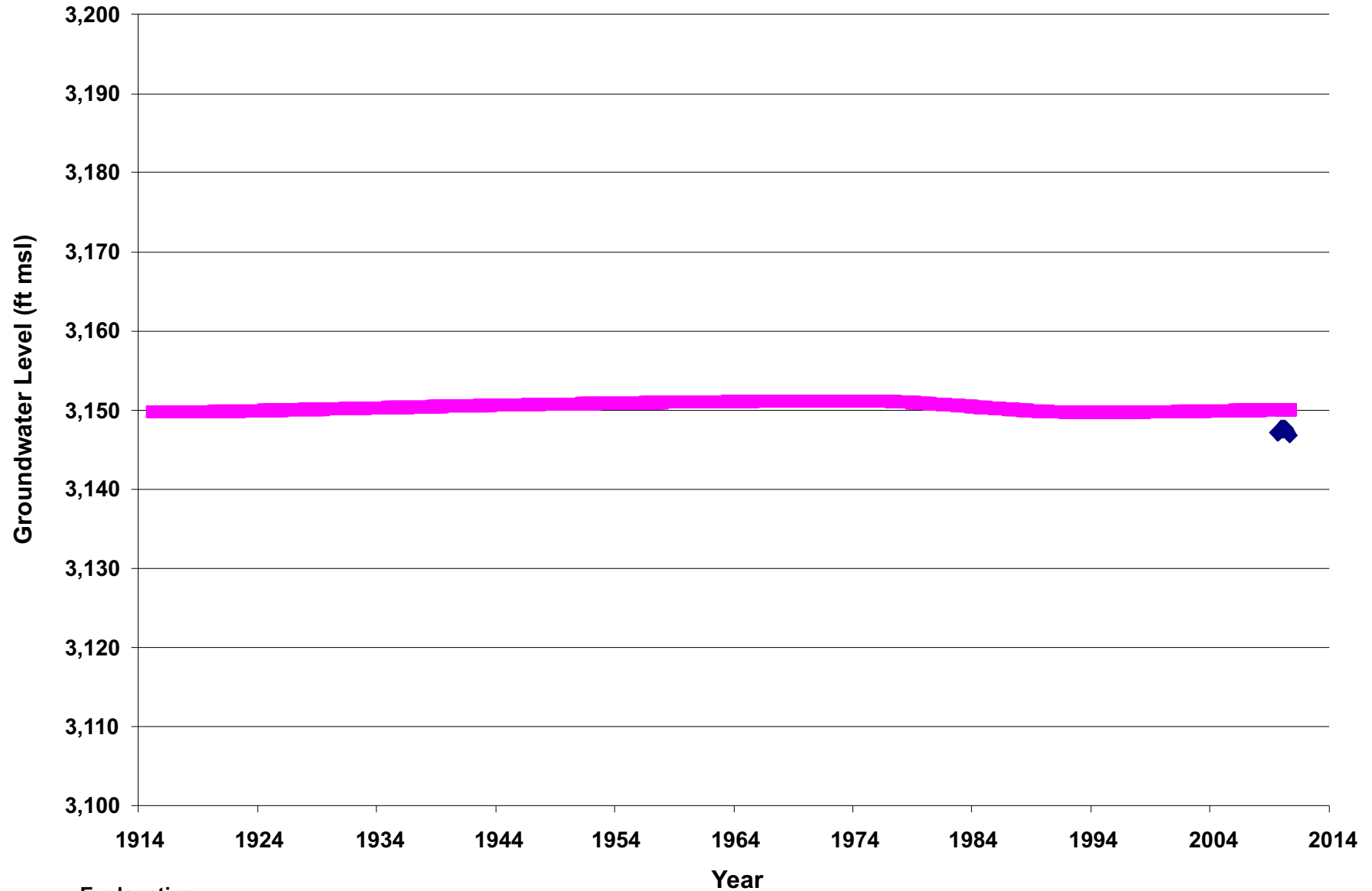
ROSE VALLEY MODEL
Well RV180 Hydrograph



Explanation

- Simulated water level
- Observed water level





Explanation

- Simulated water level
- Observed water level



Appendix D

Report and Model Files



Appendix D. Report and Model Files

The attached compact disc contains a PDF version of the complete report, as well as model files discussed in the report. The input and output files are divided into three directories as follows:

- Steady-state run
- Transient 1915–2010 period calibration run
- Predictive simulations (contains Scenarios A, B and C)

The transient and predictive simulations were executed using MODFLOW 2000. The steady-state run was conducted using the MODFLOW-SURFACT code, Version 3, which is proprietary but available for purchase from HydroGeoLogic Inc. located in Reston, Virginia. This code was used to conduct the steady-state simulation to avoid dry cells that occurred during convergence of the numerical solution when the MODFLOW 2000 code was applied. The simulated steady-state head output file is provided as obtained from MODFLOW-SURFACT, and as amended for the dry reach in the narrows as discussed in the text. The amended head file should be used as the initial head file for the transient simulation.

All simulations were conducted using the Groundwater Vistas pre- and post-processing package distributed by Environmental Simulations, Inc.

**The complete report PDF and model files are provided on the CD
included in the hard copy reports.**